

NN 8201

649

C

# genesis and solution chemistry of acid sulfate soils in thailand

n.van breemen



NN08201.649

**Genesis and solution chemistry of acid sulfate soils in Thailand**

**Aan mijn ouders & Gerard  
Aan Riekje**

Dit proefschrift met stellingen van Nico van Breemen, landbouwkundig ingenieur, geboren te Haarlem op 9 juli 1942, is goedgekeurd door de promotoren dr.ir. L.J. Pons, hoogleraar in de regionale bodemkunde, en dr.ir. J. van Schuylenborgh, lector in de bodemchemie en bodemfysica aan de Universiteit van Amsterdam.

De rector magnificus van de Landbouwhogeschool,  
J.P.H. van der Want

Wageningen, 11 februari 1976

# Genesis and solution chemistry of acid sulfate soils in Thailand

Proefschrift  
ter verkrijging van de graad van  
doctor in de Landbouwwetenschappen  
op gezag van de rector magnificus,  
dr.ir. J.P.H. van der Want, hoogleraar in de virologie,  
in het openbaar te verdedigen  
op vrijdag 23 april 1976 des namiddags te vier uur  
in de aula van de Landbouwhogeschool te Wageningen



*Centre for Agricultural Publishing and Documentation*

*Wageningen - 1976*

# Abstract

Breemen, N. van (1976) Genesis and solution chemistry of acid sulfate soils in Thailand. Agric. Res. Rep. (Versl. landbouwk. Onderz.) 848, ISBN 90 220 0600 X, (xvi) + 263 p., 75 figs, 18 tables, 254 refs, 3 App., Eng. and Dutch Summaries

Also: Doctoral thesis Wageningen.

To study short-term and long-term chemical processes in periodically flooded acid sulfate soils in the Bangkok Plain and in various smaller coastal plains along the Gulf of Thailand, 16 acid sulfate soils and one non-acid marine soil were examined for distribution of iron-sulfur compounds, elemental composition of soil and clay, clay mineralogy, redox potential, pH, and ionic activities in the soil solution.

The application of thermodynamics to mineral-water interactions enlightened various aspects of sulfate reduction, weathering and transformation of minerals (with emphasis on iron oxides, jarosite and clay minerals), and acid production and pH buffering reactions in the soils.

Free descriptors: paddy soils, mangrove swamps, redox potential, sulfate reduction, pyrite oxidation, jarosite, ferric oxides, clay mineral equilibria, amorphous silica, pH buffering.

This thesis will also be published as Agricultural Research Reports 848.

© Centre for Agricultural Publishing and Documentation, Wageningen 1976.

No part of this book may be reproduced or published in any form, by print, photoprint, microfilm or any other means without written permission from the publisher.

# Stellingen

1. Maak geen slapende kattekleien wakker.

Dit proefschrift

2. De verbouw van rijst op geïnundeerde velden is een van de grootste landbouwkundige vindingen.

3. Bij onregelmatige inundatie van natte rijst kan oogstderving optreden als gevolg van stikstofverlies door afwisselende nitrificatie en denitrificatie. Dit verschijnsel heeft waarschijnlijk al spoedig na domesticatie van het gewas geleid tot het perfectioneren van de waterbeheersing.

F.R. Moormann, W.J. Veldkamp & J.C. Ballaux, 1975. The growth of rice in a toposequence. A methodology. Draft for publication, IITA, Ibadan. Nigeria.

4. De uitdrukking 'Groene revolutie' was taktisch verstandig gekozen, maar is, door de hooggespannen verwachtingen die zij opwekte, tevens verantwoordelijk voor de dikwijls in publiciteitsmedia geproclameerde 'mislukking' van de Groene revolutie.

5. Het effect van 'shifting cultivation' op de bodemvruchtbaarheid is onvoldoende bestudeerd.

P.H. Nye & D.J. Greenland, 1960. The soil under shifting cultivation. Commonwealth Bur. Soils Techn. Comm. 51.  
FAO, 1974. Shifting cultivation and soil conservation in Africa. Soil Bull. 24.

6. De geringe omvang en intensiteit van sodaverzouting in de Konya-vlakte hangen samen met de aard van het aldaar aanwezige vulkanisme.

P.M. Driessen, 1970. Soil salinity and alkalinity in the Great Konya Basin, Turkey. Versl. Landbouwk. Onderz. 743, Pudoc, Wageningen.

7. Bij de behandeling van het onderwerp 'soil acidity' wordt door veel auteurs onvoldoende aandacht besteed aan de mogelijke oorzaken van verzuring van de grond.

E.W. Russel, 1973. Soil conditions and plant growth. 10<sup>th</sup> Edition. Longmans.

N.T. Coleman & G.W. Thomas, 1967. In: Soil acidity and liming. Agronomy ser. 12, Amer. Soc. Agronomy, p. 1-41.

8. Voor de studie van bodemverzouting is potentiometrie met behulp van anionen-/of kationselectieve elektroden, zonder gebruik van een referentie-elektrode, in principe zeer bruikbaar.

R.A. Berner, 1971. *Principles of chemical sedimentology*. Mc Graw-Hill.

9. Tot op heden gepubliceerde thermodynamische gegevens over kleimineralen, verkregen uit experimenteel bepaalde ionenactiviteitsprodukten in waterige suspensies zijn i.h.a. weinig betrouwbaar. In verband hiermee is het van belang dat door calorimetrie verkregen vrije vormingsenthalpiën beschikbaar komen.

J.A. Kittrick, 1971. *Proc. Soil Sci. Soc. Am.* 35:140-145.

W.H. Huang & W.D. Keller, 1973. *Am. Mineralogist.* 58: 1023-1028.

A.L. Reesman, 1974. *Clays Clay Minerals* 22:443-454.

10. De aanwezigheid van de redoxkoppels  $S_{\text{rhombisch}}^{2-}$ - $S^{2-}$  en  $\text{Fe}^{2+}$ - $\text{Fe(OH)}_3$ , gevonden in respectievelijk zeebodemsedimenten en bodemoplossingen van geïnundeerde gronden is waarschijnlijk een gevolg van oxydatie door  $\text{O}_2$  na bemonstering of tijdens de meting van de redoxpotentiaal.

R.A. Berner, 1963. *Geochim. Cosmochim. Acta* 27:563-575.

F.N. Ponnamperuma et al., 1967. *Soil Sci.* 103:374-382.

11. Ook bij een homogene verdeling van pyriet in de grond mag men verwachten dat na pyriet-oxydatie de vorming van stabiele aluminiumverzadigde klei allereerst rond open wortelgangen zal plaatsvinden.

G.E. Kamerling, 1974. *Bodemfysisch en agrohydrologisch onderzoek in de jonge kustvlakte van Suriname*. Versl. Landbouwk. Onderz. 825. Pudoc, Wageningen.

12. Boekbesprekingen in vaktijdschriften zouden bij voorkeur begeleid moeten worden door frequentiediagrammen van publikatiedata van de in de besproken boeken aangehaalde literatuur.

13. Het hardnekkige misverstand dat 'klassieke' muziek per se 'ernstig' is leidt dikwijls tot feestelijke radiouitzendingen op dagen van nationale rouw.

14. De techniek der transcendentale meditatie zoals wordt onderwezen door Maharishi Mahesh Yogi kan goede diensten bewijzen bij het verminderen van het gebruik van psychofarmaca en verdient daarom meer aandacht in de medische wereld.

# Contents

<b>1</b>	<i>Introduction</i>	<b>1</b>
<b>2</b>	<i>Physical environment, vegetation and land use</i>	<b>4</b>
2.1	Physiography	4
2.2	Climate	7
2.3	Hydrology and tidal regimes	10
2.4	River water composition and sediment load	15
2.5	Vegetation	16
2.6	Land use	16
<b>3</b>	<i>Distribution and characteristics of coastal plain soils</i>	<b>21</b>
3.1	Soil mapping and classification	21
3.2	The Bangkok Plain	24
3.3	The Cha-am Lagoon	31
3.4	Southern Peninsular Thailand	33
3.5	The Southeast Coast Region	35
3.6	Comparison of the soils	38
<b>4</b>	<i>Processes involving iron, sulfur and manganese</i>	<b>46</b>
4.1	Measurement and interpretation of redox potentials	47
4.2	Accumulation of pyrite	50
4.2.1	Sulfate reduction and dissolved sulfide	51
4.2.2	Formation of iron sulfides	55
4.3	Oxidation of pyrite	62
4.3.1	Pyrite oxidation under field conditions	63
4.3.2	Pyrite oxidation in artificially aerated samples	71
4.4	Oxidation products of pyrite	75
4.4.1	Jarosite	75
4.4.2	Iron oxides	85
4.4.3	Gypsum and other sulfates	96
4.5	Manganese	100

4.6	Reduction processes	103
4.6.1	Soil reduction in acid sulfate soils	104
4.6.2	Soil reduction in non-acid soils	110
4.7	Redistribution of iron, sulfur and manganese	113
5	<i>Silica and silicates</i>	117
5.1	Mineralogy	117
5.2	Dissolved silica	126
5.3	Silicate stability diagrams	128
6	<i>Buffering of pH</i>	136
6.1	Buffer intensity and pH	136
6.2	Extensive properties in acid buffering	140
	<i>Summary</i>	144
	<i>Epilogue: the agronomists' viewpoint</i>	149
	<i>References</i>	153
	<i>Appendix A. Field procedures and methods for soil and water analysis</i>	161
	<i>Appendix B. Profile descriptions and analytical data on soil samples</i>	167
	<i>Appendix C. Analytical data of water samples and calculated thermodynamic activities</i>	225

## Acknowledgments

My thanks are due to:

- My promotor, Prof Dr L.J. Pons, for his enthusiastic support for this research on muddy tropical lowland soils to which both of us entertain some inexplicable attachment.
- My second promotor, Dr J. van Schuylenborgh, who put me on such a promising and rewarding track for the study of soil genesis.
- Dr Bancherd Balankura, Director General of the Land Development Department, Kingdom of Thailand, and Mr Ying Watcharakhup, Mr Samarn Panichapong and Mrs Bunsom Pramonchant and other staff members of the Land Development Department, for providing excellent facilities for field and laboratory work.
- Dr F.R. Moermann, then Project Manager of the FAO Soil Survey and Land Classification Project, Bangkok, for his invaluable guidance during the first stages of my work in Thailand.
- Mr W. van der Kevie and Mr G.W. Arnott of the FAO, Bangkok, for their generous help on field work and trouble shooting in the laboratory.
- Mr Paul L.G. Vlek for his excellent cooperation in many stages of the research.
- Dr Samran Sombatpanit, Mr Kien Apichonthiwhong, Mr Nakhon Thawornwong and Mr Manob Tandatemiya of the Land Development Department, Bangkok, and staff of the Rangsit Acid Sulfate Soil Research Station, for their enthusiastic collaboration during field work.
- Miss Suwatana Rangsikul of the Soil Survey Division, Land Development Department, Bangkok, and Mr L.Th. Begheyn, Mr J.D.J. van Doesburg, Mr A. Engelsma, Mr J.R.M. Huting, Mr A.T.J. Jonker, Mr H. Krechting, Mr R. Schoorl, Mr W. Stamm and Miss Y. Wubben, of the Department of Soil Science and Geology, Agricultural University Wageningen, whose laboratory work formed the foundation for this study.

- Mr G.J. van de Waal and Mr Th. Pape of the Department of Soil Science and Geology, Agricultural University Wageningen, for preparing and interpreting the many thin sections.
- Mr G. Buurman, Mr O.D. Jeronimus and Mr P.G.M. Versteeg of the same department for their skilled draftsmanship that was not affected by my whimsical demands.
- Mr R. Brinkman and Mr K. Harmsen of the Agricultural University Wageningen for many stimulating discussions.
- Mr R.J.P. Aalpol and Mr J.C. Rigg, editors of Pudoc, Wageningen, who interfered mercilessly where necessary.
- Mrs M.N.E. Tyrol, Mrs P. Rozendaal, Mrs W.M. Laoh of the Words Processing Centre and Miss M.M. Rosbag of the Department of Soil Science and Geology both of the Agricultural University Wageningen, for typing the voluminous manuscript.

This study was supported by a grant (W 89-2) from the Netherlands Foundation for the Advancement of Tropical Research, The Hague.

Finally I wish to express my deep gratitude to my wife, Riekje, and my children, Barbara, Sanneke, Onno and Marjolein, who had to put up with a husband and father deep in acid and muddy thoughts.

# Curriculum vitae

Na het behalen van het einddiploma HBS-B aan het Coornhert Lyceum te Haarlem begon de auteur in 1960 zijn studie aan de Landbouwhogeschool te Wageningen. Tijdens zijn praktijktijd was hij lid van de 'Rijstgroep', een groep van negen studenten van verschillende specialisaties die de rijstcultuur in verschillende landen in de beide Amerika's, Azië en het Midden Oosten bestudeerde. In september 1968 studeerde hij (met lof) af in de richting bodemkunde en bemestingsleer met als specialisatie de bodemgenese (hoofdvak tropische bodemkunde, bijvakken bodemmineralogie en bemestingsleer).

Vervolgens trad hij in dienst als wetenschappelijk medewerker van de afdeling Bodemkunde en Geologie van de Landbouwhogeschool en werd in de gelegenheid gesteld om, met financiële steun van de WOTRO, gedurende twee jaar onderzoek te verrichten aan de genese van kattekleigronden in Thailand. Na zijn terugkomst in Nederland werd hij onder meer belast met het onderwijs in de chemische aspecten van de bodemgenese.

Met ingang van mei 1976 zal hij voor twee jaar als Postdoctoral Fellow verbonden zijn aan het International Rice Research Institute te Los Banos, Philippijnen.

# Samenvatting

Over de gehele wereld vindt men kustgebieden waar kleirijke sedimenten worden afgezet onder zoute tot brakke omstandigheden. Terwijl zulke getijdengebieden in gematigde streken dikwijls weinig begroeid zijn, zijn zij in de tropen meestal gekarakteriseerd door de aanwezigheid van dichte mangrovebossen. Door de overvloedige aanvoer van organische stof, verzadiging met water en aanwezigheid van sulfaat uit het zeewater vindt in dergelijke sedimenten een sterke reductie van sulfaat tot sulfide plaats. In de aanwezigheid van ijzer wordt een deel van het gevormde sulfide vastgelegd als pyriet, kubisch  $\text{FeS}_2$ . Het grootste deel van de alkaliniteit dat als opgelost bicarbonaat tijdens de sulfaatreductie naast sulfide wordt gevormd, verdwijnt met het afstromend getijdewater naar de zee, waardoor een potentieel zuur residu (pyriet) achterblijft. Aeratie van deze sedimenten door natuurlijke of kunstmatige drainage leidt tot oxydatie van het pyriet en de vorming van zwavelzuur. Bij afwezigheid van neutraliserende bestanddelen, zoals calciumcarboonaat, kan de pH dalen tot 3 - 4 en worden de typische gele vlekken van jarosiet,  $\text{KFe}_3(\text{SO}_4)_2(\text{OH})_6$ , gevormd.

In de tropen komen enkele miljoenen hectaren van deze zogenoamde 'katteklei-gronden' (acid sulfate soils) voor, terwijl het areaal aan potentiële katteklei-gronden (niet gedraineerde pyrietrijke sedimenten) nog groter is. Al deze gronden zijn ongeschikt of minder geschikt voor de landbouw. Niettemin worden alleen al in Thailand ongeveer een drielikwart miljoen hectaren katteklei-gronden voor de verbouw van natte rijst gebruikt. Verbetering is technisch gezien gemakkelijk (op grote schaal bekalken) maar financieel dikwijls onhaalbaar. Fundamenteel en praktisch onderzoek is gewenst om nieuwe methoden en technieken te ontwikkelen ter verbetering van deze gronden. Naast dit praktisch aspect is de studie van de genese van deze gronden ook uit theoretisch oogpunt van belang. Zo verlopen, anders dan in de meeste gronden, verschillende bodemvormende processen en verwerkingsreacties in katteklei-gronden betrekkelijk snel en zijn daarom (relatief) gemakkelijk te volgen.

Terwijl bij de meeste bodemgenetische onderzoeken voornamelijk of uitsluitend aandacht wordt besteed aan de vaste fasen, is bij deze studie

vooral gebruik gemaakt van watermonsters. Bij periodieke bemonstering is de chemische samenstelling van het bodemwater dikwijls een veel gevoeliger maat voor chemische processen die zich in de grond afspelen dan de samenstelling van de grond zelf. Omdat potentiële katteklei-gronden in een marien milieu worden gevormd kan men door vergelijking van zeewater en bodemwater van gronden in diverse ontwikkelingsstadia bovendien inlichtingen verkrijgen over de processen die zich op langere termijn hebben afgespeeld. Tenslotte geven de thermodynamische concentraties (activiteiten) van de opgeloste bestanddelen, die berekend kunnen worden uit de geanalyseerde concentraties, inlichtingen over de mate waarin het water is oververzadigd of onderverzadigd met verschillende mineralen. Hierdoor wordt het mogelijk de richting van verschillende processen vast te stellen (wordt een bepaald mineraal gevormd of lost het juist op?), terwijl men soms de fasen en variabelen kan identificeren die de concentraties van bepaalde elementen in oplossing bepalen.

Het onderzoek werd uitgevoerd in het zuidelijke deel van de Chao Phraya delta, de zogenaamde Bangkok Plain, en in drie van de kleinere kustvlakten langs de Golf van Thailand. De meeste katteklei-gronden in de Bangkok Plain zijn goed ontwikkeld en bevinden zich op tenminste 10-30 km van de huidige kust (zie achterflap). In de kuststrook zelf vindt men voornamelijk niet-zure marine gronden; slechts in het zuidoostelijk deel van de vlakte komen kleinere oppervlakten met jonge, zoute katteklei-gronden voor. De Bangkok Plain is gedurende de natte moesson grotendeels geïnundeerd en staat de rest van het jaar droog. Bijna alle gronden in het gebied worden voor de natte rijstverbouw gebruikt.

In totaal werden 16 katteklei-gronden van de Bangkok Plain en van drie kleinere kustvlakten langs de Golf van Thailand beschreven en bemonsterd. Naast de samenstelling van ijzer en zwavel verbindingen, de elementaire samenstelling van de grond en van de kleifracie en de kleimineralogie, werd veel aandacht geschonken aan de pH en de redoxpotentiaal. Op 23 plaatsen werden 480 watermonsters genomen. Bovendien zijn grond- en watermonsters verzameld tijdens enkele laboratoriumexperimenten waarbij grondmonsters werden onderworpen aan kunstmatige aëratie of inundatie. De belangrijkste bevindingen van het onderzoek kunnen als volgt worden samengevat:

## *Pyrietvorming*

In mangrove-modders met actuele sulfaatreductie komen de  $E_H$  (redox-potentiaal)-pH-gegevens redelijk overeen met de theoretische waarden van het sulfaat-sulfide-koppel, en niet met die van het elementair zwavel-sulfide-koppel die werden gevonden door andere onderzoekers. Verversing van het interstitieel water als gevolg van de getijdewerking zorgt voor een snelle aanvulling van het gereduceerde en als sulfide gebonden sulfaat. FeS-gehalten zijn laag en pyriet is de enige gereduceerde zwavelverbinding die kwantitatief belangrijk is. Het gehalte aan pyrietzwavel is 2-3% in de ondergronden van katteklei-gronden en potentiële katteklei-gronden, en in het algemeen lager dan 1% onder in niet-zure marine gronden. In de ondergronden van kattekleigronden uit het zuidelijk deel van het schiereiland is bijna alle voor de vorming van pyriet beschikbare ijzer inderdaad in pyriet omgezet. In de Bangkok Plain is minder beschikbaar ijzer omgezet in pyriet: ongeveer de helft in het geval van katteklei-gronden, en ongeveer een derde in niet-potentieel zure gronden.

Uit onderzoek in Maleisië bleek dat pyrietaccumulatie sneller verloopt langs estuaria dan langs aangroeiente kusten. Dit verschil is waarschijnlijk gelegen in de sterkere doorspoeling van het getijdewater in de estuaria, waardoor (a) opgeloste alkaliniteit gemakkelijker verdwijnt (dit leidt tot een lagere pH hetgeen kinetisch gesproken gunstig is voor pyrietvorming) en (b) partiële oxydatie van sulfide tot elementair zwavel optreedt ( $S_{\text{elem}}$  is een noodzakelijk tussenproduct bij de vorming van pyriet). De verspreiding van katteklei-gronden en niet-zure gronden langs de huidige kust in Thailand geeft aanleiding te veronderstellen dat hetzelfde verschil ook hier een rol speelt.

## *Oxydatie van pyriet*

Pyrietoxydatie wordt uiteindelijk veroorzaakt door atmosferische zuurstof, maar het proces verloopt waarschijnlijk via opgelost ferri-ijzer als tussen-oxidant. Dit blijkt uit het micromorfologische beeld van de distributie van pyriet en ferri-oxyde langs holten en scheuren en verklaart de waarneming dat pyrietoxydatie zelfs na inundatie nog enige tijd doorgaat (nl. door reductie van ferri-oxyde dat in de voorafgaande droge tijd vlak naast pyriet werd gevormd).

In de diep ontwikkelde katteklei-gronden is de oxydatie van pyriet gedu-

rende de droge tijd een vrij langzaam proces met de aanvoer van zuurstof als beperkende factor. In jonge gronden waar, door geringe dikte van het geoxydeerde pakket, zuurstof gemakkelijker in de pyrietrijke ondergrond kan doordringen, verloopt dit proces iets sneller. Een zeer snelle pyrietoxydatie treedt daarentegen op bij kunstmatige aëratie van gereduceerde grondmonsters.

#### *Sulfaten*

Het opvallende stroo-gele mineraal jarosiet komt voor in dichte massa's van kleine ( $0,1-5 \mu\text{m}$ ) deeltjes en geeft een scherp röntgendiffractiepatroon. Jarosiet is verder gekarakteriseerd door (a) een abnormaal hoog watergehalte, (b) geringe substitutie van K voor Na (zelfs bij hoge concentraties aan  $\text{Na}^+$  in de omringende oplossing) en (c), in enkele gevallen, partiële vervanging van  $\text{K}^+$  door  $\text{H}_3\text{O}^+$ . In overeenstemming met theoretische stabiliteitsdiagrammen wordt jarosiet alleen gevormd onder zure ( $\text{pH}<4$ ), geoxideerde omstandigheden in afwezigheid van pyriet, en wordt het mineraal uiteindelijk door hydrolyse omgezet in goethiet.

Andere vormen waarin sulfaat in katteklei-gronden voorkomt, zijn gips, geadsorbeerd sulfaat en het hypothetische basische aluminiumsulfaat  $\text{AlOHSO}_4$  dat de concentratie van opgelost Al lijkt te reguleren. Uitbloeiingen van wateroplosbare sulfaten, waarvan er sommige aluminium en ferro-ijzer bevatten, kunnen ontstaan onder zeer droge omstandigheden.

#### *Ferri-oxyden*

Behalve in pyriethoudende gronden en in sterk gereduceerde bovengronden, is de bodemoplossing meestal oververzadigd met grofkorrelige goethiet en onderverzadigd met amorf ferrihydroxyde. Het aanvankelijk röntgenamorfe materiaal in de bruine (roest)vlekken veroudert tot steeds meer grofkorrelige goethiet. Hematiet komt voor in rode vlekken boven in het profiel van vele oudere katteklei-gronden. De omzetting van goethiet tot hematiet wordt waarschijnlijk bevorderd door periodieke sterke uitdroging en door zure tot zwak zure omstandigheden.

#### *Mangaan*

Zwarte mangaanoxyde-vlekken komen vrijwel steeds voor in de B-horizont van niet-zure mariene gronden, maar ontbreken altijd in katteklei-gronden.

Bij lage pH wordt mangaan gemakkelijk gemobiliseerd en is dan voornamelijk aanwezig in wateroplosbare en uitwisselbare vorm.

#### *Afwisselende reductie en oxidatie in de bovengrond*

Vergeleken met de meeste niet-zure gronden vertonen katteklei-gronden in het algemeen een langzame reductie na bevloeiing. Dit blijkt onder andere uit de langzame stijging van de pH en het late optreden van sulfaatreduceertie. Reductie van ferri-oxyden tot opgelost  $Fe^{2+}$  gaat gepaard met desorptie van sulfaat en met hydrolyse van basische sulfaten. Een deel van het aldus gevormde (opgeloste) ferrosulfaat wordt weer geoxydeerd tot ferri-oxyde en zwavelzuur aan het grensvlak van grond en oppervlaktewater. Het zwavelzuur wordt met het zijwaarts afstromende oppervlaktewater meegevoerd, zodat periodieke bevloeiing van katteklei-gronden leidt tot ontzuring van de bovengrond.

Een geheel ander proces treedt op in bevloeide niet-zure gronden. Hier verloopt de reductie veel sneller en wordt FeS gevormd terwijl een deel van de bij de sulfaatreduceertie geproduceerde alkaliniteit in het oppervlaktewater verdwijnt. Oxydatie van het FeS in de daaropvolgende droge tijd levert zwavelzuur, zodat elkaar afwisselende bevloeiing en droogzetting in deze gronden juist tot verzuring leiden. De uiteindelijke pH zal echter nooit dalen beneden 4,5-5 omdat, na tijdelijke verzuring tot een lagere pH, het eerder genoemde ontzuringsproces in werking zal treden. Om eenzelfde reden zal de (aërobe) pH van katteklei-gronden aan de oppervlakte niet boven het traject pH 4,5-5 uitkomen.

#### *Verplaatsing van ijzer*

Een gedeelte van het in de gereduceerde bovengrond en in de pyrietrijke ondergrond opgeloste Fe diffundeert naar de B-horizont die het hele jaar door sterk geoxydeerd blijft en waar de concentraties aan opgelost ijzer bijna steeds lager zijn dan in de onder- en bovenliggende horizonten. Oxydatie van het verplaatste ijzer gedurende de droge tijd leidt uiteindelijk tot een sterke aanraking van ferri-ijzer in deze horizont. Jarosiet wordt vooral in het onderste deel van de B-horizont gevormd, en hydrolyseert tot goethiet op geringere diepte. Naarmate de gronden ouder worden en dieper zijn gedraineerd, vindt men de verschillende accumulatiehorizonten op grotere diepte. Ook de B-horizont van niet-zure gronden blijft na inundatie in

geoxydeerde toestand. Als gevolg van de geringere mobiliteit van ijzer bij een hogere pH, is de ijzeraanrijking hier echter minder uitgesproken.

#### *Verwering en omzetting van silikaten*

De kleifractie van alle gronden bevat kaoliniet, illiet en smectiet. In het zuidelijk deel van het schiereiland en in het zuidwesten worden echter betrekkelijk geringe hoeveelheden aan 2:1-kleimineralen aangetroffen.

Bij katteklei-gronden van de Bangkok Plain zijn drie afzonderlijke processen van invloed op de kleimineralogie: (a) magnesium in oktahedrische posities van smectitische klei, aanwezig in pyrietrijke ondergronden, wordt na aëratie vervangen door ferri-ijzer dat vrijkomt bij de oxidatie van pyriet; (b) in periodiek gereduceerde bovengronden worden tussenlagen van aluminium-hydroxyde in zwellende kleimineralen ingebouwd en (c) een klein deel van de 2:1-klei verweert tot amorf silica en, mogelijk, tot kaoliniet.

Vergelijkbare processen spelen zich af in niet-zure gronden, maar hier is de intensiteit van de verwering geringer en wordt geen amorf silica gevormd.

#### *Verzuring en pH-buffering*

Het zeer nauwe pH-traject (3,6-3,8) van jarosiet-rijke B-horizonten kan worden verklaard door evenwichtsinstelling van een vrij groot aantal vaste fasen met de bodemoplossing. De fasenregel van Gibbs voorspelt dat toevoeging van componenten van het systeem (bijvoorbeeld zwavelzuur of calcium-hydroxyde), bij behoud van de evenwichtssituatie, geen verandering zal brengen in de pH en in de samenstelling van de oplossing. Als de verzuring (dus de pyrietoxydatie) echter sneller verloopt dan de pH-buffering, kan de pH tot beneden 2 dalen. In de oudere katteklei-gronden houdt het buffermechanisme de verzuring bij; in de jongere gronden is dit niet steeds het geval, hetgeen dikwijls resulteert in pH waarden tussen 3 en 3,5.

De resultaten van de chemische (totaal-)analysen van vele profielen geven aanleiding te veronderstellen dat een deel van het bij de pyrietoxydatie gevormde zwavelzuur in een of andere ongenuutraliseerde vorm de grond verlaat. Mogelijk speelt het gasvormige  $\text{SO}_2$  hierbij een rol, tenminste in de jongere gronden. Het reeds eerder genoemde ontzuringsmechanisme in de bovengrond van geïnundeerde kattekleien heeft eenzelfde effect, maar het kwantitatieve belang van deze processen is niet geheel duidelijk.

Bij lage pH wordt mangaan gemakkelijk gemobiliseerd en is dan voornamelijk aanwezig in wateroplosbare en uitwisselbare vorm.

#### *Afwisselende reductie en oxidatie in de bovengrond*

Vergeleken met de meeste niet-zure gronden vertonen katteklei-gronden in het algemeen een langzame reductie na bevloeiing. Dit blijkt onder andere uit de langzame stijging van de pH en het late optreden van sulfaatreductie. Reductie van ferri-oxyden tot opgelost  $Fe^{2+}$  gaat gepaard met desorptie van sulfaat en met hydrolyse van basische sulfaten. Een deel van het aldus gevormde (opgeloste) ferrosulfaat wordt weer geoxydeerd tot ferri-oxyde en zwavelzuur aan het grensvlak van grond en oppervlaktewater. Het zwavelzuur wordt met het zijwaarts afstromende oppervlaktewater meegevoerd, zodat periodieke bevloeiing van katteklei-gronden leidt tot ontzuring van de bovengrond.

Een geheel ander proces treedt op in bevloeide niet-zure gronden. Hier verloopt de reductie veel sneller en wordt  $FeS$  gevormd terwijl een deel van de bij de sulfaatreductie geproduceerde alkaliniteit in het oppervlaktewater verdwijnt. Oxydatie van het  $FeS$  in de daaropvolgende droge tijd levert zwavelzuur, zodat elkaar afwisselende bevloeiing en droogzetting in deze gronden juist tot verzuring leiden. De uiteindelijke pH zal echter nooit dalen beneden 4,5-5 omdat, na tijdelijke verzuring tot een lagere pH, het eerder genoemde ontzuringsproces in werking zal treden. Om eenzelfde reden zal de (aërobe) pH van katteklei-gronden aan de oppervlakte niet boven het traject pH 4,5-5 uitkomen.

#### *Verplaatsing van ijzer*

Een gedeelte van het in de gereduceerde bovengrond en in de pyrietrijke ondergrond opgeloste Fe diffundeert naar de B-horizont die het hele jaar door sterk geoxydeerd blijft en waar de concentraties aan opgelost ijzer bijna steeds lager zijn dan in de onder- en bovenliggende horizonten. Oxydatie van het verplaatste ijzer gedurende de droge tijd leidt uiteindelijk tot een sterke aanraking van ferri-ijzer in deze horizont. Jarosiet wordt vooral in het onderste deel van de B-horizont gevormd, en hydrolyseert tot goethiet op geringere diepte. Naarmate de gronden ouder worden en dieper zijn gedraaineerd, vindt men de verschillende accumulatiehorizonten op grotere diepte. Ook de B-horizont van niet-zure gronden blijft na inundatie in

geoxydeerde toestand. Als gevolg van de geringere mobiliteit van ijzer bij een hogere pH, is de ijzeraanrijking hier echter minder uitgesproken.

#### *Verwering en omzetting van silikaten*

De kleifracie van alle gronden bevat kaoliniet, illiet en smectiet. In het zuidelijk deel van het schiereiland en in het zuidwesten worden echter betrekkelijk geringe hoeveelheden aan 2:1-kleimineralen aangetroffen.

Bij katteklei-gronden van de Bangkok Plain zijn drie afzonderlijke processen van invloed op de kleimineralogie: (a) magnesium in oktahedrische posities van smectitische klei, aanwezig in pyrietrijke ondergronden, wordt na aëratie vervangen door ferri-ijzer dat vrijkomt bij de oxidatie van pyriet; (b) in periodiek gereduceerde bovengronden worden tussenlagen van aluminium-hydroxyde in zwellende kleimineralen ingebouwd en (c) een klein deel van de 2:1-klei verweert tot amorf silica en, mogelijk, tot kaoliniet.

Vergelijkbare processen spelen zich af in niet-zure gronden, maar hier is de intensiteit van de verwering geringer en wordt geen amorf silica gevormd.

#### *Verzuring en pH-buffering*

Het zeer nauwe pH-traject (3,6-3,8) van jarosiet-rijke B-horizonten kan worden verklaard door evenwichtsinstelling van een vrij groot aantal vaste fasen met de bodemoplossing. De fasenregel van Gibbs voorspelt dat toevoeging van componenten van het systeem (bijvoorbeeld zwavelzuur of calcium-hydroxyde), bij behoud van de evenwichtssituatie, geen verandering zal brengen in de pH en in de samenstelling van de oplossing. Als de verzuring (dus de pyrietoxydatie) echter sneller verloopt dan de pH-buffering, kan de pH tot beneden 2 dalen. In de oudere katteklei-gronden houdt het buffermechanisme de verzuring bij; in de jongere gronden is dit niet steeds het geval, hetgeen dikwijls resulteert in pH waarden tussen 3 en 3,5.

De resultaten van de chemische (totaal-)analysen van vele profielen geven aanleiding te veronderstellen dat een deel van het bij de pyrietoxydatie gevormde zwavelzuur in een of andere ongenuutraliseerde vorm de grond verlaat. Mogelijk speelt het gasvormige  $\text{SO}_2$  hierbij een rol, tenminste in de jongere gronden. Het reeds eerder genoemde ontzuringsmechanisme in de bovengrond van geïnundeerde kattekleien heeft eenzelfde effect, maar het kwantitatieve belang van deze processen is niet geheel duidelijk.

Het boek wordt afgesloten met een nawoord waarin verschillende praktische aspecten van de bevindingen van het onderzoek nader worden beschouwd. Hierbij ligt de nadruk op het herkennen en karteren van katteklei-gronden enerzijds en de ontginding en verbetering anderzijds.

# 1 Introduction

In many coastal regions all over the world clayey sediments are deposited over extensive areas under brackish to saline conditions. Such tidal marshes are often sparsely vegetated under temperate climates, but they are normally covered by dense mangrove forests in the tropics. Abundance of organic matter from mangrove trees, saturation with water and ubiquity of sulfate from sea water lead to anaerobiosis characterized by prolific bacterial sulfate reduction. If iron is available from ferric oxides or iron-bearing silicates, much of the sulfide produced is fixed as pyrite (cubic  $\text{FeS}_2$ ). The greater part of the alkalinity ( $\text{HCO}_3^-$ ) formed during sulfate reduction is removed to the sea by tidal action, leaving a potentially acid residue as pyrite.

Aeration of these pyritic sediments leads to microbial oxidation of pyrite and, in the absence of sufficient acid-neutralizing substances such as calcium carbonate, to the formation of sulfuric acid.

Aeration and acidification can be brought about by natural or artificial drainage of pyritic sediments. The resulting acid sulfate soils commonly have a pH between 3 and 4 and show yellow mottles of the mineral jarosite,  $\text{KFe}_3(\text{SO}_4)_2(\text{OH})_6$ .

In the tropics several million hectares of acid sulfate soils occur, and potentially acid sediments cover at least 7.5 million hectares (Kawalec, 1973). Acid sulfate soils are less widespread in the temperate zones, possibly because of less production of organic matter in tidal areas and generally higher lime content of the sediments. Agricultural productivity is often seriously hampered on acid sulfate soils, and the presence of potentially acid sediments poses problems when reclaiming tidal areas. Technically such soils can easily be improved: liming will eliminate most, if not all, problems. But the amounts of lime required are usually economically excessive. Fundamental and practical research on these soils may reveal cheaper ways.

The study of acid sulfate soils also enables us to trace certain weathering and soil-forming processes. Most soil-forming processes proceed slowly, but the high acidity in acid sulfate soils causes a rapid transformation of certain

minerals and a rapid differentiation of soil horizons. Moreover the predominant-ly 'chemical' nature of weathering and soil formation greatly facilitates identification of the relevant processes: microbes involved in oxidation and reduction of iron and sulfur can be conveniently treated as black boxes.

Recent reviews (Dost, 1973; Bloomfield & Coulter, 1973) show that most research done on acid sulfate soils is highly empirical, and has added little to knowledge of the chemical processes involved in acidification discovered by van Bemmelen in 1886. One of the aims of my study was to investigate these processes by approaches used successfully in recent geochemical work on interactions between minerals and aqueous solutions at the earth's surface (e.g. Garrels & Christ, 1965; Berner, 1971; Helgeson et al., 1969).

The coastal plain areas of Thailand were chosen for this study because of the widespread occurrence of acid sulfate soils in various stages of development, the availability of good soil maps and excellent facilities for field and laboratory work. The selected areas were (a) the Bangkok plain, having the largest area (about 8000 km<sup>2</sup>) of acid sulfate soils in Thailand, (b) the estuary of the Chanthaburi River in the southeast, (c) the Cha-am Lagoon to the west of the head of the Gulf of Thailand and (d) the Songkhla-Pattani region of Peninsular Thailand.

The emphasis was placed on the development of acid sulfate soils from existing pyritic sediments, and little attention was paid to pyrite formation itself. Seventeen soils were selected for detailed description and sampling for chemical and morphological analysis. Most emphasis was placed, however, on the study of ground and surface water. The benefit of data on water chemistry is manifold. In the first place, owing to the large mass ratio of solids to dissolved matter for most elements in a soil-water system, undetectably small changes in the composition of the soil may appear as relatively large changes in the composition of the water. Thus water sampling at intervals of a few months allows identification of certain chemical processes measurable in the soil itself only after decades or centuries. Moreover, because sea water can be considered as a starting point, the long-term changes in the groundwater composition as a result of mineral-water interactions can be evaluated by comparing the actual soil solution with sea water.

Another advantage of water analysis is that calculated ionic activity products indicate to what extent the solution is in equilibrium with certain minerals. This approach helps to identify the variables and phases that control the concentration of different elements in the soil solution. Such knowledge may be useful in studies on plant nutrition and on toxicity, and has the

advantage that it may be used to predict solute concentrations under circumstances not encountered during the original research.

Between March 1969 and March 1971, about 150 soil samples were taken for elemental analysis of the fine earth and the clay, and for X-ray diffraction analysis. Various sulfur fractions were analysed in 74 soil samples collected and dried with special precautions to minimize oxidation of reduced sulfur compounds. Special samples were taken also to measure pH of the fresh soil ( $n = 700$ ), soil moisture (130), pF and bulk density (27) and to study micro-morphology (63). Periodical or single samples of ground water (360) and surface water (120) were taken at 23 sites. Most were collected from permanently installed porous pots, placed at different depths at four sites, and 120 samples were extracted from mud previously used for measuring redox potential ( $E_H$ ) and pH. A further 130 water samples were collected during laboratory experiments on the behaviour of different soil samples upon flooding and aeration in the laboratory. Water analysis, most of the sulfur analysis, and determinations of  $E_H$ , pH, pF and moisture were done in the laboratory of the Soil Survey Division, Department of Land Development, Bangkhen. All other measurements were made at the Department of Soil Science and Geology, Agricultural University, Wageningen. Field and laboratory procedures are described in Appendix A.

Some of the results of this study have been reported earlier (Vlek, 1971; van Breemen, 1971, 1973a, 1973b, 1973c, 1975; Buurman et al., 1973; van Breemen et al., 1973; van Breemen & Harmsen, 1975; Harmsen & van Breemen, 1975). Most of these publications focus on details of the chemistry and mineralogy of acid sulfate soils. This book gives a broader outline of the geochemistry of iron and sulfur compounds and the behaviour of silica and silicates, and supplies chemical and mineralogical data on acid sulfate soils in Thailand.

## 2 Physical environment, vegetation and land use

### 2.1 PHYSIOGRAPHY

Thailand is situated between  $5^{\circ}$  and  $21^{\circ}$ N, and between  $97^{\circ}$  and  $106^{\circ}$ E, and covers about  $5.14 \times 10^5 \text{ km}^2$ . Physiographically the country can be subdivided into six regions (Fig. 1). The Central Plain, which includes the Bangkok Plain, is a deep syncline filled with sediments. It forms the lower Chao Phraya river basin which is characterized by riverine sediments in its upper reaches and marine and tidal marsh deposits near to the coast. The Continental Highlands (200-500 m high)

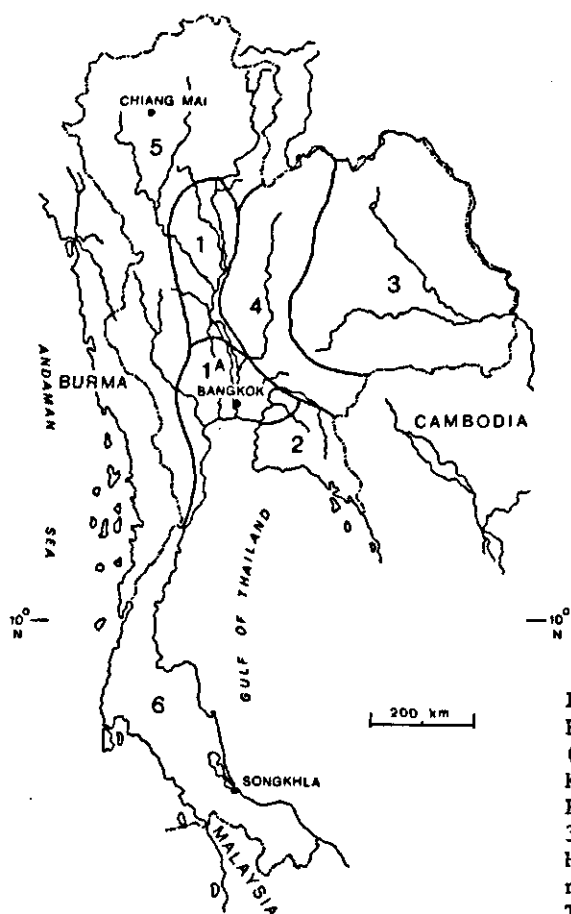


Figure 1  
Physiographic Regions of Thailand  
(Moormann & Rojanasoothon, 1968)  
Key: 1, Central Plain: 1A Bangkok  
Plain; 2 Southeast Coast Region;  
3 Northeast Plateau; 4 Central  
Highlands; 5 North and West Conti-  
nental Highlands; 6 Peninsular  
Thailand.

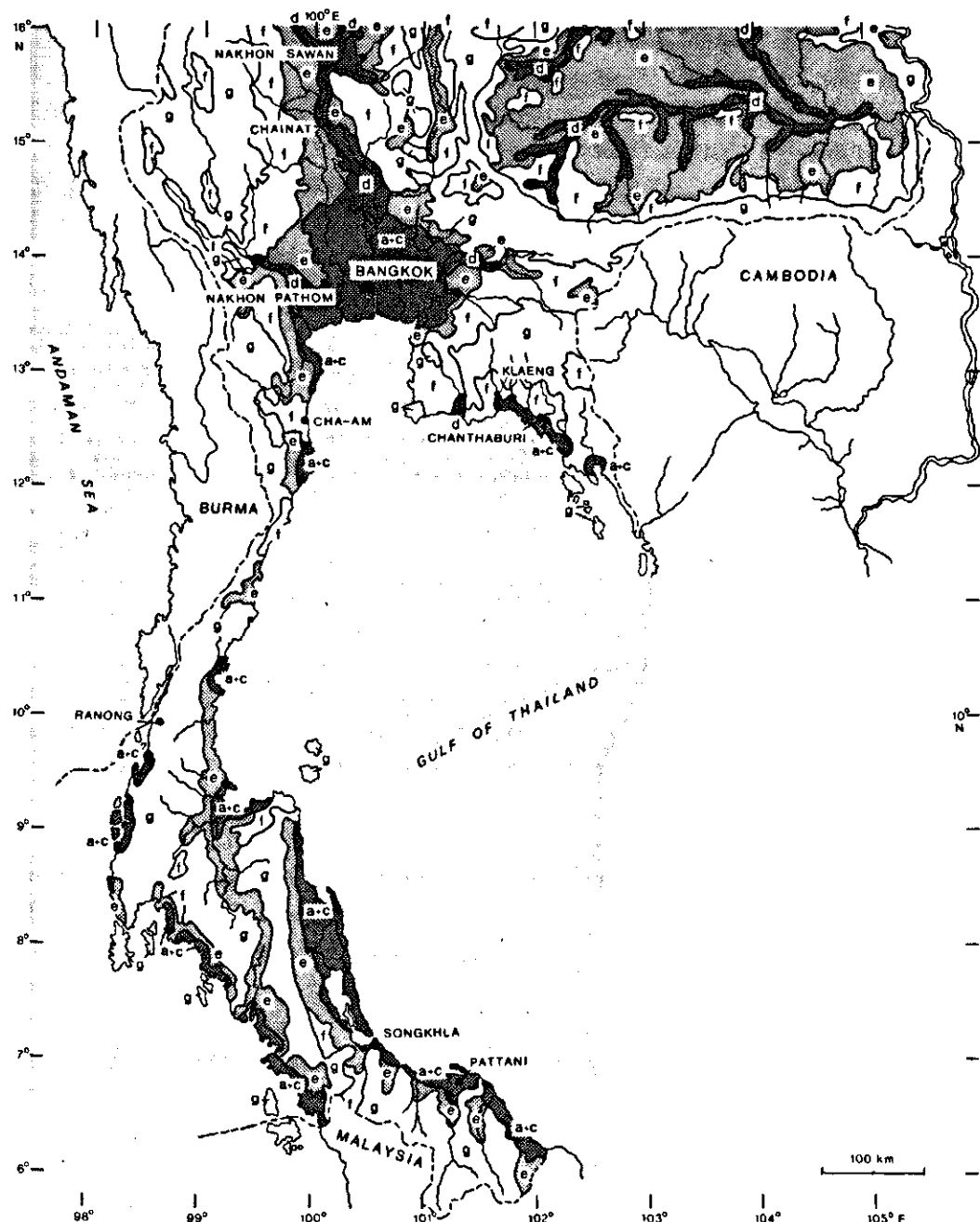


Figure 2

Parent materials in part of Thailand. Recent sediments are indicated by dark shading. Semi-recent and older sediments by light shading.

a = marine and tidal marsh deposits, non-acid; c = tidal marsh deposits, acid;  
 d = recent riverine sediments; e = semi-recent alluvium; f = older sediments;  
 g = residuum and colluvium.

and part of the Southeast Coast region belong to the catchment area of the rivers forming the delta of the Bangkok Plain. The Northeast Plateau belongs to the watershed of the Mekong River, which drains into the South China Sea. Peninsular Thailand and the Southeast Coast region are generally hilly and mountainous with altitudes between 200 and 1000 m. Fig. 2 also shows the many smaller alluvial plains fringing the coast of these regions.

The largest continuous area with acid sulfate soils covering about 8000 km<sup>2</sup>, is found in the Bangkok Plain between Bangkok and the southern boundary of the Chao Phraya riverine alluvium. Non-acid marine soils occur in a 25-40 km wide zone between the acid soils and the coast. Most of the smaller coastal plains fringing the Southeast Coast and Peninsular Thailand have small areas with acid sulfate soils, often intimately associated with potentially acid soils and non-acid marine soils.

The altitude of the Chao Phraya Delta gradually decreases from 15 m above mean sea-level at the apex near Chainat to 5 m at Ayutthaya and 1.5 m near the coast (Fig. 3). Downstream from Ayutthaya macrorelief is very flat and altitude averages 2 m, with the exception of two elongated areas parallel to the coastline that have altitudes between 3.5 and 5 m. Takaya (1969) considers the raised areas to be old barrier islands. This is corroborated by the presence here and there of bodies of fine sandy clayey to loamy material in an otherwise clayey sediment near Bangkok (van der Kevie & Yenmanas, 1972). Soil survey data by the same authors do not reveal such textural differentiation for the northernmost barrier island about 20 km south of Ayutthaya.

The recent riverine sediments (Fig. 2) show a distinct pattern of levees and backswamps, but levees are conspicuously lacking in the area with marine and tidal marsh deposits. The flat area of acid sulfate soils is dotted by numerous

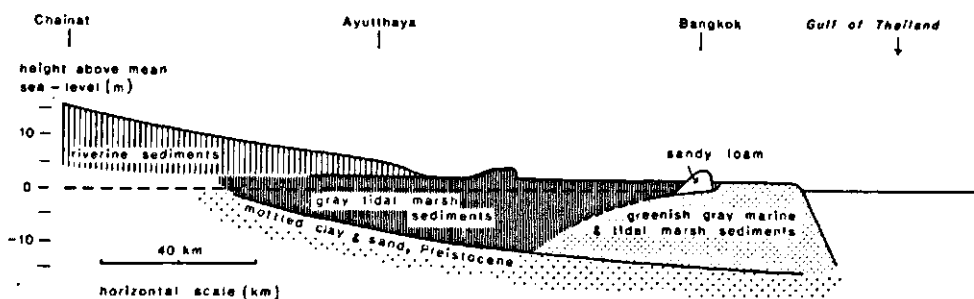


Figure 3

Schematic north-south profile through the Bangkok-Plain (after Takaya, 1969; van der Kevie, 1972; van der Kevie & Yenmanas, 1972). In the riverine area elevation shown is that of the levees.

almost circular depressions, 'elephants wallows', which may be 0.5 m deep and up to 50 m in diameter. They are probably not due to elephants or other wallowing animals, but their origin is unclear.

The substrata of the acid sulfate soils consist of non-calcareous, dark gray to gray clay with contents of 1-2.5% sulfur in the form of pyrite, and 2-8% organic carbon. To the north, these tidal sediments are overlain by recent river alluvium, whereas to the south the gray clay overlies greenish gray clay to silty clay (Fig. 3).

These greenish gray sediments generally contain up to 0.8% of pyrite sulfur, are commonly calcareous (1-8%  $\text{CaCO}_3$ , van der Kevie & Yenmanas, 1972) at least in the western part of the plain, and form the parent material of the non-acid marine soils. Higher pyrite contents, comparable to those found in the gray tidal marsh deposits are present near the mouths of the Bang Pakong River and the Khlong Dan tidal creek in the eastern part, where acid sulfate soils occur. Near Bangkok, the greenish gray sediments are about 15 m thick and cover a dissected Pleistocene surface consisting of stiff, mottled clay.

By estimation of  $^{14}\text{C}$  in material from peaty layers, van der Kevie (1972) estimated that the gray tidal marsh deposits were formed until about 3100 years before present. According to the same author sedimentation probably took place behind a relatively stable coastline marked by the sandy loam barrier island during a transgression. The influence of the sea in these swamps diminished 3500 years ago. The original mangrove vegetation (Section 2.5) gave way to a fresh-water vegetation as the influence of the tides lessened, and drainage, at least during the dry season, improved. A slight uplift of the Bangkok Plain, possibly related to the westward tilt of the Tenasserim Range along the border with Burma, may have further improved drainage. The effect of this uplift is very pronounced in the southwestern part of the Bangkok Plain where a 6700 year old pyritic sediment was observed 2 m below the soil surface but 6 m above mean sea-level (van der Kevie, 1972). After the transgression phase, most detritus was deposited on mud flats in front of the coast and the coastline extended southwards. At present, erosion and accretion of the coast alternate, but there is a net advance of the Chao Phraya Delta of 4-5 m per year (Nedeco, 1965).

## 2.2 CLIMATE

According to the classification of Köppen (1931), the climate of most of Thailand is tropical savanna (Aw), with a mean temperature above  $18^{\circ}\text{C}$  in the coldest month and a distinctly dry winter. In the Bangkok Plain, the mean annual rain-

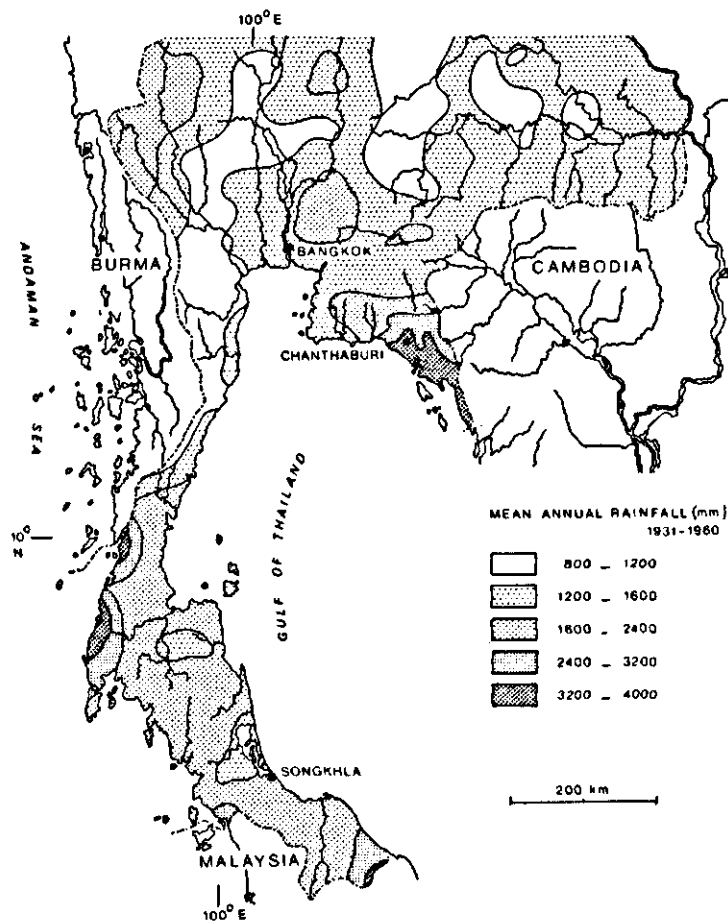


Figure 4  
Mean annual rainfall in part of Thailand (Vesa-Rajananda, 1964).

fall is between 1200 and 2000 mm (Fig. 4). During the southwest monsoon, from May to October, the monthly precipitation in that region varies between 150 and 400 mm. About 85% of the annual rainfall is in this wet season. After the onset of the northeast monsoon in October-November, the monthly precipitation drops below 50 mm. December and January are the driest months with less than 10 mm. The west coast of the peninsula (e.g. Ranong) and the Southeast Coast (e.g. Chanthaburi, Klaeng) have a rainfall distribution similar to that of the Bangkok Plain (e.g. Thanyaburi) but the intensity is much higher (Fig. 5). On the east coast of the peninsula (e.g. Cha-am, Sonkhla, Pattani) rainfall is about 100 mm per month from May to September and 200 to 500 mm monthly between September and January. The mean relative humidity is between 70 and 80% in the dry season and

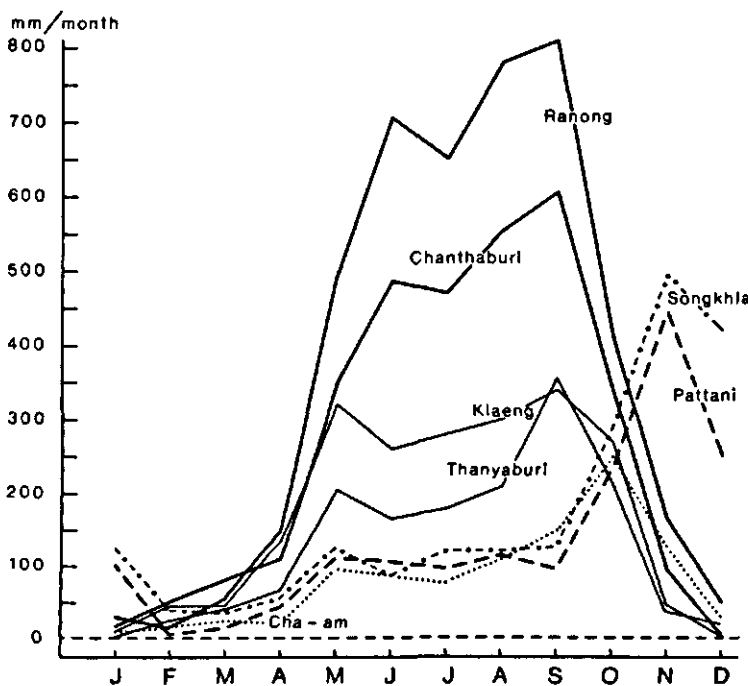


Figure 5

Monthly rainfall distribution for selected stations; means for 15-year periods between 1950 and 1970 (data, Thailand Meteorological Department).

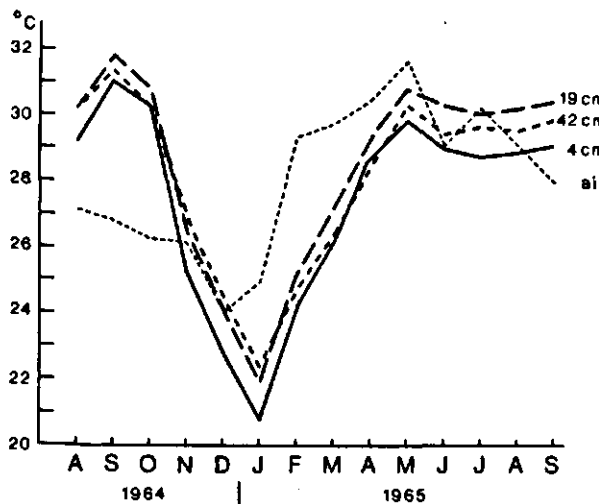


Figure 6

Ambient temperature and soil temperature at different depths at the Bangkok Meteorological station (site Bk-1): monthly averages (Rice, 1969).

between 80 and 90% in the wet season; mean maxima and minima are of the order of 45-50% in the dry season and 95 - 98% in the wet season. The average temperature is between 27 and 29 °C. Mean monthly temperatures fluctuate from about 25 °C in December and January to about 30 °C between March and June. Mean annual soil temperatures of several poorly drained soils at 42 cm depth in 1964 and 1965 were 1 to 6.5 °C below the mean air temperature (Rice, 1969). The amplitude of the annual temperature wave in a paddy soil at the Bangkok meteorological station (at site Bk-1) is surprisingly large (9-10 °C) to a depth of at least 42 cm (Fig. 6).

### 2.3 HYDROLOGY AND TIDAL REGIMES

The Chao Phraya River is by far the most important river entering the Bangkok Plain (see Insert). Its main tributaries rise at altitudes between 1200 and 1500 m in the mountains along the northern border of the country. In its upper delta, the Chao Phraya throws out a number of distributaries, all but one of which (the Suphan River) join the main branch again further downstream. The Suphan river was small originally (20 m wide in the dry season) but has recently been canalized and enlarged.

Near Ayutthaya, the Chao Phraya is joined by the Pasak River, which originates in the Petchaboon Range near the border with Laos. The mean slope between Chainat and Ayutthaya is about  $10 \times 10^{-6}$ , and drops to less than  $4 \times 10^{-6}$  in the Bangkok Plain. The deflexion in slope coincides with the transition from riverine to tidal marsh deposits (Fig. 3).

The two other rivers entering the Bangkok Plain are the Mae Klong in the west and the Bang Pakong in the east. The Mae Klong descends quite rapidly from the mountains near the Burmese border, the mean slope over the least 100 km is about  $11 \times 10^{-6}$ . It has cut quite deep into older alluvia, and has a rather narrow flood plain (Fig. 2). The Bang Pakong River is similar in size but has a smaller drop (about  $5 \times 10^{-6}$ ) and a heavily meandering course.

The mean annual flow (1905-1955) of the Chao Phraya, about 10 km north of the split forming the Suphan River, is  $31.3 \times 10^9 \text{ m}^3$  (Nedeco, 1965). The standard deviation of the annual flow is about 20 %, but deviations of + 80% and - 60% have been recorded. The other rivers entering the Bangkok Plain have considerably smaller discharges (Table 1). River discharge is low from January to May but increases rapidly a month or so after the onset of the rainy season (Fig. 7). Generally 80-90% of the annual run-off is between June and December. The high discharges between September and November cause extensive flooding. At that time,

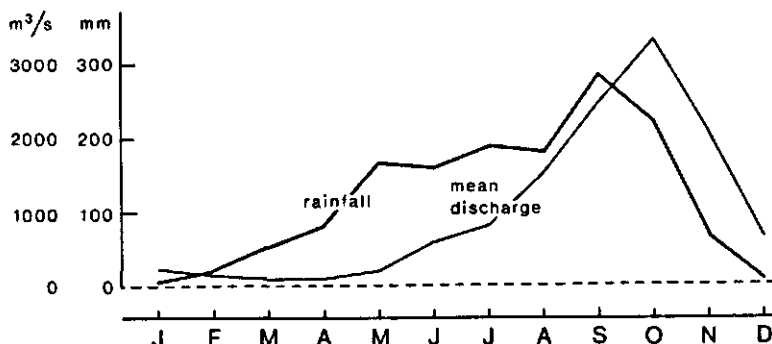


Figure 7

Monthly mean discharge ( $\text{m}^3 \cdot \text{s}^{-1}$ ) of the Chao Phraya River at Chainat (1905-1955) and mean monthly rainfall (mm) averaged for 11 stations in the Bangkok Plain.

Table 1. Hydrological data on rivers in the Central Plain (Kambhu, 1961; Nedeco, 1965).

River	Catchment area ( $\text{km}^2$ )	Annual run-off ( $10^9 \text{ m}^3$ )	Annual mean discharge $\text{m}^3 \cdot \text{s}^{-1}$
Chao Phraya	113 300 <sup>a</sup>	29.5	935
Suphan	18 200 <sup>b</sup>	1.9	60
Pasak	7 360 <sup>c</sup>	6.0	190
Prachin	162 <sup>c</sup>	4.3	136
Nakhon Nayok	25 600 <sup>c</sup>	0.1	4
Mae Klong		6.9	220

a. Above Chainat

b. Above the Rama VI barrage

c. Site not specified.

however, the land is normally already submerged by rain water.

The inundation reaches a maximum of between 0.2 and 3 m in the areas north of Bangkok, and between 0.1 and 0.3 m south of Bangkok. Greatest depths occur around Ayutthaya and along the Suphan River at the latitude of Bangsai. I have estimated the contribution of rainfall to flooding from various published data on precipitation and evapotranspiration and from soil moisture data collected during this study (Table 2). Under 'average' rainfall conditions, with a five-month rice crop and assuming that run-off and percolation are absent, precipitation seems sufficient to cause flooding to a maximum depth of about 0.3 m. In areas with non-acid soils, evapotranspiration during the dry season is greater because of more favourable conditions for root growth. As a result, the soil dries out to a greater depth, and more water is needed to flood it in the

Table 2. Precipitation, evapotranspiration and the contribution of rainwater to flooding of acid sulfate soils in the Bangkok Plain (all data in mm per month except flooding depth which is in mm).

	Rainfall <sup>a</sup>	Epan <sup>b</sup>	Evapotrans. <sup>c</sup> of rice	Actual evapotrans.	Excess precipit.	Flooding <sup>h</sup> depth
Januari	7	141	-			-
Februari	22	138	-			-
March	34	184	-			-
April	82	187	-			-
May	166	174	-			-
June	160	144	-			-
July	188	139	167	167	21	50
August	180	126	151	151	29	70
September	284	123	148	148	136	110
October	220	113	136	136	84	236
November	65	115	138	138	-73	320
December	8	126	-	126 <sup>g</sup>	-118	247
						129

- a. Mean for 11 stations, 1954-1968 (van der Kevie & Yenmanas, 1972).
- b. Class A pan evaporation at the Bangkok Meteorological Station (1961-1964).
- c. 1.2 x E pan (Kamerling, 1974).
- d. Made up of 129 mm surface water from the previous year (flooding depth in December), 145 mm rainfall, and 60 mm soil moisture (estimates at Rangsit).
- e. Assuming that the soil becomes saturated with water and flooded to 50 mm depth before rice is transplanted.
- f. Rainfall minus excess precipitation.
- g. Pan evaporation.
- h. At the end of each month.

rainy season, so rainfall may be insufficient to cause flooding. There is some uncertainty about evapotranspiration under rice. The mean daily evapotranspiration derived from Table 2 is 4.9 mm, but Kung et al. (1965) measured 5.9 mm for a 5-month rice crop grown in the second half of 1964 at Suphanburi. With the latter value, the maximum flooding depth would be about 0.15 m. The contribution of precipitation to flooding may vary from nought in the south-western part of the Bangkok Plain (1100-1200 mm rain) to almost 1 m in the north east (2000-2100 mm rain). Also because there is a considerable run-off (dikes and bunds to contain flood water on small parcels are impractical), flooding by river water must therefore be a major cause for the deep submersion as observed especially in the northern part of the acid sulfate area.

A water balance for the southern part of the Chao Phraya Basin in the second half of 1961 (Fig. 8) was compiled by Nedeco (1965). The difference between measured inflow (river water and precipitation) and outflow (drainage into the

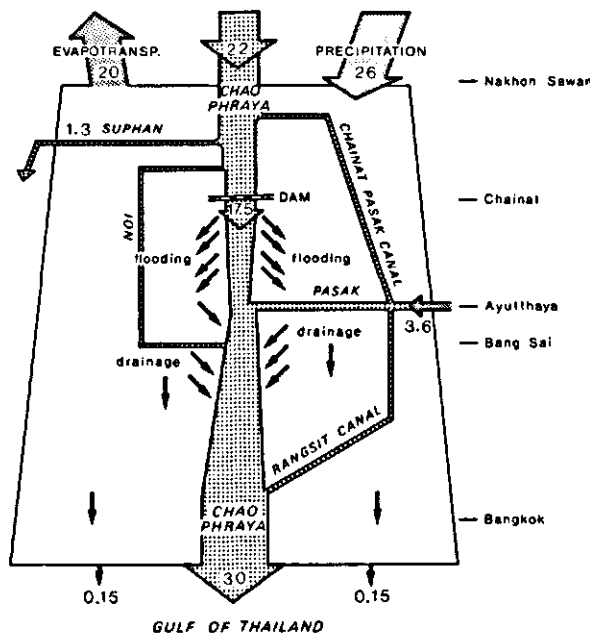


Figure 8

Scheme of the water balance of the southern part of the Chao Phraya catchment area ( $28\ 600\ km^2$ ) from 1 July to 31 December 1961. The units are  $10^9\ m^3$ . The width of the shaded bars is roughly proportional to the amount of water involved. From Nedeco, 1965.

Gulf of Thailand) was attributed to evapotranspiration. This figure corresponds with 700 mm, i.e. 166 mm lower than the figure arrived at in Table 2. The difference may be due in part to the inclusion of considerable upland areas (with lower evapotranspiration) in the Nedeco model. Fig. 8 illustrates that overflowing of the river banks takes place mainly between Chainat and Ayutthaya, in accordance with the distributive character of the river in that area. Between September and December 1961, the overflow amounted to  $10 \times 10^9\ m^3$ ; the corresponding figure for 1962 was  $7.5 \times 10^9\ m^3$ . Both years were wetter than average and the average amount of floodwater is probably lower, about  $5 \times 10^9\ m^3$  (Nedeco, 1965). This is equivalent to a layer of 0.7 m water over the Chao Phraya Floodplain between Chainat and Bangkok (about  $7000\ km^2$ ), which again illustrates the importance of river flooding to the inundation of the area. Drainage of floodwater into the river takes place mainly between Ayutthaya and Bangkok. This implies that most of the floodwater in the acid sulfate area has travelled a considerable distance overland.

A 130-year record of maximum water levels in the Chao Phraya at Ayutthaya

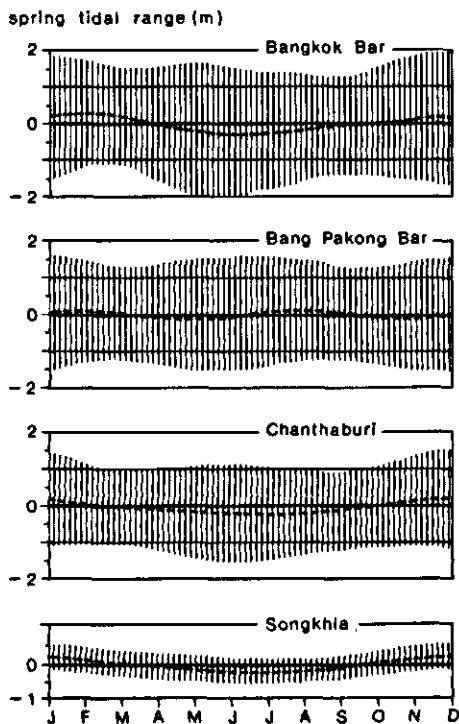


Figure 9

Seasonal variation in range of spring tides (shading) and mean sea-level (broken line) at four stations (Hydrography Department, Royal Thai Navy, 1972).

indicates that flooding is adequate for rice cultivation every second year. Crop failure due to extreme floods is rare (3%) and damage due to drought is common (Kambhu, 1961). To divert water for rice growing and transportation, numerous channels were dug during the second half of the 19th Century, when Thailand became an important rice-exporting country and most of the Bangkok Plain was brought into cultivation (Tomosugi, 1966).

The efficiency of the channels for irrigation was probably low, at least before completion of the diversion dams in the Pasak River (1924) and the Chao Phraya at Chainat (1951). According to Homan van der Heide (1904), the flat areas between Bangkok and Ayutthaya were normally inundated for maximally three months each year. If flooding is indeed more extensive and deeper at present, this may well be due to the combined effect of improved water diversion and the use of low-lying paddy land as temporary reservoir to prevent flooding of urban areas (personal communication, H. Fukui).

In the Bangkok Plain inundation of tidal areas by sea-water is most widespread in the dry season. This follows from high mean sea-level and large spring tidal ranges between November and February (Fig. 9). The combination of extensive tidal flooding and low rainfall contributes to salinization of the coastal marshes and has been used to advantage by man for saltmaking (Section 2.6).

## 2.4 RIVER WATER COMPOSITION AND SEDIMENT LOAD

Analysis of water from rivers entering the Bangkok Plain are given in Table 3. Chloride and sulfate are lower than the world average for river water. The Pasak and the Mae Klong have relatively high concentrations of calcium, magnesium and bicarbonate, reflecting the influence of limestone outcrops in their watersheds. The low discharges and high mean levels between January and June permit salt intrusion with salinities as high as 0.4 ‰ between 30 and 70 km upstream from the mouth of the Chao Phraya.

According to the Port Authority of Thailand (1967), the average annual transport of suspended sediment in the period 1962-1966 was  $12.2 \times 10^9$  kg at Nakhon Sawan and  $3.3 \times 10^9$  kg at Bangsai, indicating that about  $9 \times 10^9$  kg are supplied annually to the delta. If sedimentation were confined to the recent riverine plain between Nakhon Sawan and Ayutthaya ( $2100 \text{ km}^2$ ) the average level of the soil surface would increase by 30 cm per century. Probably little of this sediment is deposited in the very flat acid sulfate area, where the floodwater normally moves very slowly. According to van der Kevie (1972), however, the typical black surface horizon of acid sulfate soils consists mainly of riverine sediment. This is very unlikely because there were no mineralogical or textural indications for a different origin of the upper horizons of these soils apart from scattered large (100 - 200  $\mu\text{m}$ ) skeleton grains in thin sections. Possibly, the sand grains were deposited by wind or during flash floods and

Table 3. Substance concentration ( $\text{mmol.litre}^{-1}$ )<sup>a</sup> of solutes and pH of water from important rivers entering the Bangkok Plain.

River, sampling site	$\text{Cl}^-$	$\text{HCO}_3^-$	$\text{SO}_4^{2-}$	$\text{SiO}_2$	$\text{K}^+$	$\text{Na}^+$	$\text{Ca}^{2+}$	$\text{Mg}^{2+}$	pH
Chao Phraya, Uthai Thani <sup>b</sup>	0.17	1.17	0.001	0.303	0.11	0.38	0.33	0.11	6.6
Chao Phraya, Ayutthaya	0.21	1.64	0.012	0.305	0.08	0.37	0.56	0.16	6.7
Pasak, Saraburi	0.11	2.70	0.003	0.316	0.07	0.29	1.17	0.20	6.9
Prapong, near confluence <sup>c,d</sup>	0.14	1.27	0.025	0.258	0.06	0.28	0.37	0.19	7.4
Hanuman, near confluence <sup>c,d</sup>	0.07	0.64	0.017	0.122	0.05	0.15	0.18	0.09	7.2
Nakhon Nayok, Nakhon Nayok <sup>c,d</sup>	0.11	0.42	0.031	0.223	0.04	0.23	0.10	0.05	7.0
Mae Klong, Ban Pong <sup>e</sup>	0.06	2.66	0.002	0.234	0.05	0.13	0.94	0.35	7.0
world average	0.22	0.96	0.12	0.128	0.06	0.27	0.37	0.17	-

a. After Kobayashi (1958) cited by Kawaguchi & Kyuma (1969), except for d.

b. Between Nakhon Sawan and Chainat.

c. Feeder rivers of the Bang Pakong River.

d. Sampled by W. van der Kevie on 1970-1-29, and analysed by N. van Breemen.

e. After Livingstone (1963) cited by Garrels & Mackenzie (1971).

became incorporated in the soil by biological and physical homogenization. Riverine material certainly covers the tidal marsh sediments along the northern fringe of the acid sulfate area (cf. van der Kevie, 1972). Similarly up to 50 cm riverine overwash is common along the Chao Phraya as far south as Bangkok (van der Kevie & Yenmanas, 1972).

Very little is known about the mineralogical composition of the suspended material. The source of the detritus includes sedimentary and igneous rocks. Tiny limestone fragments occur in the suspended sediment of the Pasak and the Mae Klong (Kawaguchi & Kyuma, 1969).

## 2.5 VEGETATION

Outside the mangrove areas, the original vegetation in the Bangkok Plain consisted mainly of tall grasses, rushes or sedges. Trees (mainly *Dipterocarpus* species) were confined mainly to the slightly higher areas bordering the rivers (Pendleton, 1947, Murata & Matsumoto, 1974). In mangrove areas, the dominant trees are *Rhizophora apiculata*, *Avicennia officinalis*, *Bruguiera gymnorhiza*, *Xylocarpus granatum*, *Nipa fruticans*, *Ceriops decandra* and *Excoecaria agallocha*. Widespread mangrove forestry has probably obliterated the original structure and distribution of the mangrove forests. Palynological observations on samples from substrata from different places in the Bangkok Plain indicate that the vegetation in the former tidal marshes was dominated by Rhizophoraceae (Table 4).

## 2.6 LAND USE

About a fifth of the country is permanently cultivated, and about 60% of all cultivated land is under lowland rice (Kawaguchi & Kyuma, 1969). The Bangkok Plain accounts for nearly half the total rice production of the country. Between 1968 and 1970, the planted area was  $73.5 \times 10^3 \text{ km}^2$  with an average yield of 1.78 ton/ha (Fukui, 1973).

Broadcast rice is grown over about 40% of the riceland in the Central Plain, notably in the deeply flooded river basins and in the greater part of the acid sulfate area (sometimes in fields flooded to depths of 1.5-2 m, 'floating rice'), whereas transplanted rice is confined to the older river terraces, the higher parts of the riverine plain, and the non-acid soils south of Bangkok (Fig. 10). Irrigation water is rarely available during the dry season and normally only one crop is grown per year. After the first rains have sufficiently wetted the soil (May-July), the land is plowed twice. If mecha-

Table 4. Frequencies (%) of various pollen and spores in substrata in the Bangkok Plain (analysed by A.J. Hovinga in cooperation with J. Muller). Except for those from BP-1, the samples were collected by L.J. Pons (Pons & van der Kievel, 1969).

Site <sup>a</sup>	Depth (cm)	Tree pollen		Non-tree pollen		Varia
		Spores of ferns	Spores of ferns	Spores of ferns	Spores of ferns	
BP-1	18-30	1	2	48	-	
	30-40	4	2	48	-	
ATII	150-190	-	1	74	-	
	240-280	-	2	74	1	
	390-440	2	-	74	-	
CCII	170-200	5	1	52	1	
	260-300	5	-	65	1	
	340-400	3	-	69	-	
SPII	190-240	1	6	62	-	
	320-370	1	10	51	-	
	380-410	1	-	15	1	
	410-450	-	-	3	-	
PTI	150-210	-	1	66	-	
	210-310	1	-	92	-	
Sporangia of <i>Stereocaulon palustre</i>						
Acrostichum aureum <sup>b</sup>						
Trees from temperate zones						
Meliaceae						
Calophyllum						
Lithocarpus						
Dipterocarpaceae						
Nypa fruticans <sup>b</sup>						
Rhizopora type <sup>b</sup>						
Sonneatia cassolarii <sup>b</sup>						
Avicennia type <sup>b</sup>						
Mangrove species						
Chenopodiaceae						
Gramineae						
Typhaceae						
Cyperaceae						
Araliaceae						
Other ferns						

a. See Insert

b. Mangrove species

c. Includes 12% *Alnus* and 5% *Corylus*.

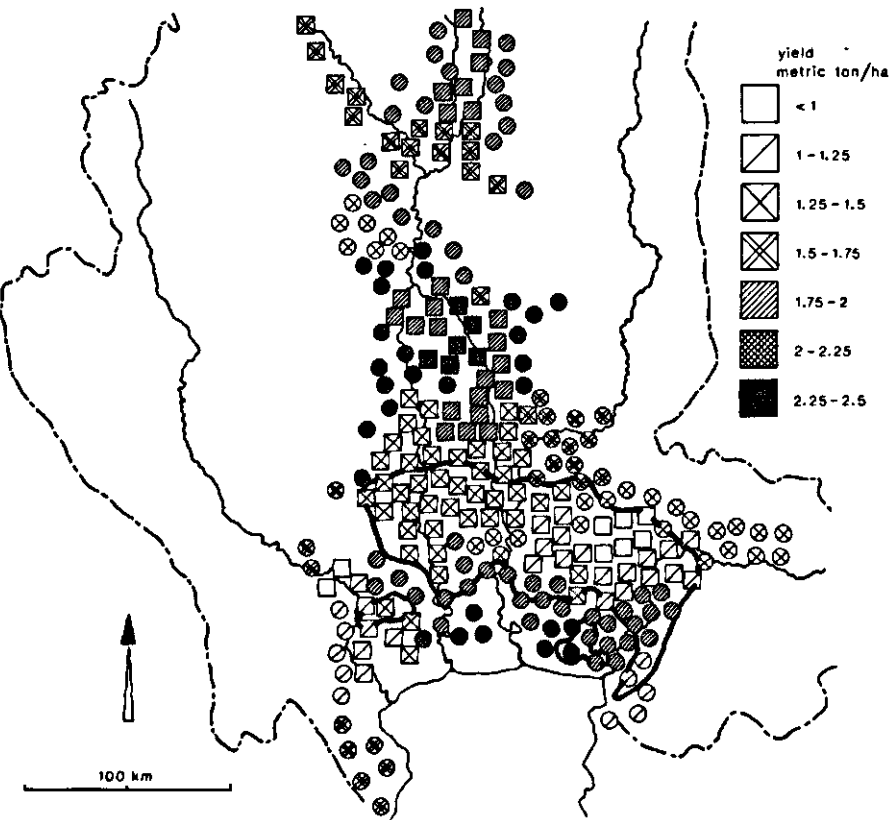


Figure 10

Distribution of broadcast rice (squares) and transplanted rice (circles), and average rice yields in the Central Plain (Fukui, 1973). Each symbol stands for 100 km<sup>2</sup> of riceland; the heavy outlines indicate the acid sulfate areas.

nical traction is available, the first plowing is earlier. Except for the seedling nursery, which is tilled more intensively, these are normally the only tillage operations both for transplanted and for broadcast rice.

Harvesting is normally still traditional with a small knife or reaping-hook. The field is generally left fallow during the dry season and the straw is burned at the end of the fallow period. Probably with increased use of fertilizers and machinery average yield was 1.2 times higher in 1969 than in 1960. High-yielding varieties played no role here. These were first introduced in 1969 and have as yet found little application, mainly because of unfavourable environmental conditions especially the poor control of depth and duration of flooding (Fukui, 1973).

Reclamation of most the Bangkok Plain for rice started only in the second

half of the 19th Century. The extension of paddy land was mainly triggered by the growing demand from newly colonized neighbouring countries (Tomosugi, 1966), and tens of thousands of peasants came to settle in the largest acid sulfate area of the country. The yield map by Fukui (1973), partly reproduced here as Fig. 10, indicates that acid sulfate soils, and especially those east of the Chao Phraya are distinctly less productive than the non-acid marine soils and the riverine soils. According to van der Kevie (1972) paddy yields of 0.5-1.0 ton/ha are typical for the acid soils in the eastern part of the plain, whereas some of the more productive acid sulfate soils of the western part produce 1.2-1.9 ton/ha.

If sufficiently desalinized, the non-acid marine soils are highly suitable for paddy and upland crops. Especially west of Bangkok, horticultural crops are grown on raised beds under intensive management. About 400 km<sup>2</sup> of these ridged soils have been mapped by van der Kevie & Yenmanas (1972).

The area of present tidal marshes in the Bangkok Plain is about 1300 km<sup>2</sup>. East of the Chao Phraya River, the active tidal zone is bound by a low dike (Sukhumvit road) equipped with floodgates, and its present width is only 0.5-2km. In the west the tidal zone extends 10-15 km inland. Table 5, taken from de Groot & Poels (1973), shows land use in the tidal areas. All types of land except the Sueda swamps are in use for collection of leaves and fruits of Nipa palms, *Rhizophora* forestry (charcoal), shrimp breeding, salt evaporation and coconut growing. Especially near the mouth of the Mae Klong River, large areas of slightly brackish tidal land have been ridged for coconut. The palms are grown mainly for sugar; fruit production is of minor importance. The returns

Table 5. Land use and vegetation in the tidal areas in the Bangkok Plain (from aerial photographs taken in 1967) and net returns (in 1971/1972, 1 Baht = \$(US) 0.05). Data from de Groot & Poels (1973).

Land use/vegetation	Area (km <sup>2</sup> )	Net annual income (Baht/ha)
Nipa swamps	294	60
Mangrove swamps (mainly <i>Rhizophora</i> )	254	400
Treeless swamps (mainly Sueda and bare land)	93	-
Salt evaporation pans	91	2500
Shrimp (and fish) ponds	199	2500
Paddy fields	12	150
Coconut plantations	353	3000
Paddy on good non-acid marine soils (Bangkok series)	-	1100

from salt farming, coconut growing and shrimp breeding considerably exceed those obtained from lowland rice on even the best soils (Table 5). Potentially acid mangrove areas north of Sukhumvit road were reasonably productive for rice during the first years after reclamation but most fields have now been abandoned. Near Khlong Dan, some paddy fields were turned into fishponds. In high rainfall areas, as near Chanthaburi, reasonably high rice yields (1-2 ton/ha) are obtained in active tidal areas on some of the better acid sulfate soils after desalinization of the surface by impounding rainwater.

### 3 Distribution and characteristics of coastal plain soils

#### 3.1 SOIL MAPPING AND CLASSIFICATION

Soil survey and research in Thailand was begun by R.L. Pendleton in 1935. His 'Provisional map of the soils and surface rocks in the Kingdom of Siam' (1959) shows units at the Great Soil Group level. Systematic soil surveying started in 1962 (Moermann, 1962) and between 1962 and 1973, 94 Soil Survey Reports were published. Of particular importance for my study were the 1:1 250 000 general soil map of the country (Moermann & Rojanasoonthon, 1968), the 1:50 000 soil map of the Chanthaburi area (Dent & Montcharoen, 1966), the soil surveys of the Southern Central Plain (1:100 000 by van der Kevie & Yenmanas, (1972) and of Peninsular Thailand (1:750 000) by Dent (1972), and the semi-detailed soil map (1:8000) of the Hup Kapong Project near Cha-am (Thailand Soil Survey Division, Bangkok 1966, unpublished).

Homan van der Heide (1904) commented on the poor quality of water from wells in the Bangkok Plain "due to the presence of alum and magnesium in the soil", but the first description of acid sulfate soils in Thailand was by Pendleton (1947). The four types described by Pendleton (the acid Rangsit and Ongkharak clays, the non-acid Bangkok clay and the slightly acid Bangkhen clay) still persist as soil series in the most recent survey by van der Kevie & Yenmanas (1972) who describe 16 non-acid marine soil series (including one potentially acid soil) and 20 acid sulfate soil series (Table 6). All soils are strongly hydromorphic. The diagnostic criteria between acid sulfate soils are the presence of yellow mottles, red mottles, gypsum, salinity, thickness of horizons, depth of the reduced substratum, pH and texture. The use of pH poses several problems. Firstly during soil survey work, the pH was estimated with the Truog-Hellige test kit which may give a pH 0.5-1.0 unit higher than by potentiometry and is useless at pH values below 4. Furthermore pH has been measured in the laboratory for recent soil survey reports (from 1972 onwards) and values have often been affected by air-drying, being too high in non-acid samples (due to loss of  $\text{CO}_2$ ) and too low in potentially acid samples (due to oxidation of pyrite). Consequently, the pH values given in Table 6 are not

Table 6. Characteristics of soil series typical for the coastal plain areas of Thailand (mainly after van der Kervie & Yemmanas, 1972).

- absent or not specified; + present; > 1.0 present below 1 m depth;  
( ) may be present.

Cartographic unit	Soil series (or complex)	Texture <sup>a</sup>	Thickness horizon A1 (m)	depth (m)	Transition to unmodified substratum	Occurrence of jarosite	Gypsum	Red mottles	Salinity	pH <sup>b</sup> 0-0.3 m
1	Tha Chin	c-sc	0.05-0.4	< 0.5	-	-	-	-	+	6-8
2	Bang Pakong	c-sc	0.05-0.4	< 0.5	(+)	-	-	-	+	5-8
3	(Tha Chin/Bang Pakong complex)									
5	Samut Songkram	c	0.05-0.2	0.5-1.25	-	-	-	-	+	5-8
6	Samut Prakan	c-sc	0.15-0.3	0.9-1.2	-	-	-	-	(+)	5-8
7	Bangkok	c-sc	0.15-0.4	1.2-1.5	-	-	-	-	-	4.5-8
9	Bang Len	c-sc	0.3-0.6	1.2-1.6	-	+	-	-	-	6-6.5
13	Bang Phae	sc-fsl	0.25-0.4	> 1.5	-	+	-	-	-	6.5-8
14	Thonburi	-	0.4-0.7	> 1.5	-	-	-	-	-	5-7
16	Hua Hin	s	< 0.1	-	-	-	-	-	-	4.5-7
17	Chao-am	c	0.1-0.3	0.6-1.5	+	-	-	-	+	3-4.4
18	Bang Nam Priso	c	0.2-0.5	> 1.5	(+)	-	-	-	-	4-6
19	Chachoengsao	c-sc	0.2-0.4	> 1.3	(> 1.0)	-	+	-	-	4.5-6
21	Bang Khen	c-sc	0.2-0.4	> 1.4	(> 1.0)	+	+	-	-	5.5-7
23	Naha Pot	c	0.2-0.4	-	> 1.0	-	+	-	-	4.5-5.5
25	Ayutthaya	c-sc on c	0.3-0.7	> 1.2	> 1.0	+	+	-	-	4.5-7
26	Rangsit	c	0.2-0.5	> 1.5	> 0.4	-	+	-	-	4-5
29	Rangsit, very acid phase	c	0.2-0.5	> 1.5	> 0.4	(+)	+	-	-	3.5-4.5
30	Rangsit, high phase ac	-	0.2-0.5	> 1.5	+	(+)	+	-	(+)	4-5
31	Thanyaburi	c	0.25-0.4	> 1.5	> 0.4	-	-	-	-	4-5
32	Sena	c	0.25-0.4	> 1.5	0.4-1.0	+	+	-	-	4.5-5
34	Ongkharak	c	0.15-0.25	> 1.5	< 0.4	(+)	(+)	-	-	4-4.5
36	The Khwang	c-sc-scl	0.1-0.3	-	(+)	(+)	+	-	(+)	4.5-5
37	(Undifferentiated acid sulfate soils)									
90	(Fish or shrimp ponds and salt pans)									

a. c = clay; sc = silty clay; fsl = fine sandy loam; scl = silty clay loam

b. Although specified as pH water (1:1), these values are probably based in part on field (Hellige-Truog) measurements

c. pH drops to below 4 upon slow aeration

d. The colour of horizon A1 is diagnostic; all other acid sulfate soils have a dark gray to black A1

e. Approximate equivalent according to Soil Survey Staff, 1971.

pH <sup>b</sup> > 0.3 m	Remarks	Classification <sup>c</sup>	Represented in this study by:	Area in the Southern Central Plain (km <sup>2</sup> )
7.5-8	not potentially acid	Hydraqquent	Mc-27, 28	261
7-8	potentially acid <sup>c</sup>	Typic Sulfaquent	BP-1, KD-2, Ca-2, 3	21
		-		370
≥ 8	ridged for coconuts	Typic Tropaquept	-	271
5-8		Typic Tropaquept	Mc-2	397
6.5-8		Typic Tropaquept	T-1, Mc-18	1820
6-8		Typic Haplauoll	-	342
6.5-8.5		Typic Haplauoll	-	97
6.5-8	ridged for horticultural crops	Typic Tropaquept	-	367
4.5-7	beach ridge	Typic Ultipsamment	-	5
3-4.5		Typic Sulfaquent	KD-1, Ca-1, Ch-1, 28, 2C, Ch-3, 6, 7	56
4-6	pH in B horizon < 5.5 if yellow mottles are absent	Typic Tropaquept/ Sulfic Tropaquept	Mn-1, Mc-10	360
> 5		Typic Tropaquept	Bk-1	1400
5.5-6.5		Typic Tropaquept	Mc-23	934
4-6.5		Sulfic Tropaquept	Mc-8	548
6-5		Sulfic Tropaquept	Na-2, Mc-11, 12, 16	765
< 4.5		Sulfic Tropaquept	O-1, Ra-1, Mc-4, 5, 7	1800
3.5-4.5	covered with rushes and sedges	Sulfic Tropaquept/ Typic Sulfaquent	-	511
< 4.5		Sulfic Tropaquept	-	1.8
< 4.5	sandy layers present	Sulfic Tropaquept	Ra-2, 3, Mc-3, 9	264
4-4.5		Sulfic Tropaquept	Mc-17	1480
> 4		Sulfic Tropaquept	Kr-1, Sa-1	122
< 5	dark grayish-brown to brown Al <sup>d</sup>	Sulfic Tropaquept	Ch-2A	3.5
				130
				423

always representative for field conditions.<sup>a</sup>

Some soils have characteristics intermediate between those of typical acid sulfate soils (jarosite mottles and a low pH, e.g. below 4) and those of non-acid marine soils (no jarosite mottles and a relatively high pH, e.g. above 5). The soils in question (Cartographic Units 18, 19 and 21 of Table 6) are rather acid but generally lack conspicuous jarosite mottles and can be considered as para- (or 'pseudo-') acid sulfate soils (Pons, 1973). Like most non-acid marine soils, they are Typic Tropaquepts according to Soil Survey Staff (1971), whereas the acid sulfate soils are either Typic Sulfaquepts or Sulfic Tropaquepts.

A short description will be given below of the general soil conditions of each of the areas studied.

### 3.2 THE BANGKOK PLAIN

*General soil conditions* The distribution and relative importance of the various soil units in the Bangkok Plains are illustrated by Table 6 and by the generalized soil map (Insert).

The active tidal marsh area is covered largely by not potentially acid soils in the west, and partly by potentially acid soils in the east. These soils are generally poorly ripened, strongly saline and highly permeable from numerous crab holes. The reduced substratum is normally greenish gray (5GY4/1) and especially in the west, somewhat calcareous. The potentially acid soils sometimes have a dark gray (10YR4/1) substratum, but the only way to establish the potential acidity with reasonable certainty is to check pH after aeration for several weeks.

North of the active tidal land is a 10-30 km wide zone of non-acid soils. The most common soils (Bangkok series) here have a dark gray, slightly acid Ap horizon, over a yellowish brown and black mottled B horizon to 130-180 cm below the surface. East of the Chao Phraya River, small patches of acid sulfate soils and para-acid sulfate soils occur in this zone.

Still further north a zone with para-acid sulfate soils forms the transition to the northern half of the Bangkok Plain which is dominated by acid sulfate soils. The para-acid sulfate soils were developed in gray pyrite-rich

---

a. The 'soil pH' I used was potentiometric in fresh soil (Appendix A). In surface soils with seasonally fluctuating pH, values given in this chapter are for aerobic conditions.

sediments over greenish-gray sediments with lower potential acidity. Both para-acid sulfate soils and acid sulfate soils are gypsiferous in the western and central part, and lack gypsum in the east.

A typical acid sulfate soil consists of 20-60 cm dark gray to black (10YR3/2-2/1) A1 horizon over a grayish brown (2.5Y5/2) B horizon mottled mainly with red (7.5R5/6) or yellowish brown (10YR5/6) iron oxide in the upper part and with prominent yellow (2.5Y8/5) jarosite in the middle. At greater depth, both yellow and brown mottles are generally confined to channels and ped faces. The B horizon extends to 1-2 m depth and covers a dark gray (SY4/1) pyritic substratum. At the transition between the B and C horizons jarosite is usually lacking, but dark brown (7.5YR4/3) iron oxide occurs here and there around root channels or cracks that penetrate into the C horizon.

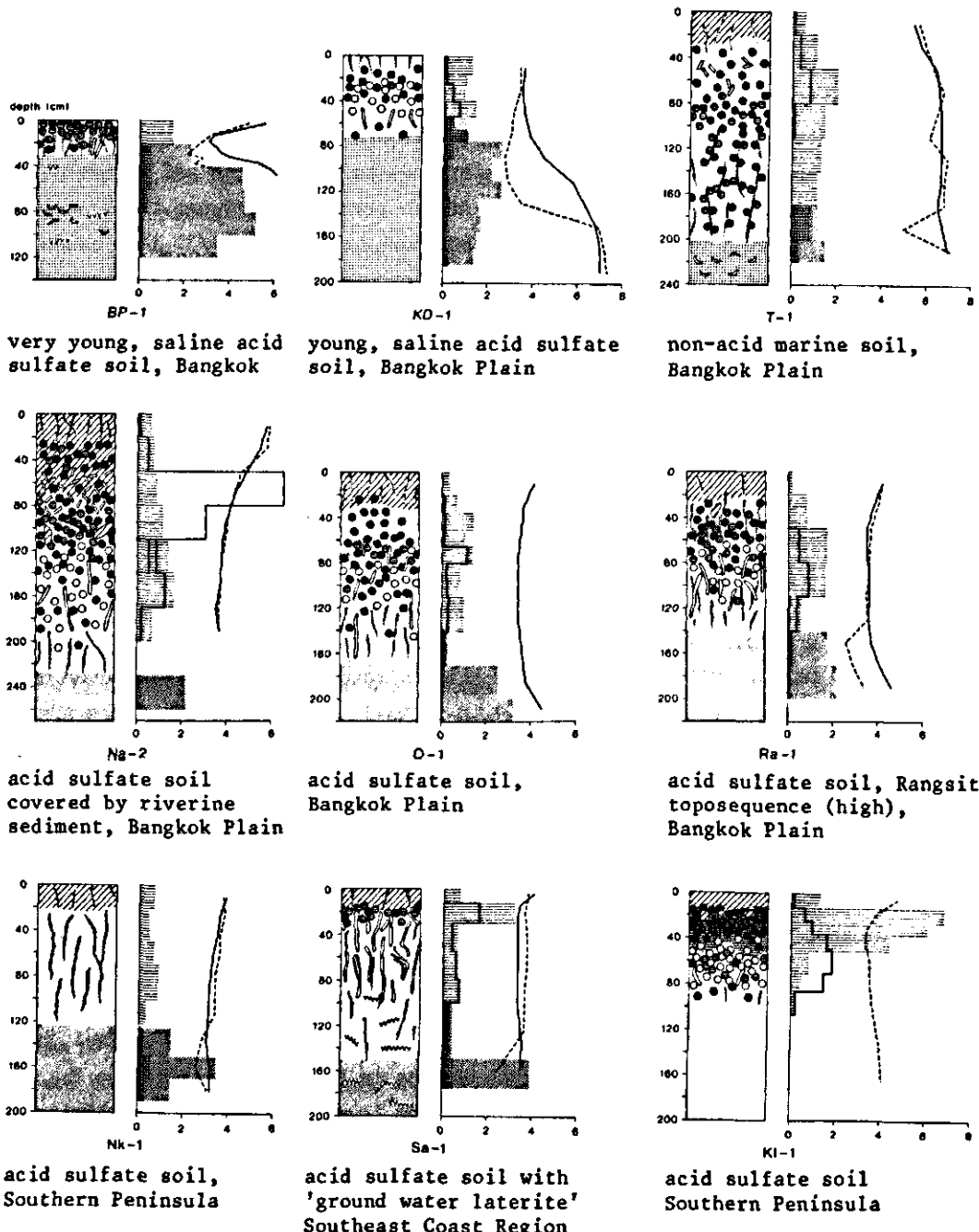
Soils on recent riverine deposits occupy only a small part of the Southern Central Plain. Except for young levee soils, which have an A-C profile, their B horizon is strongly mottled and well structured. The alluvium of the Mae Klong is calcareous; that of the other rivers contains little or no lime. Soils of the lower terraces in semi-recent and older alluvium, bordering on the formal tidal marsh areas, differ from the younger soils in having a textural B horizon.

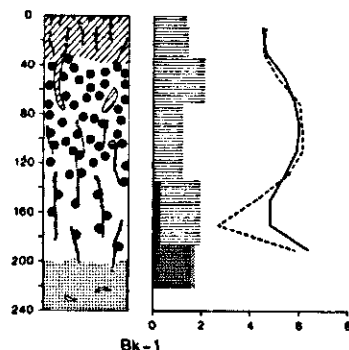
*Selected soils* Eleven soils from the Bangkok Plain were described and sampled in detail: two young, saline acid sulfate soils (BP-1 and KD-1); one non-acid marine soil (T-1); one para-acid sulfate soil (Bk-1); and seven older acid sulfate soils (KR-1, Mn-1, Na-2, 0-1, Ra-1, Ra-2 and Ra-3). Sites are shown on the generalized soil map (Insert). The profile diagrams of Fig. 11 can be used to obtain a quick impression of soil morphology, pH and distribution of iron and sulfur compounds. For further details of morphology, and chemical and mineralogical composition, see Appendix B.

Three representative soils in a toposequence, Ra-1, 2 and 3 were examined more closely. They were situated at Rangsit Acid Sulfate Soil Experimental Station near Thanyaburi. Maximum differences in altitude observed at the station (surface area  $0.17 \text{ km}^2$ ) are 40 to 50 cm. The toposequence covers 40 cm difference in altitude over a distance of 170 m. The highest soil, Ra-1, has a relatively thin Ap horizon and red mottles in the upper part of the B horizon. Ra-2, 100 m north of Ra-1 and 10 cm lower, has a thicker A horizon (45 cm), lacks red mottles and contains jarosite at shallower depth. Ra-3 lies in the center of an 'elephant wallow' 70 m north of Ra-2. It has a thick A horizon (80 cm) and contains few mottles, which are predominantly along

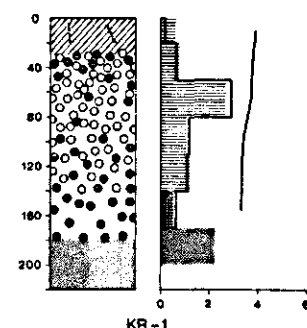
Figure 11

Diagrams showing profile morphology, distribution of iron and sulfur compounds, and pH of the described pedons.  $\text{Fe}_2\text{O}_3(\text{d})$  = dithionite extractable ferric oxide. The horizontal scale refers to pH, values on it have to be halved for mass fractions of S and doubled for  $\text{Fe}_2\text{O}_3(\text{d})$ , except in K1-1 where for  $\text{Fe}_2\text{O}_3(\text{d})$  the scale has to be multiplied by 6.

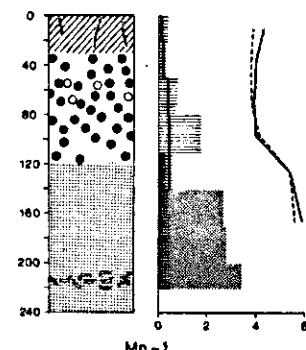




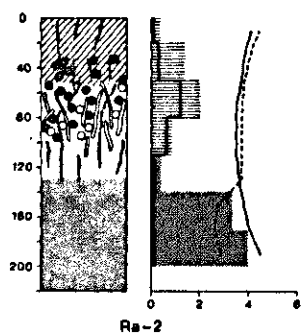
para-acid sulfate soil,  
Bangkok Plain



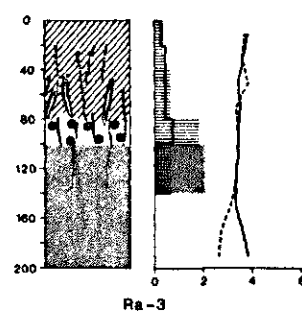
acid sulfate soil,  
Bangkok Plain



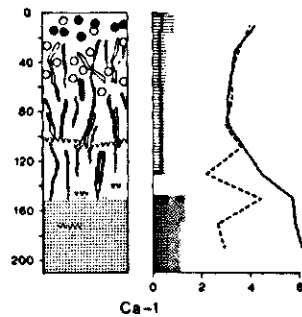
intermediate between acid  
and para-acid sulfate soil  
Bangkok Plain



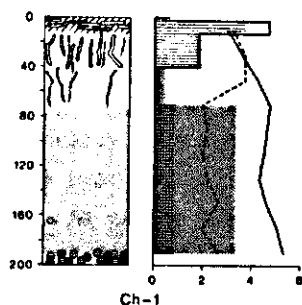
acid sulfate soil,  
Rangsit toposequence  
(middle), Bangkok Plain



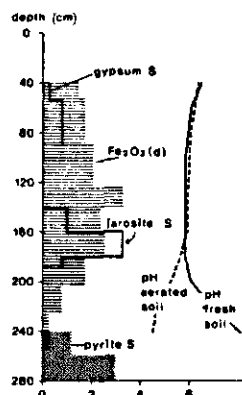
acid sulfate soil,  
Rangsit toposequence  
(low), Bangkok Plain



very saline acid sulfate  
soil, Cha-am Lagoon



saline acid sulfate soil  
Southeast Coast Region



- dark-gray to black A horizon
- dark-gray substratum
- dark greenish-gray substratum
- vvv vvv peaty layers
- brown mottles
- red mottles
- pale-yellow mottles
- black mottles
- ▨ gypsum
- ▨ sheets

vertical cracks and not, as in Ra-1 and Ra-2, mainly along large (diameter 5-10 mm) root channels. The dark-gray unmottled substratum starts at 1.4 m in Ra-1, 1.3 m at Ra-2 and at 1.0 m at Ra-3. A detailed soil survey (Fig.12) disclosed that characteristics such as thickness of the A horizon, presence of red mottles, modes of occurrence of jarosite and ferric oxide mottles, and depth of the jarosite and the pyrite show a highly significant correlation with altitude (Vlek, 1971).

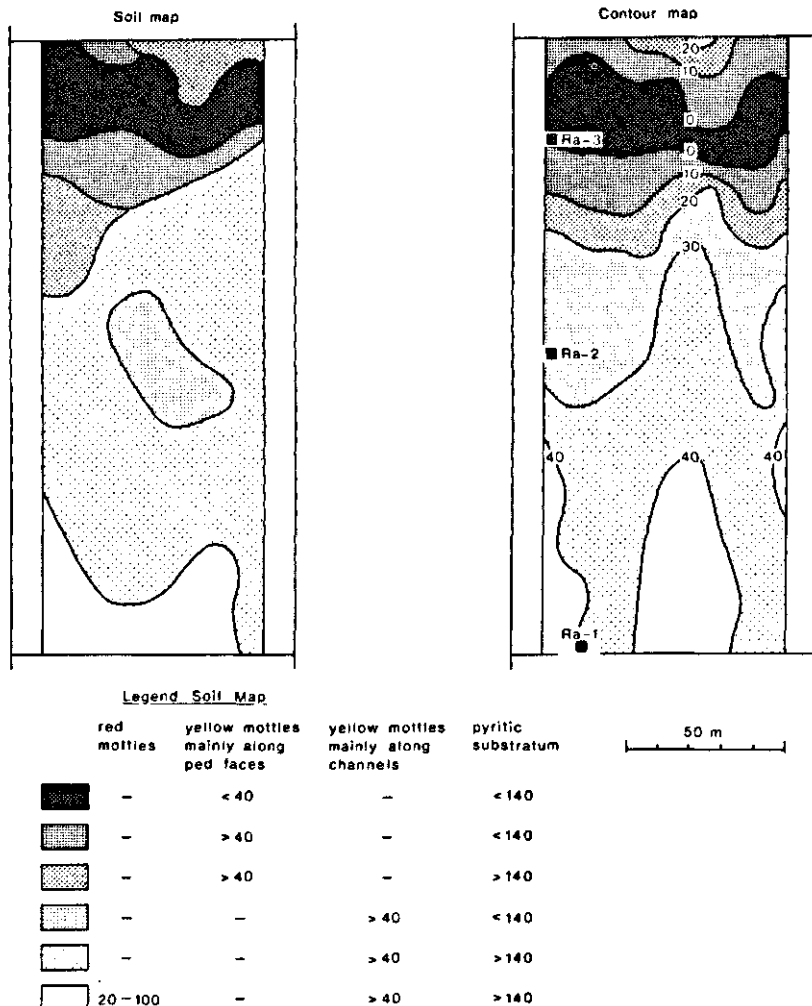


Figure 12

Detailed soil map and contour map of part of the Rangsit Acid Sulfate Soil Experimental Station (Vlek, 1971). The figures in the legend are depths in cm; those in the contour map are altitudes in cm above the zero contour.

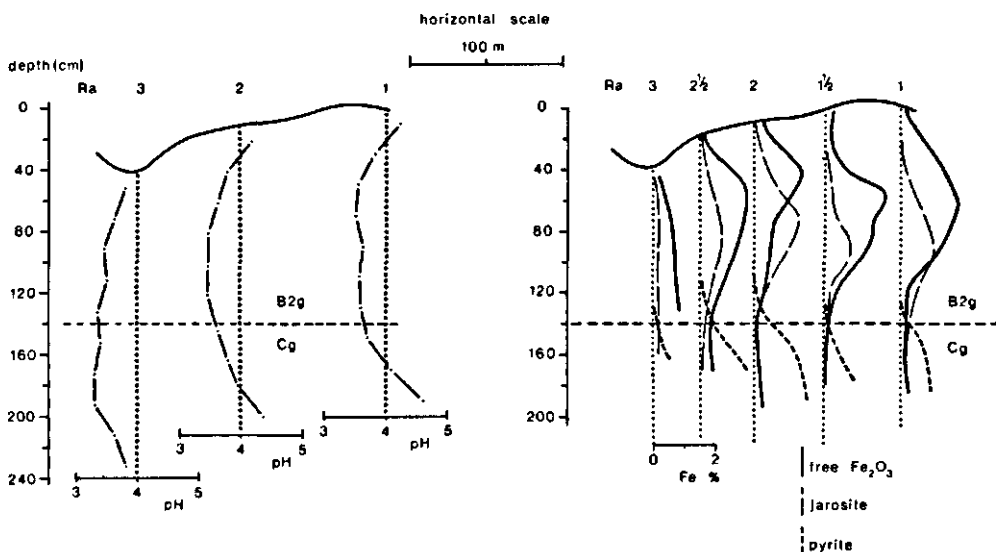


Figure 13

pH and iron fractions in the Rangsit toposequence.

Left: pH profiles (means of three measurements in the first three months of flooding in 1969).

Right: free  $\text{Fe}_2\text{O}_3$  (dithionite extractable iron minus jarosite iron), jarosite and pyrite (mass fraction Fe to oven-dried soil).

The boundary between the dark-gray, pyritic C horizon and the grayish brown, mottled B horizon is at about the same absolute level in all soils (cf. Fig. 13). In fact, pyrite-free zones sometimes penetrate as deep as 50 cm into the substratum along open channels (mainly at Ra-1 and Ra-2) and along joints of large prisms (Ra-3). In thin sections from Ra-3, pyrite was found in reduced interiors of otherwise oxidized prisms between 0,9 and 1 m depth.

Except for the lower part of the A1 horizon at Ra-3, which contains 40 to 53% clay, the clay content is very uniform (58-63%) both laterally and with depth. In Ra-1 and Ra-2 the pH of the fresh soil (in the dry season) is between 4 and 4.5 near the surface, close to 3.5 in the B horizon and gradually increases to above 4 in the unmottled substratum. Ra-3 is more acid both near the surface (pH 3.8) and at depth (pH 3.2 to 3.4).

As can be seen from Fig. 13 (left), acidification has apparently proceeded far into the pyritic substratum, notably in Ra-3 where pH values as low as 3.2 were recorded at 1.5 m depth. At the transition from the B to the C horizon, the pH at any one depth may vary, according to whether one measures in an oxidized zone associated with a channel or crack, or in unoxidized or

partially oxidized pyritic material. Variability in pH was observed, for instance, in young acid sulfate soils from polders in the Netherlands (Int. Symp. on Acid Sulfate Soils, 1972). This effect was not investigated specifically in the soils from Thailand, but the good reproducibility of pH values (of samples collected by augering) to about 1.6 m depth in all Ra pedons suggests that it is of minor importance.

In Ra-1 and Ra-2, as well as in the interposed pedons Ra-1½ and Ra-2½, free ferric oxide has accumulated in the upper, and jarosite in the lower part of the B horizon (Fig. 13, right). Samples from Ra-3 are much lower in both free ferric oxide and jarosite than from the other soils. Pyrite appears at about the same absolute level in all soils and continues to increase with depth below the lower limit of the B horizon over at least 40 cm. All soils are physically 'ripe' ( $N < 0.7$ , Pons & Zonneveld, 1965) only in the surface 60 cm. Saturation moisture contents exhibit very similar trends with depth in all soils. They are directly related to the N value, since differences in texture and organic matter contents are relatively small. Apparently they are a function of depth below the soil surface rather than of distance from the boundary between the B and C horizons (Fig. 14, left).

The same may be true for the lowest ground water tables observed (Appendix B).

The permeability (measured according to Luthin & Kirkham, 1949) is

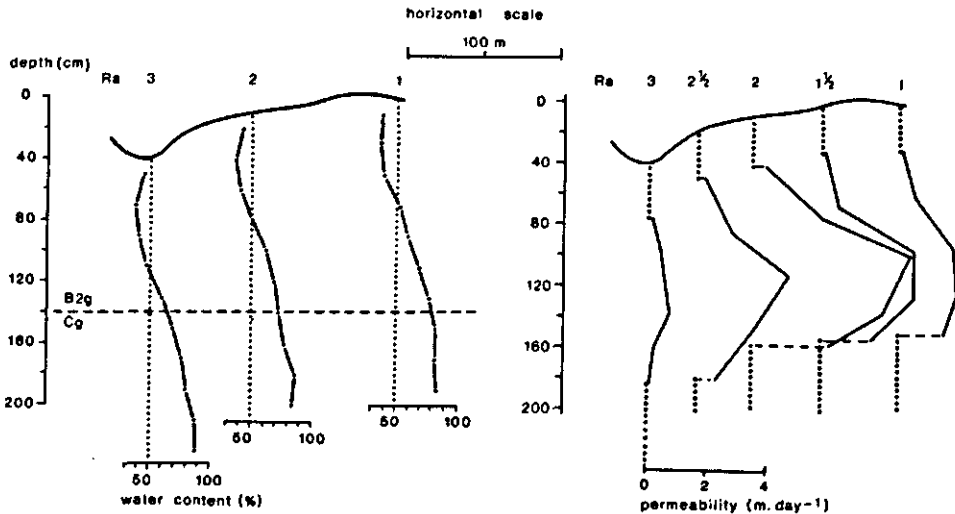


Figure 14

Saturation moisture (left) and permeability for water (right) against depth in the Rangsit toposequence.

always low near the surface, increases with depth to maximum values between 80 and 140 cm depth and finally decreases again further down (Fig. 14, right). But the maximum permeabilities vary considerably from place to place. They are rapid in pedons at intermediate heights and slow to moderately slow at lower and higher altitudes. Essentially the same pattern was found during another series of measurements 30 m to the east (Vlek, 1971).

Of the other acid sulfate soils studied, 0-1, about 25 km east of the Rangsit Station, is very similar to Ra-1. The soil KR-1, very close to the Chao Phraya, is remarkable in that jarosite is abundant at shallow depth. Na-2, in the western part of the Bangkok Plain, has a thick horizon overlying a red mottled B horizon rich in gypsum near the transition between these two horizons. Mechanical and chemical analysis suggest a lithologic discontinuity at the same depth. Deposition of calcareous Mae Klong alluvium on an acid sulfate soil or a potentially acid tidal marsh sediment may account for the strongly gypsiferous character of the transition layer, and for the relatively high pH (5.3-5.9) at the surface.

Mn-1, which lies in the para-acid sulfate zone south of the Rangsit area, is somewhat less acid (pH close to 4) than the other acid soils and shows only few inconspicuous jarosite mottles. The para-acid sulfate soil Bk-1 has a pH of about 6 in the brown and red mottled B horizon, but is rather acid (pH 4.5-5.7) between 120 and 180 cm.

The youngest of the two saline acid sulfate soils, BP-1, occurs in a mangrove area where the vegetation was cleared in 1967. The soil is distinctly acid in the top 30 cm and is high in pyrite and strongly potentially acid at greater depth. The soil conditions in this area were described in detail elsewhere (van Breemen et al., 1973). KD-1 presents a further stage of acid sulfate soil development and is mottled (partly with yellow jarosite) and strongly acid down to 65 cm.

### 3.3 THE CHA-AM LAGOON

*General soil conditions* The Cha-am Lagoon is situated in northern Peninsular Thailand, along the Gulf of Thailand (Fig.2), about 120 km southwest of Bangkok. At its greatest width, the lagoon extends 3.5 km inland, and is bordered to the west by very steep hard limestone outcrops, reaching to 200 - 370 m altitude, to the south by semi-recent alluvium and to the north by another lagoon. It is connected to the sea by a tidal creek, Khlong Cha-am, which cuts through a 0.2 to 1.1 km wide sandy beach ridge. The soil map

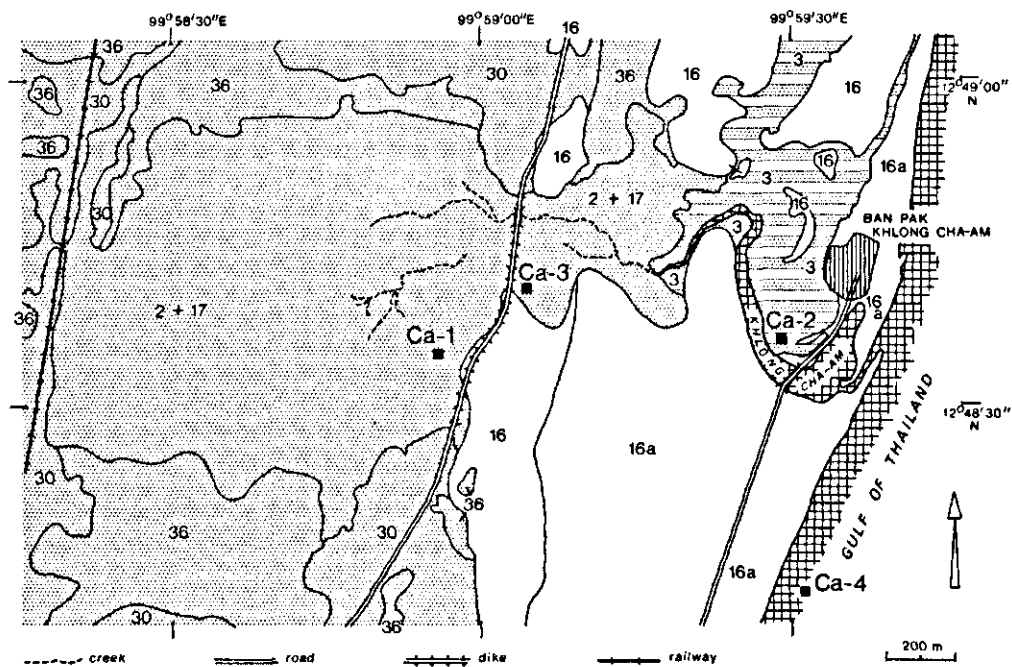


Figure 15

Semi-detailed soil map of the Cha-am Lagoon (Thailand Soil Survey Division, 1966) with sites of described soils. Areas with acid and potentially acid soils are indicated by shading.

2 = Bang Pakong series; 3 = Tha Chin / Bang Pakong complex; 16 = Hua Hin series (16a: calcareous phase); 17 = Cha-am series; 30 = Rangsit series, high phase; 36 = Tha Kwang series. For a description of the soil series see Table 6.

(Fig. 15) is derived from a much larger semi-detailed soil map (scale 1:8000) of the Hup Kapong Project Area. The creek terminates in a more or less circular depression with a complex of Bang Pakong (unit 2) and Cha-am series (unit 17). The potentially acid Bang Pakong series are found mainly east of the dike crossing the area, whereas Cha-am series occur predominantly to the west. Land surrounding the depression has been mapped either as Tha Khwang series (36) or as the high phase of the Rangsit series (30). The latter replaces the Sam Roi Yot series shown on the original survey map (cf. van der Kevie & Yenmanas, 1972).

*Selected pedons* Soil Ca-1, a saline acid sulfate soil (Cha-am series) was fully described and sampled (Fig. 11, Appendix B). Soils Ca-2 and Ca-3, both potentially acid muds (Bang Pakong series), were considered in less detail.

The Ca-1 area is barren during the dry season and is covered here and there with tufts of grasses during the wet season (September - December). Until some 20 years ago, the lagoon west of the dike was used as a salt pan. The trade was stopped when fresh water from an irrigation canal, dug to bring water to the cultivated Tha Khwang soils, started to interfere.

The Ca-3 area, immediately east of the dike, carries a forest of *Avicennia officinalis*. At Ca-2, a dense stand of *Rhizophora mucronata* fringed the tidal channel before the area was cleared at the end of 1969. Throughout the year, flooding with saline or brackish water occurs at Ca-2 and Ca-3 during high tides. Ca-1 is probably seldom flooded any more by sea-water, but is inundated with fresh water to depths of 10-20 cm during the rainy season. Ca-1 lacks an A horizon. The surface is covered by yellowish brown 'pseudo-sand' (small grains of silty clay loam), covering a grayish brown strongly acid (pH 3.0) B horizon with few red, yellow or brown mottles in the upper part and many jarosite and iron mottles in the middle. The unmottled substratum starts at 1.5 m, and is predominantly dark gray near the transition to the B horizon and dark greenish-gray at depth. The texture of the described profile is uniform silty clay loam throughout, but sandy and peaty layers occur at various depths in the immediate vicinity of Ca-1. The soil is physically 'ripe' to about 60 cm. The soil solution is saline (electrical conductivity 60-81 mS/cm, compared to 56 mS/cm for sea-water).

Ca-2 consists of very dark-gray, unmottled, 'half-ripe' silty clay with many partly decomposed plant remains. A smell of  $H_2S$  emerges after adding HCl, indicating the presence of FeS. To a depth of 80 cm, the soil acidifies strongly upon aeration. The permeability is high because of numerous crab holes.

Ca-3 has a gray silty clay-loam matrix down to 1 m depth, and consists of greenish grey silty clay-loam to fine-sandy loam below. The topsoil has olive brown to green mottles. The pH is 6 throughout and the soil is potentially acid below 40 cm depth. The groundwater is extremely saline (electrical conductivity 76-86 mS/cm) in the dry season and appears to be influenced by fresh water in the rainy season (59-71 mS/cm).

### 3.4 SOUTHERN PENINSULAR THAILAND

*General soil conditions* Figure 16 is a generalized soil map of the relevant area, derived from the reconnaissance soil map by Dent (1972). Recent marine deposits occupy a zone 10-30 km wide along the Gulf of Thailand. The coast is fringed by a beach ridge 1-8 km wide, which in turn is bordered

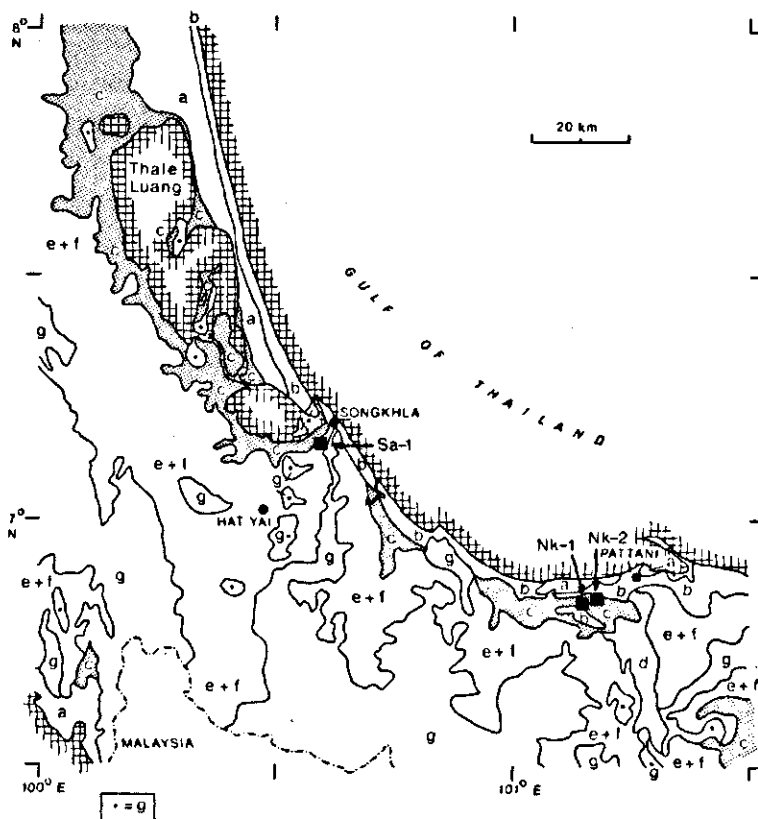


Figure 16

Generalized soil map of Southern Peninsular Thailand (after Dent, 1972) with sites of described soils. Acid sulfate soils are marked by dotted shading.  
 a = non-acid marine soils; b = soils of beach ridges and dunes;  
 c = acid sulfate soils; d = soils on recent riverine alluvium;  
 e + f = soils on older alluvium; g = soils on residuum and colluvium.

by non-acid marine soils and, especially in the southern part of the area, by acid sulfate soils. The most extensive area with acid soils is associated with the large lagoon Thale Luang.

*Selected pedons* Three acid sulfate soils were described and sampled; one (Sa-1) 2.5 km south of the edge of the smaller lagoon Thale Sap Songkhla and two (Nk-1 and Nk-2) near the village of Nong Chick, close to Pattani. Nk-1 is situated in paddy field and is characterized by a thin dark Ap, a light gray and grayish brown, mottled B horizon, over a dark gray C horizon below 125 cm. Chromas are low (1) in the upper part of the B horizon, and high (2.5) in the lower part, whereas they are almost invariably 2 in the acid sulfate soils of the Bangkok Plain. The pH is 3.8 near the surface and 3.0-3.2 in

the lower part of the B and the upper part of the C horizon. Samples from 125 - 170 cm depth further acidify on aeration.

The total sulfur content in the substratum, presumably in the form of pyrite, is between 0.7 and 1.7 %. Remarkably enough, jarosite is lacking in the B horizon, as evidenced by the low total S contents (0.04-0.02 %) and the absence of yellow mottles. But fine yellow mottling, resembling jarosite was observed in a profile about 30 m south. The nearby soil Nk-2 also lacks jarosite and has similar matrix colours. Total sulfur in the peaty substratum is too high to be accommodated as pyrite by the iron present, and at least 1.6% S must be in organic or elemental form.

The third pedon in Peninsular Thailand (Sa-1) differs from the other two, especially in that it contains appreciable amounts of jarosite in the B horizon.

### 3.5 THE SOUTHEAST COAST REGION

In the Southeast Coast Region, two acid sulfate soils from quite different sites were described and sampled in detail. One was in the estuarine swamps near Chanthaburi (Ch-1) and one in a semi-recent terrace near Klaeng (Kl-1). Occasional water samples were taken from six other sites in the coastal plain near Chanthaburi.

*General soil conditions* The landscape in the Chanthaburi area is colourful and varied. The following exposé is based in part on the soil map (Fig. 17) and the description by Dent & Montcharoen (1966). The coast is lined by beach ridges (b) and occasionally interrupted by monadnocks (h). Behind these, the intricately patterned estuary of the Chanthaburi River dominates the swampy lowlands where mangroves (including Nipa palms) fringe the tidal creeks, and rice fields, groves of paperbarks (*Melaleuca leucodendron*) and bare areas are found further inland.

Granitic hills (h) border the area to the east. A Tertiary volcanic plug 130 m high of dense olivine basalt, surrounded by an undulating to hilly basaltic plateau (5-50 m high) with red soils lies to the northwest (g). Older terrace alluvium, 3-10 m high, frequently separates the hills from the recent estuarine plain.

Most of the recent tidal marsh sediments have developed into acid sulfate soils (17 and 38 in Fig. 17). Part of the soils mapped as Cha-am series (17) may in fact be potentially acid (i.e. Bang Pakong series).

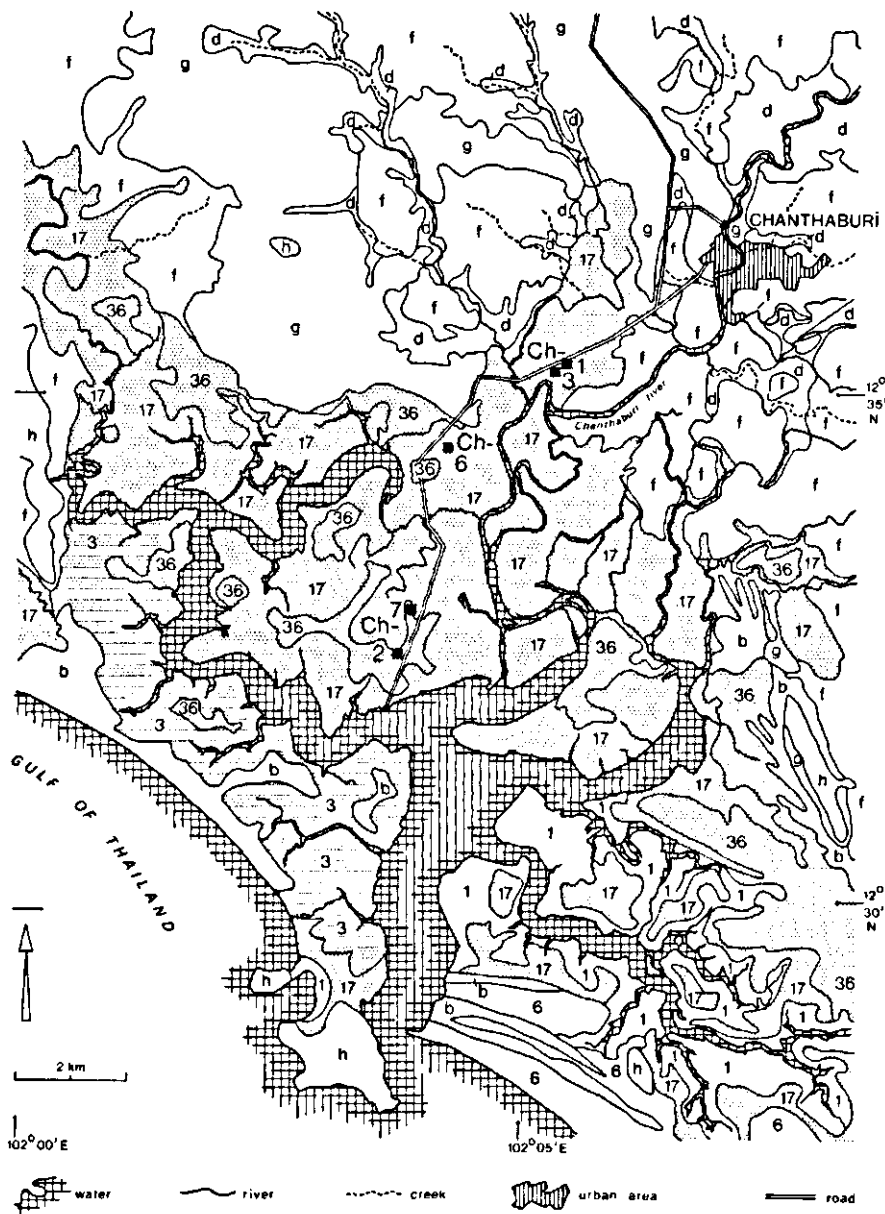


Figure 17

Generalized soil map of the Chanthaburi area (after Dent & Montcharoen, 1966) with sites of described soils. Acid sulfate soils are marked by dotted shading.

1 = Tha Chin series; 3 = Tha Chin / Bang Pakong complex; 6 = Samut Prakan series; 17 = Cha-am series; 36 = Tha Khwang series (soil series are described in Table 6); b = soils of beach ridges and dunes; d = soils on recent riverine sediments; f = soils on terrace alluvium and slope colluvium; g = soils on residuum and colluvium; h = shallow soils of hills.

*Selected soils* The soil Ch-1 is in a slightly depressed, completely barren, approximately circular area (diameter 150 m), which is partly surrounded by thickets of *Melaleuca leucodendron* on elevated land 20-30 cm higher. The yellowish surface is predominantly sandy sediment. The soil profile is made up of (a) a surface soil 13 cm thick consisting of alternating horizontal strata 1-3 cm thick of very dark-gray clay-loam and almost pure yellow jarosite, (b) a dark-brown horizon with jarosite fillings in cracks and root channels (c) a dark-gray horizon with few dark-brown mottles, and (d) from 70 cm downwards, a dark-gray unmottled substratum over a stiff red-mottled clay at 190 cm depth.

Micromorphological examination of the top 30 cm showed the presence of thin clayey, silty or sandy layers, sometimes rich and sometimes poor in organic matter. Iron shows pronounced differences with depth. It is high in the surface 40 cm (mainly in the form of jarosite), low in the B3 horizon where it is present as ferric oxide, and higher again in the substratum as pyrite. The pH is 3.0 at the surface and increases with depth but remains rather low (4.2-5.1) even in the C horizon. Samples from below 40 cm depth acidify strongly upon aeration.

The soil is saline (conductivity 19-40 mS/cm) with white salt efflorescences of halite and gypsum on the higher parts during the dry season. Under similar conditions, 60 km to the southeast, efflorescences included sodium alum and tamarugite.

The soil in the paperbark grove (Ch-3) near Ch-1 differs strikingly from Ch-1. The upper 20 cm is homogeneously brown and has a crumb to granular structure, whereas only a few jarosite mottles occur between 20 and 40 cm.

The site marked as Ch-2 in Fig. 20 represents a toposequence of acid sulfate soils. The first sampling site, Ch-2A, was in a paddy field, enclosed by small bunds. Ch-2B lies 25 m northeast from Ch-2A at slightly lower altitude in a barren area. The surface of Ch-2C, 90 m further west in the same barren area, is about 0.5 m below that of Ch-2B. Ch-2C is regularly flooded by brackish water.

Ground water was acid to moderately acid at Ch-2A (pH 3.2 and 4.1), strongly acid at Ch-2B (pH 3-3.3) and again moderately acid at Ch-2C (pH 3.7). Salinity strongly increased with depth at Ch-2A (5 and 16 mS/cm at 40 and 60 cm respectively) and was much higher at Ch-2B (39-46 mS/cm) and at Ch-2C (63 mS/cm). The conductivity at Ch-2C was higher than of sea-water, indicating the strong concentration taking place during the dry season, even in this high rainfall area (3200 mm/year).

The soil Kl-1 was about 50 km west of Chanthaburi, near Ban Thang Kwia, just south of Sukhumvit road. The land was used for transplanted rice, and lies 3-4 m above sea-level. The parent material was probably semi-recent terrace alluvium.

The rather thin (0-15 cm) very-dark grayish-brown clayey Ap covers a partly indurated brown and red B horizon, containing almost 50% of  $Fe_2O_3$  in the upper part and having yellow jarosite mottles in the lower part. Between 40 and 60 cm, the iron pan covers a sandy clay-loam horizon with yellow and yellowish-brown mottles. The substratum is unmottled sandy loam. Between 80 and 150 cm the soil seems poorly ripened, and at that depth the profile pit caved in badly during description.

Thin sections revealed clear sedimentary layering below 45 cm. The red, strongly indurated parts of the B horizon are confined mainly to zones along the larger channels and vughs. Goethite is present in the brown material and haematite in the red material.

The pH is 4.7 in the Ap, drops to a minimum of 3.3 in the B horizon and gradually increases to about 4 in the substratum. This substratum does not contain pyrite and hence is not potentially acid.

The groundwater is very low in dissolved solids (conductivity 0.1-0.7 mS/cm). As will be explained later, this soil must be considered as a 'groundwater laterite' formed by lateral supply of water rich in ferrous sulfate.

### 3.6 COMPARISON OF THE SOILS

The differences and similarities between the soils described in the previous sections are discussed below with special emphasis on profile morphology, physical characteristics, Fe-S minerals, the distribution of iron and manganese oxides, soil pH, clay mineralogy and water composition.

Most soils are very clayey throughout, but a considerable vertical and lateral variation in texture may be found in smaller coastal plains, as near Cha-am and Chanthaburi. In the Bangkok Plain, textures are more uniform in the older acid sulfate soils (typically 60-65% clay in most soils) than in the zone closer to the coast, where both silty clay (BP-1, T-1, Mn-1, Bk-1) and very heavy clay (KD-1) can be found.

All soils except Kl-1 have an unmottled, pyritic substratum. In the Bangkok Plain, the substratum is generally greenish gray in soils near the coast, regardless of whether they are acid or not (BP-1, KD-1, Bk-1, T-1 and Mn-1) and dark gray in the older soils. Both dark-gray and greenish-gray

substrata were observed in the acid sulfate soils and potentially acid soils of the Cha-am Lagoon and the Chanthaburi area, whereas dark-gray and dark-grayish-brown substrata appear to be typical for the acid sulfate soils of the Songkhla-Pattani region.

Pons & van der Kevie (1969) reported that greenish-gray colours correlate with the absence of potential acid sulfate conditions, whereas gray colours predict potential acidity. At the time of their study, the soils in the southeastern part of the Bangkok Plain were not yet mapped, so that they missed the relatively small patches of soils with potentially acid greenish-gray substrata. We must probably reject their hypothesis, that green minerals such as chlorite, chamosite and glauconite inhibit acidification of such reduced substrata upon aeration, even if they are highly pyritic. Trafford et al. (1973) observed that overnight exposure to the air caused the green colour to fade. As the colour did not reappear when the soils were rewetted, they concluded that it was caused by something considerably less stable than any of the green silicates mentioned. Most likely the lack of potential acidity in most greenish gray substrata must be ascribed to a combination of relatively low amounts of pyrite and the presence of some calcium carbonate. In the soils analysed for this study, pyrite (S) contents are generally 1-2.6% in potentially acid substrata, and 0.5-0.8% in not potentially acid substrata.<sup>a</sup> The substrata of the non-acid soils described by van der Kevie and Yenmanas (1972) and of the two non-acid soils considered here (T-1; Mc-24 used for an oxidation experiment) invariably contain 0.5-8%  $\text{CaCO}_3$ .

Possible reasons for the origin of the green colour and for the differences in pyrite content among the soils from various sites will be discussed in Sections 4.4.2 and 4.2.2 respectively.

In most acid sulfate soils the pH is only moderately low near the surface (4.0-4.5) and distinctly lower in the B horizon: 3.5-4.0 in the older soils from the Bangkok Plain and 2.9-3.5 in the majority of the younger soils closer to the coast. Below the B horizon, pH increases with depth and eventually attains near-neutral values at some distance below the upper boundary of the unmottled substratum (Fig. 18). This distance is only about 20 cm in a very young acid sulfate soil such as BP-1, but may exceed 1 m in the older soils. Downward diffusion of sulfuric acid and occasional pyrite oxidation at great

---

a. The sole exception was a sample from Mn-1, which was moderately high in pyrite (1.35% S), but hardly acidified upon aeration.

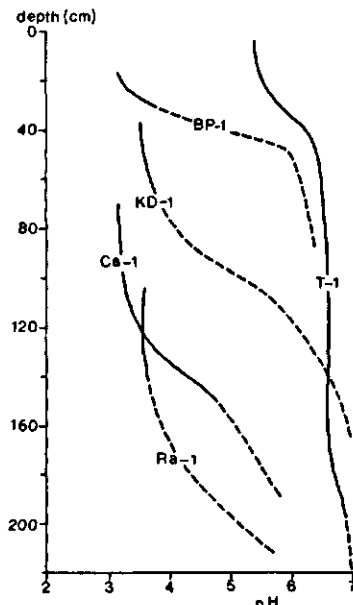


Figure 18  
pH against depth in some representative soils. The broken parts of the curves indicate the pyritic substratum

depth during a severe dry season probably account for the typical pH profiles depicted in Fig. 18.

Possible reasons for the high frequency of pH values close to 3.5 will be discussed in Chapter 6. Non-acid marine soils show little or no difference in pH between the C and the B horizon, but very often have a distinctly acid A horizon. This is exemplified by the pH profile of T-1 (Fig. 18). By contrast, in acid sulfate soils A horizons are less acid than B horizons. Deacidification and acidification processes in the surface soils were identified and account for these trends. They have been described elsewhere (van Breemen, 1975) and will be touched upon in Section 4.6.

All acid sulfate soils, except two from southern Peninsular Thailand (Nk-1 and Nk-2), show an accumulation of jarosite in the profile. The yellow mottled jarositic horizon is distinctly separated from the pyritic substratum and has a markedly lower sulfur content (0.1-0.8% against 1-2.6% in the substratum). The further the soils are developed, the greater the depth at which jarosite occurs. In most acid sulfate soils dithionite-extractable iron is low in the pyritic substratum<sup>a</sup>, considerably higher in the B horizon.

a. Relatively high contents in some substrata (Bk-1, Ch-1, Sa-1 and Nk-1) are artefacts due to pyrite oxidation upon slow air-drying of the samples.

and lower again in the A1. Part of the accumulation is due to jarosite, which is also extracted by dithionite. But a considerable amount of free ferric oxide is normally present above the jarosite horizon. In the older soils at higher altitudes, some of this free ferric oxide occurs as red haematite.

The two saline acid sulfate soils from small coastal plain areas, Ca-1 and Ch-1, differ radically in the distribution of iron oxide and jarosite. The lack of a clear accumulation of these substances in Ca-1 can be explained if it be assumed that this soil was influenced by an artificial (and hence sudden) and relatively deep drainage during utilization of the area for salt extraction or after construction of the dike through the lagoon. At Ch-1, a tidal-influenced fluctuating watertable with minimum levels of 40-70 cm may account for the extreme depletion of iron in this zone, and its accumulation as jarosite near the surface. The absence of jarosite from the Nk pedons is puzzling. A detailed profile study might have given some clues, but unfortunately only descriptions and samples from auger holes were available.

The mineralogy of the various oxidation products of pyrite, their thermodynamic stability, and the oxidation-reduction processes and hydrolytic reactions, accounting for their accumulation in various horizons, will be treated in Chapter 4.

Total manganese contents are generally very low (<0.02% as MnO) in strongly acidified soil material, and distinctly higher in non-acid soils and non-acid substrata of acid soils, indicating a considerable mobility of Mn at low pH. Several aspects of the chemistry of manganese will be dealt with in Section 4.4.

Except if very young (BP-1, KD-1), most coastal plain soils have a typical profile of organic matter, characterized by higher contents in both the top-soil and the reduced substratum, and lower contents in the B horizon. The organic matter in the substratum is often oriented parallel to the surface, and probably stems from a former mangrove vegetation at the time of deposition. Apparently, most of the organic matter originally present at the depth of the present B horizon has been decomposed upon aeration. Organic matter in the A horizon reflects, of course, the effect of a more recent vegetation. Both in the A and in the B horizons, organic matter contents are significantly higher in acid sulfate soils than in non-acid marine soils (Kawaguchi & Kyuma, 1969), suggesting slow decay of organic matter under strongly acid conditions.

In all soils, the physical ripening, expressed as the N value (Pons & Zonneveld, 1965), decreases with depth, but the differences among the soils are very large (Fig. 19). BP-1 which emerged from the mangrove mud stage only

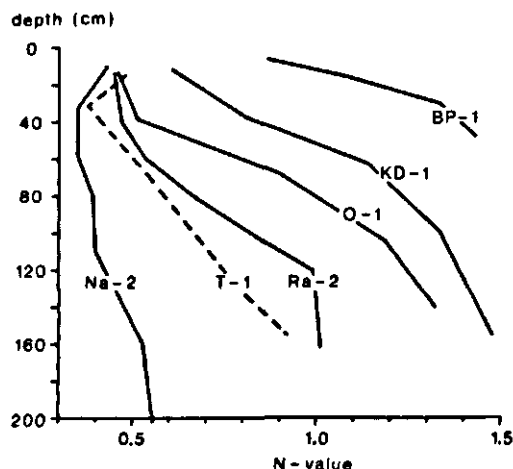


Figure 19  
 Physical ripening, expressed as N value (Pons & Zonneveld, 1965) at different depths in some soils. Solid lines, acid sulfate soils; broken line, non-acid marine soil;  $N < 0.7$ , 'ripe';  $0.7 < N < 1.0$ , 'nearly ripe'

recently, has relatively low N-values only at shallow depth. The older soils Ra-2 and O-1 have undergone physical ripening to a much greater depth, but the difference between a morphologically well developed old acid sulfate soil such as O-1 and the much younger KD-1 is rather small. Apparently, physical ripening is slow in these acid soils. This may be due to low evapotranspiration associated with a comparatively meagre and shallow root system. A more luxuriant deeper-rooting vegetation probably grew at the non-acid T-1, which has far lower N values than most acid soils.

Permeability is generally high throughout the profile in mangrove muds and very young soils but, notably in the surface 50 cm, much lower in the older soils. The crab holes and remnants of tree roots presumed to cause the high permeability of the young soils are probably short-lived, and the moderate to moderately high permeabilities observed in the subsoils of older pedons appear to be caused mainly by the large (diameter 5-10 mm) root channels of a post-mangrove vegetation.<sup>a</sup> Indeed, the typical character of the toposequential series of permeability profiles observed at the Rangsit station (Fig. 14) can be explained by differences in density and rooting habits of the vegetation due to differences in hydrology. Part of the root channels have been filled with jarosite. In some cases, for instance in KR-1, this may have strongly decreased the permeability. The widespread mass illuviation of surface material,

a. If due to a former mangrove vegetation, the root channels would probably not be confined to a zone about 1 m thick (Fig. 14, right).

observed in thin sections, may be important also in this respect. Incidentally, the apparent mechanical instability of the Ap material is somewhat surprising in view of the allegedly strong structural stability of (partly aluminium-saturated) channel walls and ped faces in acid and para-acid sulfate soils (Pons, 1973; Kamerling, 1974).

Fig. 20 shows the average clay mineral composition, in terms of both normative contents and percentages of total area of X-ray diffraction peaks for three groups of soils. Normative kaolinite contents are about 60% for acid sulfate soils of Peninsular Thailand (Group C) between 40 and 55% in

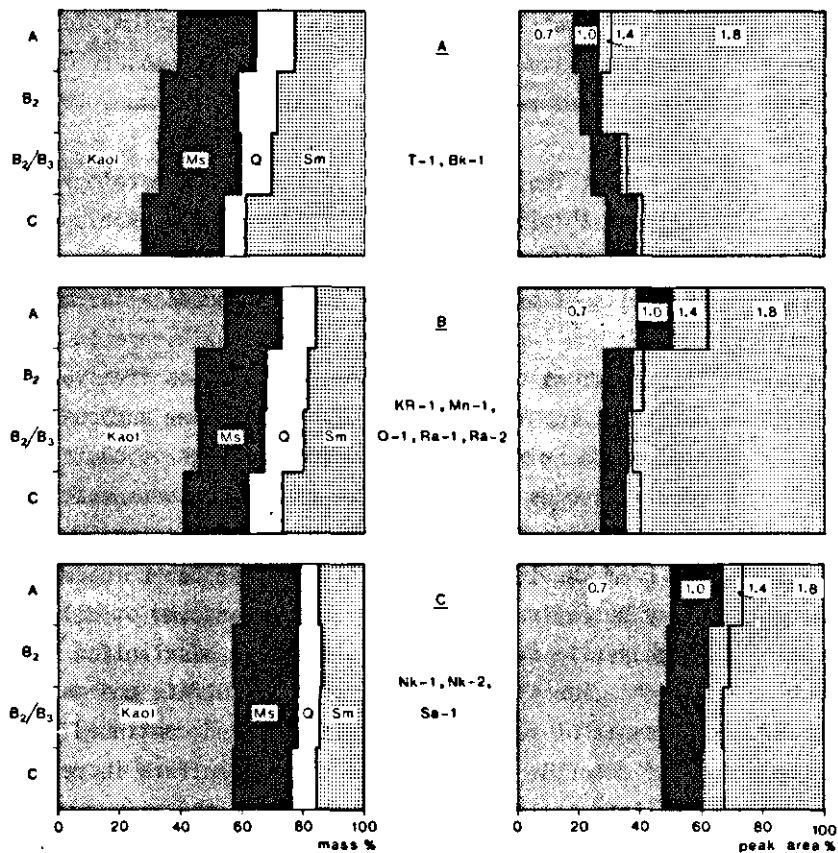


Figure 20

Cumulative plots of normative mineralogical composition and of X-ray diffraction peak area percentages in different soil horizons. A. Non-acid soil plus para-acid sulfate soil (averaged), Bangkok Plain; B. Acid sulfate soils, Bangkok Plain; C. Acid sulfate soils, Southern Peninsular Thailand. Each figure is averaged for the pedons listed. The original data were recalculated to 100%.

Kaol = kaolinite; Ms = muscovite; Q = quartz; Sm = smectite

the Bangkok Plain (Group B) and between 25 and 40% in non-acid soils and para-acid sulfate soils (Group A). Normative smectite shows a reverse trend. Normative muscovite is highest in T-1 and Bk-1 and lowest in soils from the peninsula, but the differences are small. The same general trend, i.e. high kaolinite and low smectite in Group C and the reverse in Group A, is indicated by the relative X-ray diffraction peak areas.

The agreement between the two methods is less when the trends in the mineral composition within the profiles of each of the three groups is considered. For instance, the markedly lower 1.8 nm peak area of the A horizons of the Bangkok Plain acid sulfate soils is only partially reflected by the results of the normative calculations. Most of the difference can be accounted for by partial interlayering of swelling clay minerals with aluminium, leading to the formation of non-swelling (1.4 nm) 'soil chlorite', often observed in association with seasonal cycles of reduction and oxidation (Brinkman, 1970; Mitsuchi, 1974).

In the soils from Peninsular Thailand (Group C), the clay mineralogy varies little with depth. There chloritization in the surface soil was observed only in Nk-1.

Ca-1 differs from the soils of other areas in that it contains far more normative muscovite.

A quick impression of the gross composition of ground waters from various groups of soils can be obtained from Table 7, which shows ranking numbers assigned to  $\text{Cl}^-$ ,  $\text{SO}_4^{2-}$  and  $\text{Mg}^{2+}$  based on their relative abundance in terms of equivalent concentrations. The three-digit codes made up of the ranking numbers were arranged vertically in an order of decreasing  $\text{Cl}^-$  concentration and increasing  $\text{SO}_4^{2-}$  concentration. Most waters from the immediate vicinity of the coast resemble sea-water, although they may be influenced markedly by evaporation or dilution and by acidification through pyrite oxidation. In a somewhat desalinized acid sulfate soil such as KD-1, chloride still ranks first, but sulfate and magnesium have reversed order. As a result of further desalinization and continued pyrite oxidation, the importance of chloride decreases and that of sulfate increases. Finally, in the old acid sulfate soils of the Bangkok Plain, the ground water is dominated by sulfate, and chloride is reduced to a minor constituent. Partly by release of magnesium from clay minerals, the magnesium concentration also increases with time. Sodium, not considered in Table 7, ranks first in Bk-1 and T-1, and second in most older soils.

The general picture is somewhat distorted by the results from Peninsular Thailand. The waters from Nk-2 and Sa-1 are rather like sea-water in many

Table 7. Relative abundances of  $\text{Cl}^-$ ,  $\text{SO}_4^{2-}$  and  $\text{Mg}^{2+}$  expressed as ranking numbers based on equivalent concentration, electrical conductivity and pH in groundwater from various sites. Waters from surface soils were excluded.

Sites	$\text{Cl}^-$	$\text{SO}_4^{2-}$	$\text{Mg}^{2+}$	elec.cond. (mS/cm)	pH
(sea-water), BP, KD-2					
Ca, Ch, Mc-2, Mc-27, Mc-28	1	4	3	20-97	2.9-8.3
KD-1	1	3	4	15-30	3.3-6.9
Nk-2, Sa-1	1	3	4	5-7	2.9-3.5
Bk-1	2	3	4	11-20	4.4-6.7
T-1	3	2	4	4-10	6.0-7.0
Mn-1, Na-2	3	1	4	4-7	3.5-6.6
Nk-1	3	1	5	2-4	2.8-3.0
O-1, Ra-1	4	1	3	5-7	3.3-4.7
KR-1, Ra-2	5	1	3	2-4	3.3-4.5
Ra-3	5	1	2	3-4	3.2-5.4

respects, but their electrical conductivity is considerably less than that of waters from similar soils in the Bangkok Plain. Likewise, although  $\text{Cl}^-$  is third in abundance in Nk-1, the electrical conductivity is here lower than of otherwise similar waters from Mn-1 and Na-2. Moreover in Nk-1, the concentration of  $\text{Mg}^{2+}$  is relatively low (in fact it is lower than of aluminium). The deviant results for the waters from Peninsular Thailand must probably be ascribed to a limited release of bases from minerals upon acidification and to the absence of a pronounced dry season, resulting in a rather rapid desalinization,

A typical aspect of acid sulfate waters, regardless of age and site, is the high concentration of dissolved silica ( $\text{H}_4\text{SiO}_4$  2mmol/litre). Most acid soil solutions are in fact saturated with amorphous silica, undoubtedly formed from silica released during weathering of silicates under acid conditions.

## 4 Processes involving iron, sulfur and manganese

The mobility of iron, sulfur and manganese is strongly influenced by redox potential ( $E_H$ ) and pH. This common trait is mainly responsible for the marked depletion and accumulation of these elements in certain horizons, illustrated in Fig. 21 for a young acid sulfate soil (KD-1), an older acid sulfate soil (Ra-1½) and a non-acid soil (T-1).

Iron and sulfur, moreover, combine in two minerals characteristic for acid sulfate soils: pyrite and jarosite. The stability relations of these minerals as a function of  $E_H$  and pH are exhibited succinctly by the  $E_H$ -pH diagram for pyrite, jarosite, ferric oxide, and dissolved iron and sulfur species, presented in Fig. 22. The diagram reveals that pyrite is stable

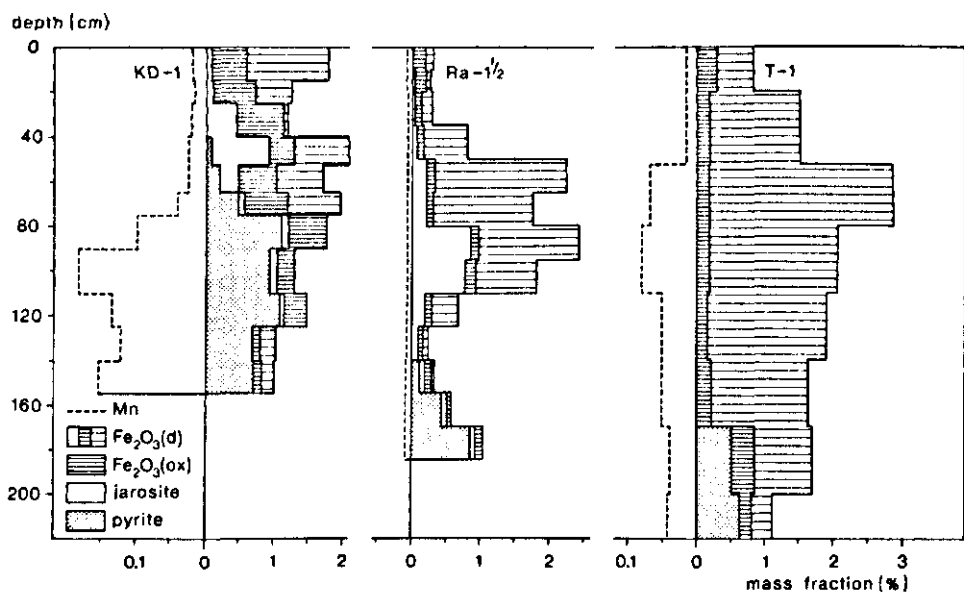
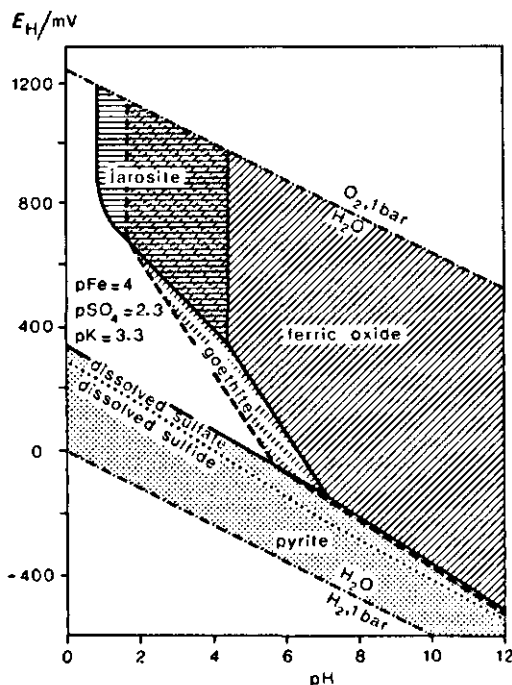


Figure 21  
Distribution of dithionite extractable manganese and of different forms of iron in two acid sulfate soils (KD-1 and Ra-1½), and one non-acid marine soils (T-1).  $\text{Fe}_2\text{O}_3(\text{d})$  = dithionite extractable  $\text{Fe}_2\text{O}_3$ ;  $\text{Fe}_2\text{O}_3(\text{ox})$  = oxalate extractable ('amorphous')  $\text{Fe}_2\text{O}_3$ .

Manganese expressed as % Mn, iron fractions as % Fe.



**Figure 22**  
 $E_H$ -pH diagram of ferric oxide ( $pK_{so} = 39.9$ ), jarosite and pyrite at 25 °C. Solid phases are indicated by hatching and shading. The broken hatched shading shows the extension of the  $Fe_2O_3$  field at  $pK_{so} = 42.6$  (goethite).

over a wide pH range but only under reduced conditions, whereas jarosite is limited to strongly oxidized and acid conditions, and ferric oxide occurs over a wide  $E_H$  range at pH values above 4.

$E_H$ -pH data will be used extensively in this chapter and therefore it is appropriate first to describe the methods used for the measurement of  $E_H$  and pH and various problems in interpreting  $E_H$ .

#### 4.1 MEASUREMENT AND INTERPRETATION OF REDOX POTENTIALS

Redox potential can be defined as the potential of a chemically inert electrode, such as a Pt electrode, with reference to a hydrogen electrode. Although measurement of  $E_H$  is simple in principle, its interpretation involves complex problems.

One problem is to obtain reproducible measurements that in some way reflect the redox state and not some other property of the system. For instance, at low concentrations of electro-active species, the low exchange current density on the Pt electrode gives rise to instability and poor reproducibility. Moreover the Pt electrode may lose its inertness, especially under aerated conditions probably by formation of non-stoichiometric Pt-O

complexes at the surface or, if kept long in strongly anaerobic environments, by formation of platinum sulfide (Whitfield, 1974). Measurements in these conditions may be highly reproducible, in contrast to those in poorly poised systems but they are also of little value. These difficulties can be alleviated by avoiding measurements in near-neutral aerobic environments, by relatively short contact between the Pt electrode and sulfide-rich soils or waters and by discarding poorly reproducible measurements.

If such precautions are taken, the  $E_H$  can certainly be useful to characterize the gross redox state of natural environments, but it is not necessarily amenable to interpretation by the Nernst equation (Stumm & Morgan, 1970). Such interpretation is impossible if the measured  $E_H$  is a mixed potential, i.e. if the oxidized and reduced species exchanging electrons at the Pt surface belong to different couples. No difficulty arises under acid oxidized conditions in the presence of dissolved iron. There the  $E_H$  can be interpreted quantitatively in terms of the  $\text{Fe}^{2+}/\text{Fe}^{3+}$  couple (van Breemen, 1973a). In a moderately reducing near-neutral environment, the ferric/ferrous couple may also regulate the potential of a Pt electrode, (Ponnamperuma, et al. 1967; Langmuir & Whittemore, 1971), although under such conditions dissolved ferric iron concentrations are presumably too low to sustain exchange currents that are sufficiently high for reproducible measurements (Stumm & Morgan, 1970). This strange phenomenon has been explained by direct participation of the ferric oxide (probably sorbed at the surface of the electrode) in the redox reaction (Doyle, 1968). Another possibility is that concentrations of dissolved uncharged  $\text{Fe}(\text{OH})_3$  are high enough to build a well poised couple with  $\text{Fe}^{2+}$ ; the activity of dissolved  $\text{Fe}(\text{OH})_3$  in equilibrium with a given ferric oxide depends only on the nature of the oxide and is independent of  $E_H$  and pH. Except for the  $\text{Fe}(\text{III})/\text{Fe}^{2+}$  couple and perhaps the  $\text{Mn}(\text{IV})/\text{Mn}^{2+}$  couple, most redox systems important in soils (e.g.  $\text{NO}_3^-/\text{NO}_2^-$ ,  $\text{SO}_4^{2-}/\text{H}_2\text{S}$  and many organic systems) are not electro-active (Stumm & Morgan, 1970).

Redox potentials were always measured in the laboratory and only in samples saturated with water or very wet. These samples were collected either in the field (generally by auger, placed immediately in a 1-litre glass jar while excluding air as much as possible by tapping the jar) or taken from a laboratory experiment involving artificial submergence or aeration of soil samples. Each sample was fitted with three bright Pt electrodes, inserted 2-3 days before measuring. During potentiometry, the reference electrode was placed onto a soaked filter and put on the surface of the soil sample. The pH was measured likewise, using a sturdy glass electrode, pressed into the

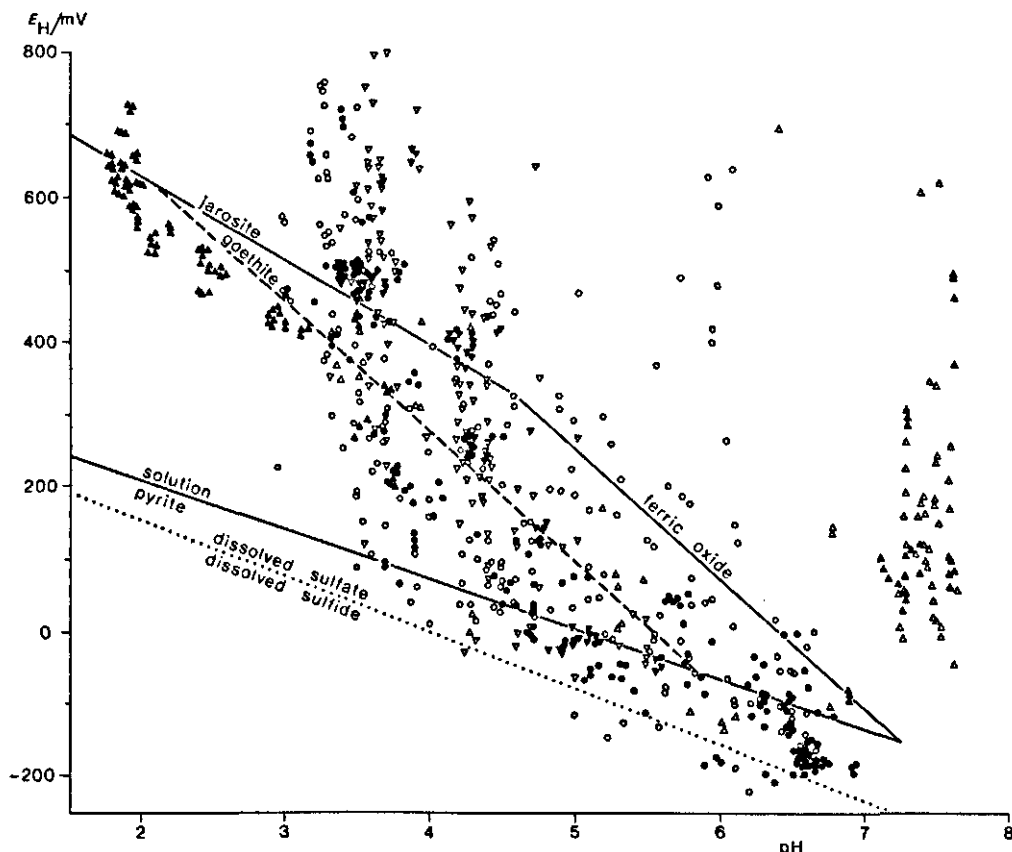


Figure 23

Plot of all  $E_H$ -pH measurements of this study. Solid symbols indicate a reproducibility (in triplicate) within 50 mV and 0.3 pH unit. Open symbols represent poorly reproducible measurements. The phase boundaries are similar to those of Fig. 22. Key:  $\circ\bullet$  field samples;  $\triangle\blacktriangle$  artificially aerated pyritic samples;  $\nabla\blacktriangledown$  artificially flooded samples.

mud after removal of the Pt electrodes, using an equilibration time of at most 2-3 min.

Fig. 23 shows unaveraged measurements of  $E_H$ -pH in triplicate, depicted by different symbols for each of three categories of samples. Many measurements were poorly reproducible (open symbols). Variations in  $E_H$  were most important in this respect; different pH measurements within each sample generally yielded results within 0.1-0.2 pH unit.

Reasons for a poor reproducibility may be twofold: the redox couples operative in the samples are poorly poised or redox conditions vary spatially in a given sample. An example of differences in redox poise was furnished by the oxidation experiment. All samples from this experiment were thoroughly mixed with excess

water about three days before measuring the  $E_H$ . Samples of one group were strongly acid ( $\text{pH} < 3$ ) as a result of pyrite oxidation and invariably showed  $E_H$  reproducible within 50 mV and generally within 2-5 mV (see Fig. 23). The exceptionally good reproducibility was due to the presence of appreciable amounts of dissolved ferrous and ferric iron. By contrast, equally well-mixed partially oxidized calcareous pyritic samples from the same experiment, with pH values above 7 were often poorly reproducible, presumably through poorly poised redox conditions.

In field samples, heterogeneity and poor redox buffering probably played a role in poorly reproducible  $E_H$  measurements. Both the occurrence of oxidized zones in an otherwise reduced medium (e.g. an aerated channel penetrating into a pyritic substratum) and the reverse situation (e.g. small active colonies of sulfate-reducing organisms in a sediment that was not entirely anoxic; Rickard, 1973) are possible. Also, heterogeneity may be induced artificially by inclusion of air bubbles in reduced muds during sampling. Because averages of triplicate  $E_H$  measurements in heterogeneous and poorly poised samples are certainly of little significance thermodynamically, quantitative interpretation in terms of oxidation-reduction equilibria was almost exclusively with measurements reproducible within 50 mV and 0.3 pH units.

Fig. 23 shows that most of the reproducible measurements fall roughly in the area where pyrite, ferric oxides, jarosite and sulfate-sulfide may play a role in determining the redox state. The correspondence between the actual  $E_H$ -pH data and the various possible chemical equilibria will be dealt with in the appropriate sections.

#### 4.2 ACCUMULATION OF PYRITE

Whereas syn-sedimentary pyrite formation has been studied extensively by oceanographers and geochemists (Rickard, 1973; Goldhaber & Kaplan, 1974), little work has been done on pyrite formation in mangrove swamps.

The concentration of detrital organic matter in tropical near-shore waters may be low, so that little syn-sedimentary or 'primary' pyrite is formed. Especially in the tropics, however, large amounts of pyrite can be formed in tidal muds above mean sea-level where mangrove trees supply ample amounts of organic matter (Pons, 1973).

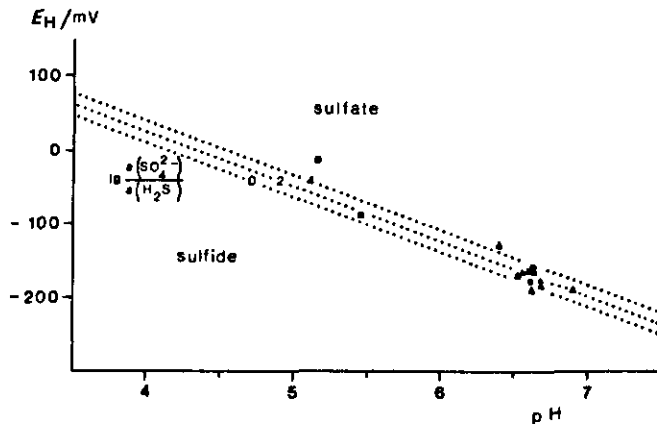


Figure 24

$E_H$ -pH data for samples with ongoing sulfate reduction. The symbols are averages of well-reproducible triplicate measurements. Key: ■ flooded surface soil; ▲ reduced mangrove mud. The dotted lines separate the predominance fields of sulfate and sulfide at different logarithmic quotients of activities of sulfate to sulfide.

#### 4.2.1 Sulfate reduction and dissolved sulfide

My few data on the concentrations of dissolved sulfide in mangrove muds come from measurements with an Orion silver sulfide electrode. Most of these measurements (by direct insertion of the electrode) were unsuccessful because both pH and total dissolved sulfide were too low to give a reliable electrode response<sup>a</sup>. Ongoing sulfate reduction can easily be detected otherwise: from the enrichment of dissolved  $\text{HCO}_3^-$  at the expense of  $\text{SO}_4^{2-}$ , the blackening of the soil (formation of  $\text{FeS}$ ) and the smell of  $\text{H}_2\text{S}$ .

Figure 24 gives the  $E_H$ -pH data on samples including surface horizons of flooded soils where ongoing sulfate reduction was suspected. With one exception all measurements were highly reproducible (generally within 10 mV and 0.05 pH unit), and corresponded closely to the theoretical  $E_H$ -pH values for the sulfate-sulfide equilibrium. To quantify this correspondence, the observed  $E_H$  was compared with the  $E_H$  calculated from the pH and the activities of dissolved  $\text{SO}_4^{2-}$  (computed from measured concentrations, van Breemen, 1973a) and  $\text{S}^{2-}$  (measured with an  $\text{Ag}_2\text{S}$  electrode) assuming equilibrium according to, for instance, Garrels & Christ (1965) by

a. The electrode senses the activity of  $\text{S}^{2-}$ , which depends on total dissolved sulfide and pH.



$$E_H = 0.148 - 0.059pH - 0.0074pSO_4 + 0.0074pS \quad (1a)$$

where  $pSO_4$  and  $pS$  are the negative decadic logarithms of the activities of the respective ions  $SO_4^{2-}$  and  $S^{2-}$ , and  $E_H$  is expressed in volts.

To investigate the possible control of  $E_H$  by polysulfides and elemental S, as found in anoxic sea-bottom sediments by Berner (1963) and others (Whitfield, 1974), the following equilibrium was considered also



$$E_H = -0.485 + 0.0295pS \quad (2a)$$

Table 8 shows that the observed redox potentials agree well with Eq. 1a, but are much lower than those for equilibrium involving elemental sulfur (Eq. 2a). The agreement with Eq. 1a is surprising in view of the non-electro-active character of the sulfate-sulfide redox couple, but can be explained by a certain degree of internal equilibrium involving other (electro-active) redox couples (Berner, 1971). The much higher potentials corresponding to those predicted by Eq. 2a, that were observed by Berner (1963), come from measurements taken brief-

Table 8. Negative logarithmic activities of dissolved sulfide and dissolved iron, pH and redox potential (in mV) in some reduced mangrove muds.

sample	pS <sup>a</sup>	pH	$E_H$ found	$E_H$ calc. <sup>b</sup>	$E_H$ calc. <sup>c</sup>	pFe	pFeS	total dissolved sulfide mmol/litre <sup>e</sup>
Ca-2 58	13.2	6.62	-172	-165	-86	5.9	19.1	0.005
Ca-2 59	12.0	6.67	-184	-177	-121	5.7	17.9	0.067
Ca-2 60	12.4	6.68	-177	-174	-109	5.7	18.1	0.026
Ca-2 77	13.6	6.55	-172	-160	-74	5.2	18.8	0.003
Ca-2 78	13.9	6.56	-168	-158	-65	5.0	18.9	0.001
Ca-3A 26	16.2 <sup>d</sup>	6.92	-191	-162	+3	4.3	20.5	0.00
Ca-3A 27	24.6 <sup>d</sup>	6.49	-124	-74	+251	5.5	30.1	0.00

a. Measured with an Orion  $Ag_2S$  electrode, calibrated by the method of Berner (1963)

b. Calculated assuming Eq. 1a

c. Calculated assuming Eq. 2a

d. Probably below detection limit; assumes the calibration line to be valid beyond  $pS > 17$

e. Calculated from pS and pH

ly after insertion of the electrodes (i.e. within a few hours against about three days in my study). Possibly, Berners results are due to oxidation of  $H_2S$  by oxygen introduced during placing of the electrodes, and may thus represent artefacts.

The general reaction between organic matter ( $'CH_2O'$ ) and sulfate:



shows that the depletion of sulfate is accompanied by an increase in bicarbonate. Changes in  $SO_4^{2-}$  and  $HCO_3^-$  can be evaluated by comparison with sea-water, which is a convenient starting point for processes affecting the composition of water in sediments of marine origin. If  $[Cl^-]$  be influenced only by dilution and concentration, the change in the concentration of dissolved species B,  $\Delta[B]$ , with respect to its concentration in sea-water can be written as

$$\Delta[B] = [B]_{\text{sample}} \times \frac{[Cl^-]_{\text{sea-water}}}{[Cl^-]_{\text{sample}}} - [B]_{\text{sea-water}} \quad (4)$$

Average values of  $\Delta[B]$  for the most important dissolved species in water from the Gulf of Thailand and samples from several mangrove areas and reduced substrata of young acid sulfate soils are given in Table 9. Samples from the Gulf were very close to standard sea-water, but slightly less saline. There was more bicarbonate relative to chloride than in sea-water at all sites, but there was

Table 9. Difference from standard sea-water in equivalent concentration (in mmol/litre) of solutes in interstitial water from reduced zones and sea-water from the Gulf of Thailand. Values are adjusted by Eq. 4 for differences in  $[Cl^-]$ . Equivalent concentrations in standard sea-water from Garrels and Thompson (1962) were:  $[HCO_3^-]$  2.2,  $[SO_4^{2-}]$  56.8,  $[Ca^{2+}]$  20.8,  $[Mg^{2+}]$  108,  $[Na^+]$  475,  $[K^+]$  10 and  $[Cl^-]$  550 mmol/litre. n, number of samples; \*\* significantly different from Gulf sea-water at  $P < 0.01$ ; + the same at  $< 0.1$ .

Site	Equivalent substance concentration difference $\Delta[B]$							$[Cl^-]$	n
	$HCO_3^-$	$SO_4^{2-}$	$Ca^{2+}$	$Mg^{2+}$	$Na^+$	$K^+$	$Fe^{2+}$		
BP	12.2**	19.3**	6.2**	17.9**	3.7 <sup>+</sup>	1.2	1.8**	284	20
Ca-2	12.0**	-11.3 <sup>+</sup>	-0.1	-7.3	5.9	1.9**	0	363	3
Ca-3	0.9	-0.8	2.3	4.4	-6.9	0.3	0.1	939	8
Ca-3A	2.0	-3.6	1.2	3.7 <sup>+</sup>	-6.5	0.1	0.0	860	7
KD-1	46.0**	98.1**	7.5**	83.6**	45.7**	4.3**	0.0	226	2
Gulf of Thailand	-0.3	-0.6	1.2	-2.7	0.3	0.6	0.0	501	4

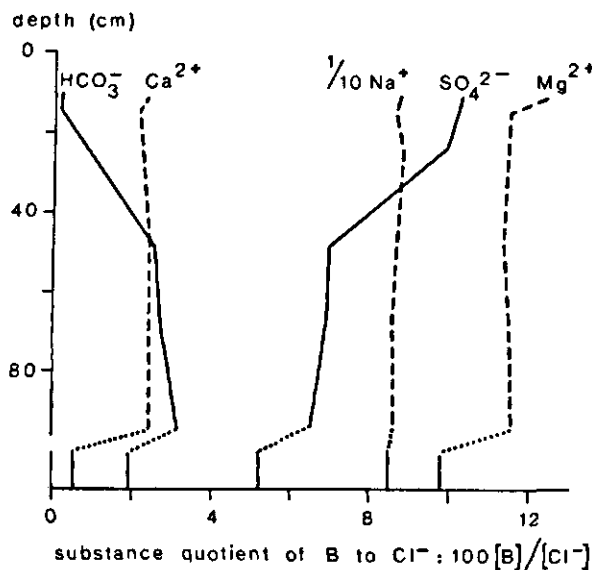


Figure 25

Means of  $[B] / [Cl^-]$  against depth at site BP-1. The vertical bars plotted on the abscissa give values in sea-water.

a significant decrease in dissolved sulfate only at Ca-2<sup>a</sup>. This supports the results for sulfide, which indicated that sulfate reduction was more intense at Ca-2 (*Rhizophora* forest) than at Ca-3 (*Avicennia* forest).

The common presence of black FeS and high values of  $[HCO_3^-]$  in substrata at the Bang Pakong station (BP) show that sulfate reduction is ongoing there also. Therefore the excess of sulfate, indicated by the positive values of  $\Delta [SO_4^{2-}]$ , must probably be ascribed to downward migration of  $SO_4^{2-}$  produced by pyrite oxidation at nearer the surface. This is corroborated by Figure 25, which depicts the substance<sup>b</sup> quotient of various dissolved species to  $Cl^-$ , plotted against depth. Especially in the oxidized surface soil, sulfate, magnesium and calcium are high compared to sea-water. This must be due to the release of sulfate and cations (liberated by cation exchange and mineral weathering) during pyrite oxidation. The decrease in  $SO_4^{2-}/Cl^-$  and the concomitant increase in  $HCO_3^-/Cl^-$  with depth, together with the relative constancy of

a. Only 3 out of 6 samples available from Ca-2 were considered because it was suspected that the other samples were affected by inadvertent oxidation during  $E_H$ -pH-pS measurement and water sampling.

b. The quantity 'amount of substance' is expressed in moles and is used in reporting amounts of any chemically analysable species (e.g.  $SO_4^{2-}$  or  $\{SO_4^{2-}\}$ ) or group of species (e.g. exchangeable bases,  $\{Ca^{2+} + Mg^{2+} + Na^+ + K^+\}$ ). (International Organization for Standardization, ISO—31.8, 1973, Section 3.1.)

$Mg^{2+}/Cl^-$  and  $Ca^{2+}/Cl^-$  indicates that sulfate is reduced in the substratum and that part of the sulfate reduced at depth was formed earlier by pyrite oxidation nearer the surface. The  $SO_4^{2-}/Cl^-$  ratio in the substratum still exceeds that of sea-water so that oxidation of pyrite predominates over sulfate reduction.

The high concentrations of  $HCO_3^-$ ,  $SO_4^{2-}$  and  $Mg^{2+}$  in the reduced substratum of KD-1 suggest that similar processes take place also in somewhat further developed acid sulfate soils. An increase in  $HCO_3^-$  is not necessarily a consequence of sulfate reduction alone. Solution of carbonates ( $CaCO_3 + H^+ \rightarrow Ca^{2+} + HCO_3^-$ ) and bacterial ammonification (amino acids  $\rightarrow NH_4^+ + HCO_3^-$ ) may contribute too, but are probably of minor importance.

Sulfate reduction in a closed system generally leads within days or weeks to a virtually complete disappearance of dissolved sulfate. The same has been observed in some anoxic sea-bottom sediments indicating that diffusion of  $SO_4^{2-}$  limits sulfate reduction (Berner et al., 1970). In the mangrove muds studied here, however, at most 20 % of the sulfate was removed. Tidal flushing, aided by the high permeability of the muds is probably far more important than diffusion for the replacement of sulfate in mangrove sediments.

#### 4.2.2 Formation of iron sulfides

Dissolved sulfide reacts rapidly with dissolved ferrous iron or with ferric oxides to form black ferrous sulfide, which is amorphous according to X-ray diffraction or gives broad lines of mackinawite, tetragonal FeS. In the presence of oxidants such as  $O_2$  or ferric iron part of the dissolved or solid sulfide can be oxidized to elemental S. Elemental sulfur reacts with dissolved sulfide to form aqueous polysulfide, which in turn reacts with FeS to form pyrite,  $FeS_2$ , either directly or with greigite (cubic  $Fe_3S_4$ ) as intermediate (Rickard, 1973). The pathway involving greigite, which apparently requires atmospheric oxygen, yields framboidal pyrite, whereas the other reaction, in the absence of oxygen, gives non-framboidal pyrite (Rickard, 1975; Sweeny & Kaplan, 1973).

Of the various forms of reduced sulfur, only pyrite was identified by X-ray diffraction and by scanning electron microscopy (Figure 26). Along with other sulfur fractions (jarosite and water-soluble sulfate), pyrite was analysed chemically in samples vacuum-dried immediately after sampling to preclude oxidation. Analysis of pyrite (Appendix A) actually includes assay of elemental sulfur, part of the organic sulfur (Melville et al., 1971), and sulfides volatile with acid (i.e. ferrous monosulfide and greigite). Estimates of organic S from organic matter content and C/S ratio of 'average' organic matter

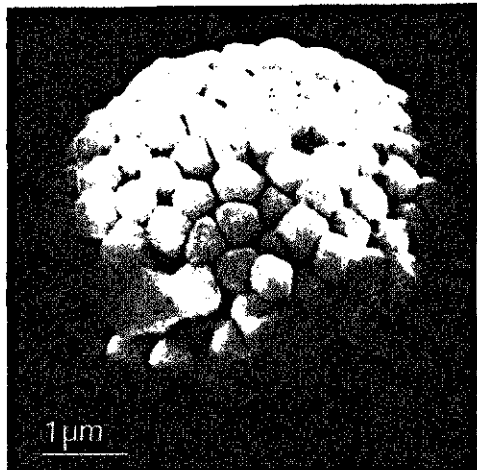
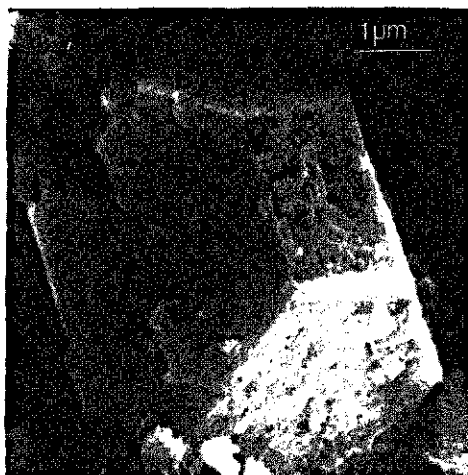


Figure 26

Scanning electron micrographs of pyrite in HF-treated residues of samples from KD-1 (left) and BP-1 (right). By courtesy S. Henstra, Technische en Fysische Dienst voor de Landbouw, Wageningen.

(Berner, 1971) and occasional estimates of FeS (by boiling the fresh soil with HCl and trapping and analysing the  $H_2S$  released) and elemental S (by extraction of fresh soil with chloroform and treating the residue as for estimation of pyrite) indicated that generally more than 95 % of the sulfur found can be attributed to pyrite. Analytical results for samples used both for total S analysis and analysis of pyrite, jarosite and water-soluble sulfate are plotted in Figure 27. Generally the calculated total sulfur was only slightly less than that measured by X-ray fluorescence, except for Mc-24 and the deepest substratum of KD-1, where this difference was much larger. The presence of relatively coarse-grained pyrite (Figure 26), which is not readily dissolved during pyrite analysis may explain the discrepancy.

In sulfidic marine sediments ferrous monosulfide is normally less than 0.01 %, expressed as mass fraction of S, and rarely exceeds 0.6 %, even in black muds (Berner, 1971). No sulfide volatile with acid was found in substrata of the older acid sulfate soils, and the highest amounts found in any of 10 dark greenish-gray samples from BP-1 and BP-6 was 0.001 %, although there FeS occurred in larger amounts in pockets rich in organic matter. Somewhat higher FeS contents were probably present at Ca-2, which is very dark gray - but not black - throughout. The negative logarithm of the solubility product of mackinawite,  $pK_{SO} = 17.55$  (Berner, 1967), is lower than pFeS observed at Ca-2 and Ca-3A (Table 8), indicating that the interstitial water is undersaturated

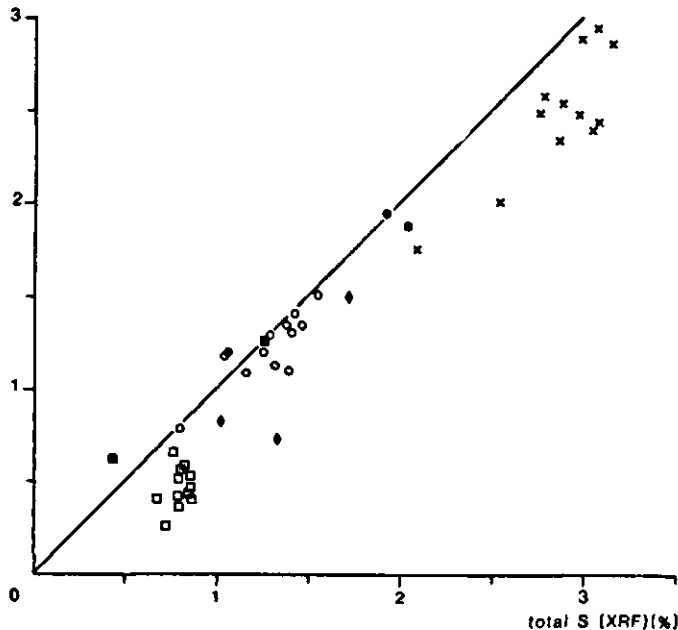


Figure 27

Relation of mass fraction of total sulfur calculated from pyrite + jarosite + water-soluble S with that measured by X-ray fluorescence spectroscopy (XRF) in oven-dried soil.

Artificially aerated samples:  $\times$  BP-1;  $\circ$  Ra-2;  $\square$  Mc-24

Field samples:  $\blacklozenge$  KD-1;  $\bullet$  Mn-1;  $\blacksquare$  KR-1.

with both amorphous FeS ( $pK_{SO} = 16.9$ ) and mackinawite. In the presence of elemental sulfur, the solubility product of pyrite can also be expressed as  $a(Fe^{2+}) \times a(S^{2-})$ , as follows from the reaction equation (Goldhaber & Kaplan, 1974):



The value for  $pK_{SO}$  for Eq. 5 is 27.6, so the pyrite solubility product (at least in the presence of elemental S) is 8-10 orders less than the observed FeS ionic activity products. This illustrates the strong driving force to pyrite formation. The relatively high pFeS found in the Cha-am Lagoon may indicate removal of ferrous iron and sulfide for pyrite.

Although the disappearance of FeS as a result of pyrite formation is in accord with thermodynamic principles, its paucity in mangrove muds is not at all obvious. Experiments by Rickard (1974, 1975), suggest that the rate-limiting step in formation of (non-framboidal) pyrite is pyritization of FeS (by the

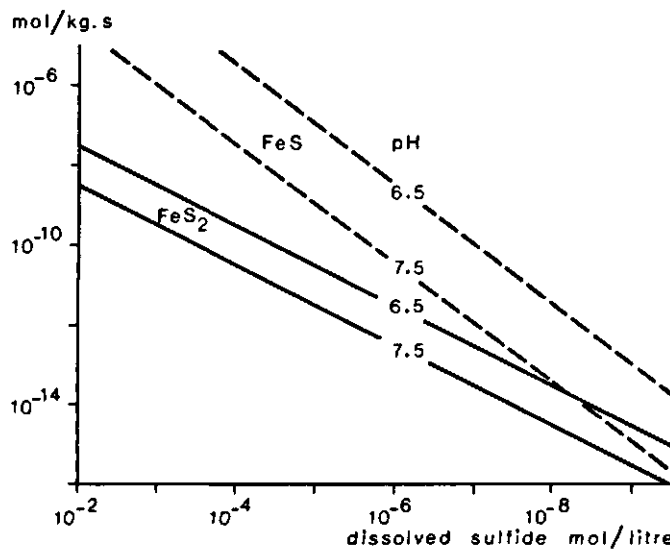


Figure 28

Substance content rate of formation of  $\text{FeS}_2$  (S) and  $\text{FeS}$  (S) expressed to oven-dried soils (mol/kg.s) as a function of total dissolved sulfide at  $25^\circ\text{C}$ , 0.5% reactive  $\text{Fe}_2\text{O}_3$  (with a specific surface of  $50 \text{ m}^2/\text{g}$ ), 0.1% elemental S ( $1.5 \text{ m}^2/\text{g}$ ), 0.005% FeS ( $70 \text{ m}^2/\text{g}$ ) and mass quotient of moisture 100% (from rate equations by Rickard, 1974, 1975).

reaction of FeS, elemental S and dissolved sulfide) and not sulfidation of goethite to FeS. This is illustrated by Figure 28, constructed from the rate equations given by Rickard. Under the specified conditions, FeS is formed much faster than pyrite at pH below 7.5 and dissolved sulfide above  $10^{-10}$  mol/litre. If so, FeS and not  $\text{FeS}_2$  ought to be accumulated. This is clearly at variance with the natural situation. The rate of FeS formation, however, is for the initial reaction only and rapidly decreases with time, especially at low pH (Rickard, 1974). Furthermore, as FeS is formed, the surface area of reactive iron oxide decreases, which also depresses FeS formation.

Under conditions that may be typical for BP-1 and Ca-2 (pH = 6.5; dissolved sulfide =  $5 \times 10^{-5}$  mol/litre; otherwise as for Figure 28), the percentage of pyrite S would increase by about  $1.5 \times 10^{-2}$  per year. This is in the order expected in view of the probable age of the sediments (several centuries to a thousand years) and the pyrite contents observed. In this respect, the assumed FeS content is particularly critical, because the rate of pyrite formation is second-order with respect to the FeS surface and first-order with respect to  $a(\text{H}^+)$ , dissolved sulfide and elemental sulfur. For instance, with a steady-state FeS content of 0.1% FeS, as much as 6% of pyrite S would be formed annually.

Under favourable conditions, large amounts of pyrite can be formed in the mangrove muds. Yet, as is described in Section 3.6, the not potentially acid substrata have distinctly lower pyrite contents than the potentially acid ones. In trying to account for this important difference, possible limiting factors in pyrite formation have been listed. Essential ingredients for pyritization are sulfate, organic matter, sulfate-reducing bacteria, anaerobic conditions, iron and time. Depletion of dissolved sulfate has never been observed in any sample from Thailand, and sulfate reducers are probably ubiquitous. If the sediment is saturated with water for longer than days or weeks, small amounts of organic matter are sufficient to lead to anaerobic conditions characterized by sulfate reduction. Such circumstances are normally present over large areas in most coastal marshes. So far, the conditions are similar to those in sea-bottom sediments, where organic matter is normally limiting (Rickard, 1973; Berner, 1971). In mangrove swamps, where large amounts of organic matter are supplied not only during sedimentation, but also later in the form of plant material, iron rather than organic matter could be in short supply.

The fraction of total iron readily available for pyritization probably includes part of the octahedral lattice iron of smectite clays, besides fine-grained ferric oxides (Berner, 1971; Drever, 1971). This fraction was estimated by assuming that only illitic iron (calculated on the basis 'average' illite with 4.6 %  $Fe_2O_3$  and 7.3 %  $K_2O$ , Weaver & Polard, 1973) is not available for pyrite formation. The ratio of pyrite Fe (calculated from total S contents) to total available iron (including the pyritized part), or the degree of pyritization,  $Py$  (see Berner, 1971), can then be found from

$$Py = \frac{Fe \text{ (pyrite)}}{Fe \text{ (total)} - Fe \text{ (illite)}} \quad (6)$$

The degree of pyritization is high ( $0.91 \pm 0.15$ ) in five samples from the Songkhla-Pattani region, indicating that there the amount of iron limits pyrite accumulation. Far lower  $Py$  values are observed in the Bangkok Plain:  $0.51 \pm 0.12$  for nine potentially acid samples (from BP, KD, KR, Na, Ra and O), and  $0.35 \pm 0.12$  for six not potentially acid samples (from T, Bk, KD, Mc-24 and Mn). The difference between the two groups is significant ( $P < 0.05$ ), suggesting that some other factor besides amount of available iron played a role in pyritization.

Work by Diemont & van Wijngaarden on pyrite formation in mangrove areas along the east coast of Malaysia provides important clues to this problem (Diemont et al., in preparation). With regard to the chemistry of sulfur, they

found striking differences between estuarine areas, intersected by numerous tidal channels and covered mainly by *Rhizophora* species, and accretionary coastal areas, with few tidal creeks and characterized by *Bruguiera* trees. Pyrite was low and free iron relatively high in sediments of the accretionary coast, whereas the reverse was true for the estuarine environment. Little or no FeS was present in either environment. Using poles painted with red-lead (Wiedemann, 1973), they found similar levels of dissolved sulfide (estimated to be in the order of 0.05 mmol/litre) in deposits of both types. The sulfide was always present on the accretionary coast, but was absent during spring tides in the estuarine marshes. This difference was attributed to a higher intensity of tidal flushing, due to the abundance of creeks in the estuary. Much higher levels of dissolved  $\text{HCO}_3^-$  and associated higher pH values (about 7.5 under *Bruguiera* and between 6.5 and 7 under *Rhizophora*) also indicated more stagnant conditions in the sediments of the accretionary coast.

The relatively low pH and the periodic removal of dissolved sulfide offer an explanation for the higher degree of pyritization in the estuarine marshes. In the first place, pyrite formation is favoured kinetically by low pH in the range 4-8 (Goldhaber & Kaplan, 1974; Fig. 28). Secondly, partial oxidation of sulfide to elemental sulfur by an oxidant other than ferric iron is prerequisite for complete pyritization of a given amount of ferric oxide, and limited aeration<sup>a</sup> provided by tidal flushing could thus promote the formation of pyrite. The relationship between potential soil acidity and depth for groups of soils from different altitudes at the Bang Pakong Land Development Centre (van Breemen et al., 1973) shown in Fig. 29 indicates that potential acidity (and the pyrite content) is highest in a layer at a certain altitude rather than at a certain depth below the soil surface. This layer may be related to the zone dominated by tidal flushing. Above the layer, oxidized conditions predominate and no sulfate reduction occurs, whereas stagnant conditions somewhat restrict pyrite formation at greater depth.

The differences between accretionary coasts and strongly dissected estuaries in pyrite formation are helpful in understanding the pattern of acid sulfate soils and non-acid soils found in the southern strip of the Bangkok Plain. According to the generalized soil map (Insert), young acid sulfate soils

---

a. With ferric iron as the only oxidant, at most half of the available Fe(III) can be pyritized:  $2\text{Fe(III)} + 3 \text{S(II)} \rightarrow \text{FeS}_2 + \text{FeS}$ . Autoxidation according to  $\text{FeS} + \text{H}_2\text{S} \rightarrow \text{FeS}_2 + \text{H}_2\text{(gas)}$  is theoretically possible, but would lead to  $E_H$  values much lower than have been observed.

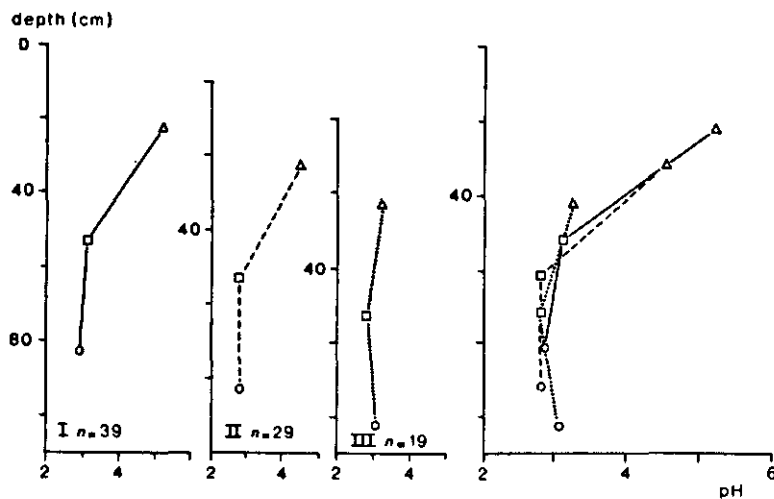


Figure 29

Average pH of aerated soil against depth in three sets of profiles from the Bang Pakong Station (near site BP-1), grouped on the basis of altitude of the soil surface (indicated by the different zero levels). In the right diagram pH values are plotted with reference to soil surface at the highest sites (Group I).  $n$  is the number of sampling sites in each group.

and potentially acid sulfate soils predominate near the Bang Pakong Estuary and the tidal creek of Khlong Dan, and are relatively scarce in between. The absence of acid and potentially acid sulfate soils near the mouths of the Tha Chin and Mae Klong Rivers is undoubtedly related to the calcareousness of the sediments of the southeastern part of the Bangkok Plain. It is not known whether the estuarine sediments there are also higher in pyrite than the sediments of the accretionary coast. By maintaining the pH at a relatively high level, the presence of lime may have depressed pyritization to some extent in these estuarine environments.

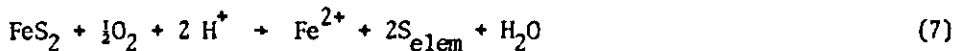
Relatively low pyrite contents in the most recent coastal sediments may be related also to the time available for pyrite formation. If the coastline advances rapidly, mangrove swamps prevail for a relatively short time at a given site, so conditions favourable for pyrite formation are short-lived (Moermann & Pons, 1974). Again, more pyrite can be fixed near estuaries where mangroves hold out longer.

A different set of conditions was probably responsible for the widespread pyrite accumulation in the older part of the Bangkok Plain, where thick deposits were formed behind a relatively stable coastline and where tidal flooding may have prevailed over large areas for a long time.

#### 4.3 OXIDATION OF PYRITE

Before discussing pyrite oxidation in relation to acid sulfate soils, the main conclusions of two recent literature surveys on this subject (van Breemen, 1973b; Bloomfield & Coulter, 1973) will be summarized briefly.

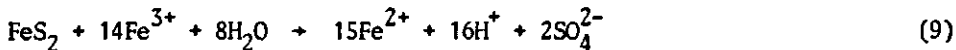
Fig. 22 illustrates that pyrite is stable only at low  $E_H$ , i.e. under reduced conditions, and will be oxidized in oxygenated environments. Dissolved aqueous oxygen, however, attacks pyrite only slowly at first, yielding ferrous iron and elemental sulfur:



Further oxidation of elemental S to sulfate with  $\text{O}_2$  as oxidant is an even slower process. Dissolved ferric iron, on the other hand, reacts rapidly with pyrite according to



Under most experimental conditions, further oxidation of elemental sulfur by ferric iron is virtually instantaneous, and the total reaction proceeds as follows



Because ferric iron is appreciably soluble only at low pH (< 4), Reactions 8 and 9 are limited to acid environments. In the presence of oxygen, the dissolved ferrous iron produced by Reaction 9 can be further oxidized to ferric iron, and pyrite oxidation can continue. Again however, there is a kinetic restriction: at low pH the oxidation of  $\text{Fe}^{2+}$  by  $\text{O}_2$  is slow.

But a number of autotrophic microbes, capable of deriving energy from the oxidation of reduced sulfur, are instrumental in breaking down the various kinetic barriers existing in the purely chemical systems considered so far. The most important bacteria belong to the genus *Thiobacillus*, usually referred to as thiobacilli. *T. thioparus* and several other thiobacilli oxidize elemental sulfur and some reduced compounds of sulfur at near neutral pH, using oxygen (and sometimes nitrate) as oxidant. These organisms may be important in oxidizing the elemental sulfur (produced by Reaction 7) to sulfuric acid, and may thus cause the initial acidification necessary for further rapid oxidation by

Reactions 8 and 9. *Thiobacillus ferrooxidans*, which grows optimally between pH 2.5 and 5.8 (Goldhaber & Kaplan, 1974) oxidizes ferrous iron and various reduced sulfur species, and is responsible for producing ferric iron. *T. thiooxidans* is also acidophilic, but cannot utilize ferrous iron.

The thiobacilli seem to be invariably present in acid sulfate soils and other environments characterized by pyrite oxidation. This factor, together with the acidophily of several thiobacilli (including *T. ferrooxidans*), the high rate of Reaction 9 and the fact that ferric iron is appreciably soluble only at low pH, explains the strong positive effect of high acidity on the rate of pyrite oxidation, noted by numerous workers.

In this study no attention was given to sulfur species with oxidation states intermediate between elemental sulfur and sulfate. These are produced during oxidation of sulfides and elemental sulfur, but their concentrations apparently remain low (Purokoski, 1958), in accordance with theoretical stability relations (Valensi et al., 1963). However there are indications that appreciable amounts of gaseous  $\text{SO}_2$ , which is released from dissolved sulfite at low pH, escape from oxidizing pyritic sediments (Section 6.2).

#### 4.3.1 Pyrite oxidation under field conditions

The profile diagrams of Fig. 11 illustrate that pyrite abruptly appears in the gray or greenish-gray substratum, and increases with depth. This increase is most pronounced in the first 10-30 cm, but continues at least 30-60 cm further, indicating oxidation of pyrite to depths considerably below the upper boundary of the C horizon. This is corroborated by thin sections of substrata showing quasi-ferrans or quasi-jarositans bordered by a pyrite-free zone. This zone may be up to 5 mm wide in the upper part of the pyrite substratum and only 0.5 mm at greater depth. Sometimes six to eight quasiferrans/jarositans, each 0.1-0.5 mm thick and up to 1 mm apart can be distinguished, indicating periodic pyrite oxidation at depth. From the presence of 'oxidized fingers' penetrating into the C horizon (van Dam & Pons, 1973; Miedema et al., 1974), one may expect a considerable heterogeneity in redox potential and pH. Average standard deviations of two to four (triplicate) measurements in pyritic substrata from the Rangsit-Ongkharak region (Table 10), however, show that the pH varies little with siting of the electrode. The same uniformity of pH in substrata was observed during systematic soil sampling for pH measurement. Redox potentials are quite variable, but the reproducibility tends to improve with the duration of flooding. This points to a heterogeneity in  $E_H$  at the end of the dry season

Table 10. Mean standard deviations ( $\bar{s}$ ) of  $E_H$  and pH in pyritic substrata of four pedons 1 month before and 1, 3 and 5 months after flooding.

Site	Depth (cm)	$\bar{s}(E_H)/\text{mV}$				$\bar{s}(\text{pH})$			
		months after flooding				months after flooding			
		-1	1	3	5	-1	1	3	5
0-1	130-190	162	.	.	.	0.03	.	.	.
Ra-1	120-220	.	76	42	17	.	0.01	0.04	0.02
Ra-2	100-200	.	17	39	.	.	0.10	0.10	.
Ra-3	100-220	.	97	.	59	.	0.04	.	0.14

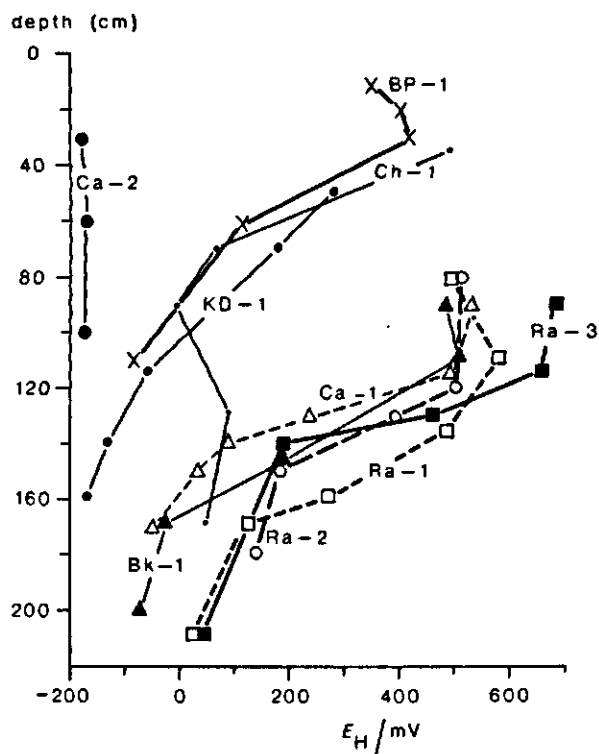


Figure 30  
 $E_H$  against depth in a mangrove mud (Ca-2), two young acid sulfate soils (BP-1 and KD-1) and a number of older acid sulfate soils.

which decreases to some extent upon flooding. The variation in  $E_H$  within a particular sample is normally small compared with the decrease in  $E_H$  with depth in the upper part of the pyritic substratum (Fig. 30). So the redox gradient is predominantly vertical, and does not have a strong horizontal component attributable to 'oxidized fingers'.

Fig. 31 summarizes all  $E_H$ -pH measurements in pyritic field samples and shows conditions for equilibrium between pyrite and dissolved sulfate plus iron

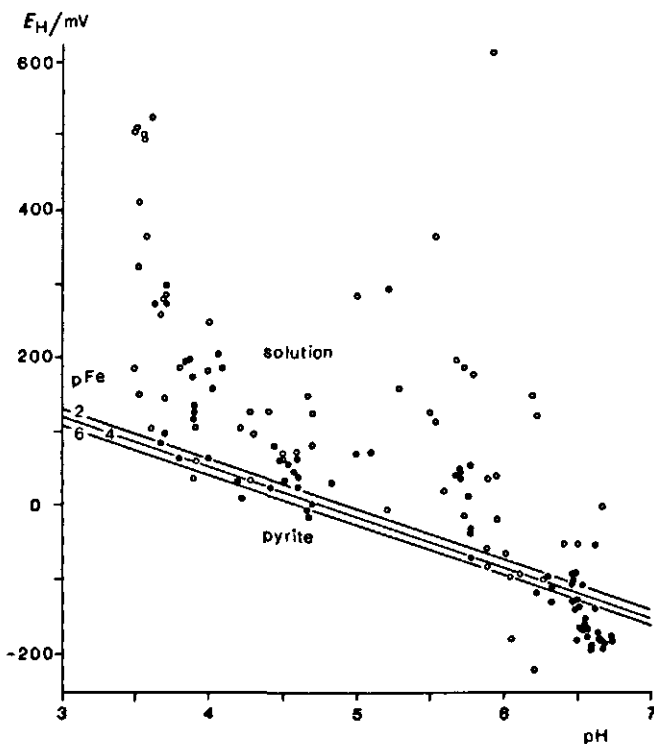
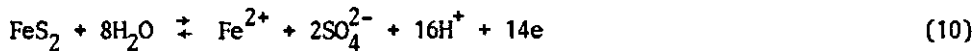


Figure 31

$E_H$ -pH data of pyritic samples. The lines are for equilibrium between pyrite and the solution at  $pSO_4 = 2.3$  and different values of  $pFe$ . Open symbols indicate poor reproducibility; solid symbols good reproducibility (compare Fig. 23).

according to



with  $pK_{10} = 85.4$  (calculated from thermodynamic data by Robie & Waldbaum, 1968) at a representative dissolved sulfate activity ( $pSO_4 = 2.3$ ) and a range of typical  $Fe^{2+}$  activities. Pyritic samples with ongoing sulfate reduction (i.e. most of the mangrove mud samples with a pH between 6.4 and 6.8) where  $pFe$  is normally about 5, are almost invariably more reduced than equilibrium according to Eq. 10 would predict. In substrata distinctly influenced by pyrite oxidation ( $pH < 6$ ), however, the pyrite-solution boundary seems to function as a lower limit of  $E_H$ . The same was observed in thermal spring waters ( $17-39^{\circ}C$ ) of Virginia (Helz & Sinex, 1974). This is surprising because it is well-nigh impossible that a complicated heterogeneous reaction such as given by Eq. 10 establishes a reversible electron exchange at a platinum electrode. Whatever

the mechanism, the result suggests that  $E_H$ -pH data and solution composition can serve to obtain a meaningful disequilibrium index with respect to pyrite. This has been done, by considering the reaction



with

$$pK_{11} = pK_{\text{so}}(\text{Pyr}) = p\text{Fe} + p\text{S}_2 \quad (11a)$$

Regardless of equilibrium, we can write for the activity product of the ions  $\text{Fe}^{2+}$  and  $\text{S}_2^{2-}$

$$p\text{FeS}_2 = p\text{Fe} + p\text{S}_2 \quad (11b)$$

The ratio of the actual ionic activity product to the theoretical solubility product, expressed as  $pK_{\text{so}}(\text{Pyr}) - p\text{FeS}_2$  is called the disequilibrium index,  $D(\text{Pyr})$ , which quantifies the extent to which the solution is removed from equilibrium (Paces, 1972). If  $D(\text{Pyr})$  is positive, the solution is supersaturated with pyrite; a negative value indicates undersaturation and at equilibrium  $D(\text{Pyr})$  is zero. To calculate  $D(\text{Pyr})$  the equilibrium equations for Eq. 10 and 11 are combined with Eq. 11b, resulting in

$$D(\text{Pyr}) = 85.4 - 2p\text{SO}_4 - p\text{Fe} - 16 \text{ pH} - 14\text{pe} \quad (12)$$

In Eq. 12, 'pe' stands for the negative logarithm of 'electron activity', which, at 25 °C, is numerically equal to  $E_H/0.059$ . Thus  $D(\text{Pyr})$  can be evaluated without recourse to thermodynamic data on the disulfide ion  $\text{S}_2^{2-}$ ; in fact, this species need not even exist.

Fig. 32 shows disequilibrium indices of pyrite (and goethite and jarosite) against depth in a development sequence of acid sulfate soils. The  $D$  values often refer to samples collected at different times and so do not necessarily represent a single profile at a given moment. In the unoxidized mangrove muds and the deeper pyritic substrata of acid sulfate soils, the soil solution appears to be relatively close to equilibrium with pyrite. By contrast strong undersaturation prevails from the upper part of the C horizon upwards. The redox potential has an overriding influence on the stability of pyrite, as can be seen by comparing Figs. 30 and 32. In pedon KD-1 two months after flood-

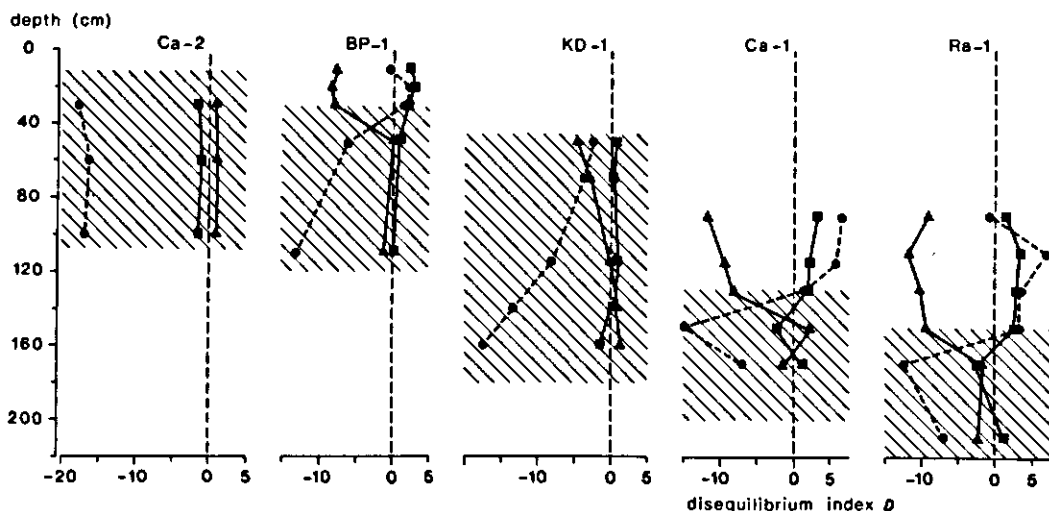
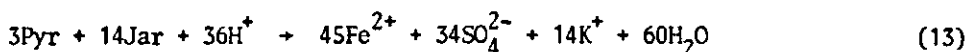


Figure 32  
Disequilibrium indices ( $D$ ) for pyrite ( $\blacktriangle$ ,  $D(\text{Pyr})/10$ ), goethite ( $\blacksquare$ ) and jarosite ( $\bullet$ ) against depth in five soils. The presence of pyrite is indicated by hatching.

ing, moderate undersaturation with both jarosite and pyrite occurs between 50 and 70 cm depth, a zone where these two minerals are in fact present (Fig. 21). Samples from 50 cm depth 2 and 4 months after flooding showed that the  $E_H$  decreased from 280 to 80 mV, whereas  $\text{Fe}^{2+}$  increased from 7 to 14 mmol/litre. Concurrently,  $D(\text{Pyr})$  changed from -48.2 (strong undersaturation) to 0.14 (close to equilibrium) and the undersaturation with jarosite deepened. Although differences in sampling site may have played a role, the results strongly suggest that after flooding jarosite (Jar) is reduced by pyrite (Pyr) according to



Conversely, this process can be visualized as oxidation of pyrite by ferric iron formed during previous dry seasons. Flooding would cut down the aeration of the larger channels and cracks, and put an end to the cause of the heterogeneity in the upper part of the substratum. Solution and diffusion of small amounts of ferric iron (present as jarosite or ferric oxide along channels) could cause oxidation of pyrite according to Eq. 9.

Dissolved ferrous iron in the upper part of the pyritic substratum increases also in Ra-1 and Ra-2, but not in the non-acid T-1 (Fig. 33). In acid sulfate soils from a chronosequence in Senegal, Vieillefon (1973, 1974) also observed a pronounced increase in dissolved iron in the upper part of the pyritic

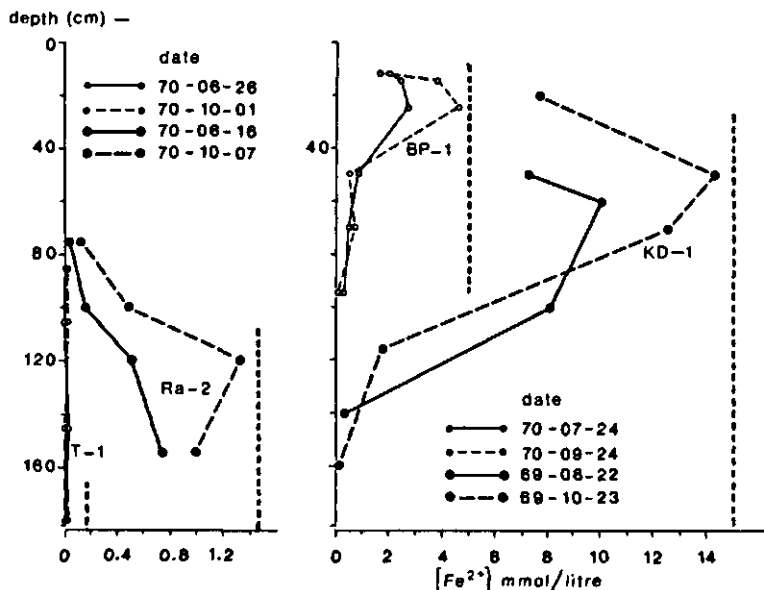


Figure 33  
 Dissolved  $\text{Fe}^{2+}$  against depth in three acid sulfate soils (Ra-2, BP-1 and KD-1) and one non-acid marine soil (T-1) at two different dates during the wet season. Broken vertical bars indicate the presence of pyrite.

substratum upon flooding. No such effect was noted in a completely reduced pyritic mangrove soil in the same sequence. The increase in  $\text{Fe}^{2+}$  in the youngest acid sulfate soil, BP-1 (Fig. 33), did not coincide with flooding, but with a periodic lowering of the watertable and must be ascribed to oxidation of pyrite by atmospheric oxygen.

Theoretically, the observed changes in pH and in dissolved iron, sulfate and potassium could suggest the causative process by considering the stoichiometry of the various reactions (See also Table 11):

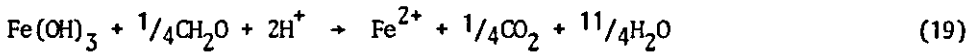
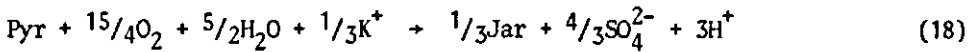
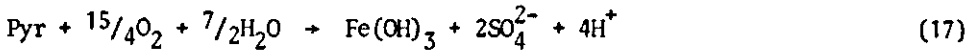
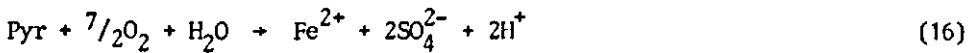
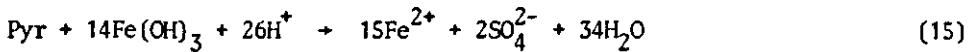
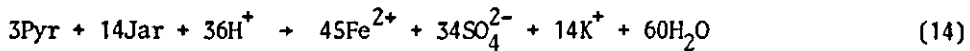


Table 11. Ratios of increments in amount of substance of products in possible reactions of pyrite, jarosite, ferric hydroxide and organic matter as calculated from stoichiometric equations.

Eq.	$\Delta [\text{SO}_4^{2-}] / \Delta [\text{Fe}^{2+}]$	$\Delta [\text{SO}_4^{2-}] / \Delta [\text{K}^+]$	$\Delta \text{pH}$
14	0.75	2.4	positive
15	0.13	$\pm \infty$	positive
16	2	$\pm \infty$	negative
17	$\pm \infty$	$\pm \infty$	negative
18	$\pm \infty$	-4	negative
19	$\pm \infty$	.	positive

Actually desorption and adsorption of sulfate (upon increase and decrease of pH, respectively) and exchange of ferrous iron against other adsorbed cations strongly affect the concentrations of the ions in question. For instance in Reactions 14, 15 and 19, adsorption of  $\text{Fe}^{2+}$  and desorption of  $\text{SO}_4^{2-}$ , would cause far higher  $\Delta \text{SO}_4 / \Delta \text{Fe}$  than expected from the stoichiometry of the reactions.

Therefore, observed high values for  $\Delta \text{SO}_4 / \Delta \text{Fe}$  (1.4-8.4 at BP-1, 3.9 at KD-1 and 2.4 at Ra-2) do not preclude reduction of ferric iron by organic matter, in fossil form in the substratum as the cause of the increase in dissolved  $\text{Fe}^{2+}$ . But in view of the ancient, and presumably somewhat humic character of the organic matter this must be of minor importance. The strong buffering capacity of the acid soil material (base equivalent content 60-120 mmol/kg per pH unit in the range 3.7-4.0; Sombatpanit, 1970) would bring the change in pH with the processes of Reactions 14-19 within analytical uncertainty. For instance, if the release of sulfate accompanying the increase in dissolved  $\text{Fe}^{2+}$  in KD-1 at 50 cm depth (Figure 33) be due to Reaction 14, and if the necessary protons be supplied by desorption of sulfate, pH would increase by at most 0.2. The changes in pH in Ra-2 and BP-1 would be much smaller. The observed increase in dissolved iron would be accounted for by a small decrement in mass fraction of pyrite S : of the order of  $10^{-2}\%$  at KD-1 and  $10^{-3}\%$  at Ra-2.

Because pyrite and ferric oxide or jarosite are normally spatially separate, diffusion of dissolved ferric iron towards pyrite is necessary. This is shown schematically in Fig. 34b. The abrupt (pyrite-facing) boundary of some quasiferrans suggests solution of ferric iron and corroborates this model.

The ultimate oxidant in pyrite oxidation is, of course, atmospheric oxygen. Pyrite oxidation during flooding can be considered as delayed oxidation from oxidative capacity stored temporarily as ferric oxide that had been formed during a preceding dry season.

Little direct information is available on pyrite oxidation in the dry

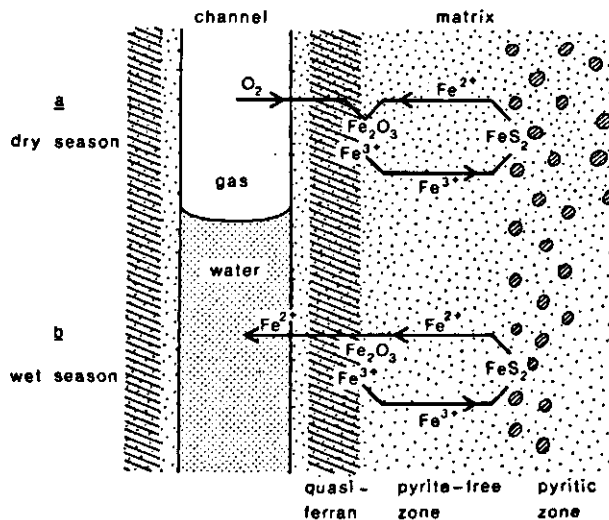


Figure 34

Model of pyrite oxidation in the substratum of acid sulfate soils during period of low watertable (a) and during flooding (b).

season. The distinct separation between pyritic soil and the ferrans or jarositans near channels and cracks, shows that oxygen is inactivated by dissolved  $Fe^{2+}$  before it can reach the pyrite. This implies that ferric iron must be the immediate oxidant of pyrite also during the dry season (Fig. 34a). At near-neutral pH, the mobility of ferric iron is extremely low, causing virtual disappearance of the pyrite-free zone. This may cause formation of ferric oxide pseudomorphs from pyrite, as observed by Miedema et al. (1974) in calcareous pyritic sediments. The same may happen if the supply of oxygen is abundant, for instance upon sudden, deep drainage. In that case, diffusion of  $O_2$  may 'overtake' the diffusion of dissolved ferric iron, causing formation of ferric oxide or even jarosite adjacent to pyrite (Miedema et al., 1974).

Pyrite oxidation during the dry season lowers the pH. For a measurable drop in pH (e.g.  $> 0.2$ ), at least 0.04-0.05% pyrite S must be oxidized if the buffering capacity is in the order of 120 mmol/kg per pH unit. The pH of soil and of soil solution in the upper part of the pyritic substratum at the Rangsit toposequence at the end of the dry season and during flooding generally differed by less than that. But at Ca-1 and Ch-1 periods with low watertables were associated with a markedly lower pH in the soil just below the boundary of the C horizon.

Especially in the older acid sulfate soils strong pyrite oxidation associated with marked acidification may take place in very dry years only. The

first dry season of fieldwork, that of 1969, can be taken as normal; that of 1970 as wetter than normal (about one in every three years is 'severely dry', Kambhu, 1961). The deepest watertable observed at Ra-3 was 116 cm below the surface, so the well developed single quasiferran at 150 cm and the series of 5-10 concentric quasiferrans at 120 cm, visible in thin sections, must have been formed in drier years.

#### 4.3.2 Pyrite oxidation in artificially aerated samples

The immediate effects of pyrite oxidation are hard to detect in the field, but are immediately evident in pyritic samples artificially exposed to the atmosphere. This came to light during an oxidation experiment with pyritic samples from substrata of two acid sulfate soils, (Ra-2, BP-1) and a non-acid marine soil (Mc-24). Relevant chemical characteristics at the start of the experiment are given in Table 12. Immediately after sampling, the soil was frozen and stored for 2-3 months. After defrosting, each sample was split. Half was mixed with distilled water to a moisture content of about 180% (relative to oven-dried mass) and the other half was treated likewise with sea-water from the Gulf of Thailand. Next, six 130 g portions of each wetted subsample were placed in 500 cm<sup>3</sup> plastic jars. All samples were aerated at 25-27 °C by simply leaving the jars open in the laboratory. After evaporation of most of the water, the samples were kept moist (approximately at field capacity) by regularly adding small amounts of distilled water. Periodically, one sample of each series was wetted and thoroughly mixed with distilled water to the original moisture content. Three days later, the redox potential and pH were measured, and the water was recovered by centrifuging and analysed for all major constituents. Except for the last lot of soil samples, which were freeze-dried, the

Table 12. Analytical data on the soil samples used for the oxidation experiment. Percentages refer to mass fraction in oven-dried soil.

Site	Depth (cm)	pH	clay (%)	soluble SO <sub>4</sub> <sup>2-</sup> S(%)	pyrite S(%)	total S <sup>a</sup> (%)	CaCO <sub>3</sub> (%)	Fe <sub>2</sub> O <sub>3</sub> (d) <sup>b</sup> (%)
BP-1	40-60	6.9	52	0.07	2.65	3.0	-	0.5
Ra-2	195-210	4.3	65	0.05	1.42	1.55	-	0.9
Mc-24	200-220	7.6	53	0.04	0.50	0.79	5.1	2.4

a. Analysed by X-ray fluorescence spectroscopy.

b. Dithionite extractable.

soils were vacuum-dried at 105 °C immediately after water sampling and used for assay of pyrite, jarosite, water-soluble sulfate and the cation-exchange complex. The duration of the experiment was about 9 months.

A separate set of samples, made up of one sample from each series, was treated alike except that after collection of the interstitial solution each soil was again mixed with distilled water or sea-water and aerated before re-wetting with distilled water and again recovering the soil solution. This leaching process, designed to simulate an open system, was repeated 5 times in 9 months.

Fig. 35 shows the effect of aeration on the pH. After an initial lag phase, the pH of the BP and Ra samples decreased rapidly to almost constant values around 2.0. The pH fell somewhat more gradually with sea-water treatment than with distilled water, but at the end there was little difference in this respect. The calcareous soil Mc did not acidify at all.

Fig. 36 shows the effect of aeration on the sulfur fractions. For samples from BP and Ra, the amounts of pyrite as a fraction of total S exhibit a course closely resembling the pH curves of Fig. 35. The concomitant increase in water-soluble and jarosite sulfate demonstrates that disappearance of pyrite is caused by oxidation. In Mc, pyrite is oxidized slower than in the acidifying samples (Fig. 37).

The decrease in the rate of pyrite oxidation after 82 days, observed in the acid soils can be explained by adverse effects of low pH on thiobacilli (Hart, 1959; Vieillefon, 1974), or increasing resistance to oxidation of the

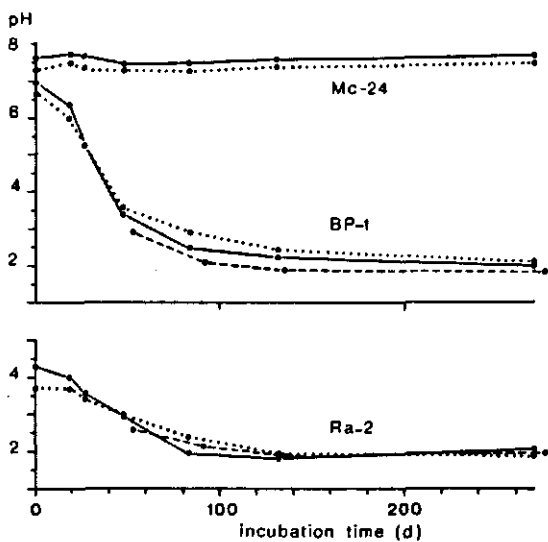
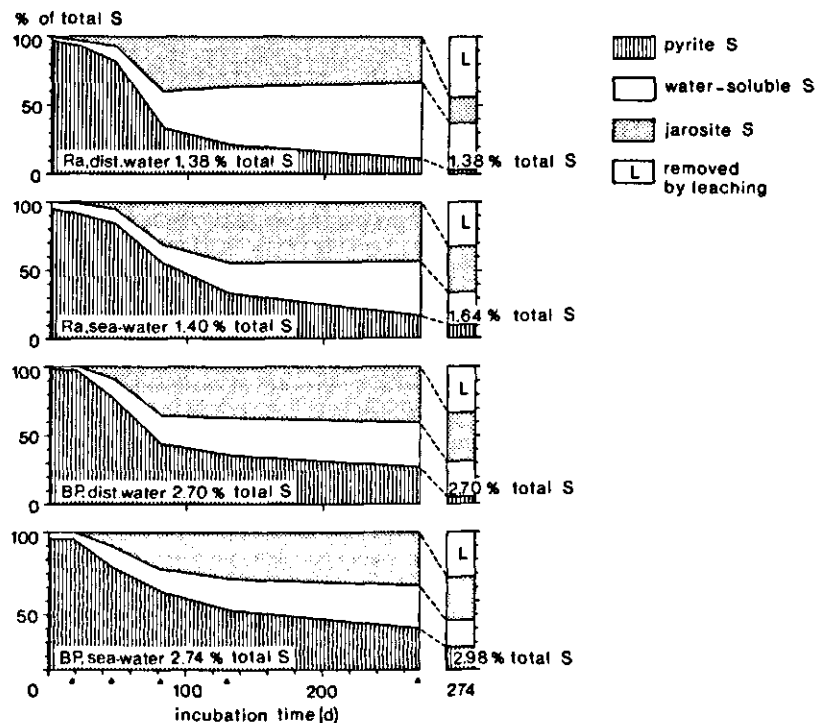
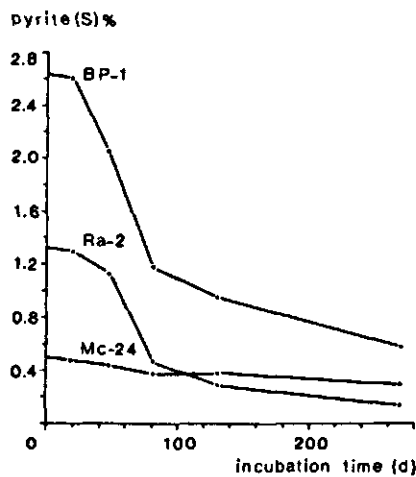


Figure 35  
Effect of artificial aeration on pH of samples from two potentially acid substrata (Ra-2 and BP-1) and one calcareous pyritic sample (Mc-24). Key:  
— distilled water, no leaching  
······ sea-water, no leaching  
- - - distilled water, plus leaching



**Figure 36**  
Changes in relative importance of different sulfur fractions upon artificial aeration of potentially acid samples, treated either with distilled water or with sea-water at the outset. The right hand columns represent samples that were leached four times with sea-water or distilled water.



**Figure 37**  
Changes in mass fraction of pyrite (S) in dried soil during artificial aeration after adding distilled water of two potentially acid soils (BP-1 and Ra-2) and one not potentially acid soil (Mc-24).

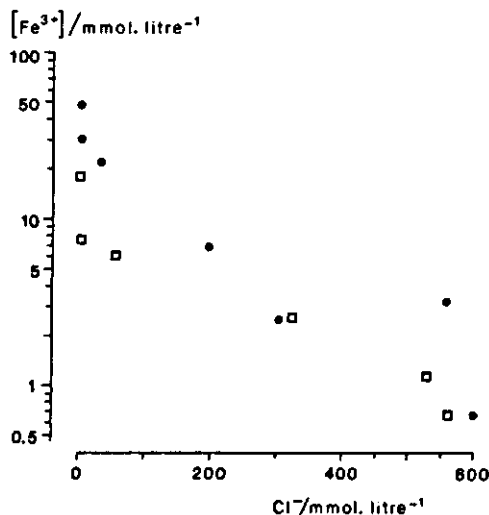


Figure 38

Relation between total dissolved ferric iron and dissolved chloride in strongly acidified (pH 1.8-2.0) pyritic soil samples.

Key:  $\square$  incubated 4½ months;  
 $\bullet$  9 months.

remaining pyrite (Hart, 1963). After 130 days, dissolved ferric iron increased at the expense of ferrous iron. Increasing resistance is therefore probably the explanation: unless the pyrite residue was indeed more resistant to oxidation, higher levels of  $Fe^{3+}$  would result in an increase, not a decrease, in oxidation rate (Garrels & Thompson, 1960). Moreover, in view of the very slow abiotic oxidation at a pH as low as 2, the ferric iron is probably produced mainly by *Thiobacillus ferrooxidans*. This is corroborated by the negative correlation between dissolved  $Cl^-$  and dissolved  $Fe(III)$  (Fig. 38) since the activity of *T. ferrooxidans* is hampered by high chloride concentrations (Silverman, 1967). The adverse effect of chloride on thiobacilli explains why samples treated with sea-water lost less pyrite than those treated with distilled water (Fig. 36).

Leaching removed between 20 and 50% of total sulfur and promoted oxidation of pyrite. This may be due to the periodic (physical) removal of intermediate reaction products such as  $Fe^{2+}$  and elemental S from near pyrite particles, removing rate-limiting diffusion steps. The leaching rate (400 ml/130 g wet soil in nine months) is undoubtedly much higher than under typical field conditions, at least in areas outside direct tidal influence. Therefore the conclusion by Bloomfield & Coulter (1973) that leaching in the field is mainly responsible for the higher pH of naturally oxidized pyritic material seems incorrect. In fact, in spite of the high rate of leaching in the laboratory, dissolved sulfate reached levels 2-10 times as high as that observed in the field. A more plausible explanation is that pyrite oxidizes far more rapidly

under the experimental conditions, most probably through intense aeration. So the supply of oxygen appears to be the rate-limiting step in pyrite oxidation in soils *in situ*, a conclusion also put forward by Rasmussen (1961). Indeed very low pH values (i.e. about 2.0), were observed in the field on several occasions: (a) when pyritic soil was dug up and directly exposed to the air, as in ridges built for improving desalinization at the Bang Pakong Station (van Breemen et al., 1973); (b) in ground water in auger holes (with a watertable below the upper limit of the pyritic substratum) left open overnight at Ch-1.

#### 4.4 OXIDATION PRODUCTS OF PYRITE

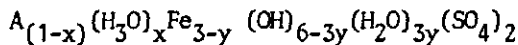
The ferrous iron, hydrogen and sulfate ions released during pyrite oxidation normally undergo various further reactions in the soil. Protons are largely inactivated by different buffering reactions (Chapter 5 and 6). Essentially all ferrous iron is ultimately oxidized to ferric iron, which precipitates as jarosite ( $KFe_3(SO_4)_2(OH)_6$ ), poorly crystallized goethite, or amorphous ferric oxide. The larger part of the sulfate released during pyrite formation, however, remains in solution and is removed from soil by leaching, and by diffusion into the surface water. The remaining sulfate is partly precipitated, either as jarosite or as the basic aluminium sulfate,  $Al(OH)SO_4$  (van Breemen, 1973c) and partly adsorbed, mainly by ferric oxides. Under relatively dry conditions, gypsum ( $CaSO_4 \cdot 2H_2O$ ) can form. Under strongly evaporative conditions, surface crusts of still more soluble sulfates such as sodium alum ( $NaAl(SO_4)_2 \cdot 12H_2O$ ), tamarugite ( $NaAl(SO_4)_2 \cdot 6H_2O$ ), pickeringite ( $MgAl_2(SO_4)_4 \cdot 22H_2O$ ) and rozenite ( $FeSO_4 \cdot 4H_2O$ ) have been observed. Under anaerobic conditions, sulfate can be reduced again to sulfide, which may, temporarily, be fixed as  $FeS$ . In very young acid sulfate soils still under tidal influence, this sulfide may even be incorporated in pyrite again.

The properties of some of the oxidation products, and the processes involved in their formation will be discussed below.

##### 4.4.1 Jarosite

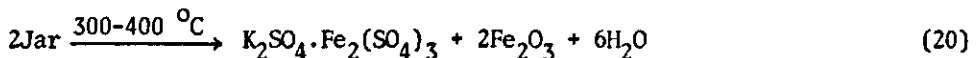
*Properties of jarosite* The most conspicuous feature of practically all acid sulfate soils is the presence of pale yellow jarosite, found in almost pure form in root channels and cracks, or closely associated with the matrix as mottles and quasicutans. Jarosite is a member of the rhombohedral alumite group (space group 3M), a series of basic sulfates with the general formula

$AB_3(SO_4)_2(OH)_6$  in which A is K, Na,  $H_3O$ ,  $\frac{1}{2}Pb$ ,  $NH_4$  or Ag and where B represents Fe(III) (jarosites) or Al (alunites). Substitution of  $K^+$ ,  $H_3O^+$  and  $Na^+$  results in a virtually complete solid solution of jarosite (the potassium form), hydronium jarosite and natrojarosite  $(NaFe_3(SO_4)_2(OH)_6)$ . There is a high preference for  $K^+$  over  $Na^+$  and  $H_3O^+$ , especially at high temperatures and pressures (Brophy & Sheridan, 1965; Brown, 1970). Many natural and artificial jarosites contain excess water. Brophy & Sheridan (1965) attribute this almost entirely to adsorbed water and to hydronium but according to Kubicz (1970) excess water is structural and is related to iron deficiency as follows:

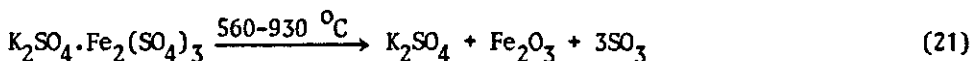


Alumite and jarosite also form a solid solution, but intermediate minerals are rare in nature. During synthesis the preference of Fe over Al was high at 105 °C, and decreased with increasing temperature and with decreasing acidity of the reagent solution (Brophy et al., 1962). For minerals synthesized between 80 and 150 °C, X-ray diffraction and thermal analysis can be used to estimate the extent of substitution of monovalent and trivalent ions (Brophy & Sheridan, 1965; Brophy et al., 1962). But jarosite and hydronium jarosite from relatively dilute solutions precipitated at room temperature showed no correlation between lattice parameters and the contents of potassium and hydronium (Brown, 1970).

Jarosite usually occurs as earthy yellow masses of individual grains generally 0.1-0.5  $\mu m$  in diameter (Figure 39). X-ray diffraction patterns of material from yellow mottles sampled in Thailand invariably yielded clear jarosite patterns (Table 13). The typical strong peaks at 0.308 and 0.311 nm permit detection, even if present at a few percent. Natrojarosite was not observed in any of the samples from Thailand, but was common in acidified lobster mounds from Sarawak (Andriesse et al., 1973). X-ray diffraction revealed the presence of jarosite also in most yellowish-brown mottles from the jarositic horizon and the horizon over it, and even in some red mottles. Differential thermal analysis (DTA) of field samples of jarosite gave endothermic peaks near 450 and 800 °C, attributed to the reactions



and



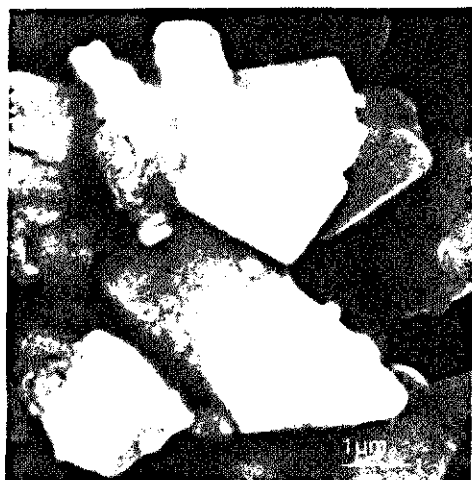
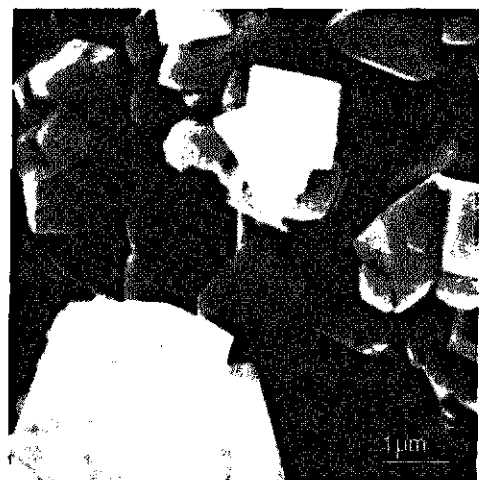


Figure 39

Scanning electron micrographs of fresh jarosite (left) and the same jarosite dialysed for about 4 months (right). Courtesy S. Henstra, TFDL, Wageningen.

Table 13. Lattice spacings (nm) and peak intensities of jarosite from yellow and brown mottles from acid sulfate soils measured from photographs taken with a Guinier-De Wolff camera. Further details about some samples are given in Table 14.

Site and code number of field samples						Reference patterns		
Ra-1 (5)	Ra-1 (8)	0-1 (2)	Ch-1 (13)	Sk-2 <sup>a</sup> (19)	intensity <sup>b</sup>	jarosite 22-827 <sup>c</sup>	natro- jarosite 11-302 <sup>c</sup>	hydronium jarosite 21-932 <sup>c</sup>
0.594	0.595	0.595	0.596	0.595	m	0.594	0.594	0.597
0.576	.	0.576	0.573	0.556	w	0.572	0.557	0.567
0.510	0.510	0.508	0.508	0.505	s	0.509	0.506	0.510
0.365	.	0.364	0.365	0.366	m	0.365	0.367	0.368
0.311	0.3105	0.3105	0.310	0.3105	vs	0.311	0.312	0.313
0.308	0.308	0.308	0.306	0.3065	vs	0.308	0.306	0.309
0.301	.	0.302	0.300	.	w	0.302	.	.
0.296	.	0.296	0.296	0.296	m	0.2965	0.296	0.298
0.287	.	0.287	0.286	0.278	w	0.2861	0.278	0.2835

a. Light-gray (2.5Y7/2) sample taken from a lobster mound in Sarawak (Andriesse et al., 1973).

b. Visually estimated peak intensities: w, weak; m, medium; s, strong; vs, very strong.

c. Card numbers of the Joint Committee on Powder Diffraction Standards.

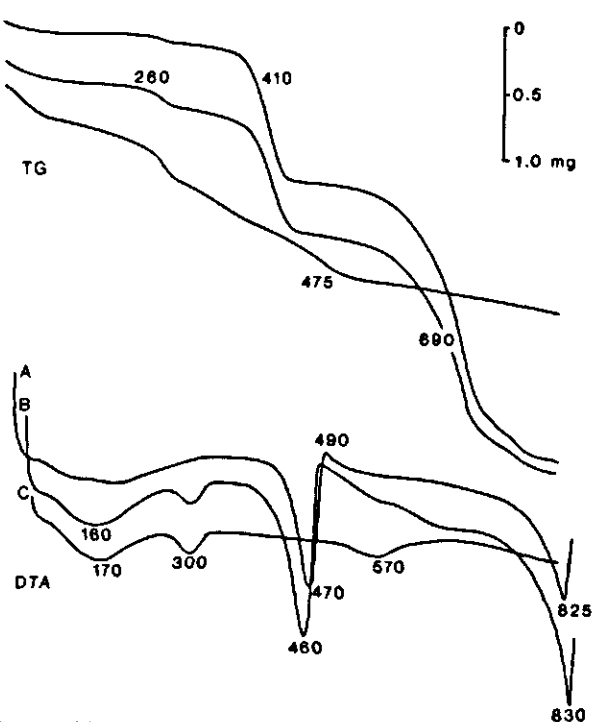


Figure 40

Thermogravimetry (TG) and differential thermal analysis (DTA) of jarosite from 0-1 of colours 2.5Y8/3 (A) and 2.5Y7/4 (B), and of goethite from Ra-1 (C). Figures denote reaction temperatures in °C.

The weight losses associated with release of water and sulfur trioxide according to Reactions 20 and 21 can be determined by thermogravimetry (TG). DTA and TG traces for samples of jarosite and ferric oxide are shown in Fig. 40.

All samples from brown mottles, and also those from very slightly brownish jarosite mottles gave a small endothermic peak at about 300 °C. This peak, which is associated with a distinct weight loss (Fig. 40) must be attributed to partial removal of water from hydronium jarosite (Kubisz, 1971) or to dehydration of very fine-grained goethite. TG data and chemical data are given in Table 14. The agreement between the two methods for  $\text{SO}_3$  is generally reasonable, and differences may be partly due to subsampling. The data show that: (a) most yellow mottles contain between 50 and 100% of jarosite; (b) jarosite from Ch-1 and BP-1 is alkali deficient and presumably contains hydronium; (c) except in Sample 13, iron is invariably present in a substance quotient greater than  $3 \text{ Fe}_2\text{O}_3$  relative to  $4 \text{ SO}_3$ , indicating the presence of free iron oxide; (d) TG analysis shows an excess of  $\text{H}_2\text{O}$  in jarosite too high to be accommodated in the lattice according to Kubisz's (1970) formula.

Table 14. Partial analysis of yellow, brown and red mottles by TG (H<sub>2</sub>O contents and SO<sub>3</sub>(TG)) and by extraction with hot HCl 4 mol/litre. SO<sub>3</sub>(TG) =  $\frac{4}{3} \times$  (weight loss upon heating from 400 to 800 °C); H<sub>2</sub>O(G) = (water in goethite) = weight loss upon heating from 150 to 300 °C; H<sub>2</sub>O(J) = (water in jarosite) = weight loss upon heating from 300 to 500 °C.

Sample no.	Site	Depth (cm)	Colour (dry)	Substance quotient to 4SO <sub>3</sub> (TG)				Free Fe <sub>2</sub> O <sub>3</sub> /H <sub>2</sub> O(G) substance quotient	Mass fract. SO <sub>3</sub> in sample	Mass fract. SO <sub>3</sub> (TG)	Mineralogy f		
				K <sub>2</sub> O	Na <sub>2</sub> O + NH <sub>4</sub> O	K <sub>2</sub> O	Fe <sub>2</sub> O <sub>3</sub> / Al <sub>2</sub> O <sub>3</sub>						
1	0-1	100-150	pale y., 2.5YR7/3	0.85	0.18	1.03	3.62	0.54	7.0	1.2	26.0	26.7	
2	0-1	100-150	pale y., 2.5Y7/4	-	-	-	-	-	1.5	-	-	Jar	
3	0-1	30-60	y. red, 5YR5/6	-	-	-	-	-	1.6	7.0	-	23.2	
4	0-1	30-60	red, 2.5YR5/6	-	-	-	-	-	1.6	-	-	Jar, Goet	
5	Ra-1	125	pale y., 2.5Y7.5/4	0.99	0.12	1.11	4.79	0.44	1.5	8.0	1.2	-	3.7
6	Ra-1	115	yellow, 10YR7/5	-	-	-	-	-	2.3	8.3	-	20.4	
7	Ra-1	115	pale y., 2.5Y8/4	-	-	-	-	-	0	7.9	-	20.4	
8	Ra-1	80	pale y., 2.5Y7/4	-	-	-	-	-	0	6.4	-	20.5	
9	Ra-1	80	y. brown, 10YR5/6	-	-	-	-	-	1.6	-	-	Jar	
10	Kl-1	50-70	brown, 7.5YR5/2	-	-	-	2.8	-	3.1	9 <sup>b</sup>	0.8	-	7.2
11	BP-1	20	yellow, 2.5Y8/6	0.62	0.08	0.70	5.75	-	-	-	-	Goet, Jar	
12	Ca-1	60	yellow, 2.5Y7/6	1.04	0.13	1.17	5.41	0.32	-	-	-	Goet, Jar	
13	Ch-1	3-13	pale y., 2.5Y7/4	0.48	0.35	0.83	2.98	0.10	0.0	6.8	-	18.3	
14	Ch-1 <sup>c</sup>	-	yellow, 10YR7/6	0.44	0.34	0.78	3.15	0.08	0.0	6.7	-	18.3	
15	Ch-1 <sup>d</sup>	-	reddish y., 7.5YR6/8	0.52	0.33	0.85	4.33	0.08	1.9	6.3	0.7	27.5	
16	Ch-1 <sup>e</sup>	-	strong br., 7.5YR5/8	0.44	0.32	0.76	6.22	0.06	4.3	6.9	0.7	23.3	
jarosite, theoretical				1	0	1	3	0	0	6	-	Jar	
									32	32			

a. as % on oven-dried (105 °C) basis, soluble in hot HCl 4 mol/litre.

b. unreliable due to low SO<sub>3</sub> or low H<sub>2</sub>O contents.

c. As Sample 13 but dialysed with distilled water for 7 weeks.

d. As Sample 13 but dialysed for 13 weeks

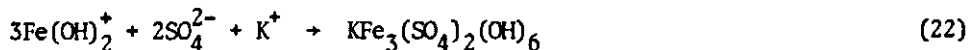
e. As Sample 13 but dialysed for 25 weeks

f. Mineralogy by X-ray diffraction:  
Jar, jarosite; Goet, goethite; Haem, haematite.

The broad goethite reflexions in some samples and the presence of endothermic peaks at about 300 °C observed in all samples with excess  $Fe_2O_3$  point to the presence of very fine-grained ('poorly crystallized') goethite.

Sulfate extracted with a hot  $Na_2CO_3$  solution 1% (w/v), which, after correction for water-soluble sulfate, has been designated as 'jarosite-sulfate' in Appendix B, may include other basic sulfates, e.g.  $AlOHSO_4$  (van Breemen, 1973b), and adsorbed sulfate. The low Al contents of the yellow mottles shows that little or no basic aluminium sulfate is directly associated with the jarosite, but  $AlOHSO_4$  may be higher in the clay matrix. Even at pH values below 4, adsorbed sulfate is probably not important quantitatively, as follows from the low contents (normally < 0.10%) of 'jarosite S' observed in horizons lacking the yellow mottles. Larger amounts of adsorbed sulfate may be present if the content of free iron oxide is high.

*Formation of jarosite* Jarosite has been synthesized at room temperature within 1-6 months by aeration of a solution of ferrous sulfate (0.06-0.6 mol/litre) and potassium sulfate (0.01-0.1 mol/litre) acidified with  $H_2SO_4$  to a pH of 0.8-1.7 (Brown, 1970). Hydronium jarosite precipitated within 5 months from a ferric sulfate solution 0.3 mol/litre of pH 1.4. In spite of the high concentrations, the rate of jarosite formation in these experiments is slower than in aerated pyritic muds. For instance, Vieillefon (1974) detected jarosite after 10 days of aerobic incubation of pyritic mangrove soil. Part of this difference may be due to the continuous neutralization of dissolved ferric iron in soil samples (by reactions involving soil minerals), leading to relatively high concentrations of the  $Fe(OH)_2^+$  complex which probably takes part in the formation of jarosite according to



(Matijević et al., 1975). In jarosite formation from solutions containing ferrous sulfate, the slow biological oxidation of  $Fe^{2+}$  at low pH may have played a role too. Ivarson (1973) observed formation of (ammonium) jarosite within 4-10 days in cultures of *T. ferrooxidans* in a medium containing ferrous sulfate. Since the organisms were isolated from natural jarosite samples, it seems likely that they do in fact take part in the formation of jarosite in situ.

Both in acid sulfate soils and in oxidized pyritic environments jarosite has been found intimately associated with pyrite (Clark et al., 1961;

Ivarson, 1973) or pseudomorphic from pyrite (Furbish, 1963; Miedema et al., 1974). In the soils studied, the two minerals were always found to be distinctly separated spatially both in profile pits and in thin sections (van Dam & Pons, 1973). This separation is in agreement with the stability relations of Fig. 22, which predicts that the assemblage jarosite-pyrite is unstable. Rapid oxidation and somewhat arid conditions could explain the presence of jarosite intimately associated with pyrite.

Appearance and grainsize of jarosite precipitated from solution during laboratory synthesis is very similar to that found in acid sulfate soils. This suggests that also *in situ* jarosite forms by precipitation from solution. Under arid conditions, water-soluble normal iron sulfates may precipitate first and may hydrolyse to more basic sulfates with jarosite as the last sulfate of the sequence (Bandy, 1938).

Fig. 41 shows all individual  $E_H$ -pH data on jarositic samples. The reproducibility of the measurements is frequently poor, at least at pH values above 3. It is clear, however, that jarosite is confined mainly to strongly oxidized acid environments with pH values normally below 3.7. Values spread far into the jarosite field, indicating appreciable supersaturation in those cases. To assess the ability of the soil solutions to precipitate jarosite, the disequilibrium index for jarosite,  $D(\text{Jar})$ , was calculated for samples with reproducible  $E_H$ -pH data.  $D(\text{Jar})$  was calculated first from the product of the ionic activities, (here symbolized by brackets),  $(\text{K}^+) \cdot (\text{Fe}^{3+})^3 \cdot (\text{SO}_4^{2-})^2 \cdot (\text{OH}^-)^6$ , in the soil solution, computed from analysed concentrations including, for  $\text{Fe}^{3+}$ , measured redox potentials (van Breemen, 1973a), and second from the solubility product of jarosite,

$$D(\text{Jar}) = pK_{\text{so}}(\text{Jar}) - pK\text{Fe}_3(\text{SO}_4)_2(\text{OH})_6 \quad (23)$$

The value of  $pK_{\text{so}}(\text{Jar})$  was taken as 98.6, from an estimate of the solubility product of jarosite from Ra-1 by Vlek et al. (1974). This material was somewhat less soluble than synthetic jarosite prepared by Brown (1970), which gave a  $pK_{\text{so}}$  between 96.5 (equilibrium approached from undersaturation) and 94.6 (approached from supersaturation)<sup>a</sup>.

The disequilibrium index for hydronium jarosite was evaluated similarly:

---

a. Calculated from data provided by Brown (pers. commun.), with the computer program described in van Breemen (1973a).

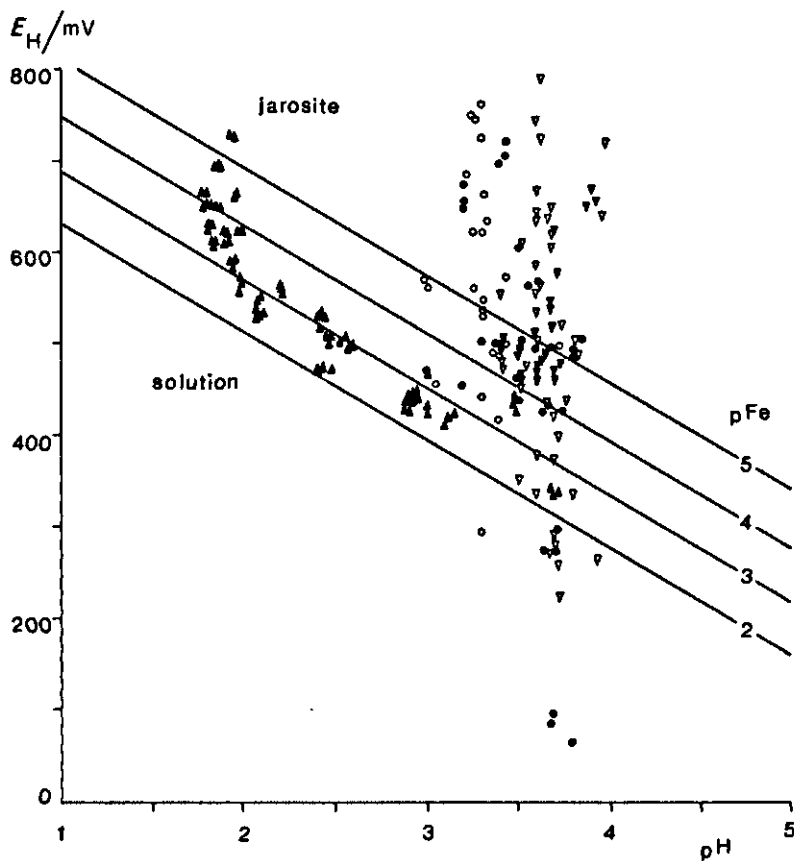


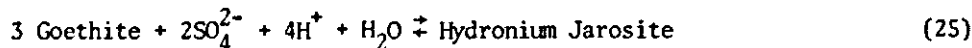
Figure 4!

Individual  $E_H$ -pH measurements in jarositic samples. Reproducibility is indicated as in Fig. 23. Lines are jarosite solubility isotherms ( $25^\circ\text{C}$ ) at fixed activities of dissolved sulfate ( $p\text{SO}_4 = 2.3$ ) and potassium ( $p\text{K} = 3.3$ ), and different levels of dissolved  $\text{Fe}^{2+}$ .

Key:  $\circ \bullet$  field samples;  $\Delta \blacktriangle$  artificially aerated samples;  $\nabla \blacktriangledown$  artificially flooded samples.

$$D(\text{Hydr.Jar}) = p\text{K}_{\text{SO}_4}(\text{Hydr.Jar}) - p\text{Fe}_3(\text{SO}_4)_2(\text{OH})_5 \quad (24)$$

The  $p\text{K}_{\text{SO}_4}$  for hydronium jarosite was estimated from the composition of a solution in equilibrium with goethite and hydronium jarosite at  $50^\circ\text{C}$  (Posnjak & Merwin, 1925) as follows. Assuming sulfate and iron to be present as  $\text{HSO}_4^-$ ,  $\text{SO}_4^{2-}$ ,  $\text{FeSO}_4^+$ ,  $\text{Fe}(\text{SO}_4)_2^-$  and  $\text{Fe}^{3+}$ , and using appropriate equilibrium constants and activity corrections (van Breemen, 1973a) the  $p\text{K}$  for the reaction



was found to be -8.24 at 50 °C. The enthalpy of Reaction 25 at 50 °C was estimated from the Gibbs free enthalpy of the reaction (calculated from the equilibrium constant) and the reaction entropy<sup>a</sup>, which was estimated in turn from entropy and heat capacity data (Kelley, 1960; Helgeson, 1969; Langmuir, 1971). Using van 't Hoff's equation, and assuming a constant reaction enthalpy in the range 25-50 °C, the  $pK$  of Reaction 25 appeared to be -8.30 at 25 °C. Assuming, moreover, that the rather coarse-grained goethite of Posnjak & Merwin (1925) had a  $pK_{SO}$  of 43.1 (Kharaka & Barnes, 1973), the solubility product of hydronium jarosite at 25 °C appears to be  $10^{-81.5}$ , or  $pK_{SO}(\text{Hydr.Jar}) = 81.5$ .

Before discussing disequilibrium indices for jarosite in actual soils, the results of  $D(\text{Jar})$  calculated for the oxidation experiments will be reviewed. Fig. 42 (left) shows how  $D(\text{Jar})$  increases from strongly negative values initially to distinctly positive values upon aerobic incubation of pyritic material from the substratum of Ra-2. The attainment of saturation ( $D = 0$ ) almost coincides with the appearance of jarosite (Fig. 36), and with an abrupt decrease in dissolved potassium. The disequilibrium index increases with time to very high supersaturation, i.e. between  $10^3$  and  $10^7$  times the solubility product. The solution becomes supersaturated with hydronium jarosite too, but after a somewhat longer incubation time. There are no noteworthy differences between treatment with distilled water and sea-water.

In BP (Fig. 42, right), jarosite saturation is reached somewhat later than in Ra, however, in agreement with the later appearance of the mineral (Fig. 36). The decrease in dissolved and exchangeable potassium is more dramatic in BP than in Ra.

The sum of  $K^+$  and  $Na^+$  removed from solution and from the exchange complex is equivalent to at most 25-50% of the jarosite found. Mineral weathering may have supplied further potassium, but some of the monovalent ion sites in the jarosite lattice have probably been filled by hydronium.

Fig. 43 plots  $D(\text{Jar})$  against  $E_H$  and against pH for samples from the field and from oxidation experiment. Jarosite is almost invariably present if the  $E_H$  is above 400 mV, does not occur at pH above 4 and is confined to saturated or supersaturated environments (Fig. 32). The three exceptions, marked in Fig. 43 by arrows refer to samples from the subsoil of KD-1 where jarosite and pyrite

a. The entropy of hydronium jarosite at 50 °C was computed from the entropy at 25 °C (estimated by summing the entropy contributions of the elements, Latimer, 1952) and its heat capacity, which was estimated by summing the heat capacity power functions of its oxide components (Kelley, 1960; Helgeson, 1969).

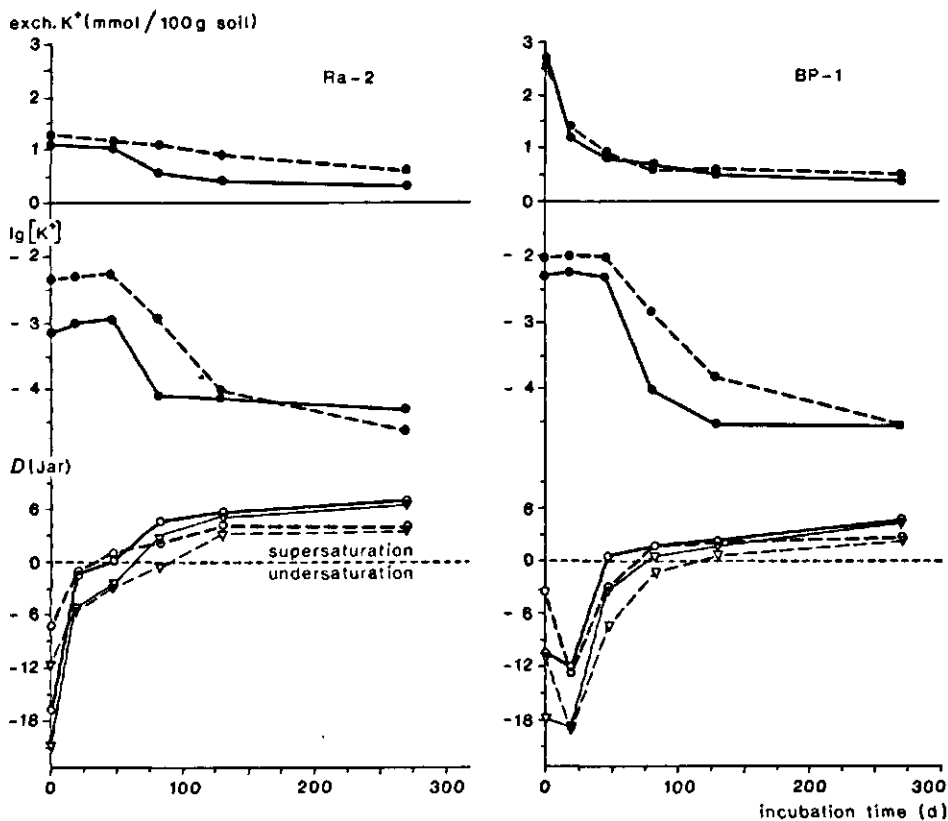


Figure 42

Exchangeable  $K^+$ , dissolved  $K^+$  and jarosite disequilibrium index,  $D(\text{Jar})$ , against time during artificial aeration of potentially acid pyritic samples. Key: solid lines, distilled water added at the outset; broken lines, sea-water added.  $[K^+]$  is value of potassium concentration in mol/litre;  $\circ D(\text{Jar})$ ;  $\nabla D(\text{Hydr. Jar})$ .

occur together, and where water saturation has led to reduction of jarosite by pyrite (Section 4.3.1).

It is puzzling that, although jarosite can be formed already at slight supersaturation (see Fig. 42), strong supersaturation often prevails in the presence of the mineral. Perhaps low concentrations of, for instance, dissolved ferric iron in situ and potassium during the oxidation experiment limit the rate of crystal growth of jarosite. Equilibrium was closely approached in the samples from the jarositic B horizons of Ra-1, Ra-2 and Na-2, after at least 4 months of water saturation in the laboratory. The  $E_H$ -pH measurements were highly reproducible and of the same order:  $E_H = (489 \pm 25)$  mV; pH =  $3.58 \pm 0.11$ . The resulting values of  $\text{pKFe}_3(\text{SO}_4)_2(\text{OH})_6$  ( $98.2 \pm 2.0$ ) were in good agreement with the solubility product ( $\text{pK}_{\text{so}} = 98.6$ ) reported by Vlek et al. (1974).

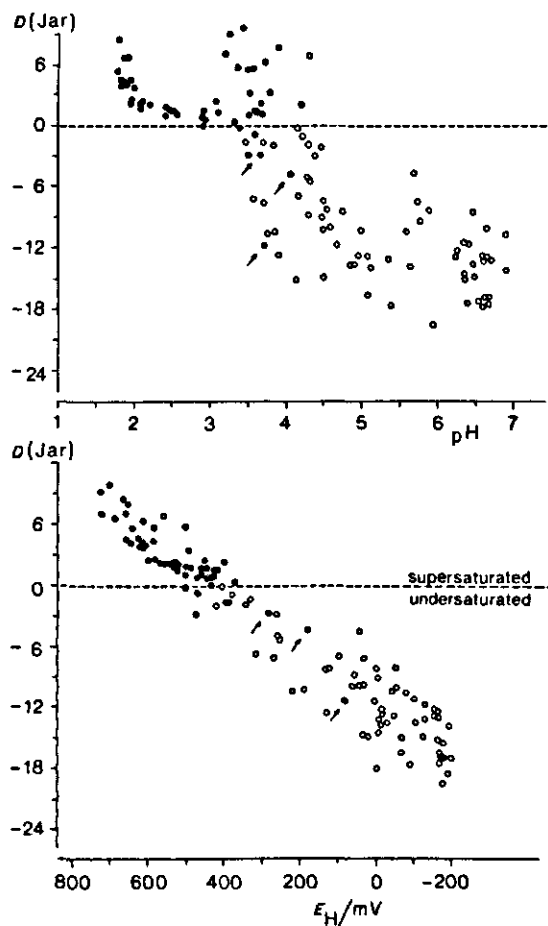


Figure 43  
 Disequilibrium index of jarosite,  $D(\text{Jar})$ , plotted against pH and against  $E_H$ . Key: arrows indicate samples from the field containing both jarosite and pyrite;  
 ● jarosite present;  
 ○ jarosite absent.

In a moderately acid ( $\text{pH} < 4.4$ ) and oxidized environment ( $E_H > 400 \text{ mV}$ ), jarosite is stable over ferric oxide with a solubility product of  $10^{-39.9}$ , but its stability field is limited to extremely acid conditions ( $\text{pH} < 1.7$ ) if equilibrium with coarser-grained goethite with  $\text{p}K_{\text{so}} = 42.6$  is considered (Fig. 22). Because the pH of acid sulfate soils is considerably higher than 1.7, jarosite is metastable and must ultimately change to goethite. Hydrolysis of jarosite to ferric oxide does indeed take place (Section 4.4.2).

#### 4.4.2 Iron oxides

*Properties of ferric oxides* In most acid sulfate soils only part of the ferric iron released as a result of pyrite oxidation is tied up in jarosite, the bulk being present in 'free ferric oxide' (Fig. 21) and in the clay mineral beidellite

(Chapter 5). Dithionite-extractable iron (Appendix A), corrected for iron present in jarosite is assumed to represent 'free ferric oxide'. Typical pedons in the older part of the Bangkok Plain show a strong accumulation of ferric oxide just above the maximum accumulation of jarosite. A notable exception was KR-1 where essentially all dithionite-extractable iron was present as jarosite. Oxalate-extractable or 'amorphous' ferric oxide (Schwertmann, 1959; Landa & Gast, 1973) is relatively abundant in young acid sulfate soils such as KD-1 (Fig. 21), and much lower in well developed acid sulfate soils and non-acid marine soils. Although its content does not change much with depth, the amorphous fraction of total free ferric oxide is higher near the surface, drops to 5-25% in the B horizon and increases again in the lower part of the B horizon (Fig. 44). The strong relative increase at still greater depths is presumably due to pyrite oxidation during storage of the samples<sup>a</sup>.

X-ray diffraction of many, but not all, brown mottles yields goethite patterns. The goethite diffraction lines were generally broad, suggesting small particles. Vague haematite patterns were obtained from red mottles sampled at 0-1 and at K1-1. No other ferric oxide phases (such as lepidocrocite or ferrihydrite) could be detected. Differential thermal analysis (DTA) of all brown mottles and of some yellow (jarosite) mottles gave endothermic peaks at 290 to 320 °C, which were associated with a weight loss at 245-275 °C during thermogravimetry (Fig. 40). The temperature of the endothermic peak from DTA for goethite dehydration is reported to vary between 390 °C for 'well crystallized' goethite and about 320 °C for 'poorly crystallized' material (Kulp & Trites, 1951; Kelley, 1956; Kihnel et al., 1974). The terms 'poorly' and 'well' crystallized are used frequently to describe samples giving broad and sharp diffraction lines, respectively. In ferric oxides, however, differences in the width of X-ray diffraction lines, and presumably in dehydration temperatures, are mainly attributable to differences in grain size although lattice defects may also play a role. Red mottles give only a weak endothermic peak at about 300 °C indicating that they contain partially dehydrated material, in accordance with the presence of haematite in most of the red mottles.

---

a. Amorphous  $Fe_2O_3$  was estimated about 4 years after sampling and vacuum-drying of the samples and was probably increased by pyrite oxidation during storage. Free iron was estimated in the same samples immediately after vacuum-drying. These free iron data have been reported by Vlek (1971) and are not repeated in Appendix B.

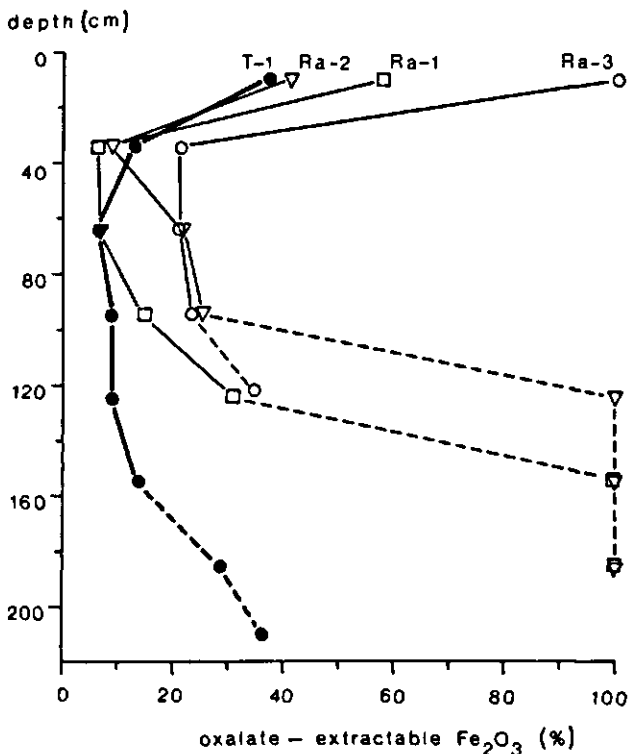
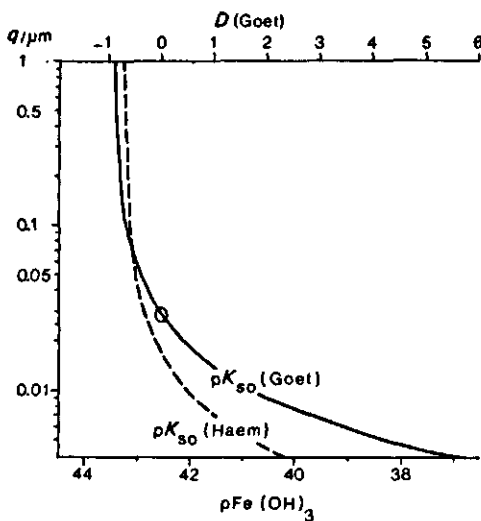


Figure 44

Fraction of oxalate extractable ('amorphous')  $\text{Fe}_2\text{O}_3$  in free  $\text{Fe}_2\text{O}_3$  against depth in three acid sulfate soils from Rangsit and one non-acid marine soil (T-1). Broken lines: data probably too high as a result of pyrite oxidation during storage.

**Solubility and particle size** At grain sizes below  $0.1 \mu\text{m}$ , mineral solubility is strongly influenced by particle size. The reference goethite used ( $\text{p}K_{\text{SO}} = 42.6$ ; Berner, 1971) consists of lath-shaped particles with average dimensions of  $0.05 \times 0.28 \times 0.013 \mu\text{m}^3$  (Langmuir, 1971). The data on this particular goethite, and values of the surface free enthalpy of the goethite-water interface ( $\bar{\gamma} = 1.6 \text{ J/m}^2$  at  $25^\circ\text{C}$ ) and the molar volume ( $V_m = 23.4 \text{ cm}^3$ ) given by Berner (1971) were used to estimate the solubility product of coarse-grained goethite (i.e. goethite with a molar surface,  $S_m$ , approaching zero or an equivalent cube width,  $q$ , approaching infinity) and to find the relationship between particle size and solubility product, by applying the equation (Berner, 1971)

$$\text{p}K_{\text{SO}}(q) = \text{p}K_{\text{SO}}(q \rightarrow \infty) - 2/3 \bar{\gamma} \cdot S_m / 2.3 R \cdot T \quad (26)$$



**Figure 45**  
Effect of equivalent cube width,  $q$ , on the solubility product of goethite and haematite. Circle denotes reference goethite for the  $D(\text{Goet})$  scale at the top of the diagram.

Where  $R \cdot T$  represents the product of the gas constant and the absolute temperature. For Berners goethite,  $q = 0.03 \mu\text{m}$  (such a cube has a similar surface to volume ratio as the described lath-shaped particles), the results are  $pK_{\text{so}}(q \rightarrow \infty) = 43.49$ , and

$$pK_{\text{so}}(\text{Goet}, q) = 43.49 - 0.0263 q^{-1} \quad (27)$$

with  $q$  expressed in  $\mu\text{m}$ . Combining Eq. (27) with Langmuir's (1971, 1972) expression for the free enthalpy change of the transformation of goethite to haematite of equal particle size yields the following relationship for the haematite solubility product as a function of particle size:

$$pK_{\text{so}}(\text{Haem}, q) = 43.295 - 0.0123 q^{-1} \quad (28)$$

Eq. (27) and (28) have been plotted in Fig. 45, which shows that the solubility of both minerals increases sharply with decreasing particle size at  $q = 0.05 \mu\text{m}$ , and that coarse-grained goethite is more stable than haematite at particle size  $> 0.07 \mu\text{m}$ , whereas the reverse is true at smaller grain sizes (Langmuir, 1971). The validity of Eq. (27) and Eq. (28) probably breaks down at very small values of  $q$ , due to the growing influence of corners and edges on the solubility, and of double-layer effects. Nevertheless, Eq. (27) predicts a solubility product of the order of that of amorphous ferric hydroxide ( $pK_{\text{so}} = 37.2$ ) at a particle size of 0.004–0.005  $\mu\text{m}$ , i.e. for stacks of about 10 goethite unit

cells, or the smallest particles that could still be called solid.

Densitometer traces of Quinier-de Wolff X-ray diffraction photographs were used to estimate line widths of the 0.418 nm goethite reflexion and the 0.268 nm haematite reflexion. With coarse-grained goethite and relatively coarse haematite ( $q = 0.06 \mu\text{m}$ ) as references, the smallest dimensions of the mineral particles in the natural samples were calculated from the Scherrer formula (Cullity, 1959). The width-length-thickness ratios of artificially prepared goethite (prepared by A. Breeuwsma, Stiboka, Wageningen) were used to calculate  $q$ . The average dimensions of the particles of the synthetic goethite were 1.66  $\mu\text{m}$  long and 0.11  $\mu\text{m}$  wide (estimated from electron micrographs) and 0.025  $\mu\text{m}$  thick (estimated from X-ray diffractogram). The results for samples giving sufficiently intense diffraction patterns are given in Table 15 together with the solubility products predicted by Eq. (27) and (28), the respective dehydration temperatures and the relative concentration of oxalate-soluble ('amorphous') ferric iron.

Relatively coarse-grained goethite occurred in the iron pan of Kl-1, more finely grained goethite in the B horizons of O-1 and Ra-1, whereas freshly precipitated ferric oxide on a ditchside near KD-1 had the smallest particle size. Decreasing particle size seems to be correlated with a decreasing DTA peak temperature and with an increase in the fraction of oxalate-soluble iron. The TG peak temperature varies little over the range of particle sizes, however. The increase in particle size of goethite and the decrease for oxalate-soluble

Table 15. Characteristics of goethite and haematite mottles in different soils.  $\text{pK}_{\text{so}}$  was calculated from Eq. (27) or (28); DTA, differential thermal analysis; TG, thermogravimetry; amorphous  $\text{Fe}_2\text{O}_3$  is oxalate-soluble  $\text{Fe}_2\text{O}_3$  as a fraction of free  $\text{Fe}_2\text{O}_3$  in surrounding soil.

Site	Depth (cm)	Mineral	$q/\mu\text{m}$	$\text{pK}_{\text{so}}$	Dehydration peak temperatures ( $^{\circ}\text{C}$ )		Amorphous $\text{Fe}_2\text{O}_3$ (%)
					DTA	TG	
Kl-1	20	haematite	0.06	43.1	.	.	.
Kl-1	20	goethite	0.065	43.1	310	275	.
Kl-1	50	goethite	0.040	43.0	320	260	.
O-1	45	goethite	0.026	42.4	300	255	.
O-1	45	haematite	0.030	42.9	.	.	.
Ra-1	40	goethite	0.021	42.2	300	260	7
Ra-1	80	goethite	0.020	42.1	290	260	10
Ra-1	125 <sup>a</sup>	goethite	0.015	41.7	.	260	31
KD-1	30 <sup>a</sup>	goethite	0.0095	40.8	.	.	95

a. Recent ferric oxide coating on a ditch side.

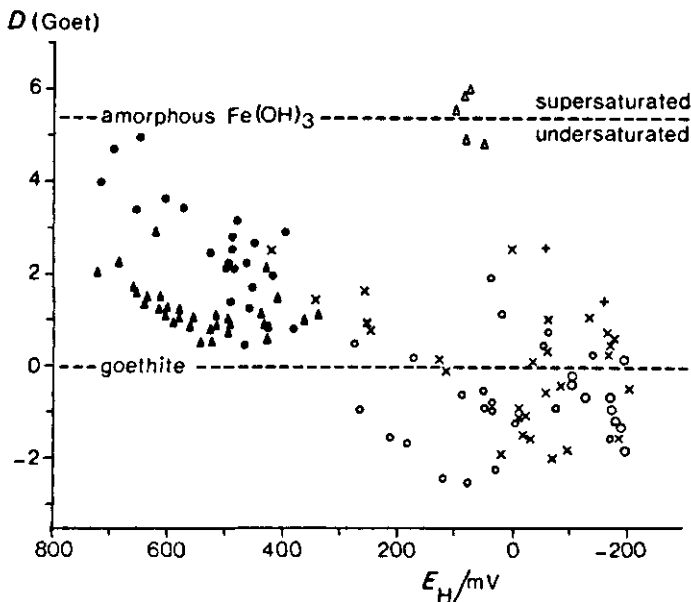


Figure 46

Disequilibrium index of goethite,  $D(\text{Goet})$ , against redox potential.

Key: ● jarositic soil, field; ▲ jarositic soils from artificially aerated pyritic samples; Δ artificially aerated calcareous pyritic sample; ○ pyritic substrata; ○ pyritic mangrove muds; X flooded surface of acid sulfate soils; + flooded surface of non-acid soils.

iron with decreasing depth above the pyritic substratum in Ra-1, and, presumably, with time in the sequence KD-1  $\rightarrow$  Kl-1, can be explained by progressive ageing of initially 'amorphous' ferric oxide. Such ageing leads to increasingly stable, i.e. less soluble, material. The appearance of haematite in the upper part of the B horizon of many acid sulfate soils also fits into this picture. Coexisting haematite and goethite was about equal in size, but the particles were still so small that haematite would be more stable than goethite (Fig. 45).

For a uniform and relatively coarse-grained mineral such as jarosite, the disequilibrium index,  $D(\text{Jar})$ , simply indicates the degree of supersaturation ( $D > 0$ ) or undersaturation ( $D < 0$ ) of the ambient solution. For fine-grained material of variable texture such as ferric oxides, however, the disequilibrium index is ambiguous. The dependance of  $pK_{\text{so}}$  on particle size implies that a positive or negative index may still pertain to equilibrium with material finer or coarser than the reference material. Disequilibrium indices for ferric oxide, with reference to goethite with  $pK_{\text{so}} = 42.6$  depicted in Fig. 32, indicate near-equilibrium or slight undersaturation (with this particular goethite) in pyritic substrata, and distinct supersaturation in the overlying B horizons.

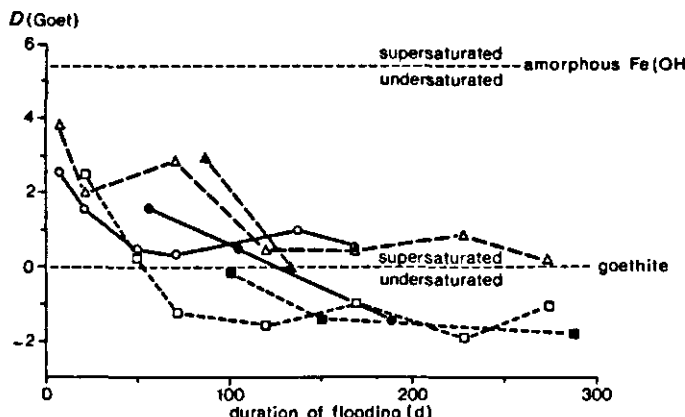


Figure 47

Effect of flooding on the disequilibrium index of goethite,  $D(\text{Goet})$ , in surface soils from Rangsit. Key: solid symbols, field samples; open symbols, artificially flooded soils in the laboratory;  $\circ$  Ra-1;  $\Delta$  Ra-2;  $\square$  Ra-3.

Apparently,  $D(\text{Goet})$  decreases again at shallower depth in the B horizon in agreement with the presence of more stable oxides, indicated by X-ray diffraction and analysis of oxalate-soluble iron. All values of  $D(\text{Goet})$  derived from reproducible  $E_H$ -pH measurements were plotted against  $E_H$  in Fig. 46. Equilibrium with moderately coarse-grained goethite ( $pK_{\text{so}} = 42.6$ ) and with amorphous ferric hydroxide ( $pK_{\text{so}} = 37.2$ ) is indicated by horizontal lines. Non-acid reduced pyritic environments (unoxidized mangrove muds) are close to equilibrium or slightly undersaturated with reference to even the most stable goethite. This probably reflects the effect of pyritization of all except the most stable ferric oxides. Partly oxidized and acid substrata, which normally have redox potentials higher than -100 mV, are often strongly undersaturated with goethite. This is probably due to the strong tendency of ferric oxide to dissolve in the presence of pyrite (Eqs. 14 and 15). A similar effect was noted in acid ground waters from oxygenated pyritic strata in New Jersey and Maryland (Langmuir & Whittemore, 1971). Soil solutions from jarosite horizons are invariably supersaturated with goethite, but still distinctly undersaturated with amorphous ferric hydroxide. Near-equilibrium with amorphous  $\text{Fe}(\text{OH})_3$  was observed only during the oxidation experiment in calcareous pyritic soils which maintained a pH between 7 and 8. Relatively rapid oxidation of  $\text{Fe}^{2+}$  at high pH (Singer & Stumm, 1970) leading to strong supersaturation may be responsible here for the formation of extremely fine-grained ('amorphous') material.

$D(\text{Goet})$  is hardly affected by flooding in the permanently oxidized B horizons, but strongly decreases with time in the surface horizons, which undergo reduction (Fig. 47; Section 4.6). The decrease in  $D$  may be due to equilibra-

tion with progressively more stable ferric oxides once the less stable material is dissolved by reduction (van Breemen, 1969) or to the prevalence of redox couples other than the ferrous-ferric couple, e.g. highly reduced organic systems. In view of the relatively large fraction of amorphous ferric oxide, and the attainment of undersaturation even with coarse-grained goethite in strongly reduced surface soils, the latter explanation is more plausible. The initial values of  $D(\text{Goet})$  which are probably least influenced by such effects, are indeed compatible with the presence of nearly amorphous ferric oxide.

If  $E_H$ , pH and pFe are in equilibrium with ferric oxide of a certain grain size, its solubility product can be found from the equation

$$pK_{\text{so}} = 42.6 - D(\text{Goet}) \quad (29)$$

For brown mottles in B horizons,  $pK_{\text{so}}$  estimated from particle size (Table 15) is higher than calculated from Eq. (29). This is to be expected because the estimate of particle size refers to the coarsest goethite in the sample, whereas the finest-grained and hence most soluble material (which does not give X-ray diffraction peaks) will determine  $D(\text{Goet})$ . The fraction of fine-grained material may be very small (Cornell et al., 1974), so  $pK_{\text{so}}$  calculated from Eq. (29) is not necessarily representative for the bulk of the ferric oxide.

*Green rust* In practically all non-acid soils and many para-acid sulfate soils, including Bk-1 and T-1, conspicuous grayish-green to green (5G4/2 or greener) mottles occur along vertical channels or ped faces in the upper part of the greenish-gray (5GY4/1) substratum (van der Kevie & Yenmanas, 1972). Nearer the surface the green colours grade to yellowish brown through shades of olive-brown (e.g. 2.5Y4/5). Green mottles have not been observed in the oldest acid sulfate soils, but they do occur in KD-1 and Mn-1. Their appearance and position between the reduced C horizon and the more oxidized B<sub>2</sub> horizon suggest the presence of hydrous oxides containing both Fe(II) and Fe(III), although the presence of greenish Fe(II) complexes with organic matter cannot be precluded. Similar, presumably transient, compounds may cause the greenish tinge of the marine substrate. This is corroborated by the rapid disappearance of the green colour upon exposure to the atmosphere (Trafford et al., 1973). Bernal et al. (1959) consider two types of Fe(II)-Fe(III) hydroxides designated as green rusts I and II. Green rust I is a non-stoichiometric compound with a substance fraction of  $\text{Fe(III)}/\{\text{Fe(II)} + \text{Fe(III)}\}$  between 0.2 and 0.5., whereas green rust II has the stoichiometry of magnetite, with a fraction of 2/3. Both compounds are reported

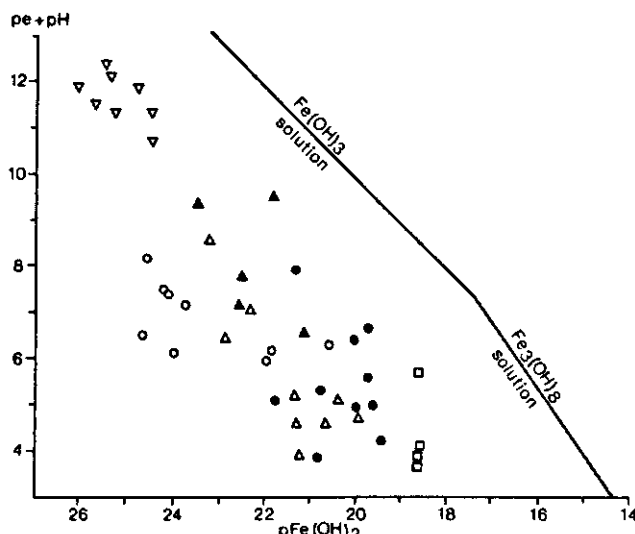


Figure 48

Redox conditions and ionic activity products of ferrous hydroxide (expressed as negative decadic logarithm,  $p\text{Fe}(\text{OH})_2$ ) in different samples compared to the solubility isotherms (25 °C) for amorphous ferric hydroxide and ferrosoferric hydroxide.

Key: • greenish gray substratum; ○ gray substratum; ▲ green mottled horizon; △ reduced surface soil (acid); □ reduced surface soils (non-acid); ▽ jarositic B horizon.

as crystalline and X-ray diffraction patterns are given. Green rust II may be similar to ferrosoferric hydroxide,  $\text{Fe}_3(\text{OH})_8$ , which, together with amorphous ferric hydroxide, may regulate the concentration of dissolved  $\text{Fe}^{2+}$  in flooded soils (Ponnamperuma et al., 1967).

Unfortunately, no samples of green mottles were available for X-ray diffraction. Fig. 48 shows the redox conditions (represented by  $\text{pe} + \text{pH}^a$ , where  $\text{pe} = E_{\text{H}}/0.059$ ) and ferrous hydroxide ionic activity products (expressed as  $p\text{Fe}(\text{OH})_2$ ) for green-mottled soil samples, greenish-gray substrata and for various other samples, together with the solubility isotherms of  $\text{Fe}_3(\text{OH})_8$  and amorphous ferric hydroxide. Green-mottled horizons are generally intermediate between well developed (jarositic) B horizons and pyritic substrata or flooded surface horizons, in redox conditions. The  $p\text{Fe}(\text{OH})_2$  values are far higher than those in equilibrium with either  $\text{Fe}_3(\text{OH})_8$  or  $\text{Fe}(\text{OH})_3$ , showing that both compounds are unstable in the samples. Formation of  $\text{Fe}_3(\text{OH})_8$  requires that

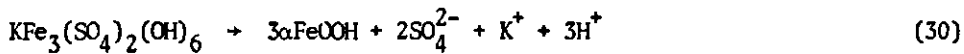
a. The sum  $\text{pe} + \text{pH}$  is a better measure for the redox condition than  $\text{pe}$  (or  $E_{\text{H}}$ ) alone, since it is directly proportional to the partial pressure of oxygen (and hydrogen).

$p\text{Fe(OH)}_2$  decreases below 17.4. Such values have never been observed in this study, so it is unlikely that the ferrosoferric hydroxide described by Ponnamperuma et al. (1967) is formed in any of the soils studied. In the flooded non-acid surface soils,  $p\text{Fe(OH)}_2$  eventually reached almost constant values around 18.7 (Fig. 48), suggesting regulation of  $\text{Fe}^{2+}$  by a compound containing ferrous iron. The soil solution was always 3-20 times supersaturated with siderite ( $\text{FeCO}_3$ ) so control by this mineral is unlikely. The ferrous iron concentrations were certainly influenced, and perhaps controlled by  $\text{FeS}$ , since numerous black spots were observed in the reduced Ap horizons of non-acid soils.

*Formation of ferric oxides* In acid sulfate soils, ferric oxides may be formed either directly by oxidation of dissolved, solid or adsorbed ferrous iron, or by hydrolysis of jarosite. The first mechanism is dominant in zones where jarosite is absent, for instance in the upper part of the pyritic substratum and in the A horizon. Ferric oxide mottles in these zones are frequently dark reddish brown (5YR3/4) or dark brown (7.5YR4/4), rather than yellowish brown (10YR5/6) as in the B horizon. Similar dark-brown and yellowish-brown colours are typical for fresh (X-ray amorphous) and aged (goethite) ferric hydroxide precipitates, respectively. Drainage, followed by oxidation of the large amounts of ferrous iron formed in the two zones upon submergence may temporarily cause high concentrations of dissolved ferric iron, leading to very fine-grained precipitates.

Part of the ferrous iron formed near the surface and in the upper part of the pyritic substratum diffuses towards the B horizon and will oxidize and precipitate there in the dry season (Harmsen & van Breemen, 1975). The calculated disequilibrium indices (Fig. 32), indicate that both goethite and jarosite can form here. Chemical and morphological changes observed in the sequence BP, KD, Ra-2, Ra-1, and 0-1 (see Fig. 11), however, are strong evidence that jarosite is formed first and that most of the ferric oxide in the B horizon of the older soils is formed later by hydrolysis of jarosite. The increase in the prevalence of brown rims around jarosite masses in thin sections from shallower depth corroborates this (van Dam & Pons, 1973; Miedema et al., 1974).

Fig. 22 shows that jarosite is more stable than ferric oxide with a  $pK_{\text{so}}$  of about 40 at pH near 4. This ferric oxide corresponds to goethite particles with a  $q$  of about  $0.008 \mu\text{m}$ . The goethite actually present (Table 15) is considerably coarser and hence can be formed at the expense of jarosite:



The reaction can be accelerated by removing one or more the soluble products, e.g. by dilution or by increasing pH. The process was simulated in the laboratory by dialysing subsamples of 100 mg jarosite from Ch-1 for about 6 months. The results of this experiment are presented in Table 14 (Samples 13-16). The pale-yellow colour of the fresh material changed to strong-brown. The residue was enriched in ferric iron and (stoichiometrically) depleted of  $K^+$ ,  $Na^+$  and  $SO_4^{2-}$ . In spite of the virtual disappearance of the pale-yellow colour, the complete jarosite X-ray diffraction pattern persisted and no ferric oxide lines were found even after 6 months. The loss of weight between 200 and 300 °C during thermogravimetry indicate the presence of hydrous ferric oxide. These observations point to the formation of coatings of amorphous ferric oxide on the jarosite surface. Scanning electron micrographs (Fig. 39) provide further evidence for such a process. Very fine-grained or amorphous ferric oxide is presumably also the initial product of jarosite hydrolysis *in situ*. Hydrolysis will certainly proceed far slower *in situ* than in the laboratory dialysis experiment where the concentrations of  $SO_4^{2-}$ ,  $K^+$  and  $H^+$  in the ambient solution were much lower. Approximately equal rates of jarosite hydrolysis and of ageing of the resulting ferric oxide would explain the low ('steady state') concentrations of amorphous ferric hydroxide in the B horizon (Fig. 44).

Even the coarsest goethite observed, in the iron pan of Kl-1, is less stable than haematite of equal particle size, leading to dehydration:



Transformation of goethite to haematite is a very slow process (Langmuir, 1971). The dehydration will be promoted by strong desiccation which explains the common occurrence of red mottles in the upper part of the B horizon of higher soils, notably in the driest (western) part of the Bangkok Plain. The presence of red mottles in soils in the much wetter peninsular region (Sa-1, Nk-2) indicates that other factors may be involved too. For instance, low pH will facilitate solution of goethite, which, in view of the completely different structures of the two minerals, must be an intermediate step in Reaction 31. This would also explain why red mottles occur only in markedly acid soils (including para-acid sulfate soils), but not in non-acid marine soils and recent or semi-recent alluvial soils, unless they cover oxidized pyritic sediments (van der Kerven & Yenmanas, 1972).

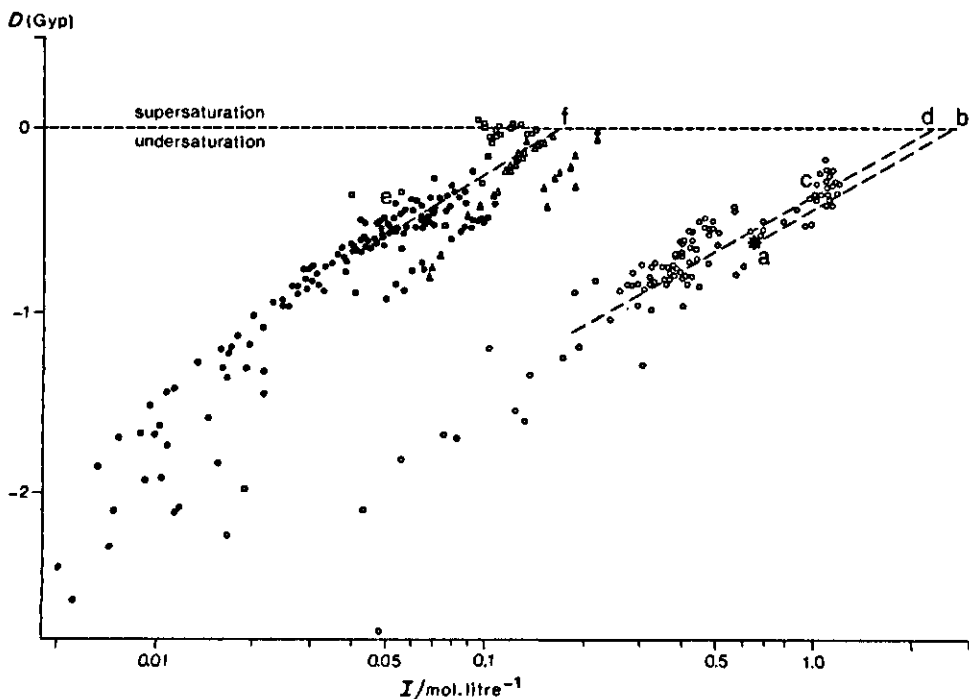


Figure 49

Disequilibrium index of gypsum,  $D(\text{Gyp})$ , against ionic strength,  $I$ . The broken lines are hypothetical evaporation paths.

Key to sample sites: • KR, Mn, Ra, O; □ Na-2; ▲ Bk-1; △ T-1;  
 ○ BP, Ca, Ch; \* standard sea-water. For a-f, see text.

#### 4.4.3 Gypsum and other sulfates

**Gypsum** Soils with gypsum are mainly found in the eastern half of the Bangkok Plain. If present, gypsum normally occurs in the upper part of the B horizon or in the lower part of the A horizon. Small amounts of gypsum may occur temporarily in thin, whitish, powdery efflorescences on ditch sides, pedfaces and on the dry soil surface everywhere in the Bangkok Plain. In the pedons studied here, appreciable amounts of gypsum occurred only in T-1 and Na-2. Gypsum was also observed, along with jarosite, in thin sections of pyritic substrata from the Rangsit Station. These are artefacts, formed after pyrite oxidation during handling and storage of the samples.

Fig. 49 plots the disequilibrium index of gypsum against ionic strength. Near-equilibrium with gypsum ( $D(\text{Gyp}) = 0$ ) occurred in the gypsiferous pedons T-1 and Na-2, and in Bk-1 where gypsum has been found in the immediate vicinity. In contrast to the commonly observed supersaturation with certain other second-

ary phases such as jarosite and goethite, appreciable supersaturation with gypsum was never observed. This shows that gypsum determines maximum ionic activity product of calcium and sulfate. The almost rectilinear relationship between  $D(\text{Gyp})$  and  $I$  for different groups of soils (Fig. 49), is due to the relative constancy of the ratios of the ions that make up the bulk of the dissolved matter. This relationship can be used to estimate the extent of evaporation necessary to bring about precipitation of gypsum. Fig. 49 predicts that sea-water becomes saturated with gypsum upon evaporation from an initial ionic strength of 0.7 (*a*) to a value of 2.1 (*b*), or to about<sup>a</sup> a third of its original volume. This is in agreement with experimental results (Berner, 1971). Similarly, the soil solutions of Ca-1 and Ca-3, even though the concentration of  $\text{SO}_4^{2-}$  and  $\text{Ca}^{2+}$  are as high as 50 and 20 mmol/litre, must be concentrated about twice (*c* + *d*) and those from Rangsit about four times (*e* + *f*) before gypsum precipitates. Concentration factors of this order certainly occur in surface horizons during the dry season, in accordance with the temporary presence of gypsum.

At T-1, gypsum is probably formed from calcium and sulfate released in the upper part of the calcareous pyritic substratum as a result of pyrite oxidation. Calcium bicarbonate from river-water has been held responsible for the ubiquity of gypsum in the eastern half of the Bangkok Plain (van der Kevie, 1972). In Na-2, however, evaporation of at least 700 m water from the Mae Klong River (with a  $\text{Ca}^{2+}$  content of 37 mg/kg) would be required to supply the 26 kg of gypsum present per  $\text{m}^2$  land surface. Through run-off only a small fraction of the solutes in the floodwater will eventually become incorporated in the soil, so it seems unlikely that all the calcium present in gypsum could have come from the floodwater in a few thousand years. Moreover, according to analysis of surface water contained in a closed cylinder (App. A, Fig. A1b) or 'inside surface water', and of normal 'outside surface water', the greater part of the solutes (including  $\text{Ca}^{2+}$ ) in the surface water comes from the soil itself, rather than from river-water. This implies that there is, at present, an outward flow of  $\text{Ca}^{2+}$ , so that gypsum may be dissolving rather than accumulating. Probably the upper 90 cm of Na-2, which is lithologically different from the subsoil, was deposited as a calcareous sediment. The material in question must have contained at least 4.8%  $\text{CaCO}_3$  to account for the gypsum present. Recent Mae

a. Due to increasing complexing at higher concentrations, ionic strength increases less than linearly with concentration.

Klong sediment contains 3-7%  $\text{CaCO}_3$ . Data by van der Kevie & Yenmanas (1972) on three profiles 10-20 km southeast to southwest from Na-2 suggest a similar lithological discontinuity, also associated with gypsum in the lower part of the upper stratum.

*Basic aluminium sulfate* The  $\text{Al}^{3+}$  activity of acid sulfate waters decreases roughly 8-fold per unit pH increase, rather than 1000-fold as would be expected from equilibrium between the solution and an aluminium oxide or aluminosilicate (at constant activities of silica and other relevant metal ions). The 8-fold increase follows from a regression of  $\text{pAl}(\text{OH})_3$  against  $2\text{pH}$  for Ra and BP samples from the oxidation experiment, which gave a slope of -1.116 and a correlation coefficient of 0.991 (van Breemen, 1973c). The regression line, which is equivalent to the expression

$$\text{pAl} = 0.77\text{pH} + 1.78 \quad (32)$$

is shown in Fig. 50. Aluminium activities in field samples can be predicted well from Eq. (32) although they have a pH that is normally 1-2 units higher than in samples from the oxidation experiment. Even more surprisingly, published values of  $\text{pAl}(\text{OH})_3$  and pH for a large number of aqueous extracts and interstitial solutions from non-acid soils fit the same relationship within an order of magnitude of the aluminium activity (Fig. 50). The strong dependence of  $\text{pAl}(\text{OH})_3$  on pH clearly demonstrates that an aluminium oxide such as gibbsite does not regulate the activity of dissolved  $\text{Al}^{3+}$  (Misra et al., 1974; Bache, 1974).

To explain the excellent rectilinear relation in the acid sulfate waters according to Eq. (25), the presence of a basic aluminium sulfate,  $\text{AlOHSO}_4$ , was postulated (van Breemen, 1973c). Its existence was substantiated for samples from the oxidation experiment by a regression of  $\text{pAl}(\text{OH})_3$  against  $\text{pH}_2\text{SO}_4$  ( $= \text{pSO}_4 + 2\text{pH}$ ), which had a regression coefficient of 1.00 and a correlation coefficient of 0.994. The regression line (Fig. 50) implies that  $\text{pAlOHSO}_4$  is constant in agreement with equilibrium according to



with  $\text{pK}_{\text{SO}_4}(\text{AlOHSO}_4) 17.23 \pm 0.16$  (mean and standard deviation, respectively). Again field samples fit this relationship very well. For instance, for 50 waters from Ra-1 and Ra-2, sampled from porous pots 30-165 cm deep over a period of

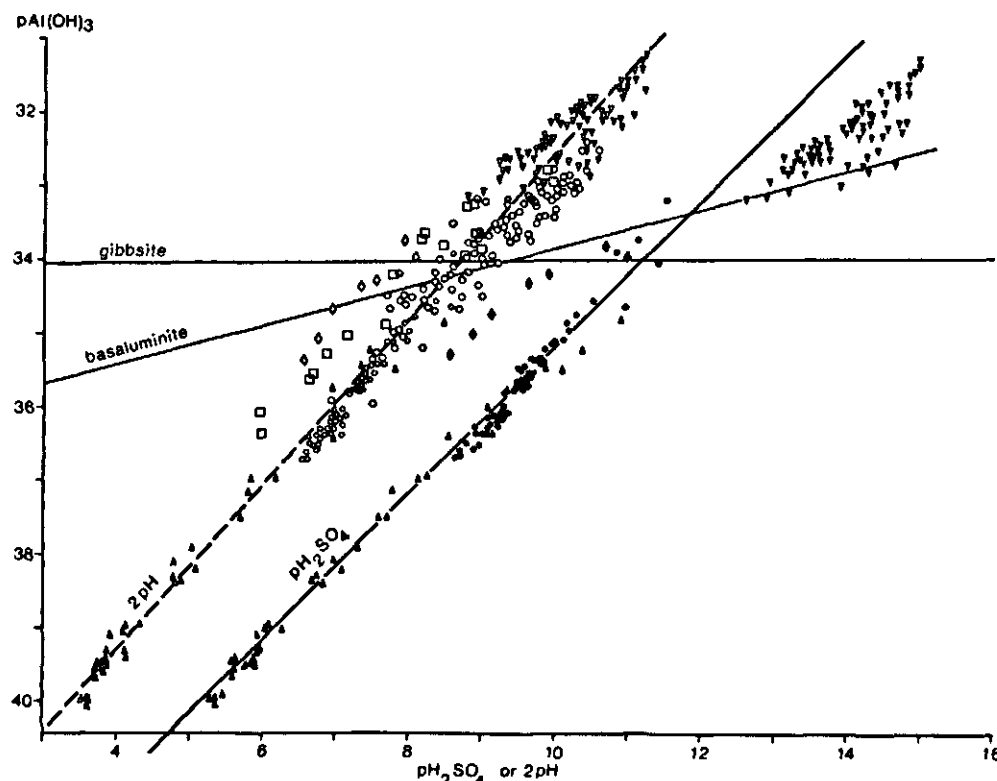


Figure 50  
 $pAl(OH)_3$  against  $2pH$  (open symbols) or  $pH_2SO_4$  (solid symbols) for acid sulfate waters from Thailand, and for published data for various soils extracts. The regression lines were calculated using only data on artificially aerated samples from Thailand.

Key:  $\circ \Delta$  Ra,0 (field samples);  $\blacktriangle \Delta$  Ra, BP (artificially aerated);  $\nabla \nabla$  soil extracts of Richburg & Adams (1970);  $\circ$  soil extracts of Bache (1974);  $\square \square$  soil extracts of Misra et al., (1974);  $\blacklozenge \lozenge$  extracts with  $H_2SO_4$  of volcanic ash soils (Gebhardt & Coleman, 1974).

6 months,  $pAlHSO_4$  was  $17.29 \pm 0.19$ . The agreement with the results for the oxidation experiment ( $pH$  1.8-4; ionic strength 0.035-1.0 mol/litre; dissolved aluminium 0.1-58 mmol/litre and dissolved sulfate 12-260 mmol/litre) is remarkable, considering that the field samples had  $pH$  values between 3.4 and 4.5, ionic strengths of the order of 0.02-0.08, aluminium concentrations between 0.04 and 0.6 mmol/litre and sulfate concentrations between 10 and 20 mmol/litre. Part of corresponding data from slightly acid coastal plain soils from the United States (Richburg & Adams, 1970), and from  $H_2SO_4$ -extracts of volcanic ash soils (Gebhardt & Coleman, 1974)<sup>a</sup> agree well with Eq. (32), but do not in

a. Recalculated to account for the presence of  $AlSO_4^+$  and  $Al(SO_4)_2^-$ .

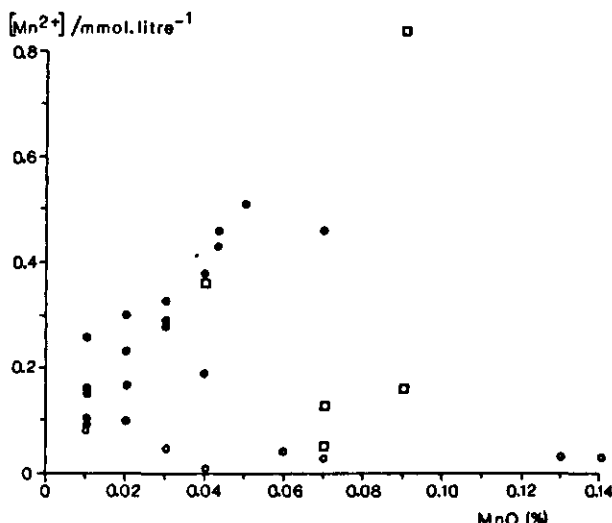


Figure 52

Relation between concentration of dissolved  $Mn^{2+}$  and mass fraction of total  $MnO$  in acid sulfate soils (●; Ra, O, KR, Na), a para-acid sulfate soil (□; Bk) and a non-acid marine soil (○; T-1).

uncertainty about the stability of the oxides, their actual nature is problematic. Oxygenation of aqueous  $Mn^{2+}$  at ordinary temperatures generally yields non-stoichiometric mixtures of different oxides with stabilities that may be quite different from those of their ideal counterparts (Morgan, 1967).

Whichever oxide is considered, the  $E_H$ -pH data normally observed in acid sulfate soils (dark-shaded area in Fig. 51) always fall in the  $Mn^{2+}$  field. This shows that none of the oxides considered is stable in these soils, as evidenced by the absence of black mottles and by the low manganese contents. Unfortunately, no redox potentials are available in black-mottled horizons of the non-acid soils. In older acid sulfate soils,  $Mn^{2+}$  may be present mainly in exchangeable and dissolved form. This is suggested by the distinct correlation between dissolved and total manganese in the acid soils, and the absence of such relationship in the non-acid T-1 (Fig. 52). Pedon Bk-1, which has a near-neutral black-mottled B2 horizon and a distinctly acid B3 horizon shares characteristics of both groups of soils. Near-equilibrium or slight supersaturation with  $MnCO_3$  ( $D(\text{Rhod}) = -0.01$  to  $+0.7$ ) was observed in some samples of mangrove muds (Ca-3) and substrata of young acid sulfate soils (BP-1, KD-1), as well as in the reduced surface horizon of T-1.

After 280 days of aeration, numerous tiny black mottles of manganese oxides were observed in calcareous pyritic soil (Mc-24) after repeated leaching with distilled water in the oxidation experiment. The  $E_H$ -pH of the sample

indeed falls in a manganese oxide field (Fig. 51), and in fact the solution was supersaturated with three oxides:  $D$ (Pyrolusite) 1.1,  $D$ (Manganite) 1.5, and  $D$ (Hausmannite) 3.8. In the other aeration experiments with the same soil (upon leaching with sea-water, and in the non-leaching treatments), no saturation with any of the oxides was reached and no black mottles were observed. This suggests that  $E_H$ -pH-pMn data may be interpretable in terms of Mn oxide equilibria, at least at the low  $Fe^{2+}$  concentrations ( $< 10^{-2}$  mmol/litre) in these samples.

#### 4.6 REDUCTION PROCESSES

Flooding brings about drastic changes in most soils. As a result of saturation with water, exchange of gases decreases dramatically. Within hours or days, the oxygen concentration is reduced to practically zero mainly by aerobic microbial respiration (Ponnamperuma, 1964). In the absence of molecular oxygen, anaerobic bacteria utilize oxidized compounds such as nitrate, manganese, ferric oxide, dissimilation products of organic matter and sulfate as electron acceptors. In agreement with standard potentials of the corresponding half cell reactions, nitrate, manganese oxides, ferric oxides and sulfate are reduced in this order. After the disappearance of nitrate, the concentrations of  $Mn^{2+}$  and, somewhat later, of  $Fe^{2+}$  generally increase to distinct peaks during the first weeks flooding, and then decrease to fairly constant values. If reduction becomes sufficiently intense, sulfate is reduced to sulfide.

Soil reduction is typically accompanied by an increase in the concentrations of  $CO_2$  (liberated by respiration) and of cations such as  $Ca^{2+}$  and  $Mg^{2+}$  that are displaced from the exchange complex by  $Fe^{2+}$ . These cations are mainly balanced by  $HCO_3^-$ , produced simultaneously with  $Fe^{2+}$ . In soils with an initial pH 5-6, the increase in alkalinity ( $HCO_3^-$ ) results in an increase in pH to 6.5-7. But in calcareous and alkaline soils, the mobilization of iron is inhibited by the high pH, and less  $HCO_3^-$  is formed. There the acidifying effect of released  $CO_2$  is more important, with a fall in pH to 6.5-7. If sufficient easily decomposable organic matter and reducible ferric iron are present, and strongly oxidized compounds such as  $NO_3^-$  and  $MnO_2$  are unimportant quantitatively, soil reduction is accompanied by a decrease in  $E_H$  from distinctly positive values, to values of the order of -0.1 to -0.2 V within a few weeks of flooding.

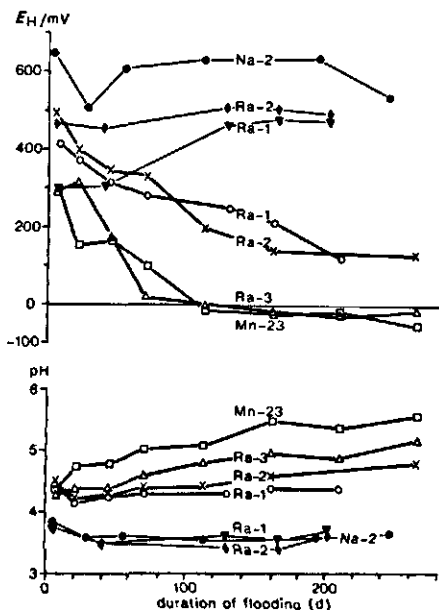


**Figure 53**  
Changes in  $E_H$  and pH in artificially flooded samples from surface horizons (open symbols) and jarositic horizons (solid symbols) from acid sulfate soils.

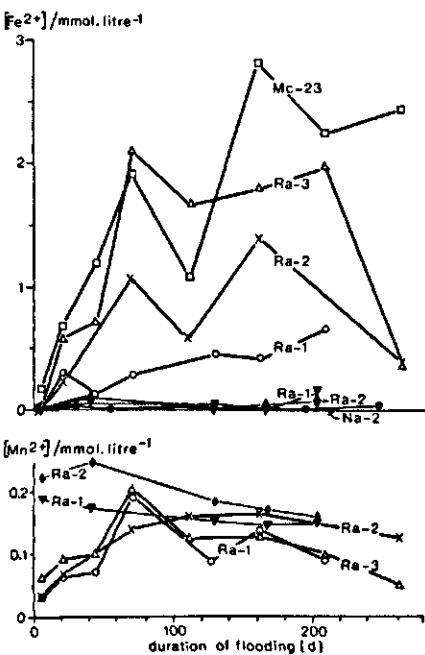


**Figure 54**  
Changes in concentration of dissolved  $Fe^{2+}$  and  $Mn^{2+}$  in artificially flooded samples from surface horizons (open symbols) and jarositic horizons (solid symbols) from acid sulfate soils.

#### 4.6.1 Soil reduction in acid sulfate soils

*Rate and intensity of soil reduction* In order to study reduction in acid sulfate soils under controlled conditions, a 'reduction' experiment was set up. Separate samples of surface soils from the Rangsit Station and from Mc-23, and of jarositic B horizons from Ra-1, Ra-2 and Na-2 were placed in 1-litre glass jars and submerged in distilled water. Periodically, the pH and  $E_H$  of the soil in one pot of each series were measured; the soil solution was collected by pressure filtration; and the soil sample was discarded.

In the surface soils, the  $E_H$  decreased and the pH increased with time as expected (Fig. 53). No such evidence for soil reduction was observed in the samples from the jarositic B horizon, even after flooding for more than 6 months.

Likewise, dissolved  $Fe^{2+}$  increased in the flooded surface soils, but remained very low in subsoil samples (Fig. 54). The somewhat erratic behaviour

Table 16. Means and standard deviations for  $E_H$ , pH, concentrations of dissolved  $Fe^{2+}$  and  $Mn^{2+}$  in field samples of surface horizons (0-10 cm) of acid and non-acid soils at the end of the flooding period (November 1969 and December 1970). The group of 'non-acid soils' includes two samples from Na-2.

	$E_H/V$	pH	pe + pH	$Fe^{2+}$ mmol/1	$Mn^{2+}$ mmol/1	n
acid soils	50 ± 150	5.35 ± 0.83	6.2 ± 1.9	0.42 ± 0.56	0.05 ± 0.01	16
non-acid soils	-140 ± 60	6.63 ± 0.01	4.3 ± 0.9	0.31 ± 0.08	0.07 ± 0.04	4

of  $Fe^{2+}$  may be due to small differences between soil samples. Dissolved manganese also increased in the surface samples, and remained almost constant in the subsoils. Because manganese oxides would be absent (Section 4.5), the increase in  $Mn^{2+}$  upon reduction must be due to the release of exchangeable  $Mn^{2+}$  or the release of  $Mn^{2+}$  incorporated in ferric oxides (Collins & Buol, 1970).

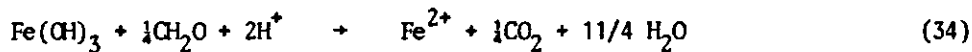
The same was observed *in situ*: soils became reduced near the surface but remained oxidized in the jarositic B horizon throughout flooding. In the surface soils reduction was somewhat more intense *in situ* than in the laboratory. Intensity of reduction was higher outside than inside the poly(vinyl chloride) tubes (App. A, Fig. A 1b). The maintenance of rather high electrolyte concentrations and the development of very low pH in the surface water, through the absence of lateral drainage, may have hampered soil reduction both in these tubes and in the laboratory samples. Another difference between 'outside' and 'inside' soil is that the latter had been disturbed when the tubes were placed, but appreciable effect on the behaviour of the soil after flooding would not be expected. Even under natural conditions, the intensity of reduction near the surface of acid sulfate soils is low compared to that observed in most 'normal' paddy soils and in non-acid soils from the Bangkok Plain (Table 16).

Other workers (Nhung & Ponnamperuma, 1966; Ponnamperuma et al. 1973, Park et al., 1971) also observed slow rates of reduction in acid sulfate soils. Data from an anaerobic incubation test<sup>a</sup> by Kawaguchi & Kyuma (1969), however,

<sup>a</sup> 10 g air-dry soil plus 20 ml deionized water incubated in a sealed cylinder at 30 °C for two weeks. An increase in pH is taken as evidence for soil reduction.

indicate that surface samples from some acid sulfate soils (pH 4.3-4.5) underwent rapid reduction whereas other did not. Some of the factors responsible for slow reduction may be (a) a low content of easily reducible  $Fe_2O_3$  (Ponnamperuma et al., 1973); (b) a low content of easily oxidizable organic matter; (c) a poor nutrient status<sup>a</sup>; and (d) an adverse effect of low pH, either directly or indirectly, on the activity of anaerobes. The last factor alone does not explain why soils with about the same pH behaved differently upon anaerobic incubation. Neither is an overriding importance of any of the other factors apparent from the chemical data on the samples used by Kawaguchi & Kyuma (1969). Their results for 18 surface horizons from the Bangkok soils fail to show a clear correlation of the pH increase with (a) the content of 'easily' (0.2 M HCl) soluble iron (b) the organic matter content (c) the release of  $NH_3$  upon anaerobic incubation and (d) various measures of available phosphorus. Total organic C is certainly not limiting, since the surface horizons of acid sulfate soils are significantly richer in organic carbon mass fraction ( $1.93 \pm 0.54\%$ ;  $n = 11$ ) than those of non-acid marine soils ( $1.28 \pm 0.34\%$ ;  $n = 11$ ) (data from Kawaguchi & Kyuma, 1969). As regards the other factors, no answer can be given at present, but it is likely that several, some perhaps unknown, operate simultaneously. In the jarositic B horizons, the persistence of oxidized conditions throughout the flooding period can be attributed to the still lower pH, the very low content of organic matter, the presence of jarosite (stable in acid, oxidized conditions), and the presence of relatively insoluble ferric oxides.

*Processes associated with reduction of  $Fe_2O_3$*  For the reduction of ferric oxide by organic matter, protons are required:



In most 'normal' paddy soils, carbon dioxide is the main proton donor in Eq. 34, since  $HCO_3^-$  appears along with  $Fe^{2+}$  and cations displaced by  $Fe^{2+}$  at the exchange complex (IRRI, 1965), leading to the total reaction:

---

a. A simple fertilizer (N 100,  $P_2O_5$  60 and  $K_2O$  20 kg/ha) roughly doubled the rate of  $Fe^{2+}$  production in an acid sulfate soil from Thailand (Sombatpanit & Wangpaiboon, 1973).

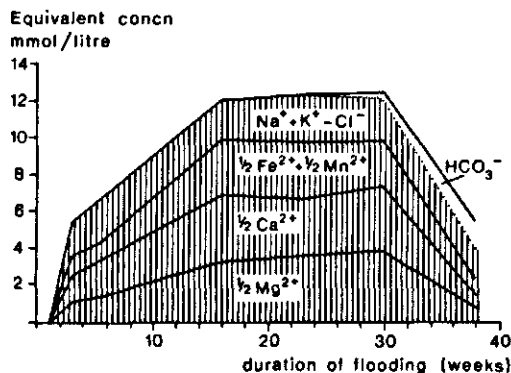
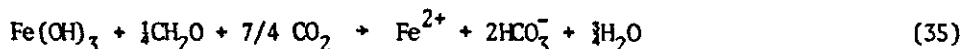
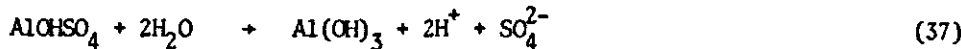
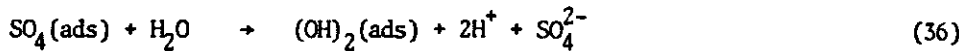


Figure 55

Changes in equivalent concentrations (with respect to initial values) of dissolved species (plotted cumulatively) in a surface sample from Ra-3, artificially flooded in the laboratory. The shaded area represents dissolved sulfate; the difference between total cations and sulfate at the end of the experiment is due to  $\text{HCO}_3^-$ .



In acid sulfate soils, however, ferrous sulfate is formed instead of ferrous bicarbonate. This is illustrated by Fig. 55, which shows the changes in the composition of the soil solution in flooded Ra-3 topsoil. Comparable changes were observed in three other soils used for the reduction experiment. Reduction of ferric oxide to  $\text{Fe}^{2+}$  followed by replacement of exchangeable  $\text{Ca}^{2+}$  and  $\text{Mg}^{2+}$  by part of the  $\text{Fe}^{2+}$  obviously account for the increase in concentration of cations during the first 24 weeks. Except for the sharp initial increase, which may be due partly to solution of easily soluble sulfates, the change in dissolved sulfate must be due to hydrolysis of basic sulfates or desorption of sulfate (Nhung & Ponnamperuma, 1966). At the same time, desorption of  $\text{SO}_4^{2-}$  or hydrolysis of a basic sulfate (e.g.  $\text{AlOHSO}_4$ ) provides protons necessary for iron reduction (Eq. 34):



Under conditions too acid for appreciable dissociation of  $\text{CO}_2$ , these protons thus have the same role as those supplied by carbon dioxide at higher pH (Eq. 35). The disappearance of exchangeable and water-soluble aluminium and the simultaneous appearance of exchangeable  $\text{Fe}^{2+}$  in flooded acid sulfate

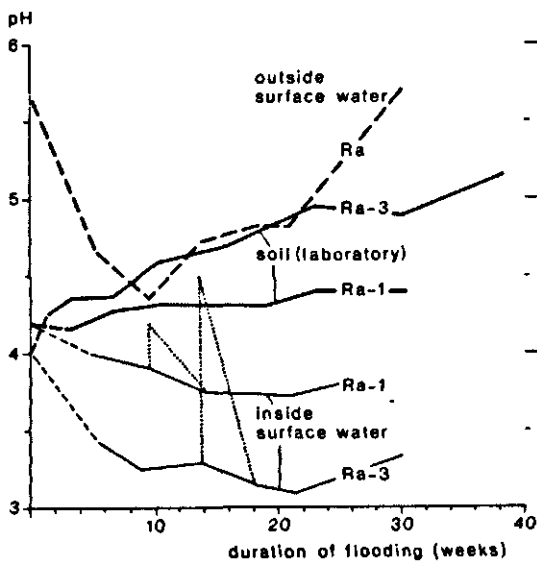


**Figure 56**  
 Changes in pH of surface soils and of 'outside' and 'inside' surface water (Fig. A.1) at Ra-1 and Ra-3. The dotted lines show the changes in pH upon replacing 'inside' surface water by less acid 'outside' surface water.

soils (Park et al., 1971; Sombatpanit & Wangpaiboon, 1973) show that the protons formed during hydrolysis of aluminium are also involved in the reduction of iron but these are not associated with an increase in dissolved sulfate.

The presence of dissolved  $\text{FeSO}_4$  in flooded acid sulfate soils explains an interesting phenomenon: the acidification of surface water standing above the soil (Fig. 56). Any ferrous sulfate that reaches the soil-water interface by diffusion (cf. Howeler & Bouldin, 1971) will produce sulfuric acid upon oxidation of  $\text{Fe}^{2+}$  to ferric oxide:



Because this effect was not anticipated, it was not studied specifically. The acidification is demonstrated clearly, however, by the change in pH of the 'inside' surface water (Fig. 56). Outside surface water, which was continuously replaced by rainwater and later also by more alkaline floodwater, underwent appreciable acidification only during the first ten weeks. Replacement of the inside surface water by less acid outside surface water after 10 and 14 weeks of flooding apparently amplified rather than reversed the drop

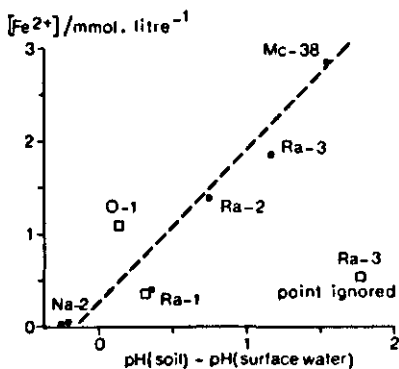


Figure 57  
 Dissolved  $\text{Fe}^{2+}$  in surface soils  
 against the difference of 'inside'  
 soil pH and the pH of 'inside'  
 surface water;  $r = 0.94^{**}$ .

One data point was ignored in  
 the regression because dissolved  $\text{Fe}^{2+}$   
 had decreased by formation of  $\text{FeS}$ .  
 Key:  $\circ$  laboratory reduction experi-  
 ment;  $\square$  field samples.

in pH. This may be due to extra supply of oxygen to the surface water, or to intensified soil reduction or diffusion upon removal of reaction products. The slight increase in pH of the inside surface water after about 30 weeks of flooding is attributable to buffering reactions involving silicate minerals. This is suggested by the release of dissolved  $\text{Si}(\text{OH})_4$  to concentrations higher than in the interstitial water in the same tube.

No such acidification was observed *in situ* for soils of pH 5.5-6 before flooding (T-1 and Na-2) and during the reduction experiment in flooded but continuously oxidized samples from jarositic B horizons. So both low pH and soil reduction are required to acidify surface water, in accordance with the hypothesis. The highly significant correlation between  $\text{pH}(\text{soil})$  minus  $\text{pH}(\text{surface water})$  and the concentration of interstitial  $\text{Fe}^{2+}$  provides further support (Fig. 57). Samples from Ra-3 showed a decrease in  $\text{Fe}^{2+}$  as a result of formation of  $\text{FeS}$  and were excluded from the correlation.

The maximum amounts of acidity and alkalinity, observed in the inside surface water at various sites are given in Table 17. As indicated by the lower  $E_H$  and higher pH reached in the soils outside the tubes, soil reduction and hence production of dissolved  $\text{FeSO}_4$  were seriously hampered in the tubes. Therefore the amounts of acid released into the open surface water must have been considerably greater. As will be explained in Chapter 6, this 'active' removal of acidity is important for deacidification of acid sulfate soils.

After 29 weeks of flooding, the concentrations of dissolved divalent ions decreased dramatically in the artificially flooded Ra-3 surface soil (Fig. 55). Moreover,  $\text{HCO}_3^-$  appeared in the soil solution and a distinct smell of  $\text{H}_2\text{S}$  was noticed when handling the soil. These observations are explained by sulfate reduction, followed by precipitation of  $\text{FeS}$  and replacement of exchangeable  $\text{Fe}^{2+}$  by  $\text{Ca}^{2+}$  and  $\text{Mg}^{2+}$ . Likewise, sulfate reduction was observed

Table 17. Acidity,  $[H^+] + [\frac{1}{3}Al^{3+}]$ , and alkalinity  $[HCO_3^-]$ , in the surface water inside the poly(vinyl chloride) tubes, and redox conditions of surface soil inside and outside the tubes at the end of flooding. The soils are classed according to their 'aerobic pH' as about 4.5 and 5.5-6.

	pH ~ 4.5					pH 5.5-6	
	KR-1	Mn-1	0-1	Ra-1	Ra-3	Na-2	T-1
$[H^+] + [\frac{1}{3}Al^{3+}]$ /depth of surface water (mmol/dm <sup>2</sup> )	1.9	4.9	3.9	2.5	18.7	0	0
$[HCO_3^-]$ /depth of surface water (mmol/dm <sup>2</sup> )	0	0	0	0	0	10	0.6
pH (inside surface water)	-	-	3.7	3.8	3.3	7.1	7.2
pH (soil in tubes)	-	-	3.85	4.15	5.1	6.6	6.5
pH (soil outside tubes)	-	-	5.2	5.25	5.5	6.6	6.6
$E_H$ (soil in tubes) /mV	-	-	433	330	-66	-163	-130
$E_H$ (soil outside tubes) /mV	-	-	0	-44	-90	-163	-153

during the reduction experiment in Mc-23, but not in Ra-1 and Ra-2. In practically all near-neutral soils, sulfate reduction took place after 2-8 weeks of submergence. The absence or late start of sulfate reduction in the acid soils is probably due to inhibition by low pH of sulfate-reducing bacteria, which are generally reported to be inactive at pH values below 5. In this respect, the reduction experiment probably exaggerated the picture. Of the 16 acid soils of Table 16, that were flooded for about 5 months, sulfate was probably being reduced in 7, since they had pH > 5 and negative  $E_H$ , low concentrations of dissolved  $SO_4^{2-}$  and sometimes black spots of FeS. Under field conditions sulfate reduction was apparent in all Rangsit soils, but only after about 6 months of flooding.

#### 4.6.2 Soil reduction in non-acid soils

Within two weeks of anaerobic incubation, the pH of non-acid marine soils increased from 5 or 5.5 to about 6 (Kawaguchi & Kyuma, 1969). In the surface horizon of T-1, dissolved manganese increased to peak values within 1 week of flooding, and concentration of ferrous iron reached peak values after 1-6 weeks (Fig. 58). After about 6 weeks, the appearance of black spots and the increase in  $HCO_3^-$  accompanied by a decrease in  $SO_4^{2-}$  marked the onset of sulfate reduction. Little or no change in dissolved iron, manganese and sulfate occurred below 50 cm depth, indicating that the subsoil remained essentially oxidized, just as in the acid sulfate soils. Oxidized conditions

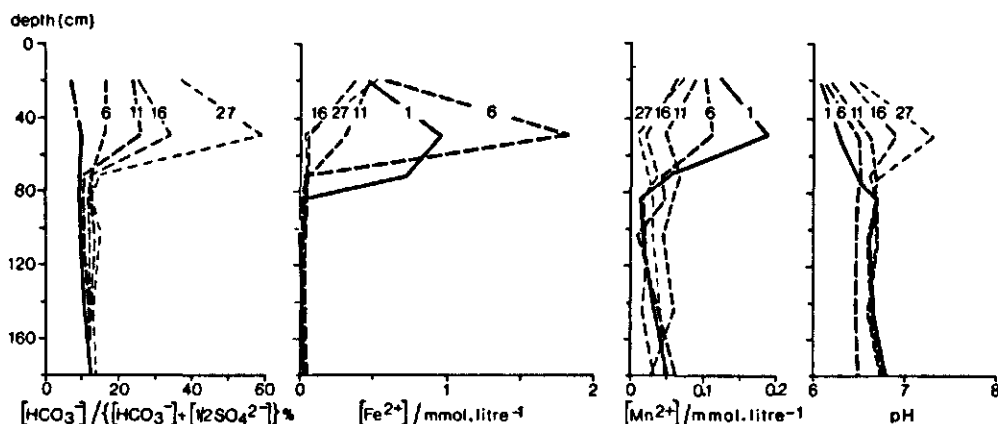


Figure 58

Changes in the extent of sulfate reduction (expressed as the substance fraction of  $\text{HCO}_3^-$  to  $(\text{HCO}_3^- + \frac{1}{2}\text{SO}_4^{2-})$ ), dissolved  $\text{Fe}^{2+}$  and  $\text{Mn}^{2+}$ , and pH with depth and time in the non-acid marine soil T-1. Numbers indicate duration of flooding in weeks.

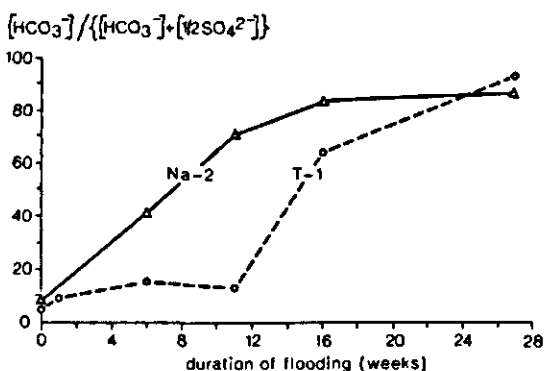


Figure 59

Changes in the relative importance of  $\text{HCO}_3^-$  with time in the 'outside' surface water at Na-2 and T-1.

are probably maintained by very low content of organic matter and a low reactivity of ferric iron.

The  $E_{\text{H}}\text{-pH}$  data given in Tables 16 and 17 demonstrate the much stronger anaerobiosis in non-acid soils than acid soils. In the surface soils of both T-1 and Na-2 dissolved bicarbonate increased relative to sulfate. Although some of the increase in  $\text{HCO}_3^-$  can be attributed to reduction of ferric oxide (Eq. 35), sulfate reduction according to Reaction 3 was far more important. A similar relative increase in  $\text{HCO}_3^-$  was observed in the (outside) surface water at both sites (Fig. 59). In the mainly rain-fed soil T-1, practically all  $\text{HCO}_3^-$  must have come from the soil. There the temporary decrease in the fraction

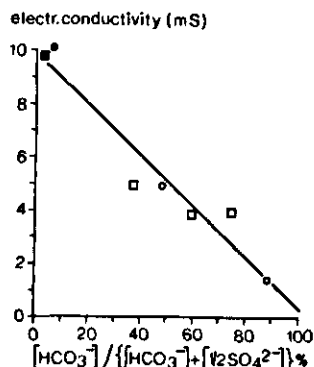


Figure 60  
 Extent of sulfate reduction (see Fig. 58) against electrical conductivity in the interstitial solution from the surface soil at Na-2 and T-1 at the end of the flooding period (November 1969; December 1970),  $r = -0.955^{**}$ .  
 Key:  $\blacksquare$  T-1;  $\bullet$   $\circ$  Na-2; solid symbols are for samples collected inside the tubes; open symbols for 'natural' samples.

$[\text{HCO}_3^-]/\{[\text{HCO}_3^-] + [\text{HSO}_4^{2-}]\}$ <sup>a</sup> after 5-11 weeks of flooding was due to a brief period with submergence during a dry spell, and associated oxidized conditions in the uppermost soil. At Na-2, river water may have contributed to the increase in  $\text{HCO}_3^-$ , but the concentrations of most electrolytes in the surface water were at least ten times as high as those of the Mae Klong and Chao Phraya Rivers, indicating that most solutes originated from the soil.

From soil solution data at the beginning and at the end of flooding, the loss of  $\text{HCO}_3^-$  at T-1 was estimated to be about  $60 \text{ mmol}/\text{dm}^2$ . Because most  $\text{H}_2\text{S}$ , formed simultaneously with  $\text{HCO}_3^-$  was probably fixed as  $\text{FeS}$ , little sulfide was lost from the soil. This implies that about  $60 \text{ mmol}/\text{dm}^2$  of potential acidity remained behind as  $\text{FeS}$ . Oxidation of this amount of  $\text{FeS}$  would contribute  $1.2 \text{ mmol}$  of acidity per  $100 \text{ g}$  soil down to  $50 \text{ cm}$  depth (bulk density  $1.5 \text{ kg/litre}$ ).

This explains why the pH of (air-dry) surface samples from periodically flooded non-acid marine soils is generally 1-3 lower than of the subsoil (van Breemen, 1975). The far lower amount of  $\text{HCO}_3^-$  in the 'inside' surface water at T-1 (Table 17) is due to inhibited sulfate reduction in soil inside the poly(vinyl chloride) tube (Fig. 60). The highly significant correlation between the extent of sulfate reduction and electrical conductivity indicates that high salinity or accumulation of reaction products is responsible for this effect.

As was discussed in Section 4.4.2, precipitation of  $\text{FeS}$ , not of  $\text{Fe}_3(\text{OH})_8$ , was probably responsible for the fall in dissolved  $\text{Fe}^{2+}$  in the flooded surface

a. Because most  $\text{HCO}_3^-$  was formed by the reaction  $\text{SO}_4^{2-} + \text{CH}_2\text{O} \rightarrow \text{H}_2\text{S} + 2 \text{ HCO}_3^-$ , this fraction indicates the extent of sulfate reduction.

soil of T-1 (Fig. 58). Because supersaturation with  $MnCO_3$  was reached only at the end of flooding, the drop in dissolved  $Mn^{2+}$  after one week cannot be ascribed to precipitation of carbonate. Precipitation of  $MnS$  was equally unlikely: simultaneous equilibrium involving  $MnS$  ( $pK_{so} 15.2$ , Morgan, 1967) and  $FeS$  ( $pK_{so} 16.9$  for the amorphous sulfide and 17.6 for mackinawite) would give  $a(Fe^{2+}) / a(Mn^{2+})$  of  $(4-20) \times 10^{-3}$ . The activity quotients observed after peak concentration of water-soluble iron were several orders of magnitude higher, so that the solutions were probably far undersaturated with  $MnS$ .

#### 4.7 REDISTRIBUTION OF IRON, SULFUR AND MANGANESE

As illustrated in Figure 21, iron, sulfur and manganese show a pronounced distribution with depth in most soils. In acid sulfate soils, iron and sulfur seemed to have been removed from the A and B3 horizons and accumulated in the B2 horizon. The oxidized part of acid sulfate soils was generally depleted of manganese, but accumulations of Mn oxides in the B horizon are common in non-acid marine soils. All these phenomena can be explained readily by considering the mobility of these elements under different conditions.

*Iron* In the upper part of the substratum low pH and the presence of organic matter and pyrite cause a high mobility of iron. With a sufficiently low water-table, ferrous sulfate and sulfuric acid are formed during pyrite oxidation. The presence of ferric hydroxide in acid pyritic substrata, for instance in ferrans, even leads to pyrite oxidation during flooding, causing an increase in dissolved  $Fe^{2+}$ . So, in the upper part of pyritic substrata,  $Fe^{2+}$  is produced throughout the year. At the same time, the B2 horizon is permanently oxidized and characterized by low concentrations of dissolved iron. This leads to a continuous upward flow of  $Fe^{2+}$  from the substratum. Moreover, during flooding,  $Fe^{2+}$  formed in the A1 horizon establishes a concentration gradient downwards. The profiles of dissolved iron at different times after the start of submergence in Ra-2 have been explained in terms of production and diffusion (Harmsen & van Breemen, 1975). The small increase in dissolved ferrous iron observed in the jarositic horizon could be accounted for by diffusion from above and below, assuming an apparent diffusion coefficient of the order of that in dilute aqueous solutions. This suggests that iron migration is little influenced by solid-solution interactions (ion exchange and oxidation followed by precipitation), which would strongly depress the apparent diffusion coefficient. This in turn implies that  $Fe^{2+}$  moves mainly through the larger vertical channels

rather than through the soil mass, which is in accordance with the close association of ferric oxide and jarosite mottles with these channels. It also implies that oxidation of the  $Fe^{2+}$  in the B horizon occurs largely in the dry season. Tentative estimates indicate that only about a fifth of the ferric iron accumulated in the B horizon can be accounted for by migration during the wet season (Harmsen & van Breemen, 1975). If this is true, most of the iron accumulation is due to upward migration of  $Fe^{2+}$  during pyrite oxidation as a result of aeration at depth in the dry season.

In the upper part of the flooded A1 horizon, iron migrates towards the soil-water interface where  $Fe^{2+}$  oxidizes to ferric hydroxide in a thin (1-10 mm) surface layer. This layer is partially disturbed by physical and biological processes during the dry season but upon detailed sampling a clear accumulation of free  $Fe_2O_3$  is noticeable in the upper 10-15 cm of most Bangkok Plain soils (Kawaguchi & Kyuma, 1969).

In addition to the vertical distribution of iron discussed above, a horizontal distribution may be important in toposequences. For instance at Rangsit, the average mass fraction of iron (Fe) in the whole profile (taking into account differences in bulk density) increases with increasing altitude of the soil surface: 2.3% at Ra-3, 3.5% at Ra-2 and 4.15% at Ra-1. Longer duration of soil reduction, due to longer periods of submergence and higher contents of organic matter, in the lowest soils and simultaneous oxidation in higher ones may be responsible for the establishment of a lateral concentration gradient.

Several soils outside the Bangkok Plain do not show the iron distribution discussed above. In Ca-1, iron oxide and jarosite are almost constant with depth throughout the B horizon. Rapid artificial drainage of the area to 1-2 m depth, and the absence of a periodically reduced A1 horizon probably account for the absence of pronounced accumulation of ferric oxide and jarosite. A permanently high watertable as a result of tidal influence, and the absence of an A1 horizon explain the peculiar distribution of iron and sulfur at Ch-1 (Fig. 11). The low mass fraction of iron in the B3 horizon, which contrasts so strongly with jarosite accumulation near the surface, must be due to the mobilization of iron when pyrite and ferric oxide are both present at low pH.

The absence of a pyritic substratum and the very pronounced iron pan in Kl-1 (see Fig. 11) point to a specific genesis of this pedon. The average iron content over the sampled depth (down to 180 cm), calculated from the analysed

contents of  $Fe_2O_3$  and estimated bulk densities, is of the order of 9% Fe. This is considerably higher than that in all other soils studied (2.1-5.0% Fe). A plausible explanation is that most of the iron in Kl-1 is accumulated by evaporation of  $FeSO_4$ -rich groundwater from an aquifer. Part of the year, this water is probably somewhat artesian, with the clay-loam to sandy-loam subsoil functioning as the water-bearing stratum, and the iron pan as the impervious layer. This would explain the wet, apparently poorly ripened character of the subsoil. The origin of the ferrous sulfate in ground water is unknown, but is probably pyrite in older and higher sediments.

The lack of jarosite and the uniform distribution of ferric oxide in Nk-1 and Nk-2 is difficult to explain. The one soil in the same region described and sampled in more detail (Sa-1) showed a distribution of iron and sulfur quite like that of soils from the Bangkok Plain.

Non-acid marine soils and para-acid sulfate soils have a less pronounced maximum in distribution of free  $Fe_2O_3$  in the B horizon than acid sulfate soils (data of Kawaguchi & Kyuma, 1969). Upward migration of  $Fe^{2+}$  from the substratum is probably small at near-neutral pH, which depresses the mobility of  $Fe^{2+}$ , prevents pyrite oxidation during flooding and slows pyrite oxidation in the dry season. Also, early precipitation of ferrous iron (e.g. as FeS) in the reduced surface soil limits downward migration of iron and probably accounts for the relatively high contents of free ferric oxide in the A1 horizon.

*Sulfur* Little of the iron leaves the soil, but most of the sulfur originating from pyrite is lost. This can be seen, for instance, from the high concentration of dissolved sulfate relative to that of iron, which points to a far greater mobility of sulfate. Neglecting surface efflorescences of easily soluble salts that may form temporarily during the dry season and the transient FeS, sulfur can be retained in the following forms: jarosite, gypsum, adsorbed sulfate and, possibly, basic aluminium sulfate. Of these, jarosite and gypsum are most important quantitatively and are generally confined to distinct horizons. Jarosite is limited to acid and oxidized conditions: it is absent from periodically reduced, and less acid, surface horizons and from acidified pyritic substrata. Jarosite is hydrolyzed in the upper part of the jarositic horizon and formed in the lower part, causing an apparent downward movement of the yellow mottled zone in a chronosequence of soils.

Precipitation of gypsum is independent of pH but requires rather high concentrations of sulfate and calcium. Its presence in certain horizons may be caused by a combination of chemical phenomena and physical phenomena, such as capillarity. Especially in non-acid soils, periodic reduction of gypsum to

sulfide would hamper accumulation of gypsum in the A2 horizon. For instance, at 50 cm depth in T-1, sulfate reduction caused a decrease in  $D(\text{Gyp})$  from -0.01 just after submergence to -1.19 at the end of flooding. Little is known about the quantitative importance and distribution of adsorbed sulfate and basic aluminium sulfate. Both forms are probably almost confined to acid ( $\text{pH} < 5$ ) soil.

Near-equilibrium with  $\text{AlOHSO}_4$  was observed throughout profiles of acid sulfate soils. Adsorbed sulfate undoubtedly occurs also at all depths in the acidified part of the soil, but because ferric oxide is probably the most important adsorbent, its content may be determined in part by that of free  $\text{Fe}_2\text{O}_3$ .

*Manganese* The rather similar response of iron and manganese to oxidation and reduction is reflected in the distinct accumulation of manganese in the B horizon of non-acid marine soils. Although it is more mobile than iron, separation of the two elements is not apparent in the pedon T-1. This difference in mobility is marked, however, in acid sulfate soils where manganese oxides were completely removed from the acidified part of the profile.

## 5 Silica and silicates

The study of silica and silicates in acid sulfate soils is of particular interest for several reasons. Firstly, the strongly acid environment enhances silicate weathering and thus affects both the soil mineralogy and the composition of the soil solution. Secondly, in the absence of lime, silicate minerals may be important in buffering the soil pH (van Breemen & Wielemaker, 1974a, 1974b). The mineralogy of the soils studied, notably the clay mineralogy, will be treated in Section 5.1, silicate weathering and dissolved silica in Section 5.2 and silicate stability diagrams in Section 5.3. The pH buffering provided by silicates and other minerals will be discussed briefly in Chapter 6.

### 5.1 MINERALOGY

The silt fraction of all soils consists predominantly of quartz but the sand fraction may contain mainly feldspars, at least in the substratum (Suraphibul, 1971). Because the sand fraction normally constitutes less than 1% of the soil, these feldspars are quantitatively unimportant. Albite was detected by X-ray diffraction in samples scraped from ped faces at Ra-2 and Ra-3. Part of the pyrite, jarosite and iron oxides also occur in the sand plus silt fraction. Most of the variation in mineralogy, however, is in the clay fraction. The clay mineralogy was studied by X-ray diffraction and elemental analysis.

Representative X-ray diffraction patterns of oriented clay separates are shown in Figures 61 and 62. Air-dry  $Mg^{2+}$ -saturated clay from the Bangkok Plain invariably shows distinct peaks at 0.7, 1.0 and 1.4 nm. Except in samples from surface horizons, saturation with glycerol results in an almost complete shift from 1.4 to 1.8 nm, whereas saturation with  $K^+$  results in a collapse of the peak at 1.4 nm, partly to 1.0 nm and partly to 1.0 - 1.4 nm. These observations demonstrate the presence of kaolinite, illite and high-charge smectite. The basal spacing of 1.4 nm is distinctly less intense in surface samples than in subsoil samples. Furthermore, swelling to 1.8 nm and collapse to 1.0 nm seem inhibited in these surface samples, and notably in the acid

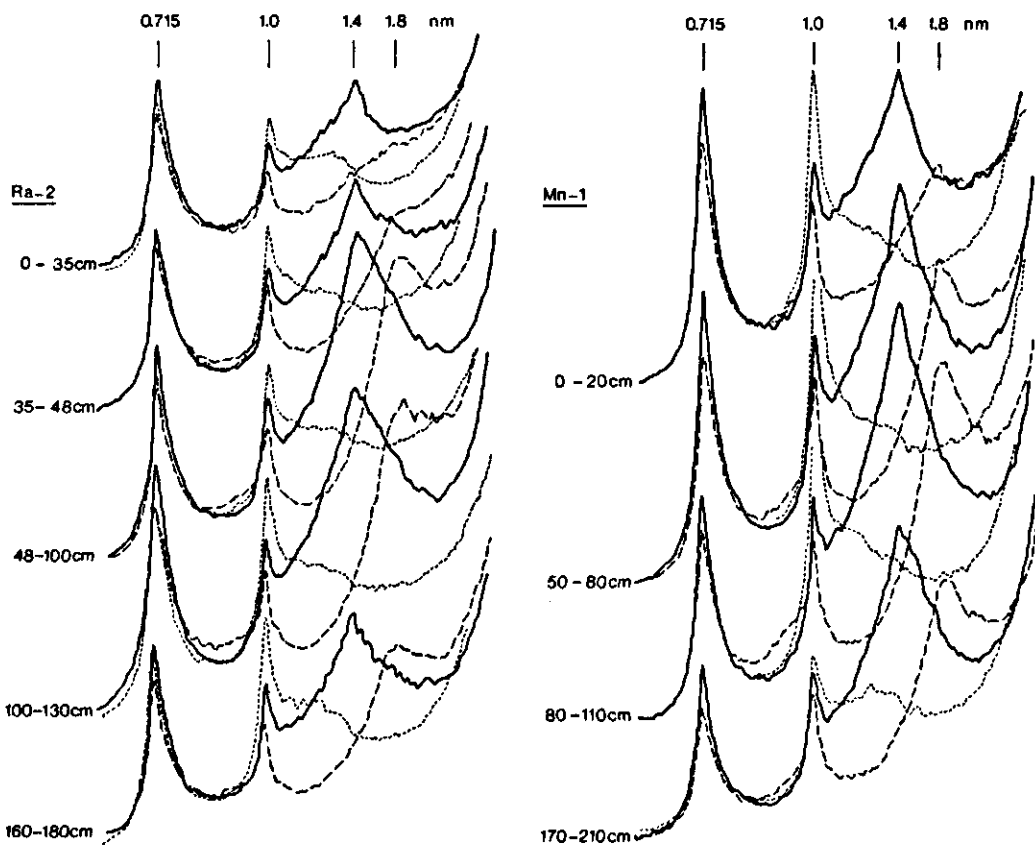


**Figure 61**  
 X-ray diffraction patterns for oriented clay separates from two acid sulfate soils from the Bangkok Plain. Key: solid line, magnesium clay; broken line, magnesium clay saturated with glycerol; dotted line, potassium clay.

sulfate soils, a distinct 'shoulder' remains present at 1.4 nm after glycerol treatment. Because the peak at 1.4 nm disappears upon heating to 400 °C, it is probably due to 'soil chlorite', formed by discontinuous interlayering of smectite with aluminium hydroxide. Others (Kawaguchi & Kyuma, 1969; Suraphibul, 1971) designated the non-swelling material with a peak at 1.4 nm as vermiculite. In view of the absence of a strongly enhanced peak at 1.0 nm upon saturation with  $K^+$ , this conclusion appears erroneous.

The non-acid T-1 has a similar clay mineralogy, except that the smectite peaks are higher and soil chlorite is essentially absent (Fig. 62 left).

X-ray diffraction patterns of clay separates from Peninsular Thailand are very different. Firstly, the kaolinite peak (0.7 nm) predominates over the peaks at 1.0 and 1.4 nm. Secondly a peak at 1.2 nm, presumably due to

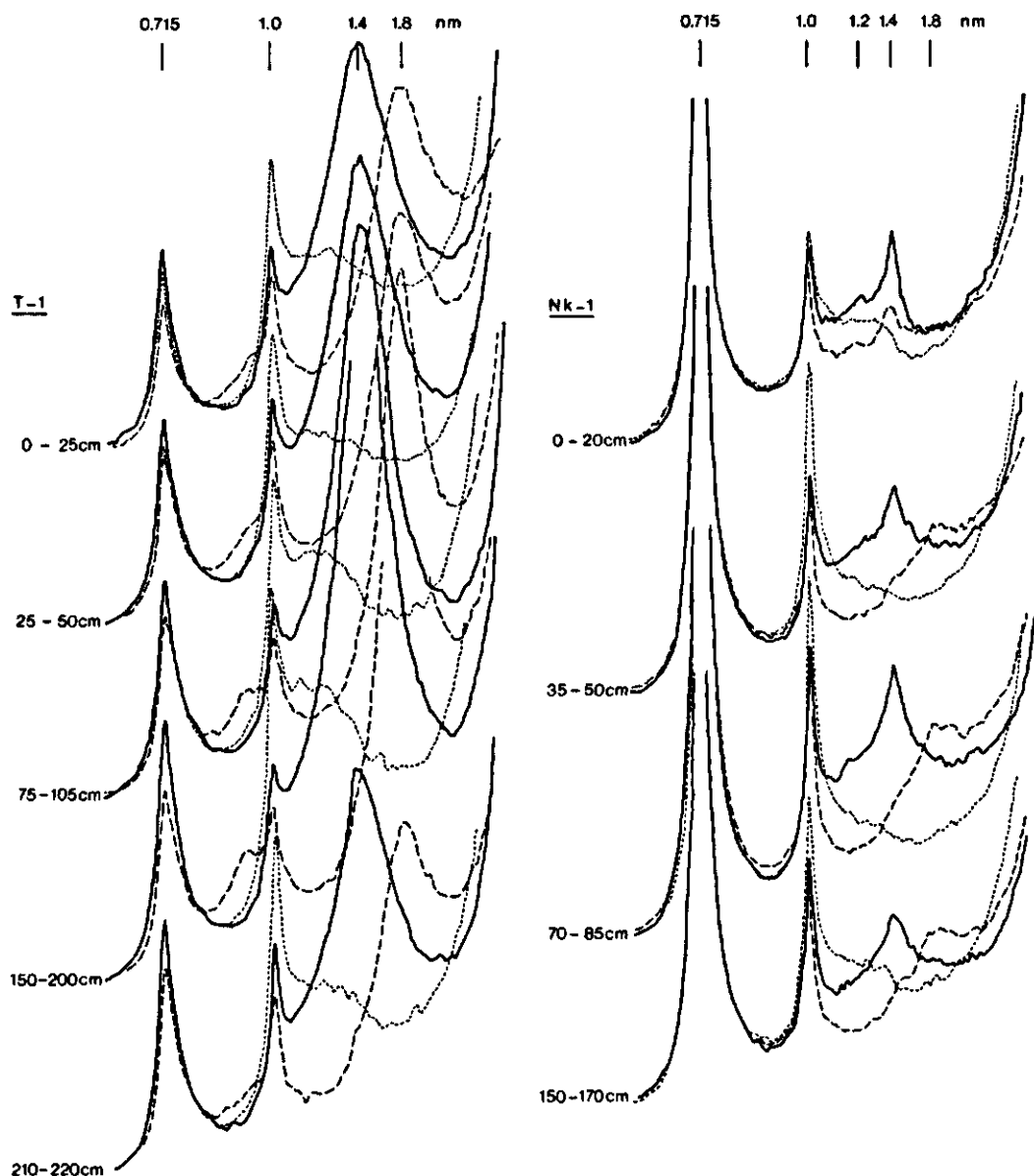


Figure 62

X-ray diffraction patterns for oriented clay separates from a non-acid soil from the Bangkok Plain (T-1) and an acid sulfate soil from Peninsular Thailand (Nk-1). For key see Fig. 61.

some mixed layer clay mineral, is present in some cases, and finally only partial expansion of the peak at 1.4 nm upon glycerol treatment indicates the occurrence of soil chlorite or vermiculite. Contrary to soils from the Bangkok Plain, there is little difference between surface soil and subsoil.

Two main approaches were used for quantitative analysis of the clay mineralogy: measurements of X-ray diffraction peak areas and normative mineralogical calculations. Peak areas can be used for accurate estimates when dealing with mixtures of a few well crystallized and pure substances (Brindley, 1961). But differences, for instance, in chemical composition, particle size and crystallinity, severely limit the utility of diffractograms for quantitative work on soil clays. Also, slight variations in pretreatment and sample size may appreciably alter peak intensities. The latter disadvantage can be overcome in part by considering relative peak areas, taking the sum of all peak areas as 100%. The relative peak areas are not directly related to the relative amounts of the individual minerals, but they are certainly helpful in identifying trends in mineralogical composition. Relative peak areas from diffractograms of oriented clay treated with  $Mg^{2+}$  and glycerol are given in Appendix B.

The normative mineralogy was calculated from elemental composition of the clay separates with the goethite norm proposed by van der Plas & van Schuylenborgh (1970). The normative mineralogy, or the 'norm' is useful when comparing different samples. It may indicate trends in the clay mineralogy. Negative or positive values of  $H_2O$ (residual) point to the presence of dehydrated minerals (e.g. haematite instead of goethite) or amorphous phases (allophane, hydroxides, amorphous silica). The norm does not necessarily agree with the actual mineralogy (the 'mode') especially since the norm minerals are idealized compounds whereas true minerals show wide ranges in chemical composition.

The normative calculations and measurements of peak areas agree fairly well for samples from different coastal plains, which are obviously very different in clay mineralogy (Fig. 20). But the two methods yield almost opposite results when considering acid sulfate soils in the Bangkok Plain. As shown by Fig. 63, the relatively low area of the peak at 1.8 nm for surface samples is not at all reflected by the standard goethite norm. The strong increase in normative smectite in the substratum does not correlate with a corresponding increase in the peak area at 1.8 nm whereas another indicator for the amount of smectitic clay, the cation-exchange capacity of the clay fraction, only shows a faint and gradual increase with depth throughout the profile.

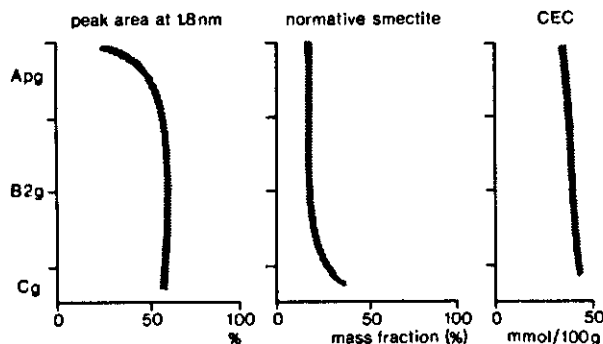


Figure 63

Trends against arbitrary depth scale of different indicators of the smectite content in acid sulfate soils from the Bangkok Plain.

The discrepant results for the A1 horizon can be explained simply by interlayering of swelling clay with aluminium hydroxide. The anomalously high normative smectite contents in the substrata could be explained if only part of the MgO in the clay fraction resides in smectite (rather than all MgO as assumed for the normative calculations), and if most of the high magnesium content in the substrata is present rather loosely bound to smectite and is replaced by an equivalent amount of ferric iron upon oxidation of pyrite. This proved correct as explained below.

Illite normally contains appreciable amounts of magnesium, and to evaluate the possible contribution of this mineral to the MgO present, K<sub>2</sub>O content (corrected for the potassium present in jarosite) of all clay separates was plotted against MgO content (Fig. 64). Disregarding the samples from very young soils and from substrata in the Bangkok Plain, and the Cha-am Lagoon, which are very high in MgO (indicated by open symbols), there is a highly significant linear relationship between MgO and K<sub>2</sub>O. In fact, the regression line is very close to the mass quotient of MgO to K<sub>2</sub>O for 'average' illite, which contains 2.75% MgO and 7.05% K<sub>2</sub>O (Weaver & Pollard, 1973). The average mass quotients vary from as low as 2.7 in the Cha-am Lagoon to as high as 4.7 in the Southeast Coast Region, but they are always within the range of illite compositions reported by Weaver & Pollard (1973). So except in substrata and young soils, all or most MgO is probably present in illite rather than in smectite. If so, the smectite present must be rich in aluminium (beidellite) or iron (nontronite).

The smectite content can be estimated from the measured cation-exchange capacity of the clay fraction, the illite content (based on illite with a

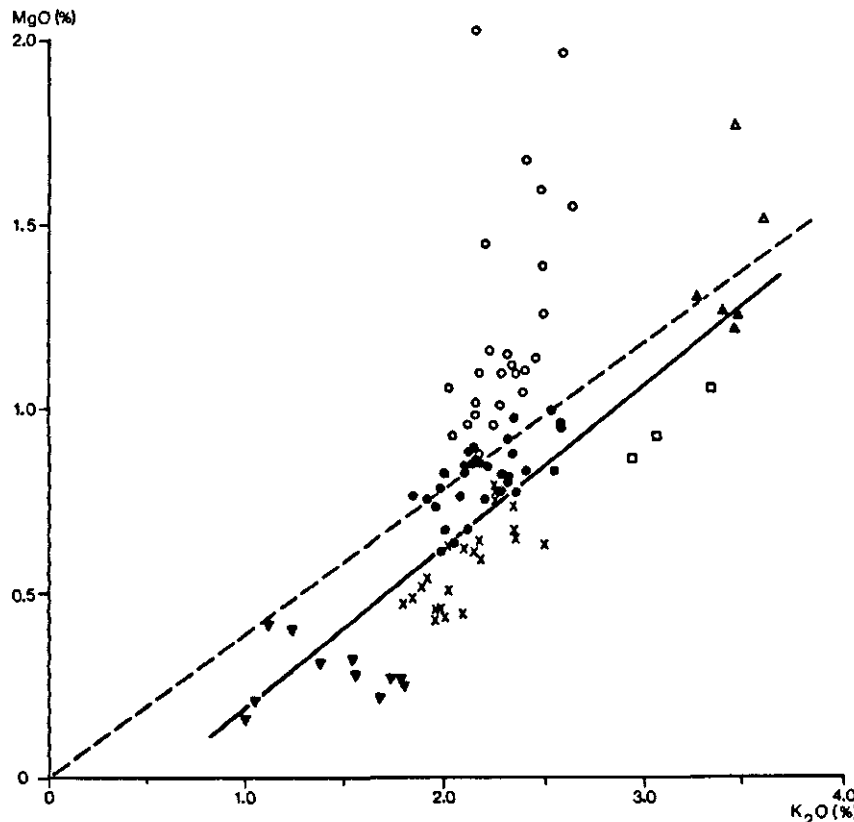


Figure 64

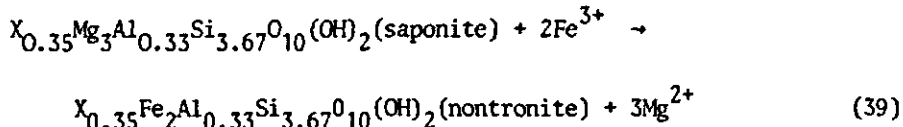
Relation between mass fraction of  $K_2O$  and  $MgO$  in the clay separates of different groups of soils. The data on the substrata relatively high in  $MgO$  (open symbols) were not used in the regression analysis. Key:  $\circ$  Bangkok Plain;  $\Delta$  Cha-am Lagoon;  $\times$  Southern Peninsula;  $\nabla$  Southeast Coast Region; broken line, average for 24 illite samples compiled by Weaver & Pollard (1973); solid line, my own regression ( $r = 0.89^{**}$ ).

$K_2O$  content of 7.0%), the cation-exchange capacity of illite (about 15 mmol/100g, Weaver & Pollard, 1973) and the cation-exchange capacity of moderately high-charge smectite (100 mmol/100 g). In the Bangkok Plain, the cation-exchange capacity of the clay fraction is generally of the order of 40-45 mmol/100 g, and the illite content between 30-35%, so about 35-40% of the clay is smectite. Total ferric iron minus free (dithionite-extractable) iron and minus illite iron (based on 'average' illite of Weaver & Pollard, 1973), amounts to 2-4% ( $Fe_2O_3$ ) of the clay. Because there are probably no other minerals that contain appreciable amounts of ferric iron, the smectite present contains 5-10% of  $Fe_2O_3$ , and is chemically intermediate between beidellite and nontronite.

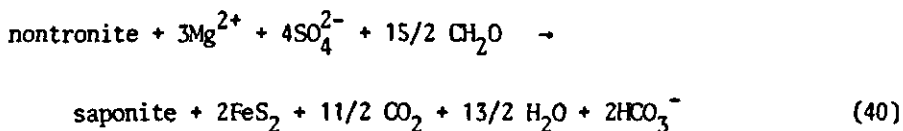
The anomalously high  $MgO$  contents in most substrata and young acid

sulfate soils are apparently due to magnesium in some mineral other than illite, presumably smectite. But cation-exchange capacity and peak area at 1.8 nm do not indicate a high smectite content. The discrepancy can be explained by the replacement of  $Mg^{2+}$  in smectite by Fe(III), under the influence of low pH and high dissolved iron from pyrite oxidation.

If the solids are represented by ideal saponite and nontronite end-members, the reaction can be written as follows (where X is exchangeable cation):



This is the reverse of the reaction proposed by Drever (1971) to account for the change in chemical composition of interstitial water and of the clay in recent anoxic sea-bottom sediments characterized by pyrite formation:



The increase in MgO in clay below the B horizon is 0.1-0.3% in most older acid sulfate soils and in BP-1, and 1-1.5% in Mn-1 and KD-1. In T-1 and Bk-1, the increase is more gradual and is about 0.6% MgO at most. If due solely to Eq. (40), these data are consistent with pyrite sulfur contents (on a whole soil basis) not exceeding those actually observed: 1.2% at KD-1, 1% at Mn-1 and 0.2-0.3% in the other Bangkok Plain soils. Some evidence for uptake of dissolved  $Mg^{2+}$  in anaerobic mangrove muds is furnished by the data on Ca-2 in Table 9. The relatively high concentrations of  $Mg^{2+}$  in soil solutions associated with pyrite oxidation (Tables 7 and 9; Fig. 25) are evidence for the reverse process (i.e. the transformation of saponite to nontronite).

Calculations of balance between dissolved and adsorbed ions for the BP samples from the oxidation experiment have shown that all the  $Na^+$  and  $Ca^{2+}$ , but only part of the  $Mg^{2+}$ , released into solution after pyrite oxidation can be accounted for by changes at the adsorption complex (van Breemen, 1973b). This shows that appreciable amounts of magnesium must indeed have come from magnesium-bearing minerals. To test the hypothesis that iron-magnesium substitution caused the removal of structural magnesium without apparent clay destruction, silicate-bound iron (assumed to be equal to total ferric iron minus dithionite-

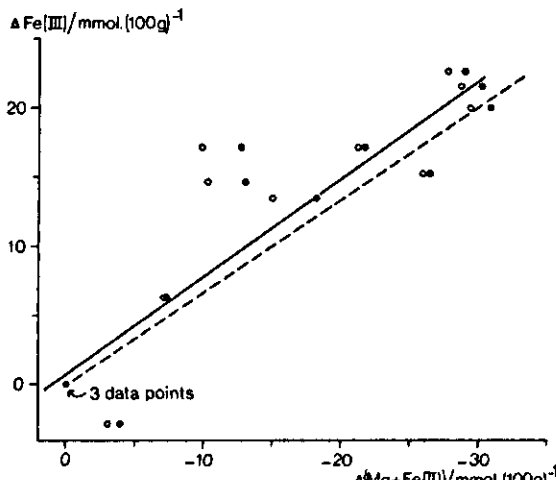


Figure 65

Comparison between the changes in silicate-bound Fe(III) and silicate-bound Mg, alone (open symbols) or with Fe(II) (solid symbols), with respect to the contents in the deepest samples from the substratum, in clay separates from three soils in the Bangkok Plain. The broken line is for theoretical substitution of 3Mg by 2Fe(III) and the solid line is the computed regression ( $r = 0.925^{**}$ ).

extractable iron) was estimated in the clay separates of three pedons (T-1, Mn-1 and Ra-2). Fig. 65 shows that the decrease in MgO content with respect to the content in the deepest sample is indeed accompanied by an increase in silicate Fe(III). If the small decrease in FeO accompanying the decrease in MgO is taken into account as well, the change in the sum FeO + MgO shows a highly significant negative correlation with the change in Fe(III), with a slope very close to that predicted by Eq. (39).

Another process that might explain the observed decrease in MgO without a concomitant change in cation-exchange capacity is solution of a magnesium-rich septochlorite such as chamosite (see Pons & van der Kervie, 1969). Chamosite contains 1-10% MgO and 10-40% FeO (Weaver & Pollard, 1973) and is authigenic in near-shore bottom sediments (Porrenga, 1967). The absence of (060) reflexions at 0.154 nm (typical for tri-octahedral layer silicates such as chamosite) in Guinier-de Wolff X-ray photographs of Mg-rich samples from Mn-1 and KD-1, and the low FeO contents of the samples suggest not. Removal of magnesium hydroxide interlayers, observed in acid sulfate soils from California (Lynn & Whittig, 1966) cannot play an important role either, because chlorite is virtually absent at depth, and cation-exchange capacity did not increase as would be expected upon release of magnesium from chlorite.

The cation-exchange capacity of the clay fraction shows a tendency to in-

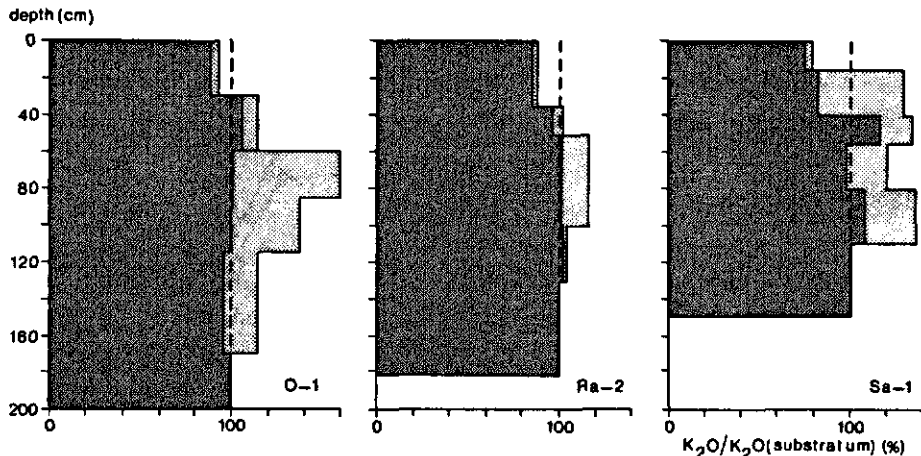


Figure 66  
 Total content of  $K_2O$  relative to that in the deepest substratum in three uniformly textured acid sulfate soils. Lighter shading indicates potassium present in jarosite.

crease with depth in all soils considered, including the non-acid T-1 and the soils from Peninsular Thailand. This increase, which is of the order of 3-6 mmol/100 g points to weathering of smectite or illite. Weathering of illite seems to be almost confined to the A1 horizons, as follows from the markedly lower  $K_2O$  contents near the surface (Fig. 66).

Potassium present in jarosite seems to have accumulated in an absolute sense indicating that potassium-bearing minerals in the B horizon are unimportant as a source of potassium for jarosite. Because illite remains practically constant at greater depth. The further slight decrease in cation-exchange capacity must be attributed to weathering of smectite. Weathering of 2:1 clays such as smectite and illite often involves incongruent solution, yielding a kaolinite residue (Garrels & Mackenzie, 1971). Formation of kaolinite from smectite can be expected at low pH and was demonstrated experimentally by Kittrick (1970). But direct proof for the formation of kaolinite in the soils studied is lacking. Although the peak areas for kaolinite are relatively high at shallow depth in most acid soils, the absolute intensities of the kaolinite peaks show no consistent trend with depth. Indirect evidence for silicate weathering is furnished by the presence of amorphous silica, notably at low pH (Section 5.2). White, powdery silicified root fragments consisting of 'opal-cristobalite' (with one X-ray reflection at 0.405 nm) or amorphous silica is common in acid sulfate soils from the Netherlands and from Senegal, but has been observed only at one site (Ca-1) in Thailand (Buurman et al., 1973;

Marius, Pons & van Breemen, in preparation). Micromorphological observations have shown the presence of diatomaceous frustules, presumably also consisting of amorphous silica, in most samples.

## 5.2 DISSOLVED SILICA

One of the most striking features of ground water in acid sulfate soils is the relatively high and constant concentration of dissolved silica. In the most acid part of the profile, where the pH is about 3.5, the soil solution is generally saturated or slightly supersaturated with amorphous silica, i.e. the concentration of  $H_4SiO_4$  is about 2 mmol/litre (Figs. 67 and 68). Slight supersaturation appears to be most prevalent near the top of the pyritic substratum. Distinct undersaturation with amorphous silica occurs near the surface and at some depth in the substratum where pH is higher. Still lower concentrations prevail in non-acid waters (pH 6-7):  $(0.92 \pm 0.38)$  mmol/litre in 39 samples from various mangrove areas and  $(0.64 \pm 0.07)$  mmol/litre in 36 samples

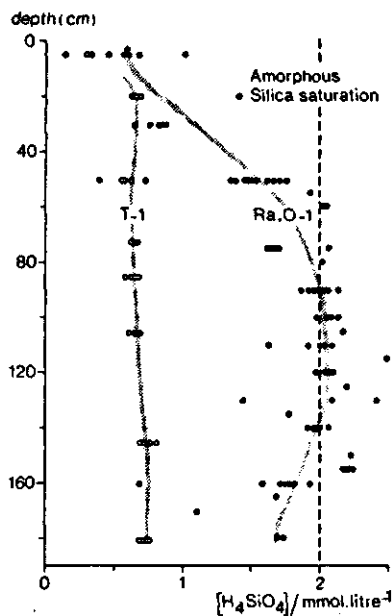


Figure 67  
Dissolved silica against depth in acid sulfate soils from the Rangsit-Ongkharak region, and in a non-acid marine soil (T-1).

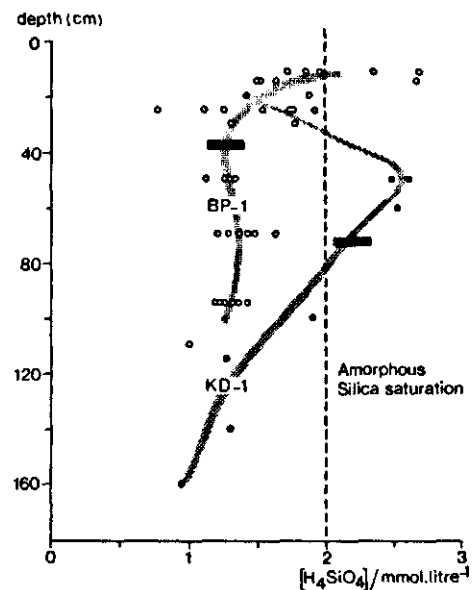


Figure 68  
Dissolved silica against depth in two young acid sulfate soils from the Bangkok Plain. The horizontal bars indicate the transition to the pyritic substratum.

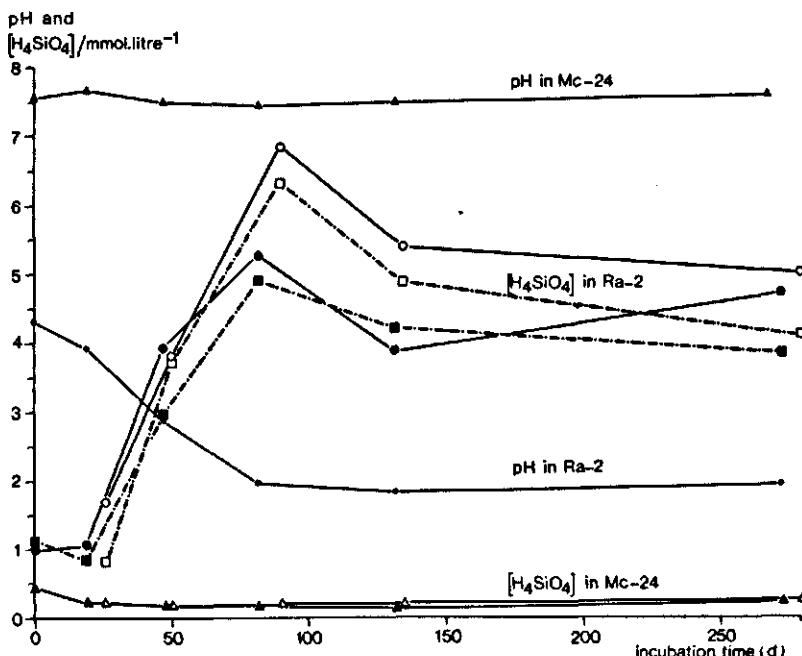


Figure 69

Changes in  $[H_4SiO_4]$  and pH upon artificial aeration of potentially acid soil (Ra-2) and not potentially acid (pyritic) soil (Mc-24). Open symbols refer to samples repeatedly leached with either sea-water ( $\square$ ) or distilled water ( $\circ\triangle\Delta$ ); solid symbols are for the treatments without leaching.

from T-1. This suggests that acidification is correlated with the higher silica concentrations in acid sulfate soils. Direct evidence for the release of silica upon acidification was furnished by the oxidation experiment. In Ra-2 samples, the drop in pH was associated with a strong initial increase in  $H_4SiO_4$  to 2.5 - 3 times saturation with amorphous silica (Fig. 69). Upon further incubation, when the pH remained very close to 2, the concentrations decreased somewhat but supersaturation was maintained. Treatments with sea-water and distilled water gave similar results but, remarkably enough, leaching resulted in concentrations slightly higher than those in the unleached treatment. Essentially, the same results were obtained with the BP samples, but there saturation with amorphous silica was already exceeded when the pH had fallen to 5-5.5. Very low and almost constant concentrations of  $H_4SiO_4$  were maintained upon aeration of the not potentially acid mud (Mc-24). Again leaching with distilled water or sea-water hardly affected concentration (Fig. 69).

Two conclusions emerge from these findings. The first one is that silicate

weathering due to acidification causes the rise in dissolved silica. Solution of diatom skeletons could also explain equilibrium with amorphous silica, but would not be enhanced by acidification and would certainly not lead to the supersaturation observed. Also, the solution rate of biogenic opal (Hurd, 1973) is far too slow to achieve saturation under the conditions encountered here. Secondly, the relative insensitivity of dissolved silica to dilution (or leaching) under a variety of conditions suggests rapid interaction between solid (or adsorbed) and dissolved silica. The same was observed *in situ* in the substratum (50-95 cm) of BP-1. There, the salinity (measured by  $\text{Cl}^-$ ,  $\text{Na}^+$  or  $\text{Mg}^{2+}$ ) was rather variable ( $s = 19\%$ ), presumably through tidal flushing and dilution with rain-water. By contrast, dissolved silica was rather constant ( $s = 8.6\%$ ) and showed only a weak positive correlation with chloride concentration ( $r = 0.45$ ).

### 5.3 SILICATE STABILITY DIAGRAMS

Mineral stability diagrams in terms of thermodynamic activities of solutes are useful to decipher the variables important in solution and transformation of minerals (Garrels & Christ, 1965; Helgeson, Brown & Leeper, 1969). Fig. 70 shows that, at a given temperature and pressure, the ionic activity products  $(\text{Mg}^{2+})(\text{OH}^-)^2$  and  $(\text{Al}^{3+})(\text{OH}^-)^3$ , together with the activity  $(\text{H}_4\text{SiO}_4)$  indicate to what extent the ambient solution is in equilibrium with kaolinite or with  $\text{Mg}^{2+}$ -saturated beidellite, and, for equilibrium or supersaturation, which of the two minerals is stable<sup>a</sup>. For instance, Fig. 70 illustrates that at high  $\text{pAl}(\text{OH})_3$  (i.e. at low pH or low  $\text{Al}^{3+}$  activity) kaolinite and beidellite may dissolve congruently, and that beidellite is more stable than kaolinite at low  $\text{pMg}(\text{OH})_2$  and  $\text{pH}_4\text{SiO}_4$  (i.e. at high pH and high activities of dissolved magnesium and silica). Because it is impractical to plot solution compositions on three-dimensional diagrams, two-dimensional projections or sections are normally used for that purpose. For the projection normal to the  $\text{pAl}(\text{OH})_3$  axis (plane *abcd* in Fig. 70), aluminium activities, which are often very small and difficult to determine, need not be known. On the other hand, without access to the value of  $\text{pAl}(\text{OH})_3$ , one does not know whether a solution composition plotted on the kaolinite-beidellite boundary (*n*) is in equilibrium (*n'*) or undersatu-

a. These ionic activity products have been expressed as negative logarithms, so  $-\lg(\text{Mg}^{2+})(\text{OH}^-)^2 = \text{pMg}(\text{OH})_2$ . Alternative variables frequently used are  $\text{pH} - \frac{1}{2}\text{pMg}$  and  $1\lg(\text{Mg}^{2+}) + 2\text{pH}$ .

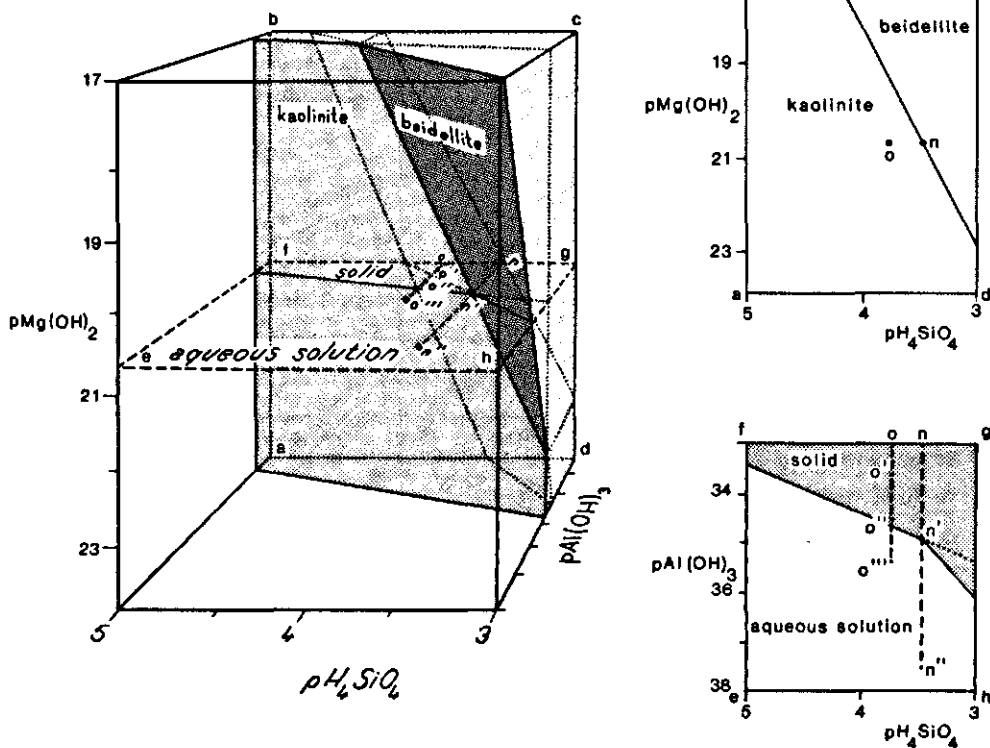
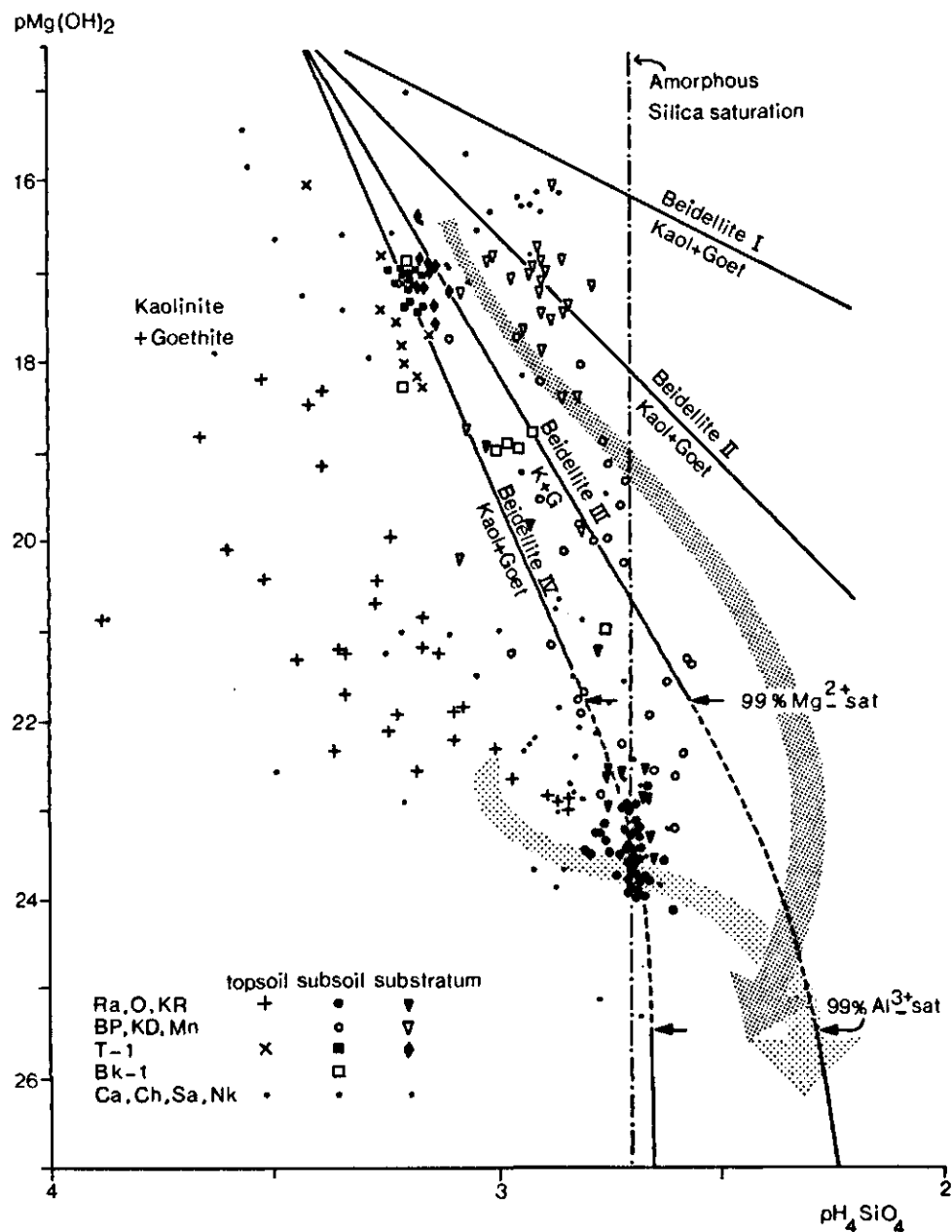


Figure 70

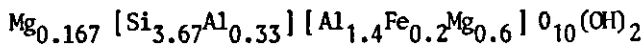
Three-dimensional stability diagram of kaolinite,  $Mg^{2+}$ -saturated beidellite and the aqueous solution. The values on the axes are approximate. A two-dimensional projection (abcd) and cross-section (efgh) are shown separately.

rated ( $n''$ ) with both minerals. Similarly, a point plotted in the kaolinite field ( $o$ ) may be supersaturated with kaolinite and beidellite ( $o'$ ), with kaolinite only ( $o''$ ), or undersaturated with the two minerals ( $o'''$ ). But if  $pAl(OH)_3$  is known, a horizontal section at a given  $pMg(OH)_2$  (plane efg) provides the necessary information.

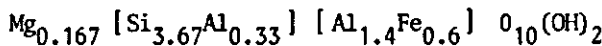
Diagrams of both kinds have been constructed for kaolinite and for beidellites containing Fe(III) and Mg of various compositions labelled I, II, III and IV (Fig. 71 and 72). Because the necessary thermodynamic data are not available for such beidellites, the method of Tardy & Garrels (1974) for estimating the Gibbs free enthalpy of formation of layer silicates was applied. This method is purely empirical but yields values close to experimental ones. For beidellite rich in magnesium, beidellite I, the following composition was chosen:



**Figure 71**  
 Stability fields of kaolinite + goethite and different hypothetical Mg-Fe(III) beidellites ( $25^{\circ}C$ ). Symbols represent composition of soil solution from various sites. The changes in the solution upon artificial aeration of two potentially acid samples are indicated by shaded arrows.

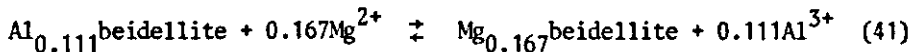


In the iron-rich beidellite IV all octahedral magnesium has been replaced by ferric iron:



In addition, beidellites with intermediate octahedral compositions were considered: beidellite II with  $[\text{Al}_{1.4}\text{Fe}_{0.46}\text{Mg}_{0.21}]$  and beidellite III with  $[\text{Al}_{1.4}\text{Fe}_{0.56}\text{Mg}_{0.06}]$ . The presence of 35-40% of beidellite I corresponds to the 1.5% of non-illitic MgO observed in the deepest substratum of KD-1. The other members have compositions in agreement with the MgO contents in the substrata of T-1 and Bk-1 (beidellite II) and of the older acid sulfate soils (beidellite III). In calculating the Gibbs free enthalpy of formation, the contribution of octahedral  $\text{Fe}_2\text{O}_3$ , in excess of the stoichiometric  $0.1 \text{ Fe}_2\text{O}_3$  in beidellite I, was assumed to be - 708.8 kJ/mol rather than the - 743.5 kJ/mol used by Tardy & Garrels (1974). The higher value was chosen in view of the supersaturation with respect to coarse-grained goethite in the B horizon of acid sulfate soils. The stability relations between the various beidellites and kaolinite in terms of  $\text{pH}_4\text{SiO}_4$  and  $\text{pMg}(\text{OH})_2$  are shown in Fig. 71 (thermodynamic data for kaolinite were taken from Helgeson, 1969).

The phase boundary for aluminium-saturated beidellites has been considered also, with the equation:



with  $\text{pK} 0.043$  (from the thermodynamic exchange constant for Ca-Mg exchange, for Clay Spur montmorillonite given by Bruggenwert, 1972). The boundaries for the phases saturated only with  $\text{Mg}^{2+}$  and  $\text{Al}^{3+}$  were assumed to be valid under conditions where at least 99% of the exchange positions are occupied by the respective cations. The  $\text{pMg}(\text{OH})_2$  values defining these conditions were calculated with the selectivity constant for divalent-trivalent ion exchange:

$$K_N = (\text{M}^{2+})^{1/2} \cdot (\text{N}^{3+})^{1/3} / (\text{M}^{3+})^{1/3} \cdot (\text{N}^{2+})^{1/2} \quad (42)$$

where  $(\text{N}^{2+})$  and  $(\text{N}^{3+})$  represent the equivalent fractions of adsorbed cations, and  $(\text{M}^{2+})$  and  $(\text{M}^{3+})$  are the activities in the equilibrium solution. The  $K_N$  used

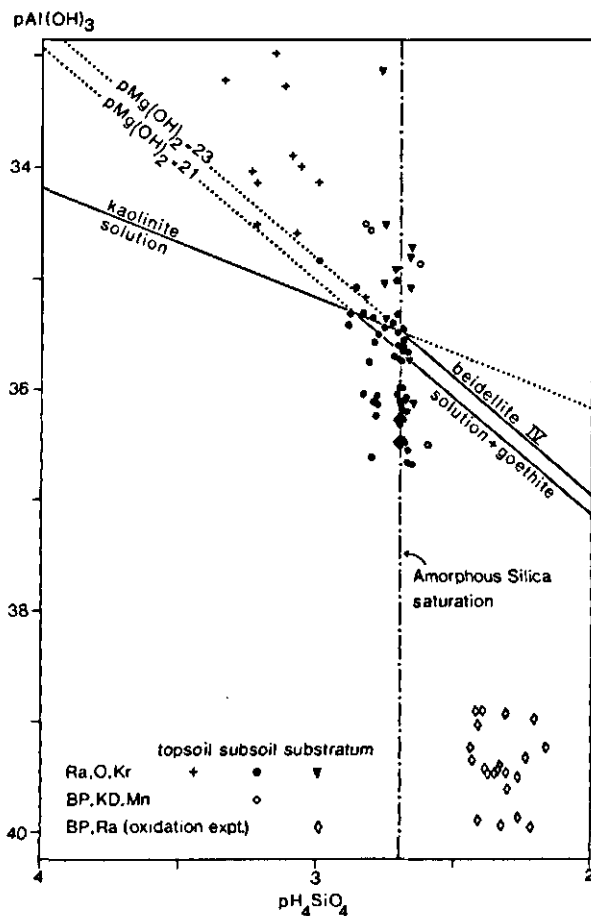


Figure 72  
Solubility isotherms (25 °C) for beidellite rich in Fe(III) and kaolinite. Symbols represent soil solutions from various sites and from artificially aerated pyritic samples.

is 1.65 (Bruggenwert, 1972). The approximate boundaries for beidellites saturated with both  $\text{Al}^{3+}$  and  $\text{Mg}^{2+}$  are indicated by broken lines in Fig. 71.

According to Fig. 71 the equilibrium between beidellite and kaolinite occurs at progressively higher  $\text{pMg}(\text{OH})_2$  (so at lower pH and  $\text{Mg}^{2+}$  activity) as more magnesium is replaced by ferric iron; and aluminium-saturated beidellites are unstable with respect to kaolinite plus amorphous silica. The composition of practically all groundwater samples collected in the field are plotted in the diagram. The kaolinite/beidellite IV boundary roughly coincides with the solution compositions typical of the subsoils of the well developed Bangkok Plain acid sulfate soils, and for the non-acid soil T-1. The clustering of data points near the beidellite IV -

kaolinite - amorphous silica triple-point suggests that this mineral assemblage plays a role in fixing the water composition at a certain  $pMg(OH)_2$ . The presence of considerable amounts exchangeable  $Mg^{2+}$  and  $Al^{3+}$  in the acid sulfate subsoils, predicted by Fig. 71, supports data on Rangsit subsoils (Sombatpanit, 1970) where about 35% of the cation-exchange capacity was filled by  $Mg^{2+}$  and 40% by  $Al^{3+}$ .

The substrata and subsoils of BP-1, KD-1 and Mn-1, with high magnesium contents in the clay fraction, have interstitial solutions that generally plot well inside the field of beidellite IV. This may reflect near-equilibrium between kaolinite and beidellite rich in magnesium. During artificial aeration of the pyritic mud from BP-1, the composition of the soil solution changed according to the darkest shaded arrow in Fig. 71. The initial course suggests near-equilibrium between kaolinite and beidellite intermediate between II and III. In contrast to waters from subsoils and substrata, those from surface soils almost invariably had a composition well within the kaolinite field.

The solid-solution boundaries in terms of  $pAl(OH)_3$  and  $pH_4SiO_4$  are depicted in Fig. 72. Near-equilibrium or slight undersaturation with kaolinite and beidellite IV is maintained in the acid subsoils, whereas supersaturation with both minerals but undersaturation with beidellites richer in magnesium prevails in the substrata and surface soils. The extent of undersaturation in the subsoils is rather small: about one order of magnitude of  $Al^{3+}$  activity, or 0.3 pH unit. The disequilibrium index for kaolinite,

$$D(Kaol) = 38.185 - pAl(OH)_3 - pH_4SiO_4 \quad (43)$$

in waters from eight porous pots at 50-100 cm depth at Ra-1 and Ra-2 slowly increased from  $-0.815 \pm 0.15$  to  $0.005 \pm 0.16$  in 4 months of flooding. This suggests equilibration with kaolinite from undersaturation, for instance by congruent solution of kaolinite, or of some other aluminium silicate such as beidellite followed by precipitation of kaolinite. The extent of equilibration with kaolinite under field conditions is especially striking in comparison to the strong undersaturation attained after several months of artificial aeration of pyritic mud in the laboratory (symbol  $\diamond$  in Fig. 72). The near-equilibrium with beidellite IV suggested by Fig. 72 and 73 may be fortuitous. The intercepts (but not the slopes) of the beidellite-kaolinite and beidellite-solution boundaries strongly depend on the solubility product of the ferric oxide present, and will move to higher values of  $pMg(OH)_2$  and  $pAl(OH)_3$  if fine-grained ferric oxide rather than goethite is considered in the equilibrium calculations.

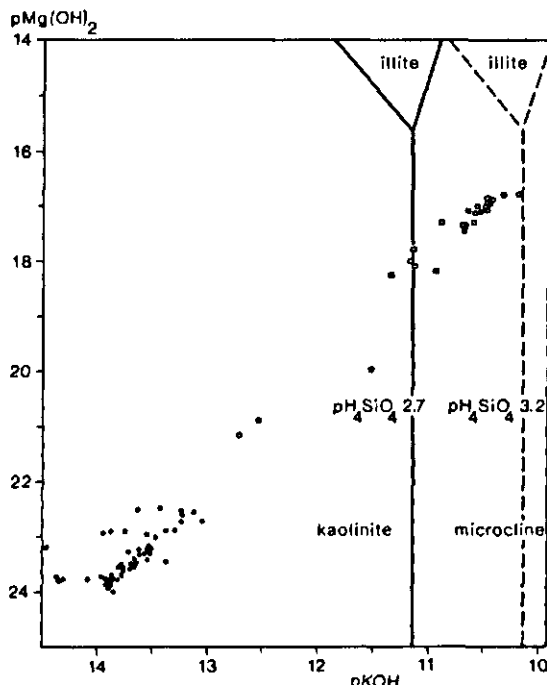


Figure 73

Stability fields of kaolinite, illite and microcline ( $25^{\circ}\text{C}$ ) at two activities of dissolved silica, and data points for soil solutions of  $\text{pH}_4\text{SiO}_4 2.7 \pm 0.05$  (solid symbols) and  $\text{pH}_4\text{SiO}_4 3.2 \pm 0.05$  (open symbols). Key:  $\bullet$  acid sulfate soils;  $\square$  non-acid soils.

However, the alignment of points along the predicted slopes lends credit to the general validity of the diagram. The lack of distinct supersaturation with kaolinite casts doubt whether appreciable amounts of kaolinite are formed, at least during flooding. Formation of kaolinite is thermodynamically possible in the surface soils and in the substrata during flooding, but the data available do not permit any conclusion as to whether this actually happens. The data on the surface soils are particularly difficult to interpret because seasonal changes, involving fluctuations in  $E_{\text{H}}$ , pH and solute concentrations, are large. The cyclic nature of physico-chemical conditions in the surface soil may be largely responsible for the relatively strong weathering of smectite and illite suggested by mineralogical analysis. Soil reduction may particularly enhance weathering of Fe(III)-bearing silicates such as beidellite IV. Furthermore, partial neutralization of  $\text{Al}^{3+}$  by reduction of ferric oxide enhances interlayering with aluminium.

Figure 73 depicts stability relations between kaolinite, microcline and illite ( $\text{K}_{0.6}\text{Mg}_{0.25}\text{Al}_{2.3}\text{Si}_{3.5}\text{O}_{10}(\text{OH})_2$ ), at two representative activities of

dissolved  $\text{H}_4\text{SiO}_4$  (thermodynamic data from Helgeson, 1969). Notably in acid sulfate soils kaolinite is stable over illite and microcline. Chemical data, on the other hand, show that marked weathering of potassium-bearing minerals is confined mainly to surface soils. Besides fluctuating physico-chemical conditions, uptake of  $\text{K}^+$  by plants may enhance illite weathering in A1 horizons.

Solubility products estimated for five different illites by Reesman (1974) yield illite stability fields obliterating the fields of kaolinite and microcline in Fig. 73, suggesting that illite is in fact stable over kaolinite in acid sulfate soils. The negative correlation between illite stability and pH of the ambient solution in the acid range (pH 3.7-5.8) that can be seen in Reesman's aqueous solution experiments, however, suggests that his data indicate the sluggishness of illite decomposition at low pH rather than the equilibrium solubilities of the illites.

## 6 Buffering of pH

In discussing pH buffering, it is useful to distinguish intensive and extensive properties. Intensive properties are characteristic of the individual phases and are independent of the amounts of the phases. Properties depending on the amounts of the phases are called extensive. Relevant intensive properties are pH and buffer intensity. Buffer intensity corresponds to the amount of substance of acid or base that must be added to a unit volume of aqueous solution to change the pH by 1. An example of an extensive property is base-neutralizing capacity, which is determined, *inter alia*, by the amounts of hydrolysable aluminium and iron in solution, at the exchange complex and in minerals (basic sulfates).

For example, two soil samples may have the same pH (intensive) but contain different masses of basic sulfates and therefore have different base-neutralizing capacities (extensive). Similarly, the presence of calcite at a given partial pressure of  $\text{CO}_2$  in a soil provides a certain buffer intensity (intensive), but the acid-neutralizing capacity of the soil (extensive) varies with the amount of lime present.

### 6.1 BUFFER INTENSITY AND pH

Jarositic B horizons from Bangkok Plain soils generally have a pH very close to 3.6-3.8. Slightly more varied pH, seldom exceeding the range 3-4, have been recorded for other sites (van Breemen, 1973b). In the acid sulfate soils from Peninsular Thailand for instance, pH values are typically 3-3.5. The occurrence of narrow pH ranges points to specific buffering reactions.

As shown by Stumm & Morgan (1970), the buffer intensity is a convenient parameter to evaluate pH buffering and equilibrium pH of mineral-water systems. The buffer intensity,  $\beta$ , for adding strong acid or base of substance concentration  $c_i$  incrementally to an equilibrium system with a constant concentration of a dissolved component  $j$ ,  $c_j$ , can be defined as

$$\beta_j^i = \frac{dc_i}{d\text{pH}} \quad (44)$$

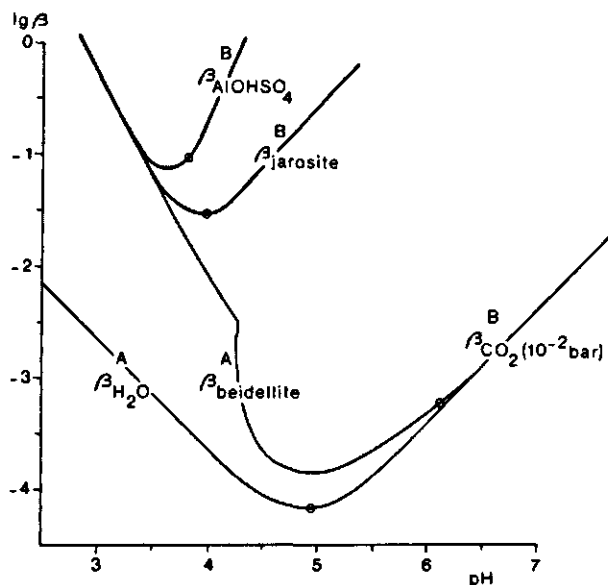


Figure 74

Buffer intensity,  $\beta$  in mol.litre<sup>-1</sup>, against pH for magnesium-saturated beidellite plus  $\text{Al}(\text{OH})\text{SO}_4$ , magnesium-saturated beidellite plus jarosite and magnesium-saturated beidellite plus  $\text{CO}_2$  at a partial pressure of  $10^{-2}$  bar, and for pure water at  $p(\text{CO}_2) = 10^{-2}$  bar (25 °C). The superscripts of  $\beta$  refer to addition of strong acid (A) or strong base (B).

Instead of  $c_j$ ,  $\beta$  may be specified for a gas at constant partial pressure, or for one or more solid compounds. The computation and interpretation of buffer intensities and equilibrium pH of minerals and soils are outlined elsewhere (van Breemen & Wielemaker, 1974a, 1974b).

Fig. 74 shows buffer intensities against pH for the incongruent solution of beidellite saturated with  $\text{Mg}^{2+}$  to kaolinite plus amorphous silica, for hydrolysis of jarosite (to ferric oxide with  $\text{pK}_{\text{SO}} 39.9$ ) and of  $\text{Al}(\text{OH})\text{SO}_4$  (to kaolinite, in the presence of amorphous silica) and for an aqueous solution at constant  $p(\text{CO}_2)$ . The presence of beidellite provides strong buffering against acidification at low pH, but a similarly strong buffering against the addition of base is provided by the two basic sulfates. The equilibrium pH (indicated by symbol o) of the beidellite-basic sulfate buffering systems, which are situated near the points of lowest buffering (van Breemen & Wielemaker, 1974b), are 3.8 for  $\text{Al}(\text{OH})\text{SO}_4$  and 3.97 for jarosite. Somewhat lower pH (about 3.1) is obtained when congruently dissolving kaolinite is considered instead of beidellite. The low pH in the presence of jarosite and  $\text{Al}(\text{OH})\text{SO}_4$  contrasts strongly with the far higher values for the same clay

minerals in an aqueous system at a constant  $p(\text{CO}_2)$  of  $10^{-2}$  bar: 6.1 for Mg-beidellite and 5.0 for kaolinite (van Breemen & Wielemaker, 1974b).

As pointed out by Sillén (1967) and by Stumm & Morgan (1970), the co-existence of a sufficient number of phases at equilibrium constitutes a chemistat or pH-stat. This means that the composition (and thus the pH) of the aqueous phase does not change upon addition or partial removal of components that make up the system. The phase rule states the relationship between the number of independent variables ( $F$ ) and the number of components ( $C$ ) and phases ( $P$ ) of a system at equilibrium:

$$F = C + 2 - P \quad (45)$$

In the jarositic horizons, a relatively large number of phases seem to be involved in regulating the composition of the soil solution. As discussed in Chapters 4 and 5, they are amorphous silica, kaolinite, beidellite saturated with  $\text{Mg}^{2+}$  and  $\text{Al}^{3+}$ , ferric oxide, jarosite,  $\text{Al}(\text{HSO}_4)_2$  and sometimes gypsum, so  $P$  is either 7 or 8. The relevant components are  $\text{H}_2\text{O}$ ,  $\text{HCl}$ ,  $\text{SO}_3$ ,  $\text{SiO}_2$ ,  $\text{Al}_2\text{O}_3$ ,  $\text{Fe}_2\text{O}_3$ ,  $\text{Na}_2\text{O}$ ,  $\text{K}_2\text{O}$ ,  $\text{MgO}$  and  $\text{CaO}$ , so  $C$  is 10. Therefore, according to Eq. (45), the number of independent variables is 4 or 5 according to whether gypsum is present. At constant temperature and pressure,  $F$  reduces to 2 or 3. These remaining degrees of freedom can be used to specify the concentrations of  $\text{Na}^+$ ,  $\text{Cl}^-$  and, in the absence of gypsum, of  $\text{Ca}^{2+}$ .

For a given water sample, the analysed concentrations of  $\text{Na}^+$ ,  $\text{Cl}^-$  and  $\text{Ca}^{2+}$  can be combined in an electroneutrality equation with expressions for the other dissolved species written in terms of the appropriate equilibrium equations for the minerals. This allows calculation of pH and of the concentrations of sulfate, silica, potassium, (calcium), magnesium, and aluminium, which can be compared with the analysed concentrations. The results of such calculation, assuming the presence of Helgeson's (1969) Mg-beidellite rather than the iron-rich beidellite saturated with  $\text{Mg}^{2+}$  and  $\text{Al}^{3+}$ , are given in Table 18. Except for  $\text{K}^+$ , the agreement between calculated and observed values is good. In fact, true equilibrium involving all phases will rarely, if ever, be established. The mineral assemblage present, however, is apparently able to 'pull' the solution composition very close to equilibrium. This may be possible by slow flow rates of the aqueous phase, comparatively rapid rates of mineral-solution interaction, and slow rates of acidification. If acidification is very rapid as in the laboratory oxidation experiment, the mineral-solution equilibration lags behind, resulting, for instance, in

Table 18. Observed and calculated concentrations (mmol/litre) in two acid sulfate waters. The concentrations in brackets were used in the calculations. Values refer to the sum of free and complexed species and not only to free ions.

Acid sulfate soil without gypsum (Ra-2)		Acid sulfate soil with gypsum (Na-2)	
found	calculated	found	calculated
pH	3.67	3.75	3.88
Cl <sup>-</sup>	10.2	(10.2)	46.6
SO <sub>4</sub> <sup>2-</sup>	20.8	18.1	34.4
H <sub>4</sub> SiO <sub>4</sub>	1.91	2.00	1.91
K <sup>+</sup>	0.681	0.075	1.02
Na <sup>+</sup>	23.2	(23.2)	55.6
Ca <sup>2+</sup>	4.16	(4.16)	13.5
Mg <sup>2+</sup>	8.35	6.70	14.2
Al <sup>3+</sup>	0.465	0.450	0.658
			0.505

strong supersaturation with amorphous silica and strong undersaturation with silicate minerals (Fig. 70 and 71). Consequently the buffering mechanism breaks down, resulting in very low pH values. In very young acid sulfate soils, the pH is frequently somewhat lower than in older soils, and the soil solution is often slightly supersaturated with amorphous silica (Fig. 68). This also points to the inability of the buffering system to keep pace with acidification during relatively rapid pyrite oxidation.

According to the phase rule, production of more sulfuric acid by (slow) pyrite oxidation would not affect pH, as long as equilibrium is maintained. Addition of lime (which completely dissolves if applied in moderate amounts) results in formation of gypsum, and pH will not increase materially until all basic sulfate is hydrolysed. The mineral assemblage of the jarositic B horizon thus constitutes an efficient pH-stat.

The number of phases known to control the activities of dissolved constituents in non-acid marine soils and in the surface horizons of acid sulfate soils is too small to allow similar considerations. Seasonal processes in surface horizons give rise to strongly fluctuating conditions, so that the concept of a pH-stat is meaningless. Another approach is possible. The processes of acidification and deacidification accompanying periodic oxidation and reduction tend to produce zero alkalinity and zero mineral acidity (van Breemen, 1975). Concentrations of HCO<sub>3</sub><sup>-</sup> and H<sup>+</sup> would become equal, leading to a pH that depends only on the partial pressure of CO<sub>2</sub>.

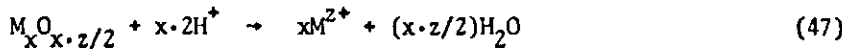
according to

$$\text{pH} = 3.91 - \frac{1}{2} \lg p(\text{CO}_2) \quad (46)$$

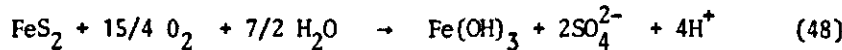
Eq. (46) yields a pH of 4.4-5.4 for a representative range of partial pressures of  $\text{CO}_2$  between  $10^{-1}$  and  $10^{-3}$  bar. As shown elsewhere (van Breemen, 1975), the pH of a large number of surface samples from periodically flooded non-calcareous coastal plain soils, either acid sulfate or non-acid marine, fell in the predicted pH range.

## 6.2 EXTENSIVE PROPERTIES IN ACID BUFFERING

The presence, not the amount of the various phases, counts in buffer intensity. If a buffering substance is used up during acidification, buffering by that substance ceases, of course. This illustrates the importance of extensive factors in pH buffering. Theoretically, all potassium, sodium, calcium and magnesium in silicates is available for buffering in near-neutral or slightly acid conditions. So the total amount of silicated metals other than aluminium and iron<sup>a</sup> (the 'bases') is a measure for the acid-neutralizing capacity. If these bases are represented by their oxide components, the acid-neutralizing capacity follows from the equation:



The pyrite content, on the other hand, is a measure for the potential acidity. Upon complete oxidation and hydrolysis of iron:



each mole of pyrite yields four moles of  $\text{H}^+$ . Less acid is produced upon incomplete oxidation and hydrolysis of the iron, but normally little or no iron escapes ultimate transformation to ferric oxide.

Fig. 75 depicts the sum of the equivalent amounts of base elements K, Na, Ca and Mg, in oven-dry soil expressed in mmol/100 g, against depth in a number of soils. The cations are mainly present in silicate minerals

a. Aluminium and iron, whether free or bound by silica, can also provide buffering, but only at pH below 2-3 (van Breemen & Wielemaker, 1974a).

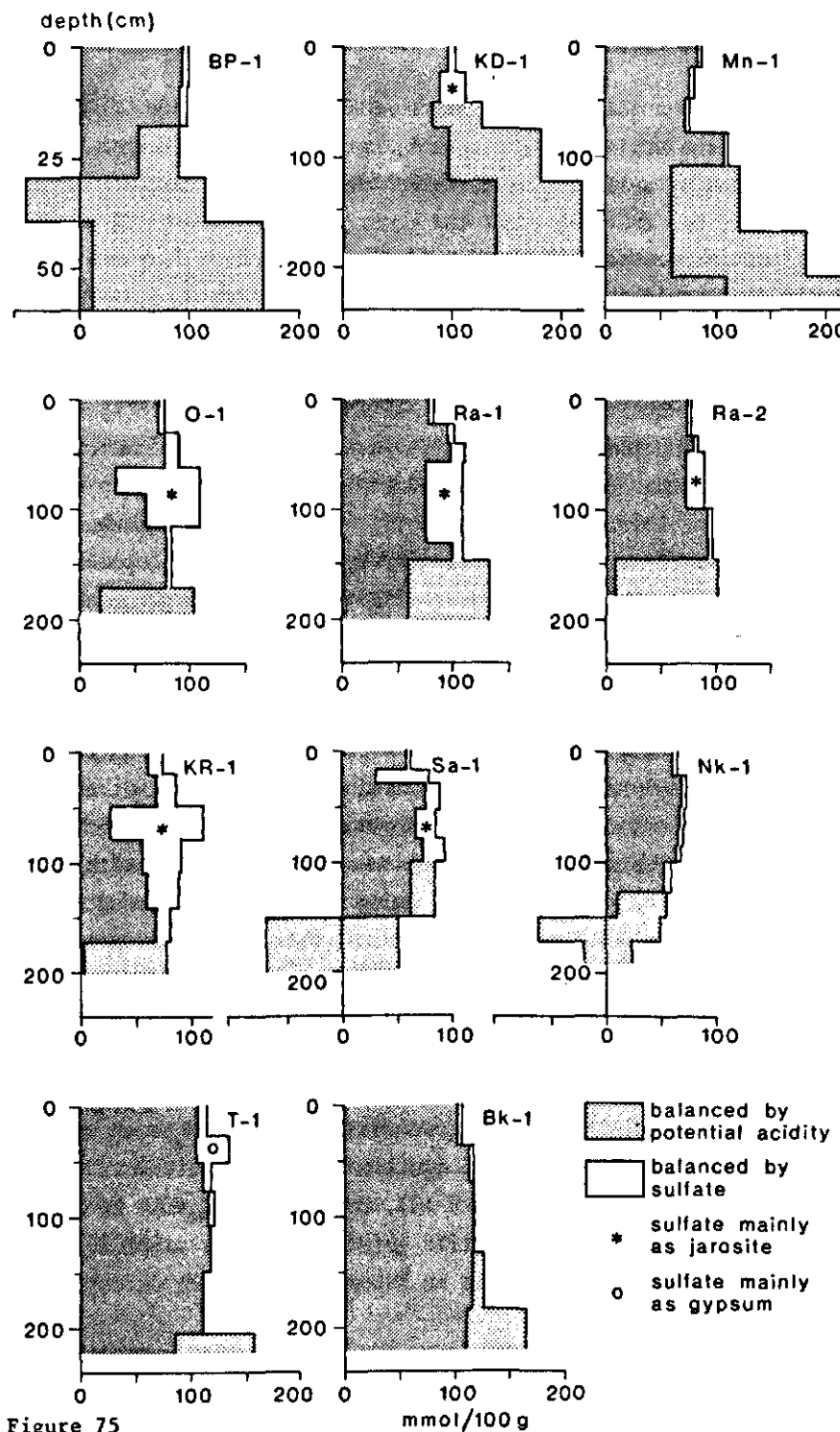


Figure 75

Total equivalent amounts of base elements in oven-dry soil (mmol/100 g) against depth in some soils and the fraction of the base elements balanced by sulfate and by potential acidity from pyrite.

but part exists in exchangeable form, and as sulfate and chloride. Chlorides are negligible on the scale of the diagrams, but appreciable amounts of cations are balanced by sulfate. The darker-shaded areas indicate total cations minus total sulfur, and thus represent the bases (i.e. cations combined with silicate and sometimes carbonate) that would remain if all sulfur was transformed into sulfuric acid and reacted with the available bases. Sulfuric acid can be produced not only by oxidation of pyrite (indicated by the lighter-shaded areas) but also by hydrolysis of jarosite. Asterisks mark the depths where most sulfur is present as jarosite.

One of the striking features of Fig. 75 is that complete oxidation of pyrite and neutralization of the acid formed would make the substrata of most acid sulfate soils far lower in bases<sup>a</sup> than the overlying horizons which have been oxidized earlier. At some sites (BP-1, Sa-1 and Nk-1), potential acidity even exceeds total available bases at some depth. This phenomenon can be explained in several ways: (a) the present oxidized horizons originally contained either less pyrite or more bases (e.g. calcium carbonate); (b) dissolved alkalinity from the surface water or rising from deeper strata has neutralized most of the acidity; (c) the sulfuric acid formed during pyrite oxidation is incompletely neutralized and most of it has left the soil in some unneutralized form. The first explanation would imply that the present upper limit of the reduced substratum chances to coincide with a lithological discontinuity in both old and young soils. Such a discontinuity would appear from other mineralogical and chemical data. Although appreciable amounts of alkalinity may be conveyed by the flood-water, it is not likely that much of it actually enters the soil. Also there is no reason to assume large amounts of dissolved alkalinity at depth.

Possible removal of unneutralized acidity (Explanation c) could involve release of dissolved sulfuric acid, and gaseous  $\text{SO}_3$ ,  $\text{SO}_2$  and  $\text{H}_2\text{S}$ . In view of its extremely low partial pressure in equilibrium with dilute sulfuric acid (e.g.  $p(\text{SO}_3) = 10^{-34}$  bar at  $\text{pH}_2\text{SO}_4 = 10$ ), removal of  $\text{SO}_3$  must be insignificant. Sulfur dioxide is far more volatile ( $p(\text{SO}_2) = 0.1$  bar at  $\text{pH}_2\text{SO}_3 = 10$ ) and because sulfite has been observed as an intermediate during oxidation of

---

a. Acidified substrata, as in older soils, have already lost some bases by ion exchange. This loss, equal to the cation-exchange capacity at the original pH (presumably 6.5-7) minus the amount of exchangeable bases still present, amounts to 10-20 mmol/100 g soil (van Breemen, 1973b) and is insufficient to explain the difference.

iron sulfide (Purokoski, 1958), the release of this gas may be important, especially if pyrite is being oxidized near the surface as in young acid sulfate soils. The weak sulfurous odour that is sometimes noticed in areas with partly aerated mangrove muds and the use of  $\text{SO}_2$  analysis in the air for prospecting of sulfide ores (Meyer & Peters, 1973) corroborate this. The steady decrease in total sulfur from 1.6% initially to 1-1.3% after 9 months in artificially aerated pyritic samples from Ra-2 may be due to escape of  $\text{SO}_2$ . But no significant decrease in total S was observed in the two other samples (BP-1 and Mc-24) used for the oxidation experiment. The importance of  $\text{SO}_2$  cannot be ascertained until field measurements have been made.

Hydrogen sulfide is certainly formed in reduced surface soils, but the smell of  $\text{H}_2\text{S}$  (which is noticeable at very low concentration) was never detected over flooded acid sulfate soils, presumably because all sulfide is fixed as  $\text{FeS}$ .

The composition of the surface waters contained in vertical poly(vinyl chloride) tubes under field conditions provides direct evidence for the release of sulfuric acid into the flood water through oxidation of ferrous sulfate near the soil-water interface. The amounts of acid produced in the tubes (Table 17) are sufficient to remove all sulfuric acid produced by oxidation of 2% of pyrite-S in soil down to 1 m depth in the course of 400-4000 years, i.e. the approximate age of the sediments in question. Because even more acid is probably released under 'natural' conditions (i.e. in the absence of the tubes), this process helps to explain the low contents of bases in most pyritic substrata. But only 1.5-4% of the  $\text{SO}_4^{2-}$  in the 'inside' surface water is balanced by  $\text{H}^+$ , and this fraction is even smaller in the outside surface water (0.5-1%). These figures underestimate the importance of free acid because they are influenced by ion exchange (in the tubes) and by dissolved alkalinity (flood water). Even so, the close resemblance of ground and surface water from acid sulfate soils, in proportion of solutes, strongly suggests that most of the dissolved  $\text{SO}_4^{2-}$  leaves the soil as sulfate and not as bisulfate ( $\text{HSO}_4^-$ ) or sulfuric acid. The question remains open.

## Summary

Acid sulfate soils cover 8000 km<sup>2</sup> of the Bangkok Plain, and occur here and there in many of the smaller coastal plains in Thailand. In the Bangkok Plain, most acid sulfate soils are well developed and are separated from the present coast by a 10-30 km wide zone dominated by non-acid marine soils. Young saline acid sulfate soils in or near active tidal areas are found only in the southeastern part of the plain. Practically all coastal plain soils are flooded during the monsoon, and most are under rice.

Sixteen acid sulfate soils from the Bangkok Plain and from three smaller coastal areas, as well as one non-acid marine soil, were described, sampled and analysed in detail (App. B). Particular attention was paid to the distribution of Fe-S compounds, redox potential and pH, elemental composition of soil and clay, clay mineralogy and the composition of interstitial water and surface water.

### *Pyrite formation*

In mangrove muds with ongoing sulfate reduction,  $E_H$ -pH data accord with the sulfate/sulfide redox couple, rather than with the elemental S/sulfide couple observed by other workers in anoxic sea-bottom sediments. Tidal flushing rapidly replenishes the reduced sulfate, which is fixed as iron sulfide. Contents of ferrous monosulfide are very low and pyrite (FeS<sub>2</sub>) is the only reduced sulfur compound that is quantitatively important. Pyrite S is 2-3% in potentially acid mangrove muds and in substrata of acid sulfate soils and is mostly below 1% in not potentially acid samples. The fraction of iron available for pyritization that is actually turned into pyrite, is close to 1 in substrata from southern Peninsular Thailand, and about 0.5 and 0.35 in potentially acid and not potentially acid samples from the Bangkok Plain, respectively.

Other research in Malaysia indicated that conditions in estuarine areas were more favourable for pyritization than in accretionary coastal areas. This phenomenon is probably due to periodic removal of dissolved alkalinity

(leading to a lower pH, which speeds up pyritization) and partial oxidation of sulfide to elemental sulfur (a necessary precursor of pyrite) under influence of stronger tidal fluctuations in the estuaria. The distribution of acid sulfate soils and non-acid soils in the present coastal zone of Thailand indicates that the same may be true there.

#### *Pyrite oxidation*

Atmospheric oxygen is ultimately responsible for pyrite oxidation, but ferric iron probably functions as an intermediate oxidant. This explains why pyrite oxidation can continue in acid substrata during flooding: ferric oxide formed during the preceding dry season is reduced by adjacent pyrite.

Pyrite oxidation during the dry season is slow with transport of oxygen as the rate-limiting factor. In young soils where oxygen penetrates more easily to the pyritic zone, pyrite oxidation is more rapid. Very rapid pyrite oxidation occurs in artificially aerated reduced samples.

#### *Sulfate minerals*

The yellow mineral jarosite,  $KFe_3(SO_4)_2(OH)_6$ , is the most conspicuous secondary mineral associated with pyrite oxidation. Jarosite occurs in dense masses of small (0.1-5  $\mu m$ ) particles and gives a sharp X-ray diffraction pattern. Furthermore it shows (a) an anomalously high water content; (b) very little substitution of  $Na^+$  for  $K^+$ , even if the ambient solution is rich in  $Na^+$ ; (c) partial replacement of  $K^+$  by  $H_3O^+$  in some cases. In agreement with theoretical stability relations, jarosite forms only under acid ( $pH < 4$ ) oxidized conditions outside the immediate vicinity of pyrite, and ultimately hydrolyses to very fine-grained goethite.

Other forms of sulfate associated with acid sulfate soils are gypsum, adsorbed sulfate and the suspected basic sulfate  $Al(OH)SO_4$  that apparently controls dissolved aluminium. Efflorescences of water-soluble sulfates, some containing aluminium and ferrous iron form occasionally under very dry conditions.

#### *Ferric oxides*

Except in pyritic soil and in strongly reduced surface horizons, the soil solution is normally supersaturated with coarse-grained goethite, and under-

saturated with amorphous ferric hydroxide. The ionic activity products for  $\text{Fe(OH)}_3$  and X-ray diffraction line widths suggests that the material from brown mottles ages to increasingly coarse-grained goethite. Haematite, found in red mottles in the upper part of the B horizon, is formed from goethite under slightly acid to acid conditions.

#### *Manganese*

Black mottles of manganese oxide are common in B horizons of non-acid soils, but are invariably absent from acid sulfate soils. At low pH, manganese is readily mobilized and is mainly present in water-soluble and exchangeable forms.

#### *Soil reduction*

Acid sulfate soils are reduced slower than most non-acid soils upon submergence. This is reflected, for instance by the slow increase in pH and the late start of sulfate reduction. Reduction of ferric oxides to  $\text{Fe}^{2+}$  is associated with desorption of  $\text{SO}_4^{2-}$  and hydrolysis of basic sulfate. Part of the dissolved ferrous sulfate formed in this way is oxidized to ferric hydroxide and sulfuric acid at the soil-water interface, and sulfuric acid is removed laterally in the flood water. Periodic flooding of acid sulfate soils thus deacidifies the surface soil.

Submergence of non-acid soils, on the other hand, causes rapid formation of  $\text{FeS}$  near the surface, and partial loss of alkalinity produced during sulfate reduction. Oxidation of  $\text{FeS}$  during the following dry season causes acidification which explains the markedly acid surface of most periodically flooded ('non-acid') coastal plain soils. The ultimate pH is not lower than 4.5-5, however, because the deacidification, also operating in flooded acid sulfate soils, would undo the effect of a temporary drop in pH below that level. Likewise, the (aerobic) pH of acid sulfate topsoils will not increase beyond the same range.

#### *Migration of iron*

Part of the dissolved ferrous iron formed in the reduced surface soil and in the pyritic substratum diffuses towards the B horizon, which remains strongly acid and oxidized throughout the year and where the concentration

of dissolved iron remains low. Oxidation of the  $Fe^{2+}$  in the dry season ultimately leads to pronounced accumulation of ferric iron in the B horizon. Jarosite is formed in the lower part of the B horizon and hydrolyses to goethite in the upper part. As the soils become older, the zones of accumulation occur progressively deeper.

The B horizon of non-acid soils is also perennially oxidized, but due to a lower mobility of iron at higher pH, accumulation of ferric iron is less pronounced.

#### *Weathering and transformation of silicates*

The clay fraction of all soils contains appreciable amounts of kaolinite, illite and smectite. The soils of Southern Peninsular Thailand and the Southeast Coast Region are much lower in 2:1 clays than those of the Bangkok Plain. In the Bangkok Plain three distinct processes affect the clay mineralogy of acid sulfate soils: (a) loosely bound smectitic Mg in reduced pyritic substrata is replaced by ferric iron upon oxidation of pyrite; (b) interlayering of swelling 2:1 clay minerals with aluminium hydroxide takes place in periodically reduced surface soils; (c) a small fraction of the 2:1 clay minerals is weathered to amorphous silica and, perhaps, to kaolinite.

Similar processes may operate in non-acid marine soils, but there the intensity of weathering is less and no amorphous silica is formed.

#### *Acid production and buffering*

The very narrow pH range (3.6-3.8) in jarositic B horizons can be explained by near-equilibrium of many minerals and the soil solution. The phase rule predicts that addition of components of the equilibrium assemblage (e.g. sulfuric acid or calcium hydroxide) will not affect pH nor composition of the soil solution. Kinetics is very important in this respect: if the rate of acid production exceeds that of the various buffering reactions, the buffering mechanism breaks down, sometimes leading to pH as low as 2. Buffering keeps pace with acid production in the older acid sulfate soils, but not always in the younger ones where relatively rapid oxidation of pyrite at shallow depth may lead to pH somewhat below 3.6-3.8.

Elemental analysis of many pedons indicates that only part of the sulfuric acid formed during pyrite oxidation is neutralized by bases. If so, most of this acid leaves the soil in some unneutralized form. In this respect,

SO<sub>2</sub> gas may be important in young acid sulfate soils. In the older flooded soils, oxidation of dissolved ferrous sulfate near the soil-water interface contributes to the release of H<sub>2</sub>SO<sub>4</sub>, but the quantitative importance of this process is not clear.

## Epilogue: the agronomists' viewpoint

This study was not aimed at answering practical questions. In spite of my academic approach, I encountered several unanticipated phenomena that may be of direct utility. Of necessity, the discussion below is speculative. I treat first some aspects of the identification and mapping of acid sulfate soils and next deal with factors of possible importance in reclamation and improvement of acid sulfate soils.

### *Identification and mapping of acid sulfate soils*

Potentially acid soil is usually identified by either estimating pyrite and lime separately, or by forced pyrite oxidation (by  $H_2O_2$ ) and then measuring pH or water-soluble sulfate. Neither method takes account of slowly buffering compounds, and the  $H_2O_2$  method may give an erroneously low pH in organic matter is only partially oxidized. Artificial aeration of potentially acid soil under moist conditions, which causes rapid and strong acidification (Section 4.3.2), does not suffer from these drawbacks and requires little if any instrumentation (visual estimation of yellow mottles or pH paper may suffice). The necessary incubation time, several weeks to several months, is far less than most laboratories need to produce analytical results for soil surveys. Zuur (1954) recommended this method for (often calcareous) pyritic soils and advised inoculation with sulfur-oxidizing bacteria by adding a little acidified soil. Theoretically acid production upon laboratory aeration might override buffering reactions operating at near-neutral pH, and might thus lead to strong acidity where none would develop *in situ*. But it is unlikely that a pH below 3.5 would then be reached in the laboratory.

Until recently acid sulfate soil areas in the tropics have not been related to any physiographic characteristic within coastal plains (van der Kevie, 1973). In Malaysia Diemont and van Wijngaarden observed stronger pyrite formation in estuarine than in accretionary coastal areas. The present Bangkok Plain coast shows this same difference, which can be explained by

physiochemical factors (relatively low pH and periodic oxidation of sulfide to elemental sulfur in estuarine sediments) influencing the rate of pyrite formation (Diemont et al., in preparation ; Section 4.2.2). Because pyritization in mangrove areas is favoured especially in that part of the soil profile where the watertable fluctuates as a result of tidal action, the (spring)tidal range may be important too: provided the sea level remains constant, the smaller the tidal range the greater the chance of pyrite being accumulated mainly in a relatively thin horizon. Time may limit pyritization if coastal accretion is sufficiently rapid (Section 4.2.2). Therefore one may expect (potentially) acid sulfate soils to be absent along the present coasts of deltas with a lateral accretion more rapid than that of the Chao Phraya Delta, for instance near the mouths of the Irrawaddy River and the Mekong River.

#### *Reclamation and improvement of acid sulfate soils*

Once the occurrence of potential or actual acid sulfate soils has been established, how should they be treated? As regards soils from tidal areas, the data of de Clopper & Poels (Table 5) clearly demonstrate the value of such soils for mangrove forestry, salt production and shrimp ponds. For potential acid sulfate soils, but also for not potentially acid soils, these types of land use should be considered first. If reclamation is to be decided all the same, two approaches are possible: (1) try to limit pyrite oxidation by maintaining a high watertable (2) drain intensively to achieve maximum oxidation and leach with sea-water to remove most of the dissolved acidity. The first method may be applicable for lowland rice cultivation in a continuously wet climate or if abundant fresh water is available seasonally (e.g. along the Gambia River) and tidal action can be used to maintain a high watertable (e.g. Driessen, 1973). The second approach has been used with some success in Sierra Leone (Bloomfield & Coulter, 1973). The extreme acidification upon intensive aeration (Section 4.3.2) can be used to advantage here for dissolving and washing out much of the acidity. Because it provides exchangeable bases capable of removing some of the exchange acidity, sea-water (conveyed and removed by tidal action) is to be preferred for leaching. Large amounts of fresh water must be available later for desalinization. In general, the method requires considerable capital and would rarely be economical.

Land with already developed acid sulfate soils is often unsuitable or hardly suitable for agriculture, forestry or pisciculture, because of

toxicity from aluminium, iron or  $H_2S$  and lack or imbalance of other nutrients. The adverse conditions are frequently more severe in young acid sulfate soils than in deeper developed older soils.

Aluminium is probably the most important toxin. Maximum dissolved  $Al^{3+}$  activities appear to depend directly on pH and the activity of dissolved sulfate, presumably as a result of near-equilibrium with  $Al(OH)SO_4$ , according to  $pAl(OH)SO_4 = 17.2$  (Section 4.4.3). Because  $pSO_4$  varies little and is close to 2.3 in most acid sulfate soils and para-acid sulfate soils, the relation  $pAl + pH = 9.0$  is sufficiently accurate for most practical purposes. If the tolerable limits of Al for various crops at different stages of development are known, this equation can be used to calculate the minimum pH for crop growth. For an example, see van Breemen, (1973). For lowland rice, either liming or prolonged flooding can of course be used to raise the pH.

In flooded soil, all dissolved aluminium will eventually precipitate as a result of the increase in pH associated with soil reduction. But then the release of  $Fe^{2+}$  and  $H_2S$  may cause new problems. Whereas dissolved aluminium seems to react similarly in all acid sulfate soils, wide difference exist between soils in production of  $Fe^{2+}$  and presumably also of  $H_2S$  (Ponnamperuma et al., 1973). In the well developed acid sulfate soils of the Bangkok Plain, dissolved  $Fe^{2+}$  attains concentration of the same order as in 'normal' paddy soils, but far higher concentrations occur in the younger acid sulfate soils. This difference is probably associated with larger fractions of easily decomposable organic matter and of fairly amorphous, easily reducible ferric oxide in the younger soils (Sections 4.4.2 and 4.6.1). In very young acid sulfate soils, pyrite may reduce ferric oxides and also cause high concentrations of  $Fe^{2+}$  (Section 4.3.1). Hydrogen sulfide is probably of little importance as a toxin in older acid sulfate soils where sulfate reduction starts late.

In the older soils of the Bangkok Plain, a small dressing of lime may be sufficient to precipitate aluminium. Because the production of  $Fe^{2+}$  does not increase much as a result of liming (Sombatpanit & Wangpaiboon, 1973), this may considerably improve the soils for rice. However, liming could promote sulfate reduction and increase concentrations of  $H_2S$ . Another effect of liming may be enhanced decomposition of organic matter and release of nitrogen.

The release of sulfuric acid into the surface water above reduced acid sulfate soils as a result of reduction of  $Fe_2O_3$  in the soil and oxidation of dissolved  $FeSO_4$  near the soil-water interface (Section 4.6.1) may have impor-

tant consequences for rice growing and pisciculture. In the absence of lateral removal and refreshing of the floodwater, acidity of the surface water may increase strongly and thus hinder growth of plants and aquatic animals and microbes. In the Bangkok Plain, the influx of somewhat alkaline floodwater from the riverine part of the delta (where *alkalinity* increases in the surface water during soil reduction!) may be an important benefit. Acidification of surface water is certainly detrimental to pisciculture in acid sulfate soil areas; liming or refreshing of water seem necessary.

## References

Andriesse, J.P., N. van Breemen & W.A. Blokhuis, 1973. The influence of mudlobsters (*Thallasina anomala*) on the development of acid sulfate soils in mangrove swamps in Sarawak (East Malaysia). In: Dost, 1973, Vol. II, 11-39.

Bache, B.W., 1974. Soluble aluminium and calcium-aluminium exchange in relation to the pH of dilute calcium chloride suspensions of acid soils. *J. Soil Sci.* 25: 320-332.

Bandy, M.C., 1938. Mineralogy of three sulfate deposits of northern Chile. *Am. Mineral.* 23: 669-760.

Bascomb, C.L., 1964. Rapid method for the determination of cation exchange capacity of calcareous and non-calcareous soils. *J. Sci. Food Agric.* 12: 821-823.

Begheijn, L.Th., in preparation. Organic and inorganic carbon analysis in soils by potentiometry.

Begheijn, L.Th. & J. van Schuylenborgh, 1971. Methods for the analysis of soils used in the laboratory of soil genesis of the Department of Regional Soil Science. Internal report, Agricultural University, Wageningen, 156 p. (Available on request.)

Bemmelen, J.M. van, 1886. Bijdragen tot de kennis van den alluviaal bodem in Nederland. Derde Verhandeling: De samenstelling en de vorming van de zure gronden in het Nederlandsche alluvium. *Verh. Acad. Wet. Amsterdam.* XXV B: 33-105.

Bernal, J.D., D.R. Dasgupta & A.L. Mackay, 1959. The oxides and hydroxides of iron and their structural interrelationships. *Clay Miner. Bull.* 4: 15-30.

Berner, R.A., 1963. Electrode studies of hydrogen sulfide in marine sediments. *Geochim. Cosmochim. Acta* 27: 563-575.

Berner, R.A., 1967. Thermodynamic stability of sedimentary iron sulfides. *Am. J. Sci.* 265: 773-785.

Berner, R.A., 1971. Principles of chemical sedimentology. McGraw-Hill, New York. 240 pp.

Berner, R.A., M.R. Scott & C. Thominson, 1970. Carbonate alkalinity in the pore waters of anoxic marine sediments. *Limnol. Oceanogr.* 15: 544-549.

Bloomfield, C. & J.K. Coulter, 1973. Genesis and management of acid sulfate soils. *Adv. Agron.* 25: 265-326.

Breemen, N. van, 1969. The effect of ill-defined ferric oxides on the redox characteristics of flooded soils. *Neth. J. Agric. Sci.* 17: 256-260.

Breemen, N. van, 1971. Methods of analysis. I. Ground and surface water samples. II. Sulphur fractions in soils. Laboratory Inform. Paper 3, Soil Survey Division, Bangkok, 23 pp.

Breemen, N. van, 1973a. Calculation of ionic activities in natural waters. *Geochim. Cosmochim. Acta* 37: 101-107.

Breemen, N. van, 1973b. Soil forming processes in acid sulphate soils. In: Dost, 1973, Vol. I, p. 66-130.

Breemen, N. van, 1973c. Dissolved aluminium in acid sulfate soils and in acid mine waters. *Proc. Soil Sci. Soc. Am.* 37: 694-697.

Breemen, N. van, 1975. Acidification and deacidification of coastal plain soils as a result of periodic flooding. *Proc. Soil Sci. Soc. Am.* 39: 1153-1157.

Breemen, N. van & K. Harmsen, 1975. Translocation of iron in acid sulfate soils. I. Soil morphology, and the chemistry and mineralogy of iron in a chronosequence of acid sulfate soils. *Proc. Soil Sci. Soc. Am.* 39: 1140-1148.

Breemen, N. van, M. Tandatemiya & S. Chanchareonsook, 1973. A detailed soil survey on the actual and potential soil acidity at the Bang Pakong Land Development Centre, Thailand. In: Dost, 1973, Vol. II, p. 159-168.

Breemen, N. van & W.G. Wielemaker, 1974a. Buffer intensities and equilibrium pH of mineral and soils. I. The contribution of minerals and aqueous carbonate to pH buffering. *Proc. Soil Sci. Soc. Am.* 38: 55-60.

Breemen, N. van & W.G. Wielemaker, 1974b. Buffer intensities and equilibrium pH of minerals and soils. II. Theoretical and actual pH of minerals and soils. *Proc. Soil Sci. Soc. Am.* 38: 61-66.

Brindley, G.W., 1961. Quantitative analysis of clay mixtures. In: G. Brown (ed.). *The X-ray identification and crystal structures of clay minerals. Mineralogical Society, London.* p. 489-514.

Brinkman, R., 1970. Ferrolysis; a hydromorphic soilforming process. *Geoderma* 3: 199-206.

Brophy, G.P., E.S. Scott & R.A. Snellgrove, 1962. Sulfate studies. II. Solid solutions between alunite and jarosite. *Am. Mineral.* 47: 112-126.

Brophy, G.P. & M.F. Sheridan, 1965. Sulfate studies. IV. The jarosite-natrogjarosite-hydronium jarosite solid solution series. *Am. Mineral.* 50: 1595-1607.

Brown, J.B., 1970. A chemical study of some synthetic potassium-hydronium jarosites. *Can. Mineral.* 10: 696-703.

Bruggenwert, M.G.M., 1972. *Adsorptie van Al-ionen aan het kleimineraal montmorilloniet.* Versl. Landb. Onderz. 768. Pudoc, Wageningen. 120 pp.

Buurman, P., N. van Breemen & S. Henstra, 1973. Recent silification of plant remains in acid sulphate soils. *Neues Jahrb. Mineral. Monatsh.*, 1973: 117-124.

Chaudry, I.A. & A.H. Cornfield, 1966. The determination of total sulfur in soil and plant material. *Analyst (London)* 91: 528-530.

Clark, J.S., C.A. Gobin & P.N. Sprout, 1961. Yellow mottles in some poorly drained soils of the Lower Frazer Valley, British Columbia. *Can. J. Soil Sci.* 41: 218-227.

Collins, J.F. & S.W. Buol, 1970. Effects of fluctuations in the  $E_{H^+}$ -pH environment on iron and/or manganese equilibria. *Soil Sci.* 110: 111-118.

Cornell, R.M., A.M. Posner & J.P. Quirk, 1974. The dissolution of synthetic goethites: the early stage. *Proc. Soil Sci. Soc. Am.* 38: 377-378.

Crerar, D.A. & H.L. Barnes, 1974. Deposition of deep-sea manganese nodules. *Geochim. Cosmochim. Acta.* 38: 273-300.

Cullity, B.D., 1959. *Elements of X-ray diffraction.* Addison-Wesley, Mass. U.S.A. 514 pp.

Dam, D. van & L.J. Pons, 1973. Micromorphological observations on pyrite and its pedological reaction products. In: Dost, 1973. Vol. II, p. 169-196.

Dent, F.J., 1972. Reconnaissance soil survey of peninsular Thailand. Rep. SSR - 94, Soil Survey Division, Bangkok. 32 pp.

Dent, F.J. & L. Moncharoen, 1966. Report on the soil survey of the MERS study area no 6, Chanthaburi. Rep. SSR - 46, Soil Survey Division, Bangkok, 39 pp.

Diemont, W.H., W. van Wijngaarden, N. van Breemen & L.J. Pons (in prep.). Coastal configuration and pyrite accumulation in mangrove swamps in Northwest Malaysia.

Dost, H. (Ed.), 1973. Acid sulphate soils. Proceedings of an International symposium, Wageningen. ILRI Publ. 18, 2 vols. (295 pp; 406 pp).

Doyle, R.W., 1968. The origin of the ferrous iron-ferric oxide Nernst potential in environments containing dissolved ferrous iron. *Am.J.Sci.* 266: 840-859.

Drever, J.I., 1971. Magnesium-iron replacement in clay minerals in anoxic marine sediments. *Science* 172: 1334-1336.

Driessens, P.M. & Ismangun, 1973. Pyrite-containing sediments of southern Kalimantan, Indonesia. Their soils, management and reclamation. In: Dost, 1973, Vol. II, p. 345-358.

Fukui, H., 1971. Environmental determinants affecting the potential dissemination of high yielding varieties of rice - A case study of the Chao Phraya river basin. *Southeast Asian Studies* (Kyoto University) 9: 348-374.

Fukui, H., 1973. Environmental determinants affecting the potential productivity of rice - A case study of the Chao Phraya river basin of Thailand. PhD thesis, Graduate school of Kyoto University. 178 pp.

Furbish, W.J., 1963. Geologic implications of jarosite, pseudomorphic after pyrite. *Am.Mineral.* 48: 703-706.

Garrels, R.M. & C.L. Christ, 1965. Solutions, minerals and equilibria. Harper & Row and Weatherhill, New York. 450 pp.

Garrels, R.M. & F.T. Mackenzie, 1971. Evolution of sedimentary rocks. Norton & Co Inc., New York. 397 pp.

Garrels, R.M. & M.E. Thompson, 1960. Oxidation of pyrite by iron sulfate solutions. *Am.J.Sci.* 258A: 56-67.

Garrels, R.M. & M.E. Thompson, 1962. A chemical model for sea water at 25° C and one atm. total pressure. *Am.J.Sci.* 260: 57-66.

Gebhardt, H. & N.T. Coleman, 1974. Anion adsorption by allophanic tropical soils. II. Sulfate adsorption. *Proc.Soil. Sci.Soc.Am.* 38: 259-262.

Glopper, R.J. & R.L.H. Poels, 1973. A general study with tentative recommendations to the Government of Thailand on reclamation possibilities in the coastal area of the Central Plain in Thailand. Unpublished report FAO, 64 pp.

Goldhaber, M.B. & I.R. Kaplan, 1974. The sulfur cycle. In: E.D. Goldberg (ed.) *The Sea*, Vol. 5: Marine chemistry. John Wiley, New York. p. 569-655.

Halma, G., 1973. Improved efficiency in XRFS routine analysis of geochemical samples - a simple sample changer and an elegant fusion technique. *Proc.Coll.Spectroscopicum Intern.* Florence, p. 626-631.

Harmsen, K. & N. van Breemen, 1975. Translocation of iron in acid sulfate soils. II. Production and diffusion of dissolved ferrous iron. *Proc.Soil. Sci.Soc.Am.* 39: 1148-1153.

Hart, M.G.R. 1959. Sulphur oxidation in tidal mangrove soil of Sierra Leone. *Plant Soil* 11: 215-235.

Hart, M.G.R., 1963. Observations on the source of acid in empoldered mangrove soils. II. Oxidation of soil polysulphide. *Plant Soil* 19: 106-114.

Helgeson, H.C., 1969. Thermodynamics of hydrothermal systems at elevated temperatures and pressures. *Am.J.Sci.* 267: 729-804.

Helgeson, H.C., Th.H. Brown & R.H. Leeper, 1969. Handbook of theoretical activity diagrams depicting chemical equilibria in geologic systems involving an aqueous phase at one atm. and 0° to 300° C. Freeman, Cooper & Co, San Francisco. 253 pp.

Helgeson, H.C., R.M. Garrels & F.T. Mackenzie, 1969. Evaluation of irreversible reactions in geochemical processes involving minerals and aqueous solutions. II. Applications. *Geochim.Cosmochim.Acta* 33: 455-485.

Helz, G.R. & S.A. Sinex, 1974. Chemical equilibria in thermal spring waters of Virginia. *Geochim.Cosmochim.Acta* 38: 1807-1820.

Homan van der Heide, J., 1904. L'irrigation au Siam. *Bull.écon. Indo-Chine* (Hanoi), n.s. 7: 490-524.

Howeler, R.H. & D.R. Bouldin, 1971. The diffusion of oxygen in submerged soils. *Proc. Soil Sci. Soc. Am.* 35: 202-208.

Hurd, D.C., 1973. Interactions of biogenic opal, sediment and sea water in the Central Equatorial Pacific, *Geochim.Cosmochim.Acta* 37: 2257-2282.

Hydrographic Department, Royal Thai Navy, 1972. Tide tables. Vol 1. Thai waters, Thonburi - 252 pp.

International Rice Research Institute (IRRI), 1965. Annual Report for 1964. Los Banos, Philippines.

Ivarson, K.C., 1973. Microbiological formation of basic ferric sulfates *Can. J. Soil. Sci.* 53: 315-323.

Jackson, M.L., 1958. Soil chemical analysis. Prentice Hall Inc., New Jersey.

Kambhu, M.L.X., 1961. Brief description of hydrologic features of river basins in Thailand. *J. Nat. Res. Council (Thailand)* 2: 39-48.

Kamerling, G.E., 1974. Bodemfysisch and agrohydrologisch onderzoek in de jonge kustvlakte van Suriname. *Versl. Landb. Onderz.* 825. Pudoc Wageningen 259 pp.

Kawaguchi, K. & K. Kyuma, 1969. Lowland rice soils in Thailand. *Natural Sci. Ser. N-4, Center for Southeast Asian Studies (Kyoto University)*, 270 pp.

Kawalec, A., 1973. World distribution of acid sulfate soils. In: H. Dost, 1973, Vol I, p. 292-295.

Kelley, K.K., 1960. Contributions to the data on theoretical metallurgy. XII. High temperature heat content, heat capacity and entropy data for the elements and inorganic compounds. *U.S. Bur. Mines Bull.* 584, 232 pp.

Kelley, W.C., 1956. Application of differential thermal analysis to identification of the natural hydrous ferric oxides. *Am. Mineral.* 41: 353-355.

Kevie, W. van der, 1972. Morphology, genesis, occurrence and agricultural potential of acid sulphate soils in Central Thailand. *Thai J. Agric. Sci.* 5: 165-182.

Kevie, W. van der, 1973. Physiography, classification, and mapping of acid sulphate soils. In: Dost, 1973, Vol I, p. 204-222.

Kevie, W. van der & B. Yenmanas, 1972. Detailed reconnaissance soil survey of southern Central Plain area. Rep. SSR-89, Soil Survey Division, Bangkok, 187 pp.

Kharaka, Y.K. & I. Barnes, 1973. SOLMNEQ: Solution-mineral equilibrium computations. Rep. U.S. Geol. Survey, Water Res. Div., no. 73-002. 82 pp.

Kittrick, J.A., 1970. Precipitation of kaolinite at 25° C and 1 atm. *Clays Clay Miner.* 18: 261-267.

Köppen, W., 1931. Die Klimate der Erde. Walter de Gruyter, Berlin.

Kubisz, J., 1970. Studies on synthetic alkali-hydronium jarosites. I: Synthesis of jarosite and natrojarosite. *Mineral. Polonica* 1: 49-59.

Kubisz, J., 1971. Studies on synthetic alkali-hydronium jarosites. II: Thermal investigations. *Mineral. Polonica* 2: 51-60.

Kühnel, R.H., D. van Hilten & H.J. Roorda, 1974. The crystallinity of minerals in alteration profiles: an example on goethite in laterite profiles. *Delft Prog. Rep. Geosci.* 1: 1-8.

Kulp, J.L. & A.F. Trites, 1951. Differential thermal analysis of natural hydrous ferric oxides. *Am. Mineral.* 36: 23-44.

Kung, P., C. Atthayodhin & S. Kruthabandu, 1965. Determining water requirement of rice by field measurement in Thailand. *Mimeogr. rep.*, Sam Chook Farm, Royal Irrigation Department, Thailand. 16 pp.

Landa, E.R. & R.G. Gast, 1973. Evaluation of crystallinity in hydrous ferric oxides. *Clays Clay Miner.* 21: 121-130.

Langmuir, D., 1971. Particle size effect on the reaction goethite = hematite + water. *Am.J.Sci.* 271: 147-156.

Langmuir, D., 1972. Correction. Particle size effect on the reaction goethite = hematite + water. *Am.J.Sci.* 272: 972.

Langmuir, D. & D.O. Whittemore, 1971. Variations in the stability of precipitated ferric oxyhydroxides. In: J.D. Hem (Ed.) *Nonequilibrium systems in natural water chemistry. Adv.Chem.Ser.* 106. American Chemical Society, Washington D.C. p. 209-234.

Latimer, W.M., 1952. The oxidation states of the elements and their potentials in aqueous solutions. 2nd edition. Prentice Hall Inc. 392 pp.

Luthin, J.N. & D. Kirkham, 1949. A piezometer method for measuring permeability of soil in situ below a water table. *Soil Sci.* 68: 349-358.

Lynn, W.C. & L.D. Whittig, 1966. Alteration and formation of clay minerals during cat clay development. *Proc. 14th Natl.Conf.Clays Clay Mineral.* p. 241-248.

Marius, C., L.J. Pons & N. van Breemen (in prep.). Contribution à l'étude de la genèse des sols sulfatés acides du Sénégal. *Cah.ORSTOM, sér Pédol.*

Matijević, E., R.S. Sapiensko & J.B. Melville, 1975. Ferric hydrous oxide soils. I: Monodispersed basic iron (III) sulfate particles. *J.Coll.Interface Sci.* 50: 567-581.

Melville, G.E., J.R. Freney & C.H. Williams, 1971. Reaction of organic sulfur compounds in soil with tin and hydrochloric acid. *Soil Sci.* 112: 245-248.

Meyer, W.T. & R.G. Peters, 1973. Evaluation of sulphur as a guide to buried sulphide deposits in the Notre Dame Bay Area, Newfoundland. In: *Prospecting in areas of glacial terrain. Inst.Min.Metall.* London. p. 55-66.

Miedema, R., A.G. Jongmans & S. Slager, 1974. Micromorphological observations on pyrite and its oxidation products in four Holocene alluvial soils in the Netherlands. In: G.K. Rutherford (ed.). *Soil Microscopy. Proceedings of the 4th international working meeting soil micromorphology.* Limestone Press, Kingston, Ontario. p. 772-794.

Misra, U.K., R.W. Blanchard & W.J. Upchurch, 1974. Aluminum content of soil extracts as a function of pH and ionic strength. *Proc.Soil Sci.Soc.Am.* 38: 897-902.

Mitsuchi, M., 1974. Chloritization in lowland paddy soils. *Soil Sci.Plant Nutr.* 20: 107-116.

Moormann, F.R., 1962. Report on the preliminary soil survey of the Mae Klong irrigation project area. Rep.Land Dev.Dept. Bangkok, no MSR-1. 17 pp.

Moormann, F.R. & L.J. Pons, 1974. Characteristics of mangrove soils in relation to their agricultural land use potential. Paper submitted to Intern.symp.biology & mangroves, Honolulu.

Moormann, F.R. & S. Rojanasoonthon, 1968. Soils of Thailand. Rep.SSR-72, Soil Survey Division, Bangkok. 43 pp.

Morgan, J.J., 1967. Chemical equilibria and kinetic properties of manganese in natural waters. In: S.D. Faust & J.V. Hunter (eds.). *Principles and applications of water chemistry.* Proc.IVth Rudolfs Research Conference John Wiley, New York. p. 561-624.

Murata, G. & E. Matsumoto, 1974. Natural vegetation and physiography of the Central Plain of Thailand. *Southeast Asian Studies (Kyoto Univ.)* 12: 280-290.

Nedeco, 1965. A study on the siltation of the Bangkok Port channel. Volume II. The field investigations. Netherland Engineering Consultants, The Hague. 474 pp.

Nhung, M.M. & F.N. Ponnamperuma, 1966. Effects of calcium carbonate, manganese dioxide, ferric hydroxide and prolonged flooding on chemical and electro-chemical changes and the growth of rice in a flooded acid sulfate soil. *Soil Sci.* 102: 29-41.

Paces, T., 1972. Chemical characteristics and equilibration in natural water-felsic rock-CO<sub>2</sub> system. *Geochim.Cosmochim.Acta* 36: 217-240.

Park, N.J., Y.S. Park & Y.S. Kim, 1971. Effect of lime on the growth of rice and changes in pH, Fe<sup>2+</sup> and Al in an acid sulfate soil. *J.Korean Soc. Soil Sci.Fert.* 4: 167-175.

Pendleton, R.L., 1947. The formation, development and utilization of the soils of the Bangkok Plain. *Natural Hist.Bull. (Thailand)* 14: 1-43.

Plas, L. van der & J. van Schuylenborgh, 1970. Petrochemical calculations applied to soils - with special reference to soil formation. *Geoderma* 4: 357-385.

Ponnamperuma, F.N., 1964. Dynamic aspects of flooded soils. In: the mineral nutrition of the rice plant. *Proceedings of a Symposium, International Rice Research Institute, Los Banos, Philippines.* John Hopkins, Baltimore, p. 295-328.

Ponnamperuma, F.N., T. Attanandana & G. Beye, 1973. Amelioration of three acid sulphate soils for lowland rice. In: Dost, 1973, Vol. II; p. 391-406.

Ponnamperuma, F.N., T.A. Loy & E.M. Tiano, 1969. Redox equilibria in flooded soils: II The manganese oxide system. *Soil Sci.* 108: 48-57.

Ponnamperuma, F.N., E.M. Tiano & T.A. Loy, 1967. Redox equilibria in flooded soils: I The iron hydroxide system. *Soil Sci.* 103: 374-382.

Pons, L.J., 1973. Outline of the genesis, characteristics, classification and improvement of acid sulphate soils. In: Dost, 1973, Vol. I, p. 3-27.

Pons, L.J. & W. van der Kevie, 1969. Acid sulphate soils in Thailand. Rep. SSR-81, Soil Survey Division, Bangkok. 82 pp.

Pons, L.J. & I.S. Zonneveld, 1965. Soil ripening and soil classification. ILRI Publ. 13, Veenman, Wageningen. 128 pp.

Port Authority of Thailand, 1967. Investigation of sedimentation in the channel at Bangkok Bar after completion of the Yanhee Dam, water year 1966-1967 (in Thai). 8 pp.

Porrenga, D.H., 1967. Clay mineralogy and geochemistry of recent marine sediments in tropical areas. *Publ.Fys.Geogr.Lab., Univ.Amsterdam*, No 9, 145 pp.

Posnjak, E. & H.E. Merwin, 1922. The system Fe<sub>2</sub>O<sub>3</sub>-SO<sub>3</sub>-H<sub>2</sub>O. *J.Am.Chem.Soc.* 44(II): 1965-1994.

Purokoski, P., 1958. Die schwefelhaltigen Tonsedimenten in dem Flachlandgebiet von Liminka im Lichte chemischer Forschung. *Agrogeol.Publ.* 70: 1-88.

Rasmussen, K., 1961. Uorganske svovlforbindelsers omsestninger i jordbunden. Thesis, Veterinaer og Landbohøjskole, København. 176 pp.

Reesman, A.L., 1974. Aqueous dissolution studies of illite under ambient conditions. *Clays Clay Miner.* 22: 443-454.

Rice, O.W., 1969. Notes on soil temperature regimes in Thailand. Rep.SSR-79. Soil Survey Division, Bangkok. 26 pp.

Richburg, J.S. & F. Adams, 1970. Solubility and hydrolysis of aluminum in soil solutions and saturated-paste extracts. *Proc.Soil Sci.Soc.Am.* 34: 728-734.

Rickard, D.T., 1973. Sedimentary iron sulphide formation. In: Dost, 1973, Vol. I, p. 28-65.

Rickard, D.T., 1974. Kinetics and mechanism of the sulfidation of goethite. *Am.J.Sci.* 274: 941-952.

Rickard, D.T., 1975. Kinetics and mechanism of pyrite formation at low temperatures. *Am.J.Sci.* 275: 636-652.

Robie, R.A. & D.R. Waldbaum, 1968. Thermodynamic properties of minerals and related substances at 298.15° K (25 °C) and one atmosphere (1.013bars) pressure and at higher temperatures. U.S.Geol.Survey Bull. 1259, 256 pp.

Schwertmann, U., 1959. Die fraktionnierte Extraktion der freien Eisenoxyden in Böden; ihre mineralogischen Formen und ihre Entstehungsweisen. Z.Pflanzenernähr.Düng.Bodenk. 84: 194-204.

Sillén, L.G., 1967. Gibbs phase rule and marine sediments. In: R.F. Gould (ed.). Equilibrium concepts in natural water systems. Adv.Chem.Ser. 67, American Chemical Society, Washington D.C. p. 57-69.

Silverman, M.P., 1967. Mechanism of bacterial pyrite oxidation. J.Bacteriol. 94: 1046-1051.

Singer, P.C. & W. Stumm, 1970. Acidic mine drainage: the rate determining step. Science 167: 1121-1123.

Soil Survey Staff, 1970. Soil Taxonomy (selected chapters from the unedited text). Soil Conservation Service, USDA, Washington D.C., 213 pp.

Sombatpanit, S., 1970. Acid sulphate soils- Their nature and properties. Unpubl.Thesis, Royal Agricultural College. Uppsala. 135 pp.

Sombatpanit, S. & L. Wangpaiboon, 1973. Study on the lime requirement of an aluminium-rich acid sulfate soil. Paper presented at the 12th Conference on agricultural Biological Sciences, Kasetsart University, Bangkok.

Stumm, W. & J.J. Morgan, 1970. Aquatic Chemistry. John Wiley, New York. 583 pp.

Suraphibul, K., 1971. Preliminary studies on chemical and mineralogical compositions of various Great Soil Groups in Thailand. Preprint, 1st Asean Soil Conference, Bangkok, 8 pp.

Sweeny, R.E. & I.R. Kaplan, 1973. Pyrite framboid formation: laboratory synthesis and marine sediments. Econ.Geology 68: 618-634.

Takaya, Y., 1969. Topographical analysis of the southern basin of the Central Plain, Thailand. Southeast Asian Studies (Kyoto University) 7: 293-300.

Tardy, Y. & R.M. Garrels, 1974. A method of estimating the Gibbs energies of formation of layer silicates. Geochim.Cosmochim.Acta 38: 1101-1116.

Tomosugi, T., 1966. Historical development of irrigation and drainage in the Chao Phraya Delta. In: Water resource utilization in Southeast Asia. The Center for Southeast Asian Studies (Kyoto Univ.). Symp.Series III. p. 165-176.

Trafford, B.D., C. Bloomfield, W.I. Kelso & G. Pruden, 1973. Ochre formation in field drains in pyritic soils. J.Soil Sci. 24: 453-460.

Valensi, G., J. van Muylder & M. Pourbaix, 1963. Soufre. De: M. Pourbaix (ed.). Atlas d'équilibres électrochimiques à 25 °C. Publ. du Centre Belge d'Etude de la Corrosion (CEBELCOR). p. 545-553.

Vesa-Rajananda, S., 1964. Mean annual and Monthly rainfall over Thailand. Meteorological Department, Bangkok (12 maps).

Vieillefon, J., 1973. Sur quelques transformations sédimentologiques et mineralogiques dans les sols sulfatés acides du Sénégal. In: Dost, 1973, Vol. 2, p. 99-113.

Vieillefon, J., 1974. Contribution à l'étude de la pédogenèse dans le domaine fluvio-marin en climat tropical d'Afrique de l'Ouest. (Importance du compartiment géochimique du soufre dans l'aquisition et le développement des caractères pédologiques.) Thèse, ORSTOM et CRG, Paris et Thonon. 361 pp.

Vlek, P.L.G., 1971. Some morphological, physical and chemical aspects of acid sulfate soils in Thailand. Rep. SSR-84. Soil Survey Division, Bangkok. 73 pp.

Vlek, P.L.G., Th.J.M. Blom, J. Beek & W.L. Lindsay, 1974. Determination of the solubility product of various iron hydroxides and jarosite by the chelation method. Proc.Soil Sci.Soc.Am. 38: 429-432.

Weaver, C.E. & L.D. Pollard, 1973. The chemistry of clay minerals. Elsevier, Amsterdam. 213 pp.

Whitfield, M., 1974. Thermodynamic limitations on the use of the platinum electrode in  $E_H$  measurements. Limnol. Oceanogr. 19: 857-865.

Wiedemann, H.U., 1973. Application of Red-lead to the detection of dissolved sulfide in waterlogged soils. Z. Pflanzenernähr. Bodenk. 113: 73-81.

Zuur, A.J., 1954. Bodemkunde der Nederlandse bedijkingen en droogmakerijen. Deel B. Directie Wieringermeer - Landbouwhogeschool, Wageningen. Mimeographed text, 100 pp.

# Appendix A

## FIELD PROCEDURES AND METHODS FOR SOILS AND WATER SAMPLES

## A.1 Field investigations and sampling procedures

### A.1.1 Descriptions

Most pedons were described from freshly dug profile pits, using 'Guidelines for Soil Description', issued by FAO, Rome. Colours were described with the Munsell Soil Color Charts (Munsell Color Co., Baltimore, USA), 1954 edition. Sometimes, time or other circumstances (e.g. submersion) prevented digging of a profile pit, and brief descriptions were made using samples collected by means of an open-bladed (diam. 7 cm) 'Edelman-type' auger.

### A.1.2 Soil samples

Of each soil horizon, representative samples were assembled from sub-samples taken randomly from each horizon of the described face. These samples were dried at 40-50 °C (without special precautions to prevent oxidation), ground to obtain aggregates < 2 mm and stored for estimation of particle size distribution, organic matter, dithionite-extractable iron, elemental analysis of soil and of clay fraction, and mineralogy. Pyritic samples for analysis of sulfur fractions were taken by augering, and were vacuum-dried at 100-110 °C within a few days of sampling. In soils described from auger samples (KD, KR, Mn, Nk) the same samples were used for analysis of sulfur fractions and for the other chemical estimations.

At several sites, auger samples from every 20 cm down to 2 m depth were collected periodically for pH and soil moisture. Samples for estimation of bulk density were taken in duplicate from profile walls, using 100 cm<sup>3</sup> metal cores.

### A.1.3 Water samples

Surface water was collected directly in 100 or 250 cm<sup>3</sup> plastic bottles from ditches, creeks or floodwater (Fig. A. 1a) or from the inside of permanently installed poly(vinyl chloride) tubes (A.1b, si). At most sites, ground water samples were collected directly in 50 or 100 cm<sup>3</sup> bottles from fresh auger holes, sometimes by means of a simple plastic hand pump. During flooding, contamination by surface water was prevented by drilling either in a drained area inside a wide poly(vinyl chloride) tube (Fig. A.1c) or inside a poly (vinyl chloride tube) that just accommodated the auger and that could easily be pressed down to a considerable depth (Fig. A.1d). Before augering, the surface water was removed by pumping (c) or bailing (d). At four sites (Ra-1, Ra-2, T-1 and BP-1), ground water was sampled also from permanently installed porous pots made of glass fibre (Whatman No. A1 filter tubes, volume 8 cm<sup>3</sup>) surrounded by acid-washed quartz sand contained in nylon fabric (Fig. A.1e, fe). The tubes were placed in horizontal auger holes drilled in the wall of a profile pit. Before refilling the pit, plastic foil was placed against the wall to prevent contamination by water from the disturbed soil. The water was drawn through a flexible plastic tube (inner diam. 4 mm) by vacuum from a simple piston pump into a 50 cm<sup>3</sup> plastic bottle. The first, and sometimes also the second 50 cm<sup>3</sup> aliquot was discarded. Drawing one aliquot took usually less than two minutes.

All gr and fe samples were sealed without air bubbles by means of a conical rubber stopper, and brought to the laboratory within 1-2 days.

Interstitial water was also collected in the laboratory by pressure filtration from about 0.5 litre of soft water-saturated soil. These soil samples were collected in the field by augering (or taken from the laboratory reduction experiment), placed in glass jars, freed from air by tapping the

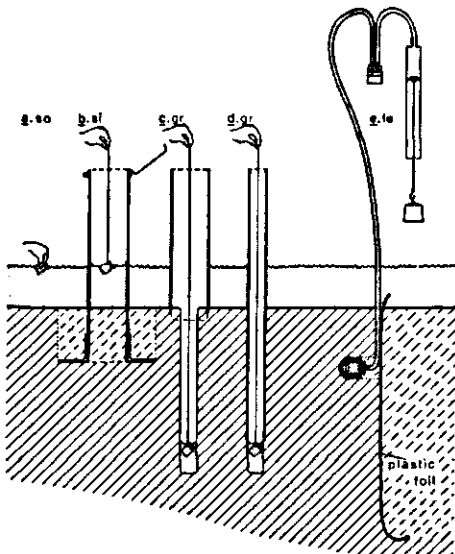


Figure A.1  
Technique of collecting surface water and ground water.

jar (and sometimes by adding soil water from the same hole), and sealed. Before collecting the water, redox potential and pH of the soil were measured in triplicate. Only flooded surface soils and samples from the lower B horizon and from pyritic substrata had sufficiently high moisture content to allow this procedure. Mud samples were filtered with a Baroid filter press, applying 1.5 bar pressure from compressed air. The collection of 25-100 cm<sup>3</sup> water took 4-6 h. To restrict evaporation and exchange of CO<sub>2</sub>, the expelled water was guided through a plastic tube into a closed plastic bottle, equipped with a balloon to allow for volume expansion. No special precautions were taken to prevent oxidation of reduced species in solution.

#### A.2 Procedures of measurement

All measurements were in the laboratory apart from a few of electrical conductivity of water samples (in the Chanthaburi area) and estimations of permeability (reported by Vlek, 1971). All analysis of waters and of sulfur fractions in soils, and those involving fresh samples (pH, E<sub>H</sub>, moisture, bulk density) were done in the laboratory of the Soil Survey Division, Department of Land Development at Bangken. All other measurements were done in the Department of Soil Science and Geology, Agricultural University, Wageningen.

##### A.2.1 Fresh samples of soil

- pH of fresh soil: a sturdy glass electrode was pressed into the soft, wet soil (if necessary wetted with distilled water to allow the electrode to be inserted), a reference electrode (Orion double-junction reference electrode) was put onto a soaked filter pad placed on the surface of the sample and the pH was measured potentiometrically. The measurement was triplicated by placing the glass electrode at three different points in the sample.
- pH of aerated soil: The soil was kept under moist aerobic conditions at ambient temperature (ca 27 °C) for 2-3 months, wetted with distilled water and the pH was measured as above.

- *Soil E<sub>H</sub>*: three bright Pt electrodes (treated with abrasive cleansing powder, and washed with dilute HCl and with water) that had been fitted into a rubber stopper were inserted 5-7 cm below the surface of samples. Three days later, the redox potential was measured with a double-junction reference electrode (cf. pH measurement). After removal of the Pt electrodes, the pH was measured in triplicate and the interstitial water was collected by pressure filtration.
- *Soil moisture*: immediately after sampling 50-100 g of soil was placed in a previously weighed container and the moisture content (by mass) was estimated by weighing before and after overnight drying at 105 °C.

#### A.2.2 Vacuum-dried and oven-dried soil samples

Samples for the analysis of sulfur fractions were either vacuum-dried (pyritic samples) or oven-dried (non-pyritic samples) within a few days of sampling, ground to a fine powder, and analysed within 1-2 weeks.

- *Sulfur fractions*: the H<sub>2</sub>S liberated from 1-5 g soil, mixed with 1.2 g granulated Sn, during boiling in 20 cm<sup>3</sup> HCl 6 mol/litre for 6 hours was attributed to FeS<sub>2</sub>. The H<sub>2</sub>S was transferred into an alkaline anti-oxidant solution (NaOH 32 and ascorbic acid 29 g/litre) by means of a stream of N<sub>2</sub> gas, and titrated potentiometrically with Pb(NO<sub>3</sub>)<sub>2</sub>, with an Orion silver sulfide electrode and an Orion double-junction reference electrode.

Jarosite plus water-soluble sulfate was extracted from 1-5 g soil by 50 cm<sup>3</sup> solution of Na<sub>2</sub>CO<sub>3</sub> 1% and of NaCl 1 mol/litre on a boiling water bath (3.5 h). If necessary the extracts were decolorized by active carbon, and sulfate was determined turbidimetrically as BaSO<sub>4</sub> (A.2.4). Jarosite was estimated after correction for the sulfate extracted<sup>4</sup> from 2-5 g soil by 50 cm<sup>3</sup> of NaCl 1 mol/litre (shaking for 3.5 h at room temperature). Further details of sulfur analysis are given elsewhere (van Breemen, 1971).

- *Dithionite-extractable iron*, Fe<sub>2</sub>O<sub>3</sub> (d), dissolved by the method by Jackson (1958) with sodium citrate and sodium bicarbonate buffer and was analysed by atomic absorption spectrometry. The results, taken from Vlek (1971), were used for the diagrams of Fig. 11, but are not given in Appendix B.

#### A.2.3 Air-dried soil samples

Except if noted otherwise, details of the analytical procedure are given by Begheijn and van Schuylenborgh (1971).

- *Particle size distribution*: the soil was treated with 10% (v/v) H<sub>2</sub>O<sub>2</sub> and HCl 0.1 mol/litre in a boiling water bath. Salts were removed by suction and washing. The fraction < 50 µm was obtained by sieving of the suspended soil, and peptized in sodium-pyrophosphate 3 mmol/litre. The fractions < 2 µm and 2-50 µm were separated by pipetting, using the Stokes formula.

- *Separation of the clay fraction for elemental analysis*: the fraction <50 µm was peptized with a few cubic centimetres of NaOH 4 mol/litre (to pH 7-8), and the fraction <2 µm was pipetted from this suspension, coagulated with HCl 2 mol/litre (to pH 3), and saturated with Li<sup>+</sup> (from LiCl 2 mol/litre). Finally excess salt was removed by dialysis for several days, and the clay was recovered by freeze-drying.

- *Dithionite-extractable iron* (Fe<sub>2</sub>O<sub>3</sub> (d)): 1 g soil was mixed with 1 g EDTA as acid, 1 g Na<sub>2</sub>S<sub>2</sub>O<sub>4</sub> and 50 cm<sup>3</sup> water, and was shaken at 85 °C for 30 min. After centrifuging, an aliquot was taken, the EDTA-Fe was digested by treatment with Se dissolved in concentrated H<sub>2</sub>SO<sub>4</sub>, and iron was estimated colorimetrically with orthophenanthroline. This procedure gives essentially the same result as the method of Jackson (1958). Fe<sub>2</sub>O<sub>3</sub> (d) includes jarosite iron and oxalate-soluble iron.

- Oxalate-soluble iron,  $Fe_2O_3$  (ox): 1 g soil was shaken in 50 cm<sup>3</sup> of Tamm's solution (oxalic acid 17.6 and ammonium oxalate 28.4 g/litre) in the dark for 1 h, and iron was estimated by atomic absorption spectrometry. Tamm's solution does not dissolve any jarosite.
- Organic matter: in non-pyritic samples, organic matter was oxidized by  $K_2Cr_2O_7$  in concentrated  $H_2SO_4$  under steady heating up to 175 °C for 90 s. The colour intensity of the green chromous ions formed during oxidation of the organic matter was measured colorimetrically. In pyritic samples, the  $CO_2$  evolved during this oxidation was collected as  $BaCO_3$ , and measured potentiometrically after dissolving the  $BaCO_3$  in EDTA (Begheijn, in prep.).
- Elemental analysis of the soil and the clay fraction: Total Si, Al, Fe, Mn, Ca, K, Ti and P were estimated with Philips PW 1540 X-ray fluorescence spectrometer after fusing the soil with sodium or lithium tetraborate (Halma, 1973). Total S was determined with the same apparatus in pellets of very finely ground material. For estimation of S, samples with known amounts of sulfur (determined by the procedure of Chaudry & Cornfield, 1966) were used as standards. There was a perfect rectilinear relationship between the chemical results and the intensity of the fluorescence due to sulfur.

Total Na was estimated by flame photometry, and total Mg by colorimetry with titan yellow, after decomposing the material with HF and  $H_2SO_4$ . For the Fe(II)-Fe(III) analysis, the soil or clay was decomposed at 180 °C for 10 min. in a HF- $H_2SO_4$  mixture in a covered Pt crucible. After transferring the reaction mixture into a saturated boric acid solution, Fe(II) was measured colorimetrically with orthophenanthroline, and total iron was measured afterwards in the same solution upon adding a reductant ( $NH_2OH.HCl$ ).

- Cation-exchange capacity (CEC): The CEC of the clay fraction was estimated by saturation with  $Ba^{2+}$  at pH 8.1, removing excess  $BaCl_2$  solution, adding an excess of  $MgSO_4$  and back-titrating the  $Mg^{2+}$  remaining in solution (Bascomb, 1964).

- X-ray diffraction analysis: the clay fraction peptized with NaOH was oriented on a porous ceramic plate and saturated with Mg, by percolating  $MgCl_2$  0.5 mol/litre. After washing and drying (40-50% relative humidity), a diffractogram was made with a Philips PW 180 diffractometer with Co K $\alpha$  radiation. Next, the same sample was saturated with glycerol and used again for X-ray diffraction. Sometimes K-saturated samples were studied before and after heating to 400 °C.

The diffractograms of the Mg-glycerol clay were analysed by means of a Du Pont 310 Curve Resolver. Peak area percentages were based on the best fit obtainable with a set of 6 peaks at about 0.7, 0.9, 1.0, 1.2, 1.4, 1.8 nm of fixed width, superimposed on a base-line curve, taken from the diffractogram of an 'empty' ceramic plate. The peak at 0.9 nm, the second-order smectite reflexion, was not considered in computing the peak area percentage.

Samples of mottles, concretions, salt efflorescences etc, were investigated with a Guinier-de Wolff camera, using Co K $\alpha$  radiation. Identifications were based on JCPDS (Joint Committee on Powder Diffraction Standards) cards.

#### A.2.4 Water

All water samples were processed within 1-2 days of sampling. Samples obtained by pressure filtration or collected from filter tubes in the field could be used without filtration; other samples often contained well flocculated suspended matter, and were filtered through Whatman No 1 filter paper. After pH, electrical conductivity and  $HCO_3^-$  had been measured, an aliquot of 10 or 20 cm<sup>3</sup> was taken, mixed with 2 cm<sup>3</sup>  $NH_2OH.HCl$  10% and diluted 5 or 10 times with distilled water. The original sample was assayed for  $Cl^-$  and  $Al^{3+}$  by the aluminium method;  $Fe^{2+}$  and  $Mn^{2+}$  were always determined in the dilution with  $NH_2OH.HCl$ ; other solutes could be estimated with either solution.

Estimates were normally single. During all analytical runs, artificially prepared samples of known compositions were included, and sometimes recoveries were checked by addition of components. Recovery was very good (99-101%) for  $\text{Cl}^-$ ,  $\text{HCO}_3^-$ ,  $\text{SO}_4^{2-}$ ,  $\text{H}_4\text{SiO}_4$ ,  $\text{Na}^+$ ,  $\text{Ca}^{2+}$  and  $\text{Fe}^{2+}$ , consistently too high for  $\text{K}^+$  (104%) and  $\text{Mn}^{2+}$  (107%), and too low for  $\text{Mg}^{2+}$  (98%) and  $\text{Al}^{3+}$  (95%). Precision was reasonable to good (coefficient of variation < 5%) for all estimates except of  $\text{Al}$  (CV 10%). Short descriptions of the methods are given below, for details see van Breemen (1971).

$\text{pH}$ : immediately after opening the sample containers, the  $\text{pH}$  was measured potentiometrically with an ORION double-junction reference electrode with an outer filling solution of 10%  $\text{NH}_4\text{NO}_3$  (instead of a calomel electrode, which would contaminate the samples with  $\text{KCl}$ ) and any commercial glass electrode. Buffers of  $\text{pH}$  4 and 7, and sometimes 2 (Merck titrisol buffers) were used for calibration. Water samples obtained by pressure filtration normally had far higher  $\text{pH}$  than the respective soil samples. The change in  $\text{pH}$  apparently involved no change in alkalinity: water from acid soil ( $\text{pH}$  3.5-4) that acquired a  $\text{pH}$  of 6-7 could be acidified with one drop of  $\text{HCl}$  5 mmol/litre. The  $\text{pH}$  of 16 samples reported are those measured in the soil before water extraction.

$\text{Electrical conductivity}$ : electrical conductivity at 25 °C was measured with a CENCO No 34501 meter, using a Philips PW 9513 pipette cell, calibrated with  $\text{KCl}$  20 mmol/litre.

$\text{HCO}_3^-$ : the alkalinity found by potentiometric titration with  $\text{HCl}$  5 mmol/litre to  $\text{pH}$  4.65 was assumed to represent bicarbonate.

$\text{Cl}^-$ : titrated potentiometrically with  $\text{AgNO}_3$ , using Orion silver sulfide electrode and double-junction reference electrode to detect the end-point.

$\text{SO}_4^{2-}$ : sulfate was determined turbidimetrically as  $\text{BaSO}_4$  in a medium of nitric acid and acetic acid after addition of  $\text{BaSO}_4$  seed suspension, ground  $\text{BaCl}_2 \cdot 2\text{H}_2\text{O}$  and a mixture of acacia gum and acetic acid.

$\text{H}_4\text{SiO}_4$ : silica was estimated colorimetrically as the blue  $\beta$ -silico-molybdenic acid, obtained after adding ammonium molybdate and a reduction mixture ( $\text{Na}_2\text{SO}_3$ , metol and  $\text{K}_2\text{S}_2\text{O}_5$ ) in a medium of sulfuric and tartaric acids.

$\text{K}^+$  and  $\text{Na}^+$ : the alkali ions were estimated by EEL flame photometer using an air-butane flame.

$\text{Ca}^{2+}$  and  $\text{Mg}^{2+}$ : were estimated with a Techtron AA 100 atomic absorption spectrometer, using an air-acetylene flame in a solution enriched with  $\text{Al}^{3+}$  8,  $\text{Na}^+$  800 and  $\text{Sr}^{2+}$  1200 mg/litre (added as chlorides) to prevent or suppress interference by aluminium and sulfate.

$\text{Fe}^{2+}$  and  $\text{Mn}^{2+}$ : analysed directly in the dilutions containing  $\text{NH}_2\text{OH} \cdot \text{HCl}$  by atomic absorption spectrometry, with an air-acetylene flame. If ferric hydroxides had formed in the original solution immediately after sampling (this often occurred in the waters collected by pressure filtration but not elsewhere), a well mixed sample of the suspension was pipetted, and the precipitate was dissolved by adding  $\text{NH}_2\text{OH} \cdot \text{HCl}$ . All iron was assumed to be  $\text{Fe}^{2+}$  in field samples; dissolved ferric iron was found in measurable amounts only in samples of very low  $\text{pH}$  (<3) from the laboratory oxidation experiment.

$\text{Al}^{3+}$ : Dissolved aluminium was estimated only in samples with a  $\text{pH}$  below 5, but not in those collected by pressure filtration<sup>a</sup>.

Two different colorimetric methods were used: the very sensitive method with pyrocatechol violet for samples low in dissolved iron ( $\text{Fe}^{2+} < 2$  mg/litre in the final reaction mixture) and the less sensitive aluminon method for higher iron concentrations.

a.  $\text{Al}^{3+}$  was lowered strongly in such samples, probably by increase in  $\text{pH}$  during pressure filtration. Dissolved  $\text{Fe}^{2+}$  and  $\text{Mn}^{2+}$  were lowered only slightly (up to 20%) in these waters.

## Appendix B

### PROFILE DESCRIPTIONS AND ANALYTICAL DATA ON SOIL SAMPLES

The pedons are grouped geographically: B.1 Bangkok Plain, B.2 Cha-am Lagoon, B.3 Peninsular Thailand and B.4 the Southeast Coast Region. Soils from the Bangkok Plain are further subdivided into (1) saline acid sulfate soils and potentially acid soils, (2) non-acid marine soils and (3) non-saline acid sulfate soils and para-acid sulfate soils.

If available, sulfur fraction analysis are reported separately, because they refer to vacuum-dried samples, different from the air-dried samples used for estimating particle size,  $\text{Fe}_2\text{O}_3$  (d), organic matter and elemental composition. Except in Mn-1, KD-1 and KR-1, total sulfur from elemental analysis was reported either as  $\text{SO}_3$  or as  $\text{FeS}_2$  according to the redox state of the original sample. The reported  $\text{Fe}_2\text{O}_3$  contents were obtained by subtracting  $\text{FeO}$  iron and  $\text{FeS}_2$  from the total iron found by X-ray fluorescence. Aeration after sampling caused much of the original  $\text{FeS}_2$  to be oxidized to  $\text{Fe}_2\text{O}_3$  and sulfate. Through preferential precipitation of ferric oxide on clay minerals, the reported values for  $\text{Fe}_2\text{O}_3$  in the clay fraction of pyritic samples are generally too high.  $\text{FeO}$  values are reported as analysed. Reduction of ferric iron by pyrite or organic matter during destruction by HF may have led to too high values for  $\text{FeO}$  in surface soils and substrata.

The normative mineralogical composition was calculated with the goethite norm by the method of van der Plas & Schuylenborgh (1970) with a computer programme written by R. Brinkman of the Department of Soil Science and Geology, Agricultural University, Wageningen. Abbreviations for the minerals are as follows: Q, quartz; P, phosphates (strengeite + apatite); Ru, rutile; Go, goethite; Ms, muscovite, Kaol, kaolinite; Sm, smectite, Ab, albite; Pyr, pyrite and Jar, jarosite.

## B.1.1 Saline acid sulfate soils and potentially acid sulfate soils

## Profile 1

BP-1 Bang Pakong Series - Typic Sulfaquept

Described by N. van Breemen and P.L.G. Vlek, 1970-07-06

Location 5151 I 1493.4 N, 716.4 E

Elevation between 1 and 2 m

Formerly mangrove forest, dominated by *Bruguiera gymnorhiza*, *Nipa fruticans* and *Xylocarpus granatum*. Since reclamation in 1967 fallow and covered with *Sueda maritima* and grasses. The soil is flooded occasionally by brackish water during spring-tides and by rainwater in the rainy season, otherwise the watertable remains close to the surface.

## Detailed profile description:

A1 0- 10 cm 50% dark grayish brown (10YR4/2) and 50% brown to dark brown (10YR4/3) silty clay; many, coarse, faint, diffuse, dark reddish brown (5YR4/3) mottles; weak coarse, angular blocky; sticky, non-plastic; few (appr. 40/dm<sup>2</sup>) medium, vertical, inped and exped, continuous, tubular pores; many, very fine roots, pores frequently filled with faecal pellets; clear, smooth boundary

B21 10- 18 cm 70% dark grayish brown (10YR4/2) and 30% brown to dark brown (10YR4/3) silty clay; many, coarse, distinct, clear to diffuse, reddish brown (5YR4/4-5YR4/3) mottles and glossy coatings on pore walls; locally many coarse, distinct, clear, strong brown (7.5YR5/6) mottles; weak, coarse angular blocky; sticky, non-plastic; common, fine to medium, vertical, inped and exped, continuous, tubular pores; many very fine roots; many pores filled with faecal pellets; clear, smooth boundary

B22g 18- 30 cm grayish brown (10YR4/2) and locally very dark gray (10YR3/1) silty clay; many, coarse, distinct, clear to diffuse, reddish brown (10YR4/4-10YR4/3) glossy coatings on pore walls; only at a few spots in the wall of the pit: many, coarse, prominent, sharp to clear, yellow (2.5Y8/6) jarosite on ped faces and in layers (appr. 3 mm thick) sandwiched in between the matrix and the reddish brown coatings on pore walls; jarosite is sometimes associated with half decayed wood (root) fragments; weak, coarse, angular blocky; slightly sticky, non-plastic; common, fine to coarse, continuous, vertical inped, tubular, mostly open pores; pores often filled with faecal pellets and root remnants; few roots; locally pieces of soft half decayed wood (up to 10 cm in diameter); moderate to very rapid permeability; gradual, irregular boundary

Cg1 30- 60 cm greenish gray (5GY4/1) clay; unmottled; weak, coarse prismatic; slightly sticky, non-plastic; common, fine to coarse, continuous vertical, inped, tubular pores, sometimes filled with faecal pellets or half decayed roots; locally remnants of *Xylocarpus* and *Nipa* roots; moderate to rapid permeability

Cg2 60 + cm greenish gray (5GY4/1) clay; unmottled; locally many soft shell fragments and black pockets of organic matter; rapid to very rapid permeability; at many spots in the wall of the pit FeS suspension seeps from these pockets of organic matter into the pit, turning the water at the bottom of the pit jet black.

## Range of profile characteristics:

The depth of the unmottled subsoil and the degree of actual and potential acidity are closely correlated with the elevation of the soil surface, which may vary up to 20 cm over 100 m

Table 1.1

BP-1 pH fresh and pH aerated.

Depth (cm)	pH fresh	pH aerated	Depth (cm)	pH fresh	pH aerated
0- 5	5.5	4.8	25- 30	3.6	2.1
5- 10	4.2	4.3	30- 35	4.0	2.8
10- 15	3.3	3.2	35- 40	5.3	2.4
15- 20	3.1	2.8	40- 45	5.9	3.5
20- 25	3.4	2.4	45- 50	6.1	3.6

Table 1.2

BP-1 and BP-6<sup>a</sup>. Sulfur fractions<sup>b</sup> and  $Fe_2O_3(d)$ 

Depth (cm)	BP-1			BP-6		
	waters.	pyrite	$Fe_2O_3(d)$	waters.	pyrite	$Fe_2O_3(d)$
	SO <sub>4</sub> -S%	S %	SO <sub>4</sub> -S%	S %	SO <sub>4</sub> -S%	S %
0- 20	0.05	0.01	3.0	0.07	0.03	3.6
20- 40	0.11	1.11	1.0	0.27	0.16	1.0
40- 60	0.28	2.30	1.1	0.21	0.99	0.3
60- 80	0.19	2.31	0.8	0.38	0.97	0.7
60-100	0.13	2.58	0.4	0.17	1.61	0.4
100-120	0.13	1.73	0.4	0.17	1.46	0.4

Table 1.3

BP-1 Particle-size distribution, organic C and  $Fe_2O_3(d)$ 

Depth (cm)	Particle-size ( $\mu m$ )			Org. C	$Fe_2O_3(d)$
	>50	50-2	<2		
0- 10	1.0	49.7	49.3	1.7	6.7
10- 18	0.6	42.9	56.5	2.7	4.0
18- 30	0.6	41.4	58.0	3.5	2.1
30- 40	0.5	32.9	66.6	3.3	2.3
40- 60 <sup>c</sup>	0.3	44.8	54.9	2.9	0.5

Table 1.4

BP-1 Saturation moisture content, N-value and bulk density.

Depth (cm)	Moisture (weight %)	N-value	Bulk density (g/cm <sup>3</sup> )
8	61	0.88	1.06
15	80	1.04	0.87
30	117	1.32	0.66
45	143	1.41	0.57

a. 100 m northwest of BP-1

b. jarosite contents are below

0.00% in all samples

c. vacuum-dried soil

Table 1.5

BP-1 Elemental composition (weight %); a: fraction < 2 mm (analysed after dialysis);  
 b: fraction < 2  $\mu\text{m}$ .

Depth (cm)	SiO <sub>2</sub>	Al <sub>2</sub> O <sub>3</sub>	Fe <sub>2</sub> O <sub>3</sub>	FeO	MnO	MgO	CaO	Na <sub>2</sub> O	K <sub>2</sub> O	TiO <sub>2</sub>	P <sub>2</sub> O <sub>5</sub>	SO <sub>3</sub>	FeS <sub>2</sub>	ign. loss
0- 10	a. 66.8	12.9	8.02	0.76	0.08	0.91	0.19	0.41	1.47	0.81	0.16	0.18	0.00	8.43
	b. 46.6	24.5	11.9	0.51	0.07	1.05	0.03	0.20	2.04	0.80	0.23	0.05	0.00	10.5
10- 18	a. 64.8	14.8	5.90	0.75	0.04	0.85	0.16	0.38	1.63	0.81	0.12	0.23	0.00	9.53
	b. 49.3	26.2	8.63	0.30	0.05	0.92	0.02	0.21	2.09	0.86	0.29	0.05	0.00	10.2
18- 30	a. 64.7	15.2	3.05	0.92	0.02	0.74	0.14	0.40	1.58	0.81	0.06	0.00	1.10	11.7
	b. 50.1	25.8	6.85	0.42	0.03	0.87	0.03	0.24	2.16	0.87	0.23	0.00	0.19	10.7
30- 40	a. 57.1	15.7	1.32	1.08	0.07	1.13	0.15	0.41	1.66	0.74	0.06	0.00	4.93	14.5
	b. 47.1	24.9	9.38	0.40	0.05	0.95	0.03	0.38	2.25	0.83	0.25	0.00	0.15	12.2
40- 60	a. 63.5	14.1	-	-	0.13	1.71	0.19	1.20	1.57	0.76	0.05	0.00	5.43	9.81
	b. 44.7	22.8	10.6	0.34	0.02	1.15	0.03	0.62	2.38	0.80	0.44	0.00	-	13.9

Table 1.6

BP-1 Normative mineralogical composition of the fraction < 2  $\mu\text{m}$  (weight %).

Depth (cm)	Q	P	Ru	Go	Ms	Kaol	Sm	Ab	Jar.	Pyr.	H <sub>2</sub> O*	rest
0- 10	7.0	0.6	0.8	13.1	17.2	31.7	23.8	1.7	0.2	0.0	1.5	
10- 18	9.5	0.8	0.9	9.6	17.7	37.8	19.3	1.8	0.2	0.0	1.2	
18- 30	9.4	0.6	0.9	7.4	18.3	38.5	19.7	2.0	0.0	0.2	2.0	
30- 60	7.6	0.7	0.8	10.0	19.0	31.5	20.7	3.2	0.0	0.2	3.8	

Table 1.7

BP-1 Peak area percentages of X-ray diffractograms of the fraction < 2  $\mu\text{m}$ , treated with Mg-glycerol.

Depth (cm)	d Value (Å)				
	7	10	12	14	18
0- 10	23	5	2	1	69
10- 18	28.5	7	2.5	2	60
18- 30	27	7	3.5	3.5	57
30- 60	28	7	2	1	61

Profile 2

KD-1 Cha-am Series - Typic Sulfaquept

Described by N. van Breemen and P.L.G. Vlek, 1970-10-20

Location 5151 I 1495.1 N, 698.6 E

Elevation 2-3 m

Former paddy field reclaimed about 30 years ago, fishpond for 1 year. Water level 55 cm above the surface during description.

*Description from auger samples:*

0 2- 0 cm organic matter debris coated with black (10YR2/1) material, (probably FeS)

B1g(?) 0- 10 cm gray (5Y5/1) clay, common olive brown (2.5Y4/4) coatings on ped faces; slow permeability

B21g 10- 25 cm gray (5Y5/1) clay, common dark yellowish brown (10YR4/4) mottles; slow permeability

B22g 25- 40 cm gray (5Y5/1) clay, common dark yellowish brown (10YR3/4) mottles and pale yellow (2.5Y7/4) jarosite mottles; moderately rapid permeability

B23g 40- 53 cm dark gray (5Y4/1) clay, few dark yellowish brown (10YR4/4) mottles, many yellow (2.5Y8/6) jarosite as mottles (mainly in the upper part of the horizon) and as coatings on ped faces (lowest part of the horizon)

B24g 53- 65 cm dark gray (5Y4/1) clay, dark greenish gray (5G4/1) mottles, few dark yellowish brown (10YR4/4) mottles, and few yellow (2.5Y8/6) jarosite coatings on ped faces

B3g 65- 75 cm dark greenish gray (5GY4/1) clay, common dark greenish gray (5G4/1) mottles; very few dark yellowish brown (10YR4/4) mottles

C1g 75- 90 cm dark greenish gray (5GY4/1) clay, common faint mottles, slightly greener than the matrix; many partly decomposed root remnants

C2g 90-125 cm dark greenish gray (5GY4/1) clay, unmottled

C3g 125-140 cm as horizon above, slightly firmer consistence

C4g 140 + cm as horizon above, few faint, diffuse light yellowish brown (2.5Y6/4) spots (silt accumulations?).

*Range in profile characteristics:*

About 20 m from the described profile, at a spot 20 cm lower, no jarosite was observed and slightly hardened ferric oxide coatings were found on ped faces in the upper part of the profile.

During an earlier visit to the area (1969-06-09), the soil had a dark grayish brown (10YR4/2) matrix colour and showed many strong brown (7.5YR5/8) mottles in the upper 50 cm. At greater depth the two profiles appeared very similar. Almost continuous flooding since August 1969 (use as fishpond) and associated soil reduction may be responsible for the differences in matrix colour and mottling.

Profile 3

KD-2 Bang Pakong Series - Typic Sulfaquent

Described by N. van Breemen and W. van der Kevie, 1969-06-09

Location 5151 I 1494.0 N, 698.6 E

Rhizophora swamp (almost pure stand of *Rhizophora apiculata*). The soil is very soft and has a low bearing capacity.

*Description from auger samples:*

C1g 0- 50 cm very dark gray (5Y3/1) to very dark greenish gray (5GY3/1) clay; unmottled; many roots (non-fibrous); rapid permeability

C2g 50-150 cm dark gray (5Y4/1) to dark greenish gray (5GY4/1) clay with dark bluish gray (5BG4/1) spots

C3g 100-200 cm dark bluish gray (5BG4/1) clay

C4g 200-230 cm dark greenish gray (5GY4/1) clay.

---

B.1.2. Non-Acid Soils

---

Profile 4

Mc-2 Samut Prakan Series

Described by W. van der Kevie and N. van Breemen, 1969-06-09

Location 5151 IV 1499.9 N, 675.0 E

Paddy field transplanted rice.

*Description from auger samples:*

Apg 0- 21 cm gray (5Y5/2) matrix; many medium brown (7.5 YR4/4) mottles

B21g 21- 66 cm gray (N6/0) matrix; many coarse yellowish brown (10YR5/8) and few, coarse, slightly hard, black (10YR2/1) mottles

B22g 66- 90 cm gray (N5/0) matrix, common coarse yellowish brown (10YRS/8) mottles

Cg 110 + cm dark gray (5Y4/1) matrix; unmottled.

Profile 5

Mc-18 Bangkok Series

Location 5052 II 1515.3 N, 646.5 E

Paddy field, transplanted rice

Profile 6

Mc-27 Tha Chin Series in *Avicennia* forest

Location 5151 IV 1497.1 N, 675.6 E

Profile 7

Mc-28 Tha Chin Series in *Avicennia* forest

Location 5151 IV 1494.3 N, 682.3 E

Profile 8

T-1 Bangkok Series - Typic Tropaquept

Described by N. van Breemen and P.L.G. Vlek, 1970-06-10

Location 5052 II 1515.0 N, 644.7 E

Elevation + 3 m

Paddy field, transplanted rice

*Detailed profile description:*

Ap 0- 25 cm black (10YR2/1) clay, few to common, fine to medium, distinct, clear, yellowish brown (10YR5/6) rootrust and coatings on pedfaces; moderate medium to coarse angular blocky; slightly sticky, plastic; broken slickensides on all ped faces; few, very fine to fine continuous, random, inped and exped, tubular pores; frequent fine to very fine roots; very slow permeability; clear, wavy boundary

B1g 25- 75 cm grayish brown (10YR5/2) silty clay; common, coarse, distinct, sharp to clear, strong brown (7.5YR4/6) mottles (increasing with depth); common coarse, distinct, clear, yellowish brown (10YR5/6) mottles, mainly in the upper part of the horizon; locally black (10YR2/1) clay in pores and cracks; moderate coarse and moderate fine to medium angular blocky; slightly sticky, plastic; continuous slickensides; common, fine to very fine, continuous, mainly vertical, inped and exped pores; common fine to very fine roots; few hard Fe-Mn nodules (up to 5 mm in diameter) associated with the strong brown mottles; common small, colourless mica flakes; locally small white gypsum aggregates; slow to moderately slow permeability; clear, irregular boundary

B21g 75-105 cm olive gray (5Y5/2) silty clay; many (more than 40% of the surface area) coarse, distinct, sharp to diffuse, brown to dark brown (7.5YR4/4) and black (10YR5/2) Fe-Mn oxide mottles, closely associated; common, medium, distinct, diffuse, light olive brown (2.5Y5/6) mottles; locally, common dark gray (10YR4/1) material in pockets; weak, medium prismatic; slightly sticky, slightly plastic; patchy slickensides; common, very fine to medium, continuous, vertical, inped and exped pores; few fine roots; common small, colourless mica flakes; common, hard brown and black Fe (outside) and Mn (inside) oxide nodules (up to 10 mm in diameter); moderately rapid permeability; clear, wavy boundary

B22g 105-200 cm gray (5Y5/1) silty clay (upper part) to clay loam (lower part); common, coarse, distinct, diffuse brown to strong brown (7.5YR4/4-7.5YR5/6) mottles along vertical pores and as pore fillings; common hard, thick brown (7.5YR5/4) coatings along pores, with thin black (10YR2/1) Mn oxide coatings inside (no Mn oxide mottles in matrix); weak, coarse prismatic; slightly sticky, slightly plastic to non-plastic; common, medium to coarse, continuous, vertical, inped and exped pores; few roots; common, small, colourless mica flakes; moderately rapid to rapid permeability

Cg 200 + cm greenish gray (5G4/1) clay loam; common dark greenish gray to grayish green (5G4/1-5G4/2) mottles along vertical pores; slightly sticky, slightly plastic; many shell fragments; many hard, large (max. dimension up to 20 cm) irregularly shaped silt (?) indurations at appr. 230 cm below the soil surface.

Table 8.1

T-1 *pH and sulfur fractions.*

Depth (cm)	pH fresh 70-06-10	pH aerated 70-06-10	Depth (cm)	Waters. SO <sub>4</sub> -S (%)	Pyrite S (%)
0- 20	5.4	5.6			
20- 40	5.7	5.8	0- 20	0.04	-
40- 60	5.4	6.3	20- 50	0.16	-
60- 80	6.5	6.7	50- 80	0.39	0.00
80-100	6.6	6.4	80-110	0.05	0.00
100-120	6.6	6.1	110-140	0.06	0.00
120-140	6.6	6.9	140-170	0.06	0.00
140-160	6.6	6.7	170-200	0.08	0.59
160-180	6.5	6.8	200-220	0.07	0.74
180-200	6.7	5.0			jarosite-S < 0.00 % in all samples.
200-220	6.9	7.0			

Table 8.2

T-1 *Particle size distribution, organic C and Fe<sub>2</sub>O<sub>3(d)</sub>.*

Depth (cm)	Particle size (mm)				(μm)			Org. C (% C)	Fe <sub>2</sub> O <sub>3(d)</sub> (%)
	2-1	1-0.5	0.5-0.25	0.25-0.1	100-50	50-2	< 2		
0- 25			4.2			37.2	58.6	0.9	2.0
25- 50			3.7			41.4	54.9	0.2	2.9
50- 75			4.8			42.1	53.0	0.0	3.9
75-105	0.0	0.0	0.1	0.2	9.5	41.8	48.4	0.2	4.0
105-150	0.0	0.0	0.0	0.1	7.1	46.1	46.6	0.3	4.5
150-200	0.0	0.1	0.1	1.3	22.0	44.5	32.1	0.0	2.4
210-230	0.0	0.1	0.2	0.5	19.2	42.7	37.5	1.1	1.2

Table 8.3

T-1 *Saturation moisture content, N value and bulk density.*

Depth (cm)	Moisture (weight %)	N-value	Bulk density (g/cm <sup>3</sup> )
17	37	0.47	1.35
36	30	0.37	1.53
70	38	0.54	1.40
100	43	0.66	1.32
130	49	0.79	1.18
154	48	0.91	1.13

Table 8.4

T-1 Elemental composition (weight %); a: fraction < 2 mm; b: fraction < 2  $\mu\text{m}$ .

Depth (cm)	SiO <sub>2</sub>	Al <sub>2</sub> O <sub>3</sub>	Fe <sub>2</sub> O <sub>3</sub>	FeO	MnO	MgO	CaO	Na <sub>2</sub> O	K <sub>2</sub> O	TiO <sub>2</sub>	P <sub>2</sub> O <sub>5</sub>	SO <sub>3</sub>	FeS <sub>2</sub>	ign. loss
0- 25	a. 65.9	15.7	4.39	0.47	0.01	0.68	0.43	0.60	2.20	0.81	0.03	0.30	0.0	6.95
	b. 50.8	25.7	7.68	0.33	0.03	0.83	0.02	0.19	2.55	0.83	0.13	-	-	9.83
25- 50	a. 64.5	15.0	5.30	0.11	0.02	0.70	1.00	0.56	2.23	0.78	0.03	1.20	0.0	6.32
	b. 51.5	26.6	8.45	0.28	0.04	0.83	0.03	0.20	2.41	0.83	0.13	-	-	9.76
50- 75	a. 65.5	15.0	6.47	0.13	0.06	0.69	0.45	0.58	2.26	0.78	0.06	0.28	0.0	5.55
	b. 50.0	25.2	9.41	0.28	0.06	0.95	0.02	0.20	2.59	0.79	0.16	-	-	9.81
75-105	a. 66.8	13.4	6.37	0.14	0.07	0.73	0.38	0.62	2.25	0.69	0.05	0.10	0.0	5.06
	b. 49.4	23.6	10.3	0.29	0.06	1.11	0.03	0.21	2.34	0.76	0.14	-	-	9.90
105-150	a. 66.9	12.7	6.31	0.16	0.14	0.71	0.40	0.60	2.21	0.68	0.07	0.08	0.0	5.22
	b. 49.2	23.0	10.9	0.32	0.07	1.14	0.02	0.19	2.32	0.75	0.14	-	-	9.97
150-200	a. 72.3	10.2	4.47	0.11	0.03	0.63	0.38	0.61	2.22	0.65	0.06	0.10	0.0	3.82
	b. 50.3	23.5	10.7	0.32	0.06	1.15	0.02	0.20	2.25	0.75	0.16	-	-	9.80
210-230	a. 68.6	11.2	1.96	0.52	0.08	0.73	1.43	0.68	2.08	0.66	0.05	0.0	2.10	6.25 <sup>a</sup>
	b. 49.0	24.2	8.33	0.51	0.05	1.54	0.03	0.22	2.64	0.81	0.33	-	-	10.3

a. including 0.52% CO<sub>2</sub>

Table 8.5

T-1 Normative mineralogical composition of the fraction < 2  $\mu\text{m}$  (weight %).

Depth (cm)	Q	P	Ru	Go	Ms	Kaol	Sm	Ab	H <sub>2</sub> O <sup>+</sup> rest
0- 25	12.2	0.3	0.8	8.4	21.6	33.6	18.0	1.6	1.4
25- 50	12.0	0.3	0.8	9.3	20.4	37.3	17.5	1.7	0.8
50- 75	11.3	0.4	0.8	10.3	21.9	31.0	19.6	1.7	1.3
75-105	11.3	0.4	0.8	11.3	19.8	27.5	22.6	1.8	1.6
105-150	11.6	0.4	0.8	11.9	19.6	25.7	23.4	1.6	1.8
150-200	11.9	0.4	0.8	11.7	19.0	27.3	23.6	1.7	1.4
210-230	6.0	0.9	0.8	8.9	22.3	21.2	32.4	1.9	2.6

Table 8.6

T-1 Peak area percentages of X-ray diffractograms of the fraction < 2  $\mu\text{m}$ , treated with Mg-glycerol, and cation-exchange capacity of the clay fraction

Depth (cm)	d-Value (Å)					CEC mmol/100g
	7	10	12	14	18	
0- 25	15	5	6	4.5	70	46.5
25- 50	19	10 <sup>r</sup>	4	1	66	45.5
50- 75	15	6	4	0	75	46.2
75-105	16	4	2	0	78	50.3
105-150	19	7	2	0	72	.
150-200	20	7	4	0	69	50.7
210-230	28	6	4	1	61	.

### 8.1.3 Non-saline acid sulfate soils and para-acid sulfate soils

#### Profile 9

Bk-1 Chachoengsao Series - Typic Tropaquept

Described by N. van Bremen, 1969-07-07

Location 5152 II 1511.4 N, 674.18 E

Elevation 1-2 m

Formerly used for paddy, now fallow (grasses and rushes)

#### Detailed profile description:

Ap1 0- 4 cm dark gray (10YR4/1) clay; many, medium, distinct, clear, brown (7.5YR4/4) mottles, mainly on ped faces and along channels; medium to fine, moderate granular; very friable; abundant grass roots; slow permeability; clear, smooth boundary

Ap2 4- 35 cm dark gray (10YR4/1) clay; common medium, distinct, sharp, dark reddish brown (5YR3/4) mottles and brown (7.5YR4/4) to dark reddish brown (5YR3/4) root rust; moderate to strong, fine to medium angular blocky; slightly sticky, slightly plastic; few fine to very fine tubular pores; many fine roots; slow permeability; clear wavy boundary

B1g 35- 70 cm light brownish gray (2.4Y6/2) clay; locally very dark gray (10YR3/1) in vertical "veins" and along pedfaces; common, medium and coarse distinct, diffuse, yellowish brown (10YR5/6) mottles; few, medium to coarse, prominent, diffuse, red (2.5YR4/6) mottles; weak, medium to coarse prismatic, moderate, medium to coarse angular blocky; slickensides on pedfaces; sticky, plastic; few, fine tubular pores; few roots; slow permeability; gradual, smooth boundary

B2g 70-135 cm gray (5Y5/1) silty clay; many, medium to coarse, distinct, clear to diffuse, very dark gray (10YR3/1) to black (10YR2/1) mottles (soft Mn-oxide concretions); common, coarse, distinct, diffuse, yellowish brown (10YR5/0) and common, medium to coarse, faint, diffuse, olive brown (2.5Y4/5) mottles along root channels; weak, medium to coarse prismatic, moderate, medium to coarse angular blocky; slickensides on pedfaces; sticky, plastic; common very fine to fine tubular pores; moderate permeability; gradual, smooth boundary

B3g 135-185 cm gray (5Y5/1) silty clay; many soft and hard ferric oxide pipes (outer Ø  $\pm$  5 mm; inner Ø 1-2 mm), frequently surrounded by greenish (greener than 5G4/2) mottles; structureless, massive; very sticky, slightly plastic; common fine to very fine pores; moderate permeability

C1g 185-220 + cm dark greenish gray (5GY4/1) to dark gray (5Y4/1) silty clay; few shell fragments.

*Range in profile characteristics:*

Essentially similar profiles were observed in two borings, about 10 m from the profile pit. A profile in the immediate vicinity described by F.R. Moormann and S. Rojanasoothon in 1966 had a very similar morphology but showed little gypsum between 10 and 70 cm.

Table 9.1

Bk-1 pH and soil moisture (weight %) on different sampling dates

Depth (cm)	pH fresh			pH aerated 69-10-06	moisture content			
	69-07-07	69-08-11	69-10-06		69-06-18	69-07-07	69-08-11	69-10-06
0- 20	4.7	4.3	4.4	4.6	29	31	36	40
20- 40	4.6	4.7	4.4	4.5	32	31	31	32
40- 60	5.8	5.4	5.0	5.1	36	32	34	33
60- 80	5.8	5.9	5.7	6.0	35	34	39	39
80-100	6.1	6.0	6.0	6.1	53	43	44	46
100-120	6.0	5.8	5.9	6.1	52	50	56	53
120-140	5.7	5.0	5.6	5.5	59	60	56	56
140-160	5.4	4.5	4.3	4.2	56	65	62	70
160-180	5.2	4.7	4.6	2.7	79	70	75	78
180-200	6.9	6.0	6.3	5.9	86	94	77	-
height of the watertable (cm):				-	-18	-21	-3	

Table 9.2

Bk-1 Particle-size distribution, organic C,  $Fe_2O_3(d)$  and N value.

Depth (cm)	Particle-size ( $\mu m$ )			Org. C (%)	$Fe_2O_3(d)$ (%)	N value
	>50	50-2	< 2			
0- 4	0.3	38.3	61.4	1.9	2.8	-
4- 35	0.4	35.0	65.6	1.1	3.0	0.41
35- 70	1.7	36.9	61.4	0.4	4.3	0.43
70-135	0.4	41.0	58.6	0.2	2.5	0.68
135-185	1.1	44.1	54.8	1.1	4.0	1.12
185-220	0.7	47.4	51.9	1.3	3.1	1.29

Table 9.3

Bk-1 Elemental composition (weight %); a: fraction < 2 mm; b: fraction < 2  $\mu\text{m}$ .

Depth (cm)	SiO <sub>2</sub>	Al <sub>2</sub> O <sub>3</sub>	Fe <sub>2</sub> O <sub>3</sub>	FeO	MnO	MgO	CaO	Na <sub>2</sub> O	K <sub>2</sub> O	TiO <sub>2</sub>	P <sub>2</sub> O <sub>5</sub>	SO <sub>3</sub>	FeS <sub>2</sub>	ign. loss
0- 4	a. 60.4	17.4	5.55	0.29	0.02	0.57	0.20	0.49	2.13	0.88	0.07	0.03	0.0	9.86
	b. 49.4	25.6	7.25	0.29	0.01	0.96	0.01	0.54	2.59	0.85	0.11	-	-	10.5
4- 35	a. 60.2	17.9	6.14	0.23	0.02	0.57	0.20	0.51	2.19	0.91	0.05	0.03	0.0	8.62
	b. 49.5	25.6	7.36	0.27	0.02	0.99	0.01	0.55	2.53	0.83	0.09	-	-	10.3
35- 70	a. 58.7	17.9	7.79	0.17	0.04	0.74	0.22	0.55	2.27	0.88	0.11	0.03	0.0	8.08
	b. 50.3	25.0	8.38	0.28	0.03	1.13	0.01	0.57	2.46	0.83	0.11	-	-	9.97
70-135	a. 62.5	18.0	6.06	0.15	0.07	0.78	0.25	0.59	2.15	0.88	0.04	0.01	0.0	7.28
	b. 50.2	24.8	7.88	0.13	0.03	1.25	0.01	0.63	2.50	0.83	0.08	-	-	10.6
135-185	a. 61.3	16.2	6.99	0.19	0.10	0.85	0.29	0.62	2.18	0.84	0.11	0.0	0.24	7.83
	b. 49.6	24.8	7.91	0.12	0.03	1.38	0.01	0.65	2.50	0.82	0.10	0.0	0.06	10.3
185-220	a. 59.6	15.3	4.73	0.42	0.20	1.11	0.71	0.75	2.02	0.79	0.08	0.0	1.65	9.63
	b. 49.7	24.6	7.27	0.18	0.03	1.59	0.01	0.57	2.48	0.84	0.15	0.0	0.02	10.3

Table 9.4

Bk-1 Normative mineralogical composition of the fraction < 2  $\mu\text{m}$  (weight %).

Depth (cm)	Q	P	Ru	Go	Ms	Kaol	Sm	Ab	Pyr	H <sub>2</sub> O <sup>+</sup>	rest
0- 4	8.8	0.3	0.8	7.9	21.9	30.5	19.9	4.6	0.0	2.6	
4- 35	8.7	0.2	0.8	8.1	21.4	30.8	20.2	4.7	0.0	2.3	
35- 70	9.1	0.3	0.8	9.2	20.8	28.2	22.8	4.8	0.0	2.0	
70-135	8.7	0.2	0.8	8.7	21.1	26.8	23.4	5.3	0.0	2.9	
135-185	7.1	0.3	0.8	8.6	21.1	25.5	25.6	5.5	0.1	2.6	
185-220	5.8	0.4	0.8	8.0	21.0	23.4	29.9	4.8	0.0	2.9	

Table 9.5

Bk-1 Peak area percentages of X-ray diffractograms of the fraction < 2  $\mu\text{m}$ , treated with Mg-glycerol.

depth (cm)	d-Value ( $\text{\AA}$ )				
	7	10	12	14	18
0- 4	25	11	3.5	2.5	58
4- 35	25	11	3.5	2.5	58
35- 70	24.5	11	3.5	2	59
70-135	23	8	5	1	63
135-185	25.5	10.5	4	4	56
185-220	27	13	5.5	3.5	51

## Profile 10

KR-1 Ongkharak Series - Sulfic Tropaquept

Described by N. van Breemen and P.L.G. Vlek, 1970-06-09

Location 5152 IV 1544.1 N, 667.7 E

Elevation  $\pm$  2 m

Paddy field, transplanted rice.

## Description from auger samples:

Ap 0- 25 cm very dark gray (10YR3/1) clay; few yellowish brown (10YR5/6) root rust; very slow permeability

B1g 25- 40 cm grayish brown to dark grayish brown (10YR5/2-4/2) clay; many yellowish brown (10YR5/6) mottles; common, fine, pale yellow (5Y8/3) jarosite; few dark yellowish brown (10YR3/6) mottles; very slow permeability

B21g 40- 70 cm grayish brown (10YR5/2) clay; many pale yellow (5Y8/3) jarosite; few yellowish red (5YR4/6) mottles; slow permeability

B22g 70-140 cm grayish brown (10YR5/2) clay; common pale yellow (5Y8/3) jarosite, decreasing with depth; few dark yellowish brown (10YR4/6) mottles, increasing with depth; moderate permeability

B23g 140-180 cm grayish brown (10YR5/2) clay; common yellowish brown (10YR4/6) mottles.

Cg 180 + cm dark gray (5Y4/1) clay, unmottled.

Table 10.1

KR-1 Particle-size distribution, pH, organic C,  $Fe_2O_3(d)$  and sulfur fractions.

Depth (cm)	Particle-size ( $\mu\text{m}$ )			pH	Org. C	$Fe_2O_3(d)$	Waters.	Jaros.	Pyrite
	> 50	50-2	< 2	fresh	(%)	(%)	$SO_4\text{-S}(\%)$	S(%)	S(%)
0- 20	1.0	38.8	60.3	3.9	1.5	1.5	0.03	0.09	-
20- 50	0.5	34.8	64.6	3.8	0.7	1.7	0.04	0.31	-
50- 80	0.4	30.7	69.0	3.7	0.6	4.2	0.04	1.41	-
80-110	0.2	33.2	66.6	3.4	0.7	2.5	0.05	0.58	-
110-140	0.3	38.2	61.5	3.3	0.4	2.9	0.06	0.54	0.002
140-170	0.2	39.7	60.1	3.3	1.2	0.7	0.08	0.29	0.27
170-200	0.1	37.2	62.7	-	1.5	0.6	0.11	0.03	1.12

Table 10.2

KR-1 Elemental composition (weight %); a: fraction < 2 mm; b: fraction < 2  $\mu\text{m}$ .

Depth (cm)		SiO <sub>2</sub>	Al <sub>2</sub> O <sub>3</sub>	Fe <sub>2</sub> O <sub>3</sub>	FeO	MnO	MgO	CaO	Na <sub>2</sub> O	K <sub>2</sub> O	TiO <sub>2</sub>	P <sub>2</sub> O <sub>5</sub>	SO <sub>3</sub>	FeS <sub>2</sub>	ign. loss
0- 20	a.	62.7	18.1	3.45	0.38	0.02	0.52	0.14	0.32	1.52	0.96	0.08	0.40	0.0	10.2
	b.	50.7	30.4	5.16	0.20	0.04	0.67	0.03	0.25	2.06	0.90	0.11	0.18	0.0	9.97
20- 50	a.	62.4	19.1	3.97	0.30	0.03	0.62	0.15	0.35	1.92	1.04	0.04	0.73	0.0	10.2
	b.	50.3	29.1	6.09	0.15	0.03	0.77	0.02	0.26	2.39	0.97	0.08	0.35	0.0	9.51
50- 80	a.	57.1	18.5	7.05	0.28	0.03	0.63	0.16	0.38	2.94	0.96	0.05	3.37	0.0	12.8
	b.	46.8	26.6	9.63	0.16	0.05	0.76	0.02	0.27	2.85	0.82	0.09	0.85	0.0	10.9
80-110	a.	61.4	18.9	5.29	0.18	0.03	0.66	0.15	0.37	1.99	0.98	0.04	1.47	0.0	10.5
	b.	50.7	27.3	6.79	0.14	0.04	0.82	0.02	0.24	2.43	0.86	0.08	0.50	0.0	9.44
110-140	a.	62.9	18.6	5.40	0.25	0.02	0.69	0.14	0.36	1.92	0.96	0.05	1.25	0.0	10.1
	b.	50.7	27.8	6.74	0.14	0.04	0.75	0.02	0.26	2.24	0.85	0.08	0.13	0.0	9.59
140-170	a.	64.3	18.0	2.95	0.26	0.04	0.66	0.11	0.37	1.69	0.95	0.05	0.60	0.32	9.42
	b.	51.0	28.6	5.79	0.14	0.04	0.85	0.02	0.25	2.17	0.82	0.09	0.0	0.07	9.23
170-200	a.	61.8	17.9	1.21	1.17	0.03	0.62	0.06	0.34	1.65	0.90	0.05	0.35	2.10	10.8
	b.	52.5	28.4	6.93	0.20	0.04	0.85	0.02	0.25	2.14	0.88	0.12	0.0	0.04	9.11

Table 10.3

KR-1 Normative mineralogical composition of the fraction < 2  $\mu\text{m}$  (weight %).

Depth (cm)	Q	P	Ru	Go	Ms	Kaol	Sm	Ab	Jar	Pyr	H <sub>2</sub> O <sup>+</sup> rest
0- 20	8.0	0.3	0.9	5.4	17.0	51.9	13.9	2.1	0.5	-	0.1
20- 50	8.7	0.2	1.0	6.2	19.4	45.4	15.1	2.1	1.2	-	0.1
50- 80	8.1	0.2	0.8	9.3	22.2	36.5	15.0	2.1	2.6	-	1.3
80-110	10.8	0.2	0.9	6.7	19.4	40.7	15.9	1.9	1.6	-	0.2
110-140	10.7	0.2	0.8	7.3	18.7	43.2	14.7	2.2	0.4	-	0.3
140-170	9.3	0.2	0.8	6.4	18.3	44.7	16.4	2.1	-	0.1	0.0
170-200	10.9	0.3	0.9	7.7	18.1	43.9	17.0	2.1	-	0.0	0.2

Table 10.4

KR-1 Peak area percentages of X-ray diffractograms of the fraction < 2  $\mu$ m, treated with Mg-glycerol.

Depth (cm)	d Value (Å)				
	7.1	10	12	14	18
0- 20	38	15	4.5	7	36
20- 50	42.5	15	3.5	4	36
50- 80	32	15	3	4	45.5
80-110	31	9	3.5	4	52
110-140	31	10	3	4	52
140-170	34	10	3	4.5	48
170-200	32	12.5	2	7.5	46

## Profile 11

Mn-1 Bang Nam Prieo Series - Sulfic Tropaquept

Described by N. van Breemen and P.L.G. Vlek, 1970-07-09

Location 5152 II 1527.6 N, 692.5 E

Elevation  $\pm$  2 m

Paddy field, transplanted rice

## Description from auger samples:

Ap 0- 30 cm very dark gray (10YR3/1) clay; few yellowish brown (10YR5/8) root rust; slow permeability

B21 30- 50 cm brown (10YR5/3) silty clay; common yellowish brown (10YR5/8) mottles; moderate permeability

B22 50- 70 cm brown (10YR5/3) silty clay; common yellowish brown (10YR5/8) and few yellow (2.5Y7/6) (jarosite ?) mottles; rapid permeability

B23g 70- 90 cm grayish brown (10YR5/2) clay; common brown to strong brown (7.5YR4/4-5/6) mottles; few fine yellow (2.5Y8/6) jarosite; very rapid permeability

B3g 90-120 cm grayish brown (10YR5/2) clay; few brown to strong brown (7.5YR4/4-5/6) mottles; very rapid permeability

Cg 120-250 cm + dark gray to dark greenish gray (5Y4/1 - 5GY4/1) clay; common dark greenish gray to grayish green (5GY4/1 - 5G4/2) mottles; many shells present between 210 and 220 cm.

Table 11.1

Mn-1 Particle-size distribution, pH, organic C,  $Fe_2O_3(d)$  and sulfur fractions

Depth (cm)	Particle-size ( $\mu\text{m}$ )			pH fresh	pH aerated	Org. C (%)	$Fe_2O_3(d)$ (%)	Waters. $SO_4\text{-S}(\%)$	Jaros. S(%)	Pyrite S(%)
	> 50	50-2	< 2							
0- 20	0.8	34.0	65.2	4.3	3.9	2.0	1.2	0.01	0.08	-
20- 50	0.3	45.7	54.0	4.0	3.8	1.2	1.0	0.03	0.10	-
50- 80	1.5	51.7	46.8	3.9	3.8	0.9	2.4	0.03	0.19	-
80-110	1.7	33.9	64.4	4.0	4.1	0.6	6.2	0.07	0.22	-
110-140				5.4	5.4			0.05	0.23	0.16
140-170	1.3	38.7	60.0	5.9	5.6	2.0	2.4	0.26	0.0	1.35
170-200				-	-			0.27	0.0	1.39
200-210	0.3	33.3	66.4	-	-	2.2	3.3	0.39	0.0	1.71
210-220	1.0	34.6	64.4	-	-	2.2	3.4	0.35	0.0	1.60

Table 11.2

Mn-1 Elemental composition (weight %); a: fraction < 2 mm; b: fraction < 2  $\mu\text{m}$ .

Depth (cm)	SiO <sub>2</sub>	Al <sub>2</sub> O <sub>3</sub>	Fe <sub>2</sub> O <sub>3</sub>	FeO	MnO	MgO	CaO	Na <sub>2</sub> O	K <sub>2</sub> O	TiO <sub>2</sub>	P <sub>2</sub> O <sub>5</sub>	SO <sub>3</sub>	FeS <sub>2</sub>	ign. loss
0- 20	a. 63.9	19.6	3.56	0.25	0.02	0.66	0.26	0.39	1.52	0.87	0.07	0.18	0.0	9.68
	b. 52.5	29.1	5.07	0.14	0.01	0.78	0.01	0.23	2.00	0.87	0.12	0.08	0.0	9.91
20- 50	a. 69.0	18.3	3.28	0.17	0.01	0.53	0.17	0.45	1.57	0.95	0.05	0.13	0.0	7.10
	b. 52.8	29.0	5.10	0.15	0.01	0.80	0.01	0.20	2.33	0.91	0.10	0.05	0.0	9.54
50- 80	a. 70.2	15.9	4.53	0.15	0.01	0.42	0.15	0.50	1.57	0.92	0.05	0.13	0.0	6.48
	b. 51.9	27.6	6.46	0.16	0.01	0.84	0.01	0.19	2.23	0.86	0.13	0.05	0.0	10.2
80-110	a. 57.5	18.6	9.48	0.22	0.02	1.01	0.22	0.46	1.88	0.84	0.09	0.23	0.0	8.30
	b. 50.0	24.8	10.4	0.21	0.02	0.91	0.00	0.18	2.33	0.77	0.14	0.05	0.0	10.0
110-170	a. 50.7	17.4	4.82	0.34	0.05	1.14	0.30	0.50	1.83	0.82	0.05	0.67	1.42	10.3
	b. 51.5	25.7	7.90	0.20	0.02	1.10	0.00	0.22	2.41	0.75	0.10	0.0	0.07	9.79
170-210	a. 55.6	16.4	4.17	0.47	0.17	2.11	0.47	0.55	1.88	0.78	0.08	0.82	3.13	12.3
	b. 49.9	23.8	9.74	0.24	0.04	1.67	0.01	0.29	2.41	0.84	0.14	0.0	0.56	10.3
210-220	a. 56.1	15.9	3.88	0.46	0.19	2.15	1.62	0.59	1.87	0.76	0.08	0.87	2.95	11.2 <sup>a</sup>
	b. 50.4	24.3	9.65	0.24	0.04	1.96	0.01	0.23	2.59	0.78	0.14	0.0	0.13	10.3

<sup>a</sup>including some  $CO_2$  (not determined)

Table 11.3

Mn-1 Normative mineralogical composition of the fraction < 2  $\mu\text{m}$  (weight %).

Depth (cm)	Q	P	Ru	Go	Ms	Kaol	Sm	Ab	Jar.	Pyr.	$\text{H}_2\text{O}^+$ rest
0- 20	10.9	0.3	0.9	5.5	16.7	48.2	15.2	1.9	0.2	-	0.5
20- 50	11.2	0.3	0.9	5.6	19.6	45.1	15.6	1.7	0.2	-	0.4
50- 80	11.7	0.3	0.9	7.1	18.8	41.7	16.4	1.6	0.2	-	1.2
80-110	12.4	0.4	0.8	11.5	19.6	33.1	18.2	1.5	0.2	-	1.2
110-170	11.3	0.3	0.8	8.7	20.4	32.7	21.4	1.9	-	0.1	1.4
170-210	7.3	0.4	0.8	11.0	20.4	21.9	31.9	2.4	-	0.6	2.5
210-220	5.2	0.4	0.8	10.6	21.9	19.2	37.0	1.9	-	0.1	2.5

Table 11.4

Mn-1 Peak area percentages of X-ray diffractograms of the fraction < 2  $\mu\text{m}$ , treated with Mg-glycerol, and cation exchange capacity of the clay fraction.

Depth (cm)	d-Value ( $\text{\AA}$ )					CEC (mmol/100g)
	7	10	12	14	18	
0- 20	34	14.5	3	11	36.5	41.6
20- 50	29	14	3	10	45	43.0
50- 80	27	12	1	4	56	44.0
80-110	18	8	1.5	0	74	45.6
110-170	21.5	9.5	1.5	2.5	65	46.4
170-210	22	9	2	3	64	47.2
210-220	20	7	3	1	69	48.0

## Profile 12

Na-2 Ayutthaya Series - Gypsiorthid

Described by N. van Breemen, 1969-05-14

Location 5052 II 1526.4 N, 618.9 E

Elevation 3-4 m

Paddy field  $\pm$  20 x 20  $\text{m}^2$ , surface 10 to 20 cm below that of the surrounding fields; transplanted rice

## Detailed profile description:

Ap1 0- 10 cm dark gray (N4/0) clay; common, fine to medium, distinct, sharp, brown (7.5YR4/4) rootrust; moderate to strong, medium to coarse angular blocky; firm; common, fine to medium pores; many fine (rice-)roots; very slow permeability; clear, smooth boundary

Ap2g 10- 44 cm 70% very dark gray (10YR3/1) clay; 30% dark grayish brown (2.5Y4.5/2) clay in pockets 10 to 20 cm across or in more or less horizontal strata; in the grayish brown matrix, common to many, medium, distinct, diffuse yellowish red (5YR4/6) and few, fine, distinct, clear yellowish brown (10YR5/8) mottles; common, fine, distinct,

sharp, strong brown (7.5YR5/6) rootrust in upper part; locally yellowish brown (10YR5/8) coatings on ped faces; strong, coarse prismatic; very firm to extremely firm; few fine to medium vertical pores; few fine roots; very slow permeability; clear, wavy boundary

A13gcs 44-70 cm 90% very dark gray (10YR3/1) and 10% dark grayish brown (2.5Y4.5/2) clay; common, medium, distinct, diffuse, red (2.5YR4/8) mottles; strong, coarse prismatic; very firm to extremely firm; few fine vertical pores; common (10-15% by volume) elongated (up to 5 mm long) gypsum; few fine roots; moderate to moderately rapid permeability; clear, wavy boundary

B1g 70- 90 cm 90% grayish brown (10YR5/2) clay with 10% very dark gray (10YR3/1) in pockets and along cracks; common, medium to coarse, distinct, diffuse red (2.5YR4/8) to dark brown (7.5YR4/4) mottles; few, medium to coarse, distinct, clear dark yellowish brown (10YR4/8) mottles; moderate, coarse prismatic; friable to firm; very few, fine pores; common (10-15% by volume) elongated gypsum; few, very fine roots; very slow permeability; gradual, smooth boundary.

II B21g 90-130 cm grayish brown (10YR5/2) silty clay; few, small pockets of very dark gray (10YR3/1) clay; many, coarse, prominent, clear to diffuse, red (2.5YR4/6) and clear yellowish brown (10YR5/8) mottles; few, medium, distinct, clear, yellow (2.5Y8/6) jarosite in lower part; few, fine, distinct, sharp yellowish brown (10YR5/8) rootrust; weak to moderate, coarse compound prismatic and moderate, coarse angular blocky; friable; very few fine vertical pores; few powdery gypsum; very few, very fine roots; very slow permeability; gradual, smooth boundary

II B22g 130-190 cm grayish brown (10YR5/2) silty clay; few light gray (10YR7/2) very fine sandy, horizontal layers; common, medium, prominent, clear, yellow (2.5Y8/6) jarosite as mottles and in root channels; common, medium, distinct, diffuse, yellowish brown (10YR5/6) mottles; few, fine, distinct, sharp, dark brown (7.5YR4/4) rootrust; few, thin, slightly hard, olive brown (2.5Y4/4), dark yellowish brown (10YR4/4) and dark brown (7.5YR4/4) coatings on ped faces; weak, coarse, compound prismatic and moderate coarse angular blocky; slightly sticky, plastic; slickensides on most vertical and on some horizontal ped faces; common, fine to medium, vertical pores; few medium pores cemented with iron oxide and filled with jarosite; very few, very fine roots

II B3g 190-230 cm (*described from auger samples*) gray (10YR5/1) silty clay; common coarse, olive brown (2.5Y4/4), yellowish brown (10YR5/8) and dark brown (7.5YR4/4) coatings on ped faces; few jarosite in the upper part of the horizon; slightly sticky, slightly plastic

II Cg 230-340 cm + gray (5Y4.5/1) silty clay, unmottled.

At the time of the description, the watertable was 190 cm below the surface. The soil surface was cracked in a polygonal (appr. 30 cm across) pattern; 2 cm wide cracks were visible down to 60 cm below the surface.

*Range of characteristics:*

An excavation along a ditchwall ca. 20 m south-west of the described pit exposed a very similar profile. A boring 4 km south (at 1522.3 N, 618.2 E) showed an A1 horizon 40 cm, underlain by gypsiferous, slightly calcareous clay without jarosite mottles, and a greenish gray reduced subsoil below 270 cm. A boring about 1 km south of Na-2 also showed the presence of gypsum and the absence of jarosite.

Table 12.1

Na-2 pH and soil moisture (weight %), on different sampling dates.

Depth (cm)	pH fresh			pH aerated 69-11-26	Moisture content			
	69-08-06	69-09-29	69-11-26		69-05-13	69-08-06	69-09-29	69-11-26
0- 20	5.5	5.9	5.6	5.8	12	39	42	37
20- 40	5.3	5.5	5.3	5.7	17	32	33	32
40- 60	4.5	5.1	4.8	4.6	20	33	30	29
60- 80	4.2	4.3	4.3	4.3	23	34	31	30
80-100	3.9	4.0	4.1	4.0	25	32	32	31
100-120	3.8	3.7	3.9	3.9	24	30	35	31
120-140	3.7	3.5	3.8	3.7	30	30	38	-
140-160	3.5	3.4	3.8	3.7	36	37	41	37
160-180	3.4	3.4	3.6	3.6	40	41	44	38
180-200	3.6	5.2	3.7	3.6	43	44	39	42
Height of the watertable (cm):					-190	+38	+70	+45

Table 12.2

Na-2 Particle-size distribution, organic C,  $Fe_2O_3(d)$ , sulfur fractions and N-value.

Depth (cm)	Particle-size ( $\mu m$ )			Org. C. (%)	$Fe_2O_3(d)$ (%)	N-value	Depth (cm)	Sulfur fractions		
	> 50	50-2	< 2					waters.	jarosite	pyrite
0- 20	2.3	30.7	67.1	1.8	2.0	0.43	0- 20	0.03	0.00	-
20- 40	3.2	26.4	70.5	1.0	2.7	0.35	20- 50	0.23	0.00	-
40- 70	3.7	31.2	65.2	0.7	2.2	0.35	50- 80	3.26	0.00	-
70- 90	2.2	36.8	61.1	0.4	2.1	0.39	80-110	1.53	0.01	-
90-130	1.9	41.4	56.7	0.4	1.9	0.40	110-140	0.25	0.41	-
130-190	1.2	40.1	58.7	0.3	1.4	0.53	140-170	0.07	0.60	0.002
190-230	1.7	43.1	55.2	1.1	1.8	0.56	170-200	0.07	0.08	0.002
230-260	0.8	45.5	53.7	1.4	1.0	-				

Table 12.3

Na-2 Elemental composition (weight %); a: fraction < 2 mm; b: fraction < 2  $\mu\text{m}$ .

Depth (cm)	SiO <sub>2</sub>	Al <sub>2</sub> O <sub>3</sub>	Fe <sub>2</sub> O <sub>3</sub>	FeO	MnO	MgO	CaO	Na <sub>2</sub> O	K <sub>2</sub> O	TiO <sub>2</sub>	P <sub>2</sub> O <sub>5</sub>	SO <sub>3</sub>	FeS <sub>2</sub>	ign. loss
0- 20	a. 59.1	20.3	4.59	0.40	0.02	0.94	0.55	0.37	2.58	0.80	0.09	0.08	0.0	9.76
	b. 50.5	27.3	6.29	0.22	0.01	0.92	0.00	0.15	3.06	0.76	0.15	-	-	9.22
20- 44	a. 55.8	22.2	5.73	0.28	0.04	1.05	0.54	0.40	3.00	0.79	0.09	0.33	0.0	8.86
	b. 48.8	27.7	6.09	0.26	0.02	1.05	0.00	0.13	3.36	0.76	0.14	0.05	0.0	9.51
44- 70	a. 56.6	20.0	4.95	0.18	0.01	0.91	2.19	0.39	2.42	0.77	0.07	3.10	0.0	8.20
	b. 49.3	28.2	5.41	0.25	0.01	0.86	0.00	0.16	2.96	0.78	0.11	0.05	0.0	9.78
70- 90	a. 58.2	17.8	4.48	0.13	0.01	0.85	3.38	0.42	2.17	0.83	0.06	4.58	0.0	9.45
	b. 50.1	28.1	5.43	0.22	0.01	0.90	0.00	0.15	2.64	0.85	0.09	0.05	0.0	10.2
90-130	a. 64.1	17.9	5.17	0.14	0.01	0.80	1.02	0.48	2.06	0.89	0.03	1.40	0.0	7.00
	b. 50.1	26.8	5.93	0.24	0.01	0.89	0.00	0.17	2.60	0.86	0.08	0.08	0.0	10.2
130-190	a. 64.9	18.4	4.79	0.09	0.01	0.80	0.28	0.48	2.15	0.90	0.02	0.53	0.0	7.17
	b. 50.3	26.7	5.68	0.22	0.01	0.92	0.00	0.16	2.62	0.87	0.07	0.18	0.0	10.4
190-230	a. 63.2	16.8	4.60	0.26	0.02	0.89	0.25	0.54	2.15	0.86	0.04	0.98	0.0	8.05
	b. 50.5	26.6	5.81	0.28	0.01	0.92	0.00	0.16	2.53	0.84	0.13	0.05	0.0	9.77
230-260	a. 66.7	16.4	1.82	0.78	0.19	0.65	0.25	0.56	2.14	0.84	0.03	0.0	2.08	8.99
	b. 51.3	26.7	6.26	0.21	0.02	1.26	0.00	0.16	2.68	0.88	0.16	0.0	0.04	9.21

Table 12.4

Na-2 Normative mineralogical composition of the fraction < 2  $\mu\text{m}$  (weight %).

Depth (cm)	Q	P	Ru	Go	Ms	Kaol	Sm	Ab	Jar	Pyr	H <sub>2</sub> O <sup>+</sup> rest
0- 20	9.9	0.4	0.8	6.8	25.9	33.4	18.5	1.3	0.0	-	0.9
20- 44	6.8	0.4	0.8	6.5	28.3	30.4	18.5	2.7	0.2	-	1.4
44- 70	8.1	0.3	0.8	5.8	25.0	36.7	17.7	1.4	0.2	-	1.3
70- 90	8.8	0.2	0.9	5.9	22.2	39.0	18.1	1.3	0.2	-	1.5
90-130	10.3	0.2	0.9	6.4	21.8	36.0	18.2	1.4	0.2	-	1.7
130-190	10.4	0.2	0.9	5.9	21.7	35.7	18.5	1.3	0.5	-	2.1
190-230	10.6	0.4	0.8	6.2	21.3	35.6	19.1	1.4	0.2	-	1.5
230-260	8.9	0.4	0.9	6.7	22.6	31.5	24.4	1.7	-	0.0	1.0

Table 12.5

Na-2 Peak area percentages of X-ray diffractograms of the fraction < 2  $\mu\text{m}$ , treated with Mg-glycerol, and CEC of the clay fraction.

Depth (cm)	d-Value (Å)					CEC (mmol/100g)
	7	10	12	14	18	
0- 20	22.5	10.5	5	2.5	60	39.6
20- 44	32.5	12.5	6	5	44	35.0
44- 70	31	15	4.5	6	42.5	36.8
70- 90	28	12.5	3	4	52.5	38.3
90-130	28	8	3.5	1	59.5	.
130-190	30.5	12	6	2.5	50	41.6
190-230	32	12	6	2	48	42.4
230-260	29	15	5	3.5	47.5	42.4

## Profile 13

0-1 Rangsit Series - Sulfic Tropaquept

Described by N. van Breemen and P.L.G. Vlek, 1970-06-05

Location 5153 II 1560.0 N, 712.7 E

Elevation  $\pm$  2 m

Paddy field, broadcasted rice

## Detailed profile description:

Ap 0- 30 cm black (10YR2/1) clay; common, fine, distinct, sharp, dark yellowish brown (10YR3/4) rootrust; common, medium, faint, diffuse, dark yellowish brown (10YR3/4) mottles on ped faces; common, medium, distinct, diffuse, yellowish brown (10YR5/6) mottles on ped faces (mainly in the lower part of the horizon); weak, coarse, and moderate, fine to medium, angular to sub-angular blocky; slightly sticky, plastic to slightly plastic; few, fine, mainly vertical, mainly impeded tubular pores; abundant fine roots, mainly along ped faces; very slow permeability; clear, wavy boundary

B21g 30- 60 cm grayish brown (10YR5/2) clay; many, coarse, prominent, clear, dark yellowish brown (10YR4/6) mottles; few, medium, distinct, clear yellowish brown (10YR5/6) mottles; weak, coarse, and moderate, fine, angular blocky; slightly sticky, slightly plastic; common, continuous slickensides; few to common, fine, vertical, impeded and expedited tubular pores; few fine to medium pores filled with black (10YR2/1) clay; very few roots, mainly in the upper part of the horizon; slow permeability; clear, wavy boundary

B22g 60- 85 cm grayish brown (10YR5/2) clay; mainly in the upper part of the horizon common, coarse, prominent, clear, red (10R4/6) mottles; common, medium to coarse, distinct, diffuse, yellowish red (5YR4/6) mottles, surrounded by medium to coarse, distinct, diffuse, yellowish brown (10YR5/6) mottles, both in the matrix, along pores and along ped faces; common, medium to coarse, prominent, sharp and clear, yellow (5Y8/6) jarosite, mainly as pore-fillings and surrounded by yellowish brown (10YR5/6) mottles; moderate, coarse and medium, angular blocky; slightly sticky, plastic; common, broken slickensides; few to common, fine to medium, continuous, vertical, mainly expedited, tubular pores; moderately slow to moderate permeability; no roots;

gradual, smooth boundary

B23g 85-115 cm grayish brown (10YR5/2) clay; few to common, medium to coarse, distinct, diffuse, yellowish red (5YR4/6) mottles and common, medium to coarse, distinct, diffuse, yellowish brown (10YR5/6) mottles along vertical pores; common, medium to coarse, distinct, sharp, yellow (5Y8/6) jarosite; weak, coarse prismatic; sticky, non-plastic; patchy slickensides; common, fine to coarse, continuous, vertical, impeded and exped, tubular pores; very few roots; moderate to moderately rapid permeability; gradual, smooth boundary

B24g 115-170 cm grayish brown (10YR5/2) clay; few, medium to coarse, distinct, diffuse, yellowish brown (10YR5/6) mottles, mainly along vertical pores; few, medium to coarse, distinct, sharp, yellow (5Y8/6) jarosite mottles; locally broken coatings of jarosite and yellowish brown (10YR5/6) rust on prism faces; common, distinct, hard, yellowish brown (10YR5/6) coatings (1-2 mm thick) along fine to medium, vertical pores, with a very thin dark yellowish brown (10YR3/4) coating inside; weak, coarse prismatic; sticky, non-plastic; common, fine to coarse, continuous, vertical, impeded and exped pores; very few roots; moderately rapid permeability; diffuse, smooth boundary

Cg 170 + cm gray (5Y5/1) clay, unmottled.

*Range of characteristics:*

A very similar profile was observed in a boring, about 20 m from the described profile. At location MC-8, about 600 m west, the Al is thicker (50 cm), and the red mottled horizon is thinner and deeper (90-110 cm).

Table 13.1

0-1 Particle-size distribution, organic C,  $Fe_2O_3(d)$ , sulfur fractions and pH.

Depth (cm)	Particle-size ( $\mu m$ )			Org.C.	$Fe_2O_3(d)$ (%)	Depth (cm)	Waters. $SO_4-S$ (%)	Jaros. S (%)	Pyrite S (%)	pH fresh
	> 50	50-2	< 2							
0- 30	0.4	36.3	63.3	1.2	1.2	0- 10	0.01	0.01	-	
30- 60	5.0	31.9	63.1	0.3	6.7	10- 20	0.02	0.02	-	4.1
60- 85	1.6	34.0	64.3	0.1	8.9	20- 35	0.04	0.04	-	3.7
85-115	1.3	34.7	64.0	0.0	5.4	35- 50	0.05	0.08	-	3.6
115-170	2.0	38.5	59.5	0.4	3.8	50- 65	0.05	0.05	-	3.5
170-200	0.3	37.3	62.5	1.9	0.8	65- 80	0.05	0.57	-	3.4
						80- 95	0.06	0.09	-	3.4
						95-110	0.07	0.10	-	3.4
						110-140	0.08	0.15	-	3.4
						140-170	0.08	0.02	0.14	3.6
						170-200	0.11	0.04	1.27	3.8
						200-220	0.11	0.01	1.58	4.5

Table 13.2

0-1 Saturation moisture content, N value and bulk density.

Depth (cm)	Moisture (weight %)	N value	Bulk density (g/cm <sup>3</sup> )
15	39	0.45	1.32
40	41	0.52	1.50
70	66	0.91	1.00
105	83	1.19	0.84
140	88	1.31	0.82

Table 13.3

0-1 Elemental composition (weight %); a: fraction < 2 mm; b: fraction < 2  $\mu$ m.

Depth (cm)	SiO <sub>2</sub>	Al <sub>2</sub> O <sub>3</sub>	Fe <sub>2</sub> O <sub>3</sub>	FeO	MnO	MgO	CaO	Na <sub>2</sub> O	K <sub>2</sub> O	TiO <sub>2</sub>	P <sub>2</sub> O <sub>5</sub>	SO <sub>3</sub>	FeS <sub>2</sub>	ign. loss
0- 30	a. 64.2	19.7	3.28	0.26	0.04	0.63	0.19	0.33	1.43	0.97	0.05	0.20	0.0	9.52
	b. 50.9	29.9	4.89	0.30	0.03	0.76	0.02	0.21	1.84	0.92	0.12	-	-	9.80
30- 60	a. 57.4	18.7	10.4	0.10	0.07	0.74	0.11	0.40	1.78	0.94	0.03	0.45	0.0	8.52
	b. 51.6	28.2	7.19	0.29	0.04	0.88	0.02	0.21	2.18	0.96	0.05	0.20	0.0	9.00
60- 85	a. 56.2	16.9	11.0	0.11	0.06	0.75	0.12	0.49	2.49	0.90	0.03	3.13	0.0	11.4
	b. 45.5	23.5	12.4	0.28	0.04	0.82	0.02	0.29	2.83	0.84	0.09	2.17	0.0	11.8
85-115	a. 59.2	17.9	7.63	0.07	0.05	0.88	0.12	0.49	2.13	0.93	0.03	1.93	0.0	9.41
	b. 51.5	25.9	8.05	0.26	0.04	0.89	0.02	0.23	2.45	0.92	0.08	1.07	0.0	9.97
115-170	a. 64.4	17.9	5.92	0.12	0.04	0.85	0.14	0.56	1.78	0.97	0.05	0.95	0.0	8.39
	b. 51.4	27.2	6.49	0.17	0.03	0.98	0.02	0.21	2.31	0.93	0.09	0.53	0.0	9.58
170-200	a. 61.9	18.3	1.72	0.41	0.04	0.97	0.17	0.55	1.56	0.92	0.05	0.0	2.54	11.8
	b. 52.4	27.4	5.97	0.17	0.04	1.09	0.02	0.21	2.18	0.92	0.11	0.0	0.09	9.02

Table 13.4

0-1 Normative mineralogical composition of the fraction < 2  $\mu$ m (weight %).

Depth (cm)	Q	P	Ru	Go	Ms	Kaol	Sm	Ab	Jar	Pyr	H <sub>2</sub> O <sup>+</sup> rest
0- 30	8.0	0.3	0.9	5.3	15.6	50.6	16.5	1.8	0.0	0.0	0.0
30- 60	9.8	0.1	1.0	7.6	18.0	49.2	18.5	1.8	0.6	0.0	-0.7
60- 85	9.6	0.2	0.8	9.9	18.9	30.6	16.3	2.1	7.1	0.0	1.0
85-115	12.4	0.2	0.9	7.1	18.4	37.0	18.4	1.8	3.4	0.0	0.5
115-170	10.6	0.2	0.9	6.3	18.4	39.8	19.0	1.7	1.6	0.0	0.4
170-200	10.4	0.3	0.9	6.8	18.4	39.2	21.0	1.8	0.0	0.1	0.2

Table 13.5

0-1 Peak area percentages of X-ray diffractograms of the fraction < 2  $\mu\text{m}$ , treated with Mg-glycerol.

Depth (cm)	d Value (Å)				
	7	10	12	14	18
0- 30	39	13	6	8.5	34.5
30- 60	38	11.5	3.5	4	46
60- 85	26	13.5	4	4	53
85-115	27	13.5	4	2	51.5
115-170	28	13	3.5	0	55.5
170-200	25.5	9.5	3	0	62

Table 13.6

0-1 Qualitative mineralogical studies (Guinier X-ray photographs).

Depth (cm)	Material	Minerals indentified (except quarz and clay minerals)
60- 85	red mottled soil	jarosite, hematite (broad lines)
60- 85	brown mottled soil	jarosite, goethite (broad lines)
60- 85	yellow mottled soil	jarosite
100-150	yellow mottled soil	jarosite

#### Profile 14

Ra-1 Rangsit Series ~ Sulfic Tropaquept

Described by N. van Breemen, 1969-03-24

Location 5153 II 1551.9 N, 690.6 E, 550 m north of Khlong Rangsit

Elevation ca 2 m

Paddy field, broadcasted rice.

#### Detailed profile description:

Ap 0- 25 cm very dark gray to black (10YR2/1-3/1) clay; few fine, distinct, yellowish brown (10YR5/8) rootrust; moderate, medium angular blocky; friable to firm; common roots in the upper 10 cm; very slow permeability; clear, irregular boundary

Big 25- 38 cm grayish brown (10YR5/2) clay; common, fine, distinct, yellowish brown (10YR5/8) rootrust, sometimes as hard pipes; few, medium, prominent, red (7.5R4/6-5/6) mottles; common, irregularly distributed, black (10YR2/1) clay in pockets and rootholes; moderate, medium, angular blocky; firm; broken, common thin organic matter cutans on 50% of the ped faces; slow permeability; gradual, wavy boundary

B21g 38- 58 cm light brownish gray (10YR6/2) clay; many, coarse, prominent, diffuse, weak red to dusky red (7.5R4/4-3/4) mottles (mainly in the matrix but sometimes on ped faces); many medium, distinct, yellowish brown (10YR5/8) rootrust diffusing into the matrix and dark brown (10YR3/3) coatings along the rootholes; few, medium, distinct, diffuse, yellowish brown (10YR5/8) mottles; weak, coarse, compound prismatic, and

moderate coarse, angular blocky; firm; thin, broken organic matter cutans on 50% of the vertical ped faces; slow permeability; gradual, wavy boundary

B22g 58-130 cm grayish brown (2.5Y5/2) clay; many coarse, prominent, diffuse, yellowish brown (10YR5/8) mottles, mostly associated with big rootholes ( $d$  1-5 mm) and, mainly in the lower part of the horizon, occurring as coatings on vertical ped faces, mixed with dark brown (10YR3/3) coatings; common to many, yellow (2.5Y8/6) jarosite, filling up rootholes ( $d$  4-6 mm), mainly between 80 and 110 cm; locally few, medium, distinct, diffuse, dusky red (7.5R3/4) mottles down to 90 cm; weak, coarse, compound prismatic, moderate, coarse angular blocky; sticky, slightly plastic; continuous slickensides and, down to 100 cm, thin broken organic matter cutans on vertical ped faces; moderate to moderately rapid permeability; clear, smooth boundary

B3g 130-140 cm grayish brown (2.5Y5/1) clay; few, dark yellowish brown (10YR4/3) root rust; structureless, massive; sticky, slightly plastic; moderate permeability; clear, smooth boundary

Cg 140 + cm dark gray to gray (N4.5/0) clay, occasionally showing a grayish brown (2.5Y5/2) zone, 5 mm thick, around rootholes.

*Range of characteristics:*

The area has a distinct microrelief, which is closely correlated with profile morphology; cf. Ra-2 and Ra-3, and Figure 11.

Table 14.1

Ra-1 pH and soil moisture (weight %) on different sampling dates in 1969.

Depth (cm)	pH fresh			pH aerated 09-24	Moisture content					
	07-01	07-30	09-24		04-17	05-01	06-04	07-01	07-30	09-24
0- 20	4.2	4.1	4.4	4.2	19	19	21	37	36	39
20- 40	3.9	3.8	3.8	4.0	26	29	27	37	33	36
40- 60	3.6	3.6	3.4	3.7	39	36	39	40	41	41
60- 80	3.5	3.6	3.4	3.6	51	41	48	54	49	52
80-100	3.7	3.7	3.5	3.6	65	55	47	50	60	64
100-120	3.7	3.7	3.4	3.5	60	63	65	65	65	70
120-140	3.7	3.6	3.5	3.6	71	69	74	74	76	77
140-160	3.9	3.5	3.7	2.6	82	73	75	82	81	81
160-180	4.2	3.5	4.5	2.9	81	82	77	77	80	84
180-200	5.0	3.5	5.4	3.4	83	83	86	86	83	77
Height of the watertable (cm):					-109	-111	-102	-10	0	+40

Table 14.2

Ra-1 Particle-size distribution, organic C,  $Fe_2O_3$ (d) and sulfur fractions.

Depth (cm)	Particle-size ( $\mu\text{m}$ )			Org.C. (%)	$Fe_2O_3$ (d) (%)	Depth (cm)	Waters. $SO_4$ -S(%)	Jaros. $SO_4$ -S(%)	Pyrite S(%)
	> 50	50-2	< 2						
0- 25	1.7	38.7	59.6	1.6	0.6	0- 20	0.03	0.005	-
25- 38	3.5	33.2	63.3	0.7	2.7	20- 50	0.04	0.003	-
38- 58	4.4	32.8	62.8	0.5	6.6	50- 80	0.05	0.22	-
58-130	2.3	35.6	62.0	0.4	6.8	80-110	0.06	0.44	-
130-140	0.1	36.7	63.2	0.8	0.5	110-140	0.06	0.20	0.06
150-200	0.2	37.8	62.0	1.5	1.8	140-170	0.11	0.06	0.83
						170-200	0.07	0.03	1.08

Table 14.3

Ra-1 Saturation moisture content, N-value and bulk density.

Depth (cm)	Moisture (weight %)	N-value	Bulk density
			( $\text{g}/\text{cm}^3$ )
20	36	0.42	1.36
40	39	0.49	1.34
65	52	0.70	1.17
85	64	0.88	1.02
110	72	1.01	0.97
125	73	0.98	0.90
150-200	80	1.03	-

Table 14.4

Ra-1 Elemental composition (weight %); a: fraction < 2 mm; b: fraction < 2  $\mu\text{m}$ .

Depth (cm)	Elemental composition (weight %)													
	$SiO_2$	$Al_2O_3$	$Fe_2O_3$	FeO	MnO	MgO	CaO	$Na_2O$	$K_2O$	$TiO_2$	$P_2O_5$	$SO_3$	$FeS_2$	ign. loss
0- 25	a. 67.5	19.1	2.35	0.40	0.01	0.44	0.22	0.35	1.30	1.01	0.05	0.15	0.0	9.38
	b. 51.1	28.2	4.13	0.20	0.01	0.76	0.00	0.23	2.07	0.98	0.10	-	-	10.4
25- 38	a. 62.8	20.3	5.03	0.16	0.01	0.53	0.17	0.35	1.78	1.03	0.02	0.18	0.0	8.49
	b. 49.6	27.6	4.84	0.17	0.01	0.81	0.00	0.22	2.33	0.96	0.12	0.03	0.0	9.67
38- 58	a. 59.4	19.3	7.62	0.18	0.01	0.59	0.18	0.38	1.96	0.96	0.03	0.48	0.0	8.43
	b. 49.2	26.9	7.11	0.14	0.01	0.87	0.00	0.22	2.45	0.90	0.14	0.38	0.0	9.79
58-130	a. 59.2	18.2	7.67	0.27	0.01	0.61	0.16	0.46	2.20	0.92	0.02	1.80	0.0	9.56
	b. 48.5	24.9	8.18	0.15	0.01	0.86	0.00	0.25	2.55	0.85	0.14	1.33	0.0	11.8
130-140	a. 64.5	19.9	3.00	0.29	0.01	0.65	0.17	0.47	1.80	0.95	0.02	0.48	0.0	8.24
	b. 51.8	27.6	4.71	0.17	0.01	0.97	0.00	0.22	2.35	0.89	0.09	0.03	0.0	9.42
150-200	a. 61.4	18.3	2.67	0.50	0.12	0.89	0.27	0.50	1.87	0.88	0.04	0.0	2.21	9.79
	b. 50.2	25.8	6.60	0.18	0.02	1.09	0.00	0.25	2.36	0.86	0.21	0.0	0.38	9.95

Table 14.5

Ra-1 Normative mineralogical composition of the fraction < 2  $\mu\text{m}$  (weight %).

Depth (cm)	Q	P	Ru	Go	Ms	Kaol	Sm	Ab	Jar	Pyr	$\text{H}_2\text{O}^+$ rest
0- 25	10.4	0.3	1.0	4.5	17.5	45.1	15.5	1.9	-	-	1.5
25- 38	9.5	0.3	1.0	5.2	19.6	41.2	16.0	1.9	0.1	0.0	1.1
38- 58	9.6	0.4	0.9	7.1	19.9	38.8	16.8	1.8	1.2	0.0	0.8
58-130	11.3	0.4	0.9	6.7	18.6	34.9	16.7	1.9	4.1	0.0	2.4
130-140	10.5	0.2	0.9	5.1	19.8	39.3	18.8	1.9	0.1	0.0	1.0
150-200	9.9	0.6	0.9	7.3	20.0	33.4	21.1	2.1	0.0	0.1	1.6

Table 14.6

Ra-1 Peak area percentages of X-ray diffractograms of the fraction < 2  $\mu\text{m}$ , treated with Mg-glycerol, and cation-exchange capacity of the clay fraction.

Depth (cm)	d Value ( $\text{\AA}$ )					CEC (mmol/100g)
	7	10	12	14	18	
0- 25	35	8	0	17	40	-
25- 38	29.5	7	4.5	5	53	41.4
38- 58	21	7.5	2	0	69.5	41.8
58-130	24	6.5	3	0	66	-
130-140	24	6.5	1.5	0	67	-
150-200	27	5	2.5	0	64.5	-

Table 14.7

Ra-1 Qualitative mineralogical studies (Quintier X-ray photographs).

Depth (cm)	Material	Minerals identified
40	red mottled soil	goethite (broad lines), quartz, clay minerals
80	brown mottled soil along a channel	goethite (broad lines), quartz, clay minerals
90-125	yellow earthy fillings of channels.	jarosite, quartz, clay minerals

Profile 15

Ra-2 Thanyaburi Series - Sulfic Tropaquept

Described by N. van Breemen, 1969-03-24

Location 5153 II 1552.0 N, 690.6 E (95 m north of Ra-1)

Elevation  $\pm$  2 m; 10 cm lower than Ra-1

Paddy field, broadcast rice

*Detailed profile description:*

Ap 0-35 cm very dark gray (moist) to dark gray (dry) (10YR3/1-4/1) clay; mainly in the upper part of the horizon few, medium, distinct, clear yellowish brown (10YR5/6) rootrust, sometimes showing a glossy surface; moderate, medium, angular blocky; firm; many rice roots; moderately slow permeability; gradual, broken boundary

A12g 35-48 cm very dark gray (10YR3/1) clay; many, medium, prominent, clear yellowish brown (10YR5/6) mottles and rootrust, mottling locally absent over the whole depth of the horizon; strong coarse, angular blocky; very firm; moderate permeability; clear, irregular boundary

B21g 48-100 cm grayish brown (2.5Y5/2) clay; many, coarse, prominent, clear, yellowish brown (10YR5/6) rootrust and mottles surrounding channels; common, pale yellow (5Y8/4) jarosite, filling up rootholes ( $\varnothing$  3-7 mm) and coated with ferric oxides; thin, patchy, dark yellowish brown (10YR4/4) coatings on ped faces; very dark gray (10YR3/1) clay along rootholes and cracks; weak, coarse, compound prismatic and medium angular, blocky; slightly sticky, slightly plastic; moderately rapid to rapid permeability; clear, wavy boundary

B22g 100-130 cm grayish brown (2.5Y5/2) clay; brown (7.5YR4/4) coatings along rootholes ( $\varnothing$  2-10 mm); in the upper part of the horizon few jarosite and very dark gray clay in rootholes; no mottles around rootholes; weak, coarse, compound prismatic and moderate medium angular blocky; sticky, plastic; rapid permeability; diffuse, smooth boundary

Cg 130 + cm dark gray (5Y4/1) clay; grayish brown (2.5Y5/2) zone around the rootholes; weak, coarse, angular blocky; moderately rapid permeability.

*Range of characteristics:*

See profile description of Ra-1 and Ra-3, and figs. 11, 13 and 14.

Table 15.1

Ra-2 pH and soil moisture (weight %) on different sampling dates in 1969.

Depth (cm)	pH fresh			pH aerated 09-24	Moisture content					
	07-01	07-30	09-24		04-17	05-01	06-04	07-01	07-30	09-24
0- 20	4.1	4.0	4.3	4.4	21	22	21	43	35	42
20- 40	3.8	3.7	3.9	4.0	31	27	30	31	35	37
40- 60	3.6	3.7	3.7	3.8	40	35	36	38	39	40
60- 80	3.5	3.5	3.5	3.7	51	45	51	48	51	50
80-100	3.5	3.5	3.5	3.7	57	60	59	61	61	62
100-120	3.5	3.6	3.4	3.7	70	68	65	61	74	69
120-140	3.6	3.7	3.6	3.7	77	76	68	66	79	72
140-160	3.8	3.9	3.6	2.7	78	76	73	70	81	77
160-180	4.0	4.1	3.9	2.6	85	81	77	83	88	82
180-200	4.2	5.1	4.0	2.9	85	86	82	78	82	85
Height of the watertable (cm):					-87	-87	-65	+7	+12	+52

Table 15.2

Ra-2 Particle-size distribution, organic C,  $Fe_2O_3(d)$  and sulfur fractions.

Depth (cm)	Particle-size ( $\mu m$ )			Org.C. (%)	$Fe_2O_3(d)$ (%)	Depth (cm)	Waters. $SO_4-S$ (%)	Jaros. $SO_4-S$ (%)	Pyrite S(%)
	> 50	50-2	< 2						
0- 35	1.3	39.3	59.4	1.8	0.6	0- 20	0.03	0.02	-
35- 48	5.7	34.6	59.7	0.7	4.6	20- 50	0.05	0.15	-
48-100	3.1	37.3	59.7	0.4	5.0	50- 80	0.05	0.58	-
100-130	0.2	36.7	63.1	0.6	0.6	80-110	0.05	0.29	-
160-180	0.3	36.9	62.9	1.4	0.7	110-140	0.06	0.04	0.23
195-210	0.1	35.9	63.9	-	0.9	140-170	0.13	0.04	1.66
						170-200	0.06	0.03	1.97

Table 15.3

Ra-2 Saturation moisture content, N-value and bulk density.

Depth (cm)	Moisture (weight %)	N value	Bulk density ( $g/cm^3$ )
20	36	0.42	1.36
40	39	0.49	1.34
65	52	0.70	1.17
85	64	0.88	1.02
110	72	1.01	0.97
125	73	0.98	0.90
150-200	80	1.03	-

Table 15.4

Ra-2 Elemental composition (weight %); a: fraction < 2 mm; b: fraction < 2  $\mu\text{m}$ .

Depth (cm)	SiO <sub>2</sub>	Al <sub>2</sub> O <sub>3</sub>	Fe <sub>2</sub> O <sub>3</sub>	FeO	MnO	MgO	CaO	Na <sub>2</sub> O	K <sub>2</sub> O	TiO <sub>2</sub>	P <sub>2</sub> O <sub>5</sub>	SO <sub>3</sub>	FeS <sub>2</sub>	ign. loss
0- 35	a. 64.6	18.7	2.60	0.39	0.01	0.56	0.19	0.30	1.51	0.99	0.04	0.15	0.0	9.89
	b. 51.8	24.5	3.87	0.27	0.01	0.61	0.00	0.20	1.99	1.01	0.09	-	-	9.87
35- 48	a. 60.2	19.0	6.87	0.29	0.01	0.65	0.15	0.32	1.74	0.96	0.03	0.28	0.0	8.87
	b. 50.7	28.1	5.95	0.19	0.01	0.63	0.00	0.18	2.10	1.00	0.08	0.18	0.0	9.80
48-100	a. 61.6	17.8	7.13	0.18	0.01	0.70	0.14	0.39	1.98	0.93	0.02	0.83	0.0	8.15
	b. 50.5	26.6	7.37	0.14	0.01	0.67	0.00	0.20	2.35	0.96	0.08	0.78	0.0	10.3
100-130	a. 65.0	20.1	3.31	0.16	0.01	0.77	0.15	0.38	1.77	1.01	0.01	0.10	0.0	7.38
	b. 52.7	28.4	4.69	0.13	0.01	0.83	0.00	0.18	2.10	0.94	0.04	.	.	9.62
160-180	a. 59.6	18.4	1.57	0.51	0.02	0.87	0.18	0.40	1.73	0.87	0.03	0.0	2.82	10.4
	b. 50.7	27.5	5.82	0.19	0.01	0.95	0.00	0.18	2.12	0.89	0.08	0.0	0.09	9.57
195-210	a. 63.0	17.6	3.37	0.40	0.03	0.44	0.07	0.39	1.67	0.90	0.05	0.0	2.80	12.6
	b. 52.5	27.8	4.85	0.27	0.01	0.96	0.00	0.20	2.29	0.91	0.03	0.0	.	10.8

Table 15.5

Ra-2 Normative mineralogical composition of the fraction < 2  $\mu\text{m}$  (weight %).

Depth (cm)	Q	P	Ru	Go	Ms	Kaol	Sm	Ab	Jar	Pyr	H <sub>2</sub> O <sup>†</sup> rest
0- 35	10.6	0.2	1.0	4.1	16.8	50.1	13.5	1.7	0.0	0.0	0.5
35- 48	11.4	0.2	1.0	6.5	17.3	46.4	13.1	1.5	0.9	0.0	0.3
48-100	12.8	0.2	1.0	6.8	18.2	41.7	13.3	1.6	2.4	0.0	0.8
100-130	11.7	0.1	0.9	5.2	17.8	45.3	16.0	1.5	0.0	0.0	0.6
160-180	9.7	0.5	0.9	6.6	17.9	41.3	18.7	1.5	0.0	0.1	0.7

Table 15.6

Ra-2 Peak area percentages of X-ray diffractograms of the fraction < 2  $\mu\text{m}$ , treated with Mg-glycerol, and cation-exchange capacity of the clay fraction.

Depth (cm)	d Value ( $\text{\AA}$ )					CEC mmol/100 g
	7	10	12	14	18	
0- 35	40	9	2.5	10	36	37.6
35- 48	31	7.5	2.5	3.5	55.5	40.0
48-100	30	7	2	0	61	43.0
100-130	31	7	2	0	60.5	39.2
160-180	26	9	0	11	54	.

Table 15.7

## Ra-2 Qualitative mineralogical studies (Guinier X-ray photographs).

A white efflorescence on a near-by ditch wall (30 cm below the soil surface) contained gypsum, quartz, albite and traces of halotrichite.

## Profile 16

Ra-3 Thanyaburi Series - Typic Sulfaquept

Described by N. van Breemen, 1969-03-24

Location 5153 II 1552.1 N, 690.6 E (170 m north of Ra-1)

Elevation  $\pm$  1.5 m; 40 cm lower than Ra-1

Paddy field, broadcasted rice.

## Detailed profile description:

Ap	0- 20 cm dark gray (dry) to black (moist) (10YR4/1-2/1) clay; no mottles or rootrust; coarse, angular blocky; very firm to extremely firm; common, coarse vesicular pores (gasbubble structure); very few roots; slow permeability; clear, smooth boundary
A12	30- 45 cm black (10YR2/1) silty clay; common, thin, broken, dark brown (7.5YR3/2) glossy coatings on ped faces; few rootrust; moderate, coarse, angular blocky; firm; few roots; slow permeability; clear, wavy boundary
A13	45- 80 cm very dark gray (10YR3/2) silty clay loam; common, thin (1mm across), hard, dark brown (7.5YR3/2) coatings on ped faces; often with a pale yellow (5Y8/4) jarosite layer sandwiched in between; moderate to strong, coarse prismatic; non-sticky, plastic; no roots; moderately slow permeability; clear, irregular boundary
B2g	80-100 cm grayish brown (2.5Y5/2) clay; dark brown coatings on ped faces as in horizon above, but no jarosite; distinct, dark reddish brown (5YR3/4) rootrust as strongly indurated pipes ( $\varnothing$ 1-15 mm) surrounded by medium, distinct, clear, yellowish brown (10YR5/6) mottles; moderate, coarse prismatic; sticky, non-plastic; moderate permeability; diffuse, smooth boundary
C1g	100-140 cm gray (5Y5/1) silty clay; few vertical cracks with dark brown (7.5YR3/2) coatings, decreasing with depth; a grayish brown (2.5Y5/2) zone, about 1 cm thick, occurs on both sides of cracks and around vertical channels; few, distinct, dark reddish brown (5YR3/4) cemented root-pipes; weak, coarse prismatic to structureless, massive; slow to moderately slow permeability; very sticky, non-plastic
C2g	140 cm + gray (5Y5/1) clay, unmottled; (down to 160 cm:) very slow permeability.

## Range of characteristics:

See the profile descriptions of Ra-1 and Ra-2, and Fig.

Table 16.1

Ra-3 pH and soil moisture (weight %) on different sampling dates in 1969

Depth (cm)	pH fresh				pH aerated 09-24	Moisture content					
	07-01	07-30	09-24	09-24		04-17	05-01	06-04	07-01	07-30	09-24
0- 20	3.8	3.9	3.7	3.7		28	35	40	44	42	43
20- 40	3.4	3.7	3.6	3.6		31	27	31	35	32	43
40- 60	3.4	3.4	3.5	3.8		31	32	41	50	35	34
60- 80	3.5	3.4	3.6	3.4		38	38	55	54	46	45
80-100	3.4	3.3	3.4	3.9 ?		50	60	71	64	68	48
100-120	3.4	3.3	3.5	3.4		65	75	83	70	76	57
120-140	3.3	3.2	3.5	3.3		72	74	84	77	83	73
140-160	3.3	3.2	3.4	3.2		81	84	86	79	89	77
160-180	3.9	3.4	3.5	2.7		71	85	86	83	92	87
180-200	4.1	3.6	3.6	2.6		84	87	85	87	89	86
Height of the watertable (cm):						-92	-102	-12	+35	+40	+80

Table 16.2

Ra-3 Particle-size distribution, organic C,  $Fe_2O_3$  (d), sulfur fractions and N-value.

Depth (cm)	Particle-size ( $\mu m$ )			Org.C.	$Fe_2O_3$ (d) (%)	Depth (cm)	Waters. $SO_4$ -S(%)	Jaros. $SO_4$ -S(%)	Pyrite S(%)	N-value
	> 50	50-2	< 2							
0- 20	0.2	38.5	61.2	2.4	0.7	0- 20	0.03	0.02	-	0.49
20- 45	0.7	46.7	52.7	3.1	0.7	20- 50	0.04	0.06	-	0.42
45- 80	1.7	58.5	39.8	1.2	1.3	50- 80	0.05	0.05	-	0.75
80-100	1.7	37.4	60.9	1.8	3.6	80-110	0.06	0.06	0.04	0.84
100-140	0.5	41.8	57.8	1.5	1.4	110-140	0.08	0.05	0.32	1.05

Table 16.3

Ra-3 Elemental composition (weight %); a: fraction < 2 mm; b: fraction < 2  $\mu m$ .

Depth (cm)	SiO <sub>2</sub>	Al <sub>2</sub> O <sub>3</sub>	Fe <sub>2</sub> O <sub>3</sub>	FeO	MnO	MgO	CaO	Na <sub>2</sub> O	K <sub>2</sub> O	TiO <sub>2</sub>	P <sub>2</sub> O <sub>5</sub>	SO <sub>3</sub>	FeS <sub>2</sub>	ign. loss
0- 20	a. 62.6	17.7	2.39	0.37	0.01	0.34	0.23	0.33	1.41	0.96	0.08	0.35	0.0	12.9
	b. 53.0	27.0	3.46	0.18	0.01	0.73	0.02	0.45	1.96	0.96	0.12	-	-	10.8
20- 45	a. 63.6	15.9	2.09	0.34	0.01	0.29	0.16	0.31	1.28	0.92	0.12	0.48	0.0	14.2
	b. 53.1	26.7	3.49	0.21	0.01	0.75	0.02	0.54	1.91	0.98	0.15	-	-	11.1
45- 80	a. 72.3	13.9	2.69	0.19	0.01	0.28	0.12	0.41	1.47	0.98	0.06	0.48	0.0	8.12
	b. 51.7	26.5	4.92	0.23	0.01	0.84	0.01	0.57	2.14	0.97	0.15	0.10	0.0	10.6
80-100	a. 61.5	18.3	6.15	0.22	0.02	0.53	0.17	0.40	1.83	0.95	0.07	0.88	0.0	9.48
	b. 51.2	25.8	5.88	0.23	0.01	1.01	0.01	0.77	2.18	0.91	0.07	0.10	0.0	10.7
100-140	a. 62.3	17.9	1.81	0.28	0.03	0.60	0.24	0.39	1.72	0.93	0.02	0.0	1.91	10.3
	b. 51.9	26.2	5.33	0.28	0.01	1.00	0.01	0.53	2.28	0.91	0.07	0.0	0.21	10.3

Table 16.4

Ra-3 Normative mineralogical composition of the fraction < 2  $\mu\text{m}$  (weight %).

Depth (cm)	Q	P	Ru	Go	Ms	Kaol	Sm	Ab	Jar	Pyr	$\text{H}_2\text{O}^+$ rest
0- 20	13.3	0.3	1.0	3.8	16.6	42.3	14.7	3.8	0.0	0.0	2.6
20- 45	13.0	0.4	1.0	3.9	16.1	41.3	15.4	4.6	0.0	0.0	3.0
45- 80	11.0	0.4	1.0	5.3	17.8	38.1	17.2	4.8	0.3	0.0	2.4
80-100	9.3	0.2	0.9	6.4	18.2	33.5	20.2	6.5	0.3	0.0	2.9
100-140	10.3	0.2	0.9	5.9	19.3	34.5	20.5	4.5	0.0	0.2	2.4

Table 16.5

Ra-3 Peak area percentages of X-ray diffractograms of the fraction < 2  $\mu\text{m}$ , treated with Mg-glycerol.

Depth (cm)	d-Value ( $\text{\AA}$ )				
	7	10	12	14	18
0- 20	28	7	2	4.5	59
20- 45	29.5	10	4	5	54
45- 80	33	7	9	2	54
80-100	26.5	10	2	0	61
100-140	24	8	3	0	65

Table 16.6

Ra-3 Qualitative mineralogical studies (Guinier X-ray photographs).

Depth (cm)	Material	Minerals indentified
90-130	white efflorescence, developed on reduced soil exposed to the air for 18 days in March 1969	gypsum, quartz, albite and halotrichite or pickeringite
65	yellow coatings associated with rust on ped faces	quartz, jarosite, albite

Profiles 17 and 18.

Ra-1½ and Ra-2½

The profiles are situated between Ra-1 and Ra-2, and Ra-2 and Ra-3, respectively.

No profile descriptions are available. The following tables give analytical data on the sulfur fractions of these profiles.

---

Table 17.1

Ra-1½ Sulfur fractions.

Depth (cm)	Waters. SO <sub>4</sub> -S(%)	Jarosite SO <sub>4</sub> -S(%)	Pyrite S (%)
0- 10	0.02	-	-
10- 20	0.04	0.01	-
20- 35	0.04	0.02	-
35- 50	0.04	0.03	-
50- 65	0.05	0.08	-
65- 80	0.04	0.08	-
80- 95	0.05	0.33	-
95-110	0.05	0.29	0.005
110-125	0.05	0.07	0.004
125-140	0.05	0.04	0.008
140-155	0.06	0.03	0.13
155-170	0.07	0.03	0.53
170-185	0.08	0.03	0.98

Table 18.1

Ra-2½ Sulfur fractions.

Depth (cm)	Waters. SO <sub>4</sub> -S(%)	Jarosite SO <sub>4</sub> -S(%)	Pyrite S(%)
0- 20	0.03	0.01	-
20- 50	0.05	0.11	-
50- 80	0.06	0.26	-
80-110	0.06	0.15	0.004
110-140	0.07	0.04	0.41
140-170	0.08	0.04	1.81

#### Profile 19

Mc-3 Thanyaburi Series

Location 5152 IV 1547.3 N, 674.6 E

Paddy field, broadcast rice.

#### Profile 20

Mc-4 Sena series

Location 5153 IV 1571.5 N, 681.05 E

Paddy field, broadcast rice. Jarosite starts at 60 cm depth.

#### Profile 21

Mc-5 Rangsit Series

Location 5153 I 1576.0, 690 E

Paddy field, broadcast rice. Red mottled with thick A1 (0-50 cm).

#### Profile 22

Mc-6 Klaeng Series (?)

Location 5153 I 1585.3 N, 699.8 E

Paddy field, transplanted rice. Strong red mottling between 20 and 100 cm, no jarosite mottles observed.

Profile 23

Mc-7 Rangsit Series

Location 5253 IV 1572.0 N, 731.5 E

Paddy field, transplanted (?) rice. A1 (0-65 cm), red mottled horizon (65 + cm) and jarosite mottles (80 + cm).

Profile 24

Mc-8 Mahapot Series

Location 5153 II 1559.9 N, 712.1 E (Close to 0-1)

Paddy field, transplanted rice. A1 (0-50 cm), few red mottles (90-110 cm) and common jarosite (110 + cm).

Profile 25

Mc-9 Thanyaburi Series

Location 5153 II 1558.5 N, 709.3 E

Paddy field, broadcast rice (poor stand). A1 (0-40 cm), no red mottles and few jarosite mottles below 60 cm.

Profile 26

Mc-10 Bang Nam Prieo Series

Location 5152 II 1527.4 N, 693.5 E

Paddy field, transplanted rice.

Profile 27

Mc-11 Ayutthaya Series

Location 5053 III 1549.0 N, 619.3 E

Paddy field, transplanted (?) rice. Red mottled, gypsiferous with little jarosite below 100 cm.

Profile 28

Mc-12 Ayutthaya Series (?)

Location 5053 III 1549.6 N, 622.7 E

Paddy field, broadcast rice. No jarosite within 120 cm.

Profile 29

Mc-15 Series unknown

Location 5053 III 1561.0 N, 614.5 E

Paddy field, broadcast rice. No boring made below 20 cm.

Profile 30

Mc-16 Ayutthaya Series

Location 5053 III 1561.3 N, 618.1 E

Paddy field, broadcast rice. No jarosite within 120 cm, somewhat gypsiferous.

Profile 31

Mc-17 Sena series

Location 5053 IV 1571.5 N, 613.0 E

Paddy field, broadcast rice.

Profile 32

Mc-23 Bangkhen Series (?)

Location 5053 III 1550 N, 610 E (exact location unknown)

Strongly gypsiferous soil without jarosite mottles.

Table 32.1

Mc-23 pH of samples taken on 1970-04-16.

Depth (cm):	0-20	20-40	40-60	60-80	80-100	100-120	120-140	140-160	160-180	180-200
pH fresh :	4.2	3.8	3.8	3.7	3.6	3.5	3.5	3.5	3.7	3.7

---

B.2 CHA-AM LAGUNA

---

Profile 33

Ca-1 Cha-am Series - Typic Sulfaquept

Described by N. van Breemen and W. van der Kervie, 1969-03-27

Location 4949 II 1416.3 N, 607.6 E

Elevation between 1 and 2 m

Small, filled-up lagoon. Flooded with fresh water from July -- December/January; occasionally with brackish or saline water during high tides. Barren except for local tufts of grasses during the rainy season.

Detailed profile description:

B1 0- 3 cm yellowish brown (10YR5/4, dry) or brown (10YR4/3, moist) silty clay loam (apparently sand: "pseudosand"); single grain, common small soft lumps; loose; many very fine interstitial pores; clear, smooth boundary

B21 3- 15 cm dark grayish brown (10YR4/3) silty clay loam; few, distinct, medium to fine, diffuse, red (2.5YR4/6) mottles; few, medium, distinct, diffuse, yellow (2Y8/6) jarosite; few, fine, faint, diffuse, yellowish brown (10YR8/6) mottles; moderate, medium to coarse, angular to subangular blocky; very fine (1-3 mm thick) more or less horizontal, wavy layers (platy structure ?); firm; common, very fine, interstitial pores along the platy layers; gradual, smooth boundary

B22g 15- 60 cm grayish brown (10YR5/2) silty clay loam; locally light gray (10YR7/1) fine sand to silt on vertical ped faces and in horizontal layers; common, medium to coarse distinct, diffuse, yellowish brown (10YR5/8) mottles often in a 3-6 mm wide zone

around rootchannels ( $d$  1-2 mm); few, fine, distinct, sharp, yellowish red (5YR5/6) rootrust; many, medium to coarse, prominent, diffuse, yellow (2.5Y7/6) jarosite as mottles and fillings of channels ( $\emptyset$  up to 12 mm); few, dark reddish brown (5YR3/2) ferric-oxide pipes ( $d$  8 mm) at the outside coated with thin, sharp jarosite; in the lower part of the horizon few ferric-oxide-jarosite pipes ( $d$  8-12 mm) filled and/or coated with white powdery silica<sup>+</sup>; very weak, coarse compound prismatic and moderate coarse angular blocky; sticky, plastic; common, very fine, tubular, horizontal pores; diffuse, smooth boundary

B23g 60-130 cm grayish brown (10YR5/2) silty clay loam; three somewhat peaty, fine sandy layers (2-3 cm in thickness) between 100 and 110 cm; common medium and few coarse, distinct, diffuse, yellowish brown (10YR5/6) mottles and coatings on vertical ped faces; esp. in the lower part: common, thin, coarse, distinct, diffuse, yellow (2.5Y8/6-7/6) jarosite on ped faces, mixed with yellowish brown (10YR5/6) coatings that become predominant over jarosite with increasing depth; common, medium and coarse, distinct, clear, yellow (2.5Y8/6-7/6) jarosite mottles, decreasing with depth; few, fine, distinct, sharp, brown (7.5YR4/4) rootrust; few, indurated, yellowish red (5YR4/6) ferric-oxide pipes ( $d$  5-13 mm), sometimes coated with thin, yellow jarosite at outside and/or inside, and occasionally coated or filled with white silica<sup>+</sup>; moderate, coarse to medium, angular blocky; sticky, plastic; many fine and very fine random tubular pores; many, medium, and coarse vertical tubular pores; abrupt, wavy boundary

B3g 130-150 cm dark gray (5Y4/1) silty clay loam, grading towards loam and sandy loam with depth; slightly peaty; few, dark reddish brown (5YR2/2-4/4), slightly indurated iron-oxide coatings on ped faces, sometimes with yellow jarosite sandwiched in between.

C1g 150-170 cm (description from auger samples) dark gray (5Y4/1) to dark greenish gray (5GY4/1) silty clay loam, somewhat peaty

C2g 170-210 cm dark greenish gray (5GY4/1) silty clay loam, somewhat peaty; few greenish mottles along rootchannels.

Remark: the permeability is slow throughout.

#### Range of characteristics:

Sandy and peaty layers may occur at various depths below 1 m within 30 m of the described profile. The top layer of pseudosand changes to a very soft mud upon inundation with fresh water. Towards the northeast, the elevation of the surface becomes gradually less and the depth of the unmottled subsoil decreases.

<sup>+</sup>) silicified plant remains.

Table 33.1

Ca-1 pH and soil moisture (weight %) at different dates

Depth (cm)	pH fresh			pH aerated 69-11-69	Moisture content			
	69-08-07	69-09-30	69-11-02		69-05-15	69-08-07	69-09-30	69-11-26
0- 20	3.3	3.5	4.2	4.0	20	26	29	30
20- 40	3.1	3.3	3.4	3.5	24	33	32	39
40- 60	3.0	3.2	3.2	3.2	35	41	38	43
60- 80	2.9	3.2	3.1	3.3	41	45	39	49
80-100	3.0	3.2	3.1	3.0	51	50	41	53
100-120	2.9	3.2	3.8	3.7	36	54	47	69
120-140	3.3	3.2	4.5	2.2	61	57	50	73
140-160	3.5	5.2	5.7	4.4	62	69	65	60
160-180	4.5	5.7	5.8	2.7	64	73	70	63
180-200	5.4	5.9	6.1	2.9	70	65	67	41
Height of the watertable (cm):					-70	+2	+20	+5

Table 33.2

Ca-1 Particle-size distribution, organic C,  $Fe_2O_3(d)$ , total sulfur content (of the undialysed soil; cf. Table 33.3) and N value.

Depth (cm)	Particle-size						Org. C. (%)	$Fe_2O_3(d)$ Total (%)	N value		
	(mm)				( $\mu m$ )						
	2-1	1-0.5	0.5-0.25	0.25-0.1	100-50	50-2	< 2	(%)			
0- 3	0.1	0.7	2.1	4.7	2.9	54.0	35.5	0.8	1.4	0.30	-
3- 15			4.5			57.3	38.3	0.6	1.8	0.28	0.38
15- 60	0.1	0.1	1.4	5.8	3.5	51.9	38.3	0.4	1.1	0.24	0.64
60-130	0.0	0.1	0.1	3.6	4.2	57.2	34.9	0.6	1.0	0.25	0.98
150-170	0.1	0.1	0.7	5.7	3.7	54.1	35.6	1.6	1.2	1.12	1.06
170-210	0.1	0.0	0.3	3.3	2.4	54.2	40.0	1.9	1.2	1.11	0.91

Table 33.3

Ca-1 Elemental composition (weight %); a: fraction < 2 mm (analysed after dialysis);  
 b: fraction < 2  $\mu\text{m}$ .

Depth (cm)	SiO <sub>2</sub>	Al <sub>2</sub> O <sub>3</sub>	Fe <sub>2</sub> O <sub>3</sub>	FeO	MnO	MgO	CaO	Na <sub>2</sub> O	K <sub>2</sub> O	TiO <sub>2</sub>	P <sub>2</sub> O <sub>5</sub>	SO <sub>3</sub>	FeS <sub>2</sub>	ign. loss
0- 3	a. 75.3	11.7	3.23	0.29	0.11	0.61	0.08	0.32	2.30	0.70	0.07	0.33	0.0	5.57
	b. 50.9	26.1	7.46	0.26	0.02	1.21	0.00	0.21	3.57	0.80	0.17	0.38	0.0	9.50
3- 15	a. 73.0	12.5	3.65	0.23	0.05	0.67	0.05	0.31	2.67	0.75	0.05	0.45	0.0	5.91
	b. 50.3	25.4	7.99	0.21	0.01	1.25	0.00	0.20	3.64	0.78	0.20	0.55	0.0	10.5
15- 60	a. 74.8	12.6	3.25	0.19	0.05	0.67	0.07	0.31	2.51	0.73	0.04	0.35	0.0	5.34
	b. 53.1	25.4	6.00	0.23	0.01	1.26	0.00	0.16	3.50	0.85	0.10	0.48	0.0	9.61
60-130	a. 75.3	12.2	3.11	0.24	0.04	0.68	0.07	0.31	2.48	0.71	0.03	0.38	0.0	5.55
	b. 52.4	25.5	6.28	0.19	0.01	1.30	0.00	0.16	3.41	0.80	0.08	0.48	0.0	9.88
150-170	a. 70.0	12.0	1.88	0.44	0.06	0.65	0.05	0.30	2.38	0.65	0.04	0.0	1.12	7.47
	b. 51.9	25.0	5.26	0.18	0.01	1.51	0.00	0.18	3.61	0.80	0.09	0.0	1.14	9.94
170-210	a. 70.1	12.2	3.22	0.41	0.08	1.10	0.11	0.30	2.50	0.71	0.04	0.0	0.99	7.26
	b. 51.5	24.0	6.21	0.31	0.02	1.76	0.00	0.19	3.49	0.81	0.21	0.0	1.07	10.1

Table 33.4

Ca-1 Normative mineralogical composition of the fraction < 2  $\mu\text{m}$  (weight %).

Depth (cm)	Q	P	Ru	Go	Ns	Kaol	Sm	Ab	Jar	Pyr	H <sub>2</sub> O <sup>+</sup> rest
0- 3	9.2	0.5	0.8	7.5	29.3	23.7	24.0	1.7	1.2	0.0	1.5
3- 15	9.5	0.5	0.8	7.7	29.5	21.6	24.2	1.6	1.7	0.0	2.5
15- 60	12.2	0.3	0.9	5.8	28.5	22.6	24.5	1.3	1.5	0.0	2.2
60-130	11.3	0.2	0.8	6.1	27.7	23.4	24.9	1.3	1.5	0.0	2.3
150-170	9.7	0.2	0.8	6.3	30.5	17.4	28.5	1.5	0.0	1.1	3.3
170-210	8.1	0.6	0.8	6.7	29.5	12.6	34.2	1.6	0.0	1.1	3.2

Table 33.5

Ca-1 Peak area percentages of X-ray diffractograms of the fraction < 2  $\mu\text{m}$ , treated with Mg-glycerol, and cation-exchange capacity of the clay fraction.

Depth (cm)	d-Value (Å)					24	CEC (mmol/100 g)
	7	10	12	14	18		
0- 3	28	19	4	2.5	45.5	-	35.2
3- 15	21	13	5	2	55	4	37.6
15- 60	26	12.5	5	2.5	54	-	40.0
60-130	27.5	9	4.5	1	58	-	40.8
150-170	24	12.5	6	2.5	55	-	40.0
170-210	22	9.5	1	3.5	64	-	40.8

Profile 34

Ca-2 Bang Pakong Series - Typic Sulfaquent

Location 4949 II 1416.3 N, 607.6 E

Rhizophora swamp (pure stand of *Rhizophora apiculata*).

Very dark gray (5Y3/1) silty clay (reduced throughout), on sand at about 100 cm.

Table 34.1

Ca-2 pH and soil moisture (weight %).

(sampled on 1969-11-26)

Depth (cm)	pH fresh	pH aerated	Moisture content
0- 20	6.7	3.0	69
20- 40	6.1	2.6	64
40- 60	6.2	1.8	67
60- 80	6.3	1.9	46 (sandy)
80-100	6.5	6.8	28 (sandy)

Profile 35

Ca-3 Bang Pakong Series - Typic Sulfaquent

Described by N. van Breemen, 1969-08-07

Location 4949 II 1416.5 N, 606.9 E

Avicennia swamp (almost pure stand of *Avicennia officinalis* (?)).

Micro-relief with differences in elevations of 20 to 30 cm. On the higher parts the soil is rather firm.

Description from auger samples:

0- 30 cm gray (5Y5/1) silty clay loam; common olive brown (2.5Y4/4) mottles along root-channels.

30- 60 cm gray (5Y5/1) silty clay loam with common greenish (appr. 5G4/2) mottles, decreasing with depth; amount of root remnants increases with depth

60-100 cm gray (5Y5/1) to greenish gray (5GY5/1) silty clay loam

100-200 cm greenish gray (5GY5/1) silty clay loam, becoming sandier below 120 cm

200 + cm light gray (5Y6/1) fine sandy loam.

A boring 4 m from this point (Ca-3A) in a creek (surface about 30 cm lower) showed a softer, dark gray to black mud, and sand starting at about 120 cm.

Table 35.1

Ca-3 pH and soil moisture (weight %).

Depth (cm)	sampling date	pH fresh		pH aerated	Moisture content
		69-08-07	69-11-26	69-11-26	69-11-26
0- 20		6.2	6.1	6.4	45
20- 40		6.1	6.1	6.5	62
40- 60		5.9	6.0	2.2	76
60- 80		5.8	6.0	1.7	69
80-100		5.8	6.1	2.5	74
100-120		5.8			
120-140		5.9			
140-160		6.0			
160-180		6.0			
180-200		6.1			

## B.3 PENINSULAR THAILAND (SONGKHLA AND PATTANI).

## Profile 36

Nk-1 Series unknown - Typic Tropaquept

Described by N. van Breemen and L. Montcharoen, 1970-12-19

Location 50 m north of the road Pattana-Songkhla, 13 km east of Pattani (appr. 5°49' N, 101°10' E).

Elevation probably between 1 and 2 m. Abandoned paddy field or pasture. Vegetation: grasses and rushes.

Horizon description (top 25 cm from small pit, at greater depths described from auger samples)

Apg	0- 22 cm	very dark gray (10YR3/1) clay; few, fine to medium, distinct, diffuse, brown to dark brown (7.5YR4/4) rootrust; weak, fine subangular blocky (upper part of horizon) and strong, fine angular blocky (lower part of horizon); very sticky, plastic; many roots; slow permeability; clear irregular boundary
B21g	22- 50 cm	gray to light gray (10YR6/1) clay; common, fine, distinct, sharp to diffuse, brown to dark brown (7.5YR4/4), yellowish brown (10YR5/6) and brownish yellow (10YR6/6) rootrust; firm, and very sticky, very plastic after wetting; slow permeability
B22g	50- 70 cm	gray to light gray (10YR6/1) clay; common, medium, distinct, sharp to diffuse, strong brown (7.5YR5/6) and brown to dark brown (7.5YR4/4) rootrust; firm, very sticky, very plastic after wetting; slow permeability
B23	70- 85 cm	grayish brown to brown (10YR5/2.5) silty clay; few, fine, distinct, diffuse, yellowish brown (10YR5/6) mottles; sticky, plastic; moderate permeability
B24	85-100 cm	grayish brown to brown (10YR5/2.5) silty clay; common coarse, distinct, diffuse, olive (5Y5/6) rootrust and mottles around rootholes; sticky, plastic; rapid permeability
B3g	100-125 cm	grayish brown to brown (10YR5/2.5) silty clay (50%) and dark gray (10YR4/1) clay (50%); unmottled; very sticky, very plastic

C1g 125-170 cm dark gray (10YR4/1) silty clay; locally, coarse, distinct, clear brown to dark brown (7.5YR4/4) rootrust; several layers (few mm thick) of medium sand, (from 170-190 cm, the sediment appears stiffer ('riper') than higher in the horizon)  
 II C2g 170 + cm dark gray (10YR4/1 to N4/0) clay loam with pockets of grayish brown (10YR5/2) clay loam; stiffer ('riper') than the overlying soil.

During the description, the field was flooded up to 5 cm depth, and dry locally. The permeability was slow in the upper part of the profile and the water rose quickly in the auger hole at depths below 85 cm.

*Range of profile characteristics:*

About 30 m south fine yellow mottling (resembling jarosite) was observed between 95 and 120 cm below the surface.

Table 36.1

Nk-1 Particle-size distribution, pH, organic C, and  $Fe_2O_3(d)$

Depth (cm)	Particle-size (mm)						pH fresh	pH aerated	Org. C. (%)	$Fe_2O_3(d)$ (%)		
	2-1	1-0.5	0.5-0.25	0.25-0.1	100-50	50-2						
0- 20				2.3			35.1	62.6	3.8	3.7	3.5	1.4
20- 35				1.8			39.8	58.4	3.6	3.8	0.9	0.9
35- 50				4.0			46.0	50.0	3.5	3.6	0.9	1.0
50- 70				3.0			44.2	52.8	3.3	3.6	0.7	1.3
70- 85				5.3			50.4	44.3	3.2	3.4	0.9	1.8
85-100				4.4			43.7	51.9	3.1	3.4	1.3	1.7
100-125	0.0	0.4	0.5	0.5	8.1	44.5	46.0	3.1	3.4	2.4	0.6	
125-150	0.0	0.1	0.7	3.9	9.3	42.7	43.3	3.0	2.8	2.2	0.5	
150-170	0.1	0.3	1.7	7.0	12.9	40.5	37.5	3.2	2.6	2.1	1.1	
170-190	0.2	0.8	2.9	11.3	17.1	33.5	34.2	3.2	3.1	0.9	0.5	

<sup>+</sup>) measured in a 1:5 aqueous suspension.

Table 36.2

Nk-1 Elemental composition (weight %); a: fraction < 2 mm; b: fraction < 2  $\mu\text{m}$ .

Depth (cm)		SiO <sub>2</sub>	Al <sub>2</sub> O <sub>3</sub>	Fe <sub>2</sub> O <sub>3</sub>	FeO	MnO	MgO	CaO	Na <sub>2</sub> O	K <sub>2</sub> O	TiO <sub>2</sub>	P <sub>2</sub> O <sub>5</sub>	SO <sub>3</sub>	FeS <sub>2</sub>	ign. loss
0- 20	a.	57.4	22.6	2.02	0.65	0.03	0.34	0.08	0.25	1.74	0.91	0.05	0.18	0.00	12.6
	b.	47.7	32.4	2.94	0.26	0.00	0.44	0.02	0.21	2.02	0.95	0.10	-	-	9.93
20- 35	a.	61.4	23.5	2.53	0.37	0.02	0.40	0.05	0.29	1.86	0.99	0.03	0.05	0.00	8.62
	b.	49.1	33.5	2.87	0.18	0.00	0.43	0.02	0.18	1.97	0.96	0.08	-	-	10.1
35- 50	a.	65.2	21.1	2.14	0.29	0.02	0.37	0.04	0.29	1.91	0.95	0.02	0.05	0.00	7.51
	b.	48.4	32.1	3.34	0.15	0.00	0.51	0.02	0.17	2.04	0.97	0.08	-	-	9.80
50- 70	a.	63.9	22.1	2.49	0.17	0.03	0.38	0.04	0.28	1.85	0.96	0.02	0.05	0.00	7.73
	b.	48.8	31.3	3.58	0.17	0.00	0.46	0.02	0.16	1.98	0.96	0.08	-	-	9.98
70- 85	a.	66.1	19.4	2.94	0.38	0.02	0.31	0.10	0.28	1.81	0.91	0.02	0.05	0.00	7.17
	b.	48.5	31.5	3.62	0.14	0.00	0.46	0.02	0.17	1.99	0.95	0.08	-	-	10.1
85-100	a.	64.1	20.2	2.73	0.55	0.03	0.36	0.04	0.27	1.79	0.93	0.03	0.10	0.00	8.14
	b.	50.9	31.6	4.52	0.17	0.00	0.45	0.02	0.18	2.11	1.07	0.09	-	-	9.41
100-125	a.	65.8	18.4	1.43	0.56	0.02	0.27	0.04	0.27	1.68	0.98	0.02	0.25	0.00	8.94
	b.	50.2	32.5	3.23	0.25	0.00	0.52	0.06	0.18	1.92	1.03	0.09	0.05	0.00	9.46
125-150	a.	66.6	16.8	0.36	0.59	0.03	0.29	0.04	0.26	1.44	0.82	0.03	0.00	1.33	9.92
	b.	50.7	32.3	3.40	0.27	0.00	0.47	0.02	0.18	1.80	0.99	0.09	0.00	0.08	9.47
150-170	a.	67.6	14.5	0.00	0.60	0.05	0.23	0.05	0.22	1.27	0.73	0.02	0.00	3.26	10.3
	b.	48.6	31.2	3.92	0.31	0.00	0.49	0.03	0.21	1.86	0.96	0.09	0.00	0.15	10.2
170-190	a.	77.0	11.1	0.61	0.23	0.03	0.07	0.06	0.13	0.64	0.79	0.03	0.00	1.35	5.72
	b.	51.4	30.5	3.52	0.30	0.00	0.22	0.03	0.16	1.05	1.23	0.10	0.00	0.11	9.57

Table 36.3

Nk-1 Normative mineralogical composition of the fraction < 2  $\mu\text{m}$  (weight %).

Depth (cm)	Q	P	Ru	Go	Ms	Kaol	Sm	Ab	Jar	Pyr	H <sub>2</sub> O <sup>+</sup> rest
0- 20	4.4	0.3	1.0	3.3	17.1	58.8	10.4	1.8	0.0	0.0	-0.2
20- 35	4.9	0.2	1.0	3.2	16.7	62.7	9.4	1.5	0.0	0.0	-0.6
35- 50	5.5	0.2	1.0	3.7	17.3	58.1	10.5	1.4	0.0	0.0	-0.4
50- 70	7.1	0.2	1.0	4.0	16.7	57.0	9.9	1.4	0.0	0.0	0.0
70- 85	6.7	0.2	1.0	4.0	16.8	57.6	9.6	1.4	0.0	0.0	0.0
85-100	8.9	0.2	1.1	5.0	17.8	56.6	9.6	1.5	0.0	0.0	-0.8
100-125	6.2	0.2	1.0	3.6	16.2	59.4	11.7	1.5	0.2	0.0	-0.9
125-150	7.3	0.2	1.0	3.7	15.2	60.2	11.1	1.5	0.0	0.1	-0.9
150-170	6.1	0.2	1.0	3.8	15.7	56.3	11.8	1.8	0.0	0.2	0.2
170-190	11.9	0.3	1.2	3.8	8.9	64.3	7.0	1.4	0.0	0.1	-0.9

Table 36.4

Nk-1 Peak area percentages of X-ray diffractograms of the fraction < 2  $\mu\text{m}$ , treated with Mg-glycerol, and cation-exchange capacity of the clay fraction

Depth (cm)	d Value (Å)					CEC (mmol/100 g)
	7	10	12	14	18	
0- 20	51	18	2	16	13	26.4
20- 35	52.5	16	0.5	10	21	28.0
35- 50	41	19	2	12	26	.
50- 70	45	19	2.5	10	25	33.6
70- 85	46	15.5	4	10	33	.
85-100	44	16	6.5	6.5	26	.
100-125	43.5	14.5	6	7	28.5	33.6
125-150	42.5	13	7	6	31.5	.
150-170	54.5	9.5	8	7.5	20	.
170-190	54.5	9.5	8.5	7	20	29.4

## Profile 37

Nk-2 Series unknown - Typic Tropaquept

Described by N. van Breemen and L. Montcharoen, 1970-12-19

Location about 5 km west of Nk-1; 30 m south of the road Pattani - Songkhla

Elevation probably between 1 and 2 m. This profile appears to be somewhat higher elevated and better drained than Nk-1.

Paddy field (abandoned) covered with grasses.

Horizon description (top 20 cm from small pit, rest of the profile described from auger samples):

Ap 0 - 13 cm dark yellowish brown (10YR4/2) silt; few, small, faint, diffuse, brown to dark brown (7.5YR4/4) rootrust and mottles; moderate, medium, angular blocky; slightly firm; many, fine, medium and coarse roots; abrupt, irregular boundary.

B21g 13- 70 cm gray to light gray (10YR6/1) (60%) and very dark gray (10YR3/1) (40%) silt loam (below 20 cm, the percentage of the dark gray matrix decreases slightly); many, coarse, distinct, diffuse, strong brown (7.5YR5/6) mottles, firm.

B22g 70-100 cm light brownish gray (10YR6/2) silt loam; common, medium to coarse, distinct, clear, yellowish brown (10YR5/6) mottles; few, fine, distinct, clear, dark reddish brown (5YR5/4) rootrust

B23 100-130 cm grayish brown to brown (10YR5/2.5) silt loam; common, distinct, yellowish brown (10YR5/6) mottles along root channels

IIC1g 130-180 + cm dark grayish brown (10YR4/2) silt with very dark grayish brown (10YR3/2) peaty layers.

## Range of profile characteristics:

4 meters west of the described site, many, coarse, prominent, clear, dark red (10R3/6) mottles were observed in a boring at 40-60 cm below the soil surface.

Table 37.1

Nk-2 Particle-size distribution, pH, organic C and  $Fe_2O_3$  (d)

Depth (cm)	Particle-size ( $\mu m$ )			pH fresh	pH aerated <sup>+</sup>	Org. C. (%)	$Fe_2O_3$ (d) (%)
	> 50	50-2	< 2				
0- 13	1.5	86.8	11.7	3.7	4.0	2.1	2.5
13- 40	2.8	82.1	15.2	3.6	3.7	0.5	3.1
40- 70	4.2	81.6	14.2	-	3.6	0.5	3.9
70-100	2.9	82.6	14.5	3.4	3.6	0.7	1.5
100-130	1.7	84.5	13.8	3.6	3.9	1.8	0.2
130-180	1.7	91.0	7.4	4.3	2.7	8.8	0.9

<sup>+</sup> measured in a 1:5 aqueous suspension.

Table 37.2

Nk-2 Elemental composition (weight %); a: fraction < 2 mm; b: fraction < 2  $\mu m$ .

Depth (cm)	SiO <sub>2</sub>	Al <sub>2</sub> O <sub>3</sub>	Fe <sub>2</sub> O <sub>3</sub>	FeO	MnO	MgO	CaO	Na <sub>2</sub> O	K <sub>2</sub> O	TiO <sub>2</sub>	P <sub>2</sub> O <sub>5</sub>	SO <sub>3</sub>	FeS <sub>2</sub>	ign. loss
0- 13	a. 66.1	16.9	3.60	0.39	0.02	0.29	0.10	0.28	1.66	0.92	0.08	0.13	0.00	9.84
	b. 47.1	30.8	5.04	0.14	0.02	0.62	0.02	0.12	2.11	0.83	0.12	-	-	11.6
13- 40	a. 62.2	21.0	4.41	0.19	0.02	0.36	0.06	0.33	2.13	1.02	0.04	0.13	0.00	8.67
	b. 46.9	32.1	4.50	0.11	0.02	0.59	0.01	0.13	2.19	0.94	0.06	-	-	11.4
40- 70	a. 61.5	21.0	4.93	0.27	0.01	0.37	0.07	0.35	2.17	1.01	0.05	0.13	0.00	8.62
	b. 47.1	32.1	5.49	0.09	0.02	0.61	0.01	0.13	2.17	0.93	0.06	-	-	11.2
70-100	a. 63.7	21.3	3.06	0.22	0.01	0.36	0.07	0.40	2.39	1.01	0.05	0.13	0.00	8.37
	b. 48.4	30.9	5.64	0.07	0.01	0.65	0.02	0.16	2.37	0.93	0.09	-	-	11.4
100-130	a. 64.5	20.6	1.51	0.40	0.01	0.40	0.08	0.44	2.33	1.00	0.05	0.23	0.00	9.28
	b. 48.7	32.5	2.89	0.10	0.01	0.67	0.01	0.16	2.36	0.99	0.08	-	-	11.1
130-180	a. 48.5	18.3	0.00 <sup>+</sup>	0.00 <sup>+</sup>	0.02	0.50	0.16	0.47	1.93	0.78	0.04	0.00	4.79 <sup>+</sup>	25.4
	b. 47.1	28.4	6.58	0.53	0.02	0.63	0.03	0.24	2.52	1.04	0.19	0.00	1.35	11.0

<sup>+</sup> Assuming all Fe to be present as pyrite. The total S content is 3.36%, which means that at least 1.57% is in organic and/or elemental form.

Table 37.3

Nk-2 Normative mineralogical composition of the fraction < 2  $\mu m$  (weight %).

Depth (cm)	Q	P	Ru	Go	Ms	Kaol	Sm	Ab	Jar.	Pyr.	$H_2O$ <sup>+</sup> rest
0- 13	2.9	0.3	0.8	5.5	17.8	50.6	17.9	1.0	0.0	0.0	1.6
13- 40	0.6	0.2	0.9	4.9	18.5	52.3	19.3	1.1	0.0	0.0	1.2
40- 70	2.1	0.2	0.9	6.0	18.4	54.0	16.2	1.1	0.0	0.0	0.8
70-100	6.3	0.2	0.9	6.0	20.0	51.3	12.2	1.4	0.0	0.0	1.4
100-130	3.3	0.2	1.0	3.1	20.0	53.9	15.4	1.4	0.0	0.0	1.2
130-180	5.8	0.5	1.0	7.7	21.3	41.2	16.6	2.0	0.0	1.4	1.7

Table 37.4

Nk-2 Peak area percentages of X-ray diffractograms of the fraction < 2  $\mu\text{m}$ , treated with Mg-glycerol, and cation-exchange capacity of the clay fraction

Depth (cm)	d-value ( $\text{\AA}$ )					CEC (mmol/100 g)
	7	10	12	14	18	
0- 13	59	11	6	5	19	41.6
13- 40	52	12.5	5	4.5	24	44.6
40- 70	55	12	4	4	23.5	40.0
70-100	57	12	3.5	3.5	24.5	45.0
100-130	50	13	4	4.5	29	43.2
130-180	intensities too low for reliable measurement					46.0

#### Profile 38

Sa-1 Ongkharak Series (?) - Typic Sulfaquept

Described by N. van Bremen and L. Montcharoen, 1970-12-20

Location 20 m south of the road Hatyai - Songkhla, 5 km southwest of Songkhla (map 47-3, appr. 791 N, 677.5 E)

Elevation probably between 1 and 2 m. Waste land covered with grasses and shrubs (*Melaleuca leucodendron* ?). About 15 years ago the area was shut off from the influence of brackish water by the construction of a dam.

#### Detailed profile description:

A1 0- 11/18 cm black (10YR2/1) clay; few, medium, distinct, clear, dark yellowish brown (10YR3/4) coatings on ped faces; weak, fine to medium subangular blocky and crumb; sticky, slightly plastic; few dark yellowish brown (10YR3/4) concretion-like lumps ( $d$  2-10 mm); many fine grassroots, many coarse shrub-roots ( $d$  up to 10 cm); clear, wavy boundary

B21g 11/18-25/35 cm gray (10YR5/1) clay; many, coarse, distinct, clear yellowish brown (10YR5/6) and brownish yellow (10YR6/6) mottles (mainly in the upper part of the horizon), associated with few, small, distinct, clear yellowish red (5YR8/6) mottles; common to many, small, distinct, sharp, yellow (2.5Y8/6) jarosite as fillings of root-channels (mainly in the lower part of the horizon); moderate, coarse and medium, angular blocky; very sticky, very plastic; pressure faces on small peds; few fine, many medium and few coarse roots; gradual, wavy boundary

B22g 25/35- 80 cm gray to light gray (10YR5/1) clay; common, medium, prominent, sharp to clear yellow (2.5Y8/6) jarosite along root-channels; few, fine to medium, prominent, clear yellow (2.5Y8/6) jarosite mottles on ped faces; few, fine, distinct, sharp brownish yellow (10YR6/8) rootrust, mainly surrounding the jarosite; moderate, medium to coarse angular blocky; very sticky, very plastic; common medium and few coarse roots; continuous slickensides; gradual, smooth boundary

B23g 80- 100 cm dark grayish brown (10YR4/2) clay; jarosite and rootrust as in the horizon above; common very dark gray (10YR3/1) to dark yellowish brown (10YR3/4) coatings on ped faces; medium to coarse angular blocky; very sticky, very plastic; common, medium roots; gradual, smooth boundary

C1g 100-150 cm grayish brown (10YR5/2) clay, many very dark gray (10YR3/1) to dark

yellowish brown (10YR3/4) partly decayed plant remnants; only locally little rootrust along living roots; many fine and medium roots

C2g 150 + cm gray (10YR5/1) silty clay; unmottled; many partly decayed plant remnants.

Table 38.1

Sa-1 pH of the fresh soil.

Depth (cm)	pH	Depth (cm)	pH
0- 10	4.0	80- 90	3.3
10- 20	3.4	90-100	3.3
20- 30	3.3	100-110	3.3
30- 40	3.3	110-120	3.4
40- 50	3.3	120-130	3.4
50- 60	3.3	130-140	3.5
60- 70	3.3	140-150	3.5
70- 80	3.3	160-180	3.5

Table 38.2

Sa-1 Particle-size distribution, pH, organic C and  $Fe_2O_3(d)$ .

Depth (cm)	Particle-size (mm)				pH <sup>+</sup> aerated			Org. C (%)	$Fe_2O_3(d)$ (%)
	2-1	1-0.5	0.5-0.25	0.25-0.1	100-50	50-2	< 2		
0- 15			5.3			39.7	54.9	3.7	4.8 1.4
15- 30	0.6	1.5	3.5	3.7	2.2	37.5	51.1	3.6	0.7 6.4
30- 55			2.9			37.9	59.2	3.7	0.8 1.3
55- 80	0.3	0.9	2.2	1.7	1.3	33.3	60.3	3.7	0.4 1.3
80-100			3.7			35.0	61.3	3.6	0.7 1.5
100-150	0.2	0.9	1.9	1.4	1.0	36.6	57.9	3.6	2.0 0.5
150-175	0.4	2.1	4.9	4.3	3.7	43.4	41.2	2.4	2.2 1.0

+) measured in a 1:5 aqueous suspension.

Table 38.3

Sa-1 Elemental composition (weight %); a: fraction < 2 mm; b: fraction < 2  $\mu\text{m}$ .

Depth (cm)	SiO <sub>2</sub>	Al <sub>2</sub> O <sub>3</sub>	Fe <sub>2</sub> O <sub>3</sub>	FeO	MnO	MgO	CaO	Na <sub>2</sub> O	K <sub>2</sub> O	TiO <sub>2</sub>	P <sub>2</sub> O <sub>5</sub>	SO <sub>3</sub>	FeS <sub>2</sub>	ign. loss
0- 15	a. 62.4	17.4	2.14	0.69	0.01	0.26	0.06	0.45	1.41	0.71	0.08	-	-	15.3
	b. 51.0	30.5	3.90	0.27	0.02	0.54	0.02	0.24	2.00	0.77	0.15	0.23	0.00	10.9
15- 30	a. 61.8	17.0	6.90	0.46	0.03	0.39	0.03	0.45	2.05	0.87	0.03	2.03	0.00	10.1
	b. 44.9	27.6	8.86	0.23	0.03	0.64	0.02	0.24	2.70	0.89	0.08	1.75	0.00	11.7
30- 55	a. 65.2	20.9	2.51	0.41	0.02	0.56	0.04	0.46	2.09	0.99	0.03	0.45	0.00	8.38
	b. 49.6	30.4	4.76	0.16	0.02	0.79	0.01	0.21	2.39	0.95	0.07	0.43	0.00	10.3
55- 80	a. 65.6	20.2	3.45	0.23	0.02	0.54	0.04	0.47	1.96	0.94	0.03	0.73	0.00	8.26
	b. 49.0	29.6	5.29	0.14	0.02	0.73	0.02	0.17	2.50	0.92	0.08	0.50	0.00	10.5
80-100	a. 63.9	20.5	3.59	0.21	0.02	0.60	0.05	0.51	2.11	0.97	0.03	0.85	0.00	8.92
	b. 45.6	29.7	5.10	0.20	0.02	0.77	0.01	0.18	2.47	0.93	0.08	0.68	0.00	10.6
100-150	a. 65.2	20.3	1.57	0.33	0.02	0.59	0.05	0.45	1.79	0.97	0.03	0.00	0.36	9.90
	b. 51.2	31.1	3.64	0.19	0.02	0.75	0.01	0.07	2.26	0.97	0.08	0.00	0.04	10.2
150-175	a. 68.9	13.6	0.00	0.07	0.03	0.32	0.05	0.33	1.00	0.78	0.02	0.00	3.62	10.7
	b. 49.6	29.8	4.99	0.19	0.02	0.63	0.02	0.17	2.04	0.96	0.09	0.00	0.13	10.2

Table 38.4

Sa-1 Normative mineralogical composition of the fraction < 2  $\mu\text{m}$  (weight %).

Depth (cm)	Q	P	Ru	Go	Ms	Kaol	Sm	Ab	Jar.	Pyr.	H <sub>2</sub> O <sup>+</sup> rest
0- 15	9.0	0.4	0.8	3.8	16.4	53.5	12.3	2.0	0.7	0.0	0.7
15- 30	5.5	0.2	0.9	6.9	18.9	44.1	13.7	1.8	5.5	0.0	0.8
30- 55	6.4	0.2	1.0	4.5	19.3	48.9	15.6	1.7	1.3	0.0	0.4
55- 80	7.6	0.2	0.9	5.0	20.0	46.9	14.3	1.4	1.6	0.0	0.8
80-100	7.3	0.2	0.9	4.5	19.4	47.1	15.6	1.4	2.1	0.0	0.6
100-150	7.9	0.2	1.0	4.0	19.1	51.6	15.2	0.6	0.0	0.0	0.5
150-170	8.3	0.2	1.0	5.6	17.3	50.9	13.0	1.4	0.0	0.1	0.5

Table 38.5

Sa-1 Peak area percentages of X-ray diffractograms of the fraction < 2  $\mu\text{m}$ , treated with Mg-glycerol, and cation-exchange capacity of the clay fraction

Depth (cm)	d-Value ( $\text{\AA}$ )					CEC (mmol/100 g)
	7	10	12	14	18	
0- 15	44	19	1	5	31	32.8
15- 30	42.5	16	3.5	8	30	30.8
30- 55	43	10	4	7	36	32.0
55- 80	37	11	3.5	4	44.5	32.0
80-100	36	10.5	3.5	3	47	36.0
100-150	35.5	9	3.5	6	46	33.6
150-170	41	12.5	4	6	36	35.2

#### B.4. SOUTHEAST COAST REGION

Profile 39

Ch-1 Cha-am Series - Typic Sulfaquept

Described by N. van Breemen and F.R. Moormann, 1969-03-13

Location 5448 IV 1393.3 N, 184.0 E

Elevation 1 - 2 m

Bare spot (more or less circularly shaped with a diameter of about 150 m, and a slightly concave relief) in an area covered with rushes and with paperbark trees (*Melaleuca leucodendron*).

##### Detailed profile description:

I C1 0- 2.5 cm yellowish brown (10YR5/8) sandy loam with many, slightly rounded quartz grains (d up to 5 mm); somewhat stratified; structureless, single grain; loose ("puffy"); no roots; abrupt, wavy boundary

II B1g 2.5-13 cm horizontal strata (2-30 mm thick) of very dark gray (10YR3/1) clay loam (alternating with strata (< 1-10 mm thick) of yellow (2.5Y7/6) jarosite; few more or less vertical channels filled with yellow (2.5Y7/6) jarosite; continuous, thin jarosite cutans on many vertical ped faces; in the upper part of the horizon patchy and broken, thin, dark yellowish brown (10YR4/4) ferric-oxide on ped faces and in channels; weak, medium, angular blocky; firm; slow permeability; clear, wavy boundary

II B2 13- 40 cm dark brown (10YR3/3) silty clay loam; few soft, black (5YR2/1) pockets (organic matter ?); common, fine to medium, prominent, clear yellow (2.5Y7/6) jarosite in (root-)channels (diameter < 1-5 mm); few, thin, continuous jarosite cutans on ped faces; few, thin, dark brown (7.5YR3/2) ferric-oxide cutans on ped faces and channel-walls; weak, medium, angular blocky; sticky, plastic; slow permeability; gradual, wavy boundary

II B3g 40- 70 cm very dark gray (5YR3/1) to dark reddish brown (5YR3/2) silty clay loam; in some parts of the profile; common, thin, broken and continuous, dark brown (7.5YR3/2) ferric-oxide coatings along vertical cracks and channel-walls; in other parts similar coatings of very dark gray (N3/0) material, that also occurs as fillings of rootchannels (diameter 5 mm); structureless, massive; sticky, very plastic; rapid

permeability; gradual, smooth boundary

II Cg 70-190 cm dark gray (5YR4/1) silty clay; unmottled.

III B 190 + cm mottled clay with laterite gravels

*Range of profile characteristics:*

Profile morphology is very similar throughout the bare area. Thin salt crusts occur locally on higher spots. In the surrounding wooded land, the elevation of the surface is about 20 cm higher, and profile morphology is different (cf. Ch-3).

Table 39.1

Ch-1 pH and soil moisture (weight %) at different dates

Depth (cm)	pH fresh		pH aerated	Moisture content	
	69-08-21	69-10-22	69-08-21	69-08-21	69-10-22
0- 20	3.0	3.0	3.2	25	26
20- 40	4.2	3.0	3.7	28	36
40- 60	4.9	3.6	3.7	51	53
60- 80	4.6	4.8	2.0	67	61
80-100	4.4	4.8	2.2	73	66
100-120	4.3	4.7	2.0	77	65
120-140	4.4	4.2	2.2	70	68
140-160	4.8	4.5	2.6	73	70
160-180	5.1	5.0	2.0	77	-
180-190	5.3	-	2.7	80	-
Height of the watertable (cm):				-15	-40

Table 39.2

Ch-1 Particle-size distribution, organic C,  $Fe_2O_3(d)$ , total sulfur content (of the undialysed soil) and N-value.

Depth (cm)	Particle-size							Org. C (%)	$Fe_2O_3(d)$ (%)	Total S (%)	N value
	2-1	1-0.5	0.5-0.25	0.25-0.1	100-50	50-2	< 2				
0-2.5	15.5	15.4	11.4	12.5	14.1	27.0	4.1	0.3	1.2	0.36	-
2.5- 13	9.3	7.0	4.0	3.6	5.1	34.7	36.5	1.7	7.5	2.49	-
13- 40	5.1	3.7	2.1	2.4	5.1	49.5	32.0	2.2	3.9	1.10	0.44
40- 70	4.0	3.0	1.9	3.7	5.0	48.8	33.6	2.2	0.4	0.24	0.97
70-190	2.0	1.3	0.7	1.7	3.3	49.1	42.0	3.1	1.7	2.07	1.04

Table 39.3

Ch-1 Elemental composition (weight %); a: fraction &lt; 2 mm (analysed after dialysis)

b: fraction < 2  $\mu\text{m}$ .

Depth (cm)	SiO <sub>2</sub>	Al <sub>2</sub> O <sub>3</sub>	Fe <sub>2</sub> O <sub>3</sub>	FeO	MnO	MgO	CaO	Na <sub>2</sub> O	K <sub>2</sub> O	TiO <sub>2</sub>	P <sub>2</sub> O <sub>5</sub>	SO <sub>3</sub>	FeS <sub>2</sub>	ign. loss
0-2.5	a. 95.2	1.99	1.49	0.13	0.06	0.01	0.02	0.15	0.27	0.29	0.02	0.32	0.0	1.39
	b. 35.4	23.0	17.5	0.26	0.01	0.21	0.00	0.49	2.17	0.95	.	0.28	0.0	19.7
2.5- 13	a. 67.0	7.20	8.51	0.52	0.06	0.05	0.04	0.59	1.71	0.69	0.03	5.70	0.0	12.7
	b. 27.6	17.8	23.0	0.29	0.01	0.14	0.00	0.85	3.16	1.07	.	3.22	0.0	24.8
13- 40	a. 72.9	10.3	4.16	0.49	0.06	0.07	0.06	0.45	1.26	1.06	0.03	2.30	0.0	9.61
	b. 40.5	27.7	10.4	0.22	0.00	0.31	0.00	0.48	1.89	1.78	.	1.70	0.0	16.9
40- 70	a. 76.5	12.2	0.76	0.31	0.05	0.12	0.08	0.29	0.86	1.05	0.04	0.0	0.28	7.70
	b. 48.3	31.4	2.55	0.17	0.00	0.40	0.01	0.16	1.24	1.79	.	0.0	0.34	12.2
70-190	a. 66.0	14.4	1.38	0.50	0.08	0.12	0.05	0.31	0.93	1.02	0.04	0.0	3.04	10.3
	b. 42.9	28.6	5.29	0.20	0.00	0.41	0.00	0.57	1.13	1.48	.	0.0	3.12	15.3

Table 39.4

Ch-1 Normative mineralogical composition of the fraction < 2  $\mu\text{m}$  (weight %).

Depth (cm)	Q	Ru	Go	Ms	Kaol	Sm	Ab	Jar.	Pyr.	H <sub>2</sub> O <sup>+</sup> rest
0-2.5	3.9	1.0	19.0	17.8	35.4	6.4	4.1	0.9	0.0	9.6
2.5- 13	1.3	1.1	20.2	19.5	20.0	5.5	6.7	10.0	0.0	13.6
13- 40	3.0	1.8	8.8	12.2	52.1	7.7	3.8	5.3	0.0	6.3
40- 70	6.9	1.8	2.7	10.5	65.0	8.8	1.3	0.0	0.3	1.5
70-190	3.2	1.5	7.6	9.6	55.6	9.3	4.8	0.0	3.1	5.1

Table 39.5

Ch-1 Peak area percentages of X-ray diffractograms of the fraction < 2  $\mu\text{m}$ , treated with Mg-glycerol, and cation-exchange capacity of the clay fraction.

Depth (cm)	d-Value ( $\text{\AA}$ )					CEC (mmol/100 g)
	7	10	12	14	18	
0-2.5 <sup>+</sup>	70	22	0	8	0	.
2.5- 13 <sup>+</sup>	69	21	0	10	0	19.5
13- 40	59	10.5	2	5	23.5	27.3
40- 70	57.5	5	2.5	7	28	31.2
70-190	60	6.5	3.5	6.5	23.5	.

<sup>+</sup>) results inaccurate as a result of poor quality diffractograms (Fe-fluorescence).

Table 39.6

Ch-1 Qualitative mineralogical studies (Guinier X-ray photographs).

Depth (cm)	Material	Minerals identified
0	white salt crust scraped from the surface, 30 m from Ch-1	halite, quartz, gypsum. Unidentified lines at 5.65, 3.99, 3.88, 3.80, 2.96 and 2.50 Å
0	white salt crust with astringent taste, scraped from a soil similar to Ch-1, between Trat and Laem Ngop about 60 km southeast of Chanthaburi	halite, Na-alum, tamarugite
25-13	yellow material	jarosite, little quartz

## Profile 40

Ch-2A Tha Khwang Series

Location 5448 IV 1388.1 N, 180.9 E

Elevation approximately 1 m

Rice field at relatively high elevation, formed by enclosing an area by a small bund (ca 30 cm high). The soil permeability is slow to moderate. Jarosite mottles occur between 30 and 120 cm below the surface; the dark gray (5Y4/1) reduced subsoil below 140 cm. Samples were taken 1 m from the border of the field.

## Profile 41

Ch-2B Cha-am Series

Location 5448 IV 1388.1 N, 180.9 E

Elevation approximately 1 m

Site 25 m west from Ch-2A, bare land. The soil permeability is rapid throughout.

- 0- 5 cm thin layers of very dark gray (10YR3/1) and light gray (10YR7/2) sandy loam
- 5- 20 cm very dark gray (10YR3/1) matrix with common yellow jarosite mottles
- 20- 60 cm dark grayish brown (10YR4/2) matrix with common jarosite along channels
- 60- 80 cm dark grayish brown (10YR4/2) matrix, unmottled
- 80-120 cm dark greenish gray (5GY4/1) matrix, unmottled

## Profile 42

Ch-2C Cha-am Series

Location 5448 IV 1388.1 N, 180.8 E

Elevation approximately 0.5 m

Site 90 m west of Ch-2B, bare land regularly flooded by brackish or saline water.

The soil permeability is rapid to very rapid throughout.

- 0- 40 cm black (10YR2/1) matrix with few, faint dark brown (10YR3/3) and very pale brown (10YR7/4) mottles
- 40- 80 cm black (10YR2/1) and dark grayish brown (10YR4/2) matrix, unmottled
- 80-140 cm dark greenish gray (5GY4/1) matrix, unmottled, many brown root remains

#### Profile 43

##### Ch-3 Cha-am Series

Location 5448 IV 1393.3 N, 184.0 E

Situated 70 m south-west of Ch-1 in a forest of *Melaleuca leucodendron* with an undergrowth of grasses. Soil surface 20-30 cm higher than at Ch-1.

0- 20 cm homogeneous brown (7.5YR4/4) matrix, crumb to granular structure  
20- 40 cm gray (N5/0) matrix; abundant, coarse yellowish brown (10YR5/6) mottles; few yellow (2.5Y8/8) jarosite  
40- 60 cm grayish brown (10YR5/2) matrix with common, faint yellowish brown (10YR5/6) mottles  
60-180 cm grayish brown (10YR5/2) matrix; unmottled; peaty material between 100 and 120 cm; weak H<sub>2</sub>S smell.

#### Profile 44

##### Ch-6 Cha-am Series

Location 5448 IV 1391.8 N, 181.9 E

Elevation approximately 1 m

Bare area, shown on the topographical map as "intermittent lake"

0- 2 cm very dark gray (5Y3/1) fine sand over sandy loam with vesicular pores in the lower part  
2- 20 cm black (5Y2/1) sandy loam with abundant yellow jarosite, in horizontal strata (upper part) and in vertical channels (lower part)  
20- 40 cm grayish brown (5Y5/2) sandy loam; few jarosite mottles.  
40-120 cm gray (N5/0) sandy loam; unmottled; many root remnants.

#### Profile 45

##### Ch-7 Cha-am Series

Location 5448 IV 1388.8 N, 181.2 E

Elevation approximately 1 m

Bare area, formerly paddy field according to the topographical map (1953-1957)

0- 2 cm fine sandy loam, platy  
2- 10 cm gray (N4/0) matrix, few brown ferric oxide  
10- 20 cm gray (N4/0) matrix, abundant yellow jarosite  
20- 40 cm dark grayish brown (2.5Y4/2) matrix, common jarosite  
40-100 cm gray (10YR5/1-4/1) matrix, unmottled.

#### Profile 46

##### Kl-1 Klaeng Series (?) - Typic Plinthaqueox

Described by N. van Breemen and S. Sombatpanit, 1971-01-11

Location 5349 III 1414.6 N, 789.6 E

Elevation 3 to 4 m. Situated on a semi-recent (?) marine terrace, about 1 km north of the northernmost extension of a tidal creek system fringed by Nipah palms, and about 10 km north of the coastline.

Paddy field, transplanted rice; (yield about 1.4 tonne/ha, no fertilizers applied).

Flooded from June/July to November/December by impounding rainwater by bunds. Watertable during description: - 60 cm.

*Detailed profile description:*

Apg 0-12/15 cm very dark grayish brown (2.5Y3.5/2) clay; common, fine, distinct, sharp to clear yellowish red (5YR5/8) mottles; structureless, massive to weak, coarse angular blocky; firm and sticky, plastic after wetting; few fine pores; common rice roots; abrupt, wavy boundary

B21ir 12/15-40/60 cm strong brown (7.5YR4.5/8) loam; common pockets of very dark gray (10YR3/1) clay, especially in the upper part of the horizon; many, coarse, prominent, diffuse, dark red (7.5R3/8-10R3/6) indurated 'mottle-like' concretion; few, medium, distinct, clear, yellow (2.5Y7.5/6) jarosite mottles in the lower part of the horizon; structureless, massive and extremely hard in the dark red indurated parts; fine to medium crumb and friable in the strong brown material (the indurated character of this horizon is best expressed in the upper part and decreases with increasing depth); no roots; clear, wavy boundary

B22g 40/60-80/90 cm pinkish gray (7.5YR6/2) to brown (7.5YR5/2) clay loam; many coarse, prominent, clear to diffuse, yellow (2.5Y7.5/6) jarosite mottles, sometimes along pores; common, coarse, distinct, diffuse, yellowish brown (10YR5/8) mottles, mostly associated with the jarosite mottles; weak, medium to coarse angular blocky; firm, after wetting slightly sticky, plastic; few to common very fine to fine pores; no roots; gradual, smooth boundary

B23g 80/90-100 cm pinkish gray (7.5YR6/2) to brown (7.5YR5/2) sandy clay loam; few, medium and coarse, distinct, diffuse, yellowish brown (10YR5/8) mottles; few medium, distinct, clear, dark brown (7.5YR3/1) Fe-Mn(?) coatings along horizontal pores; structureless, massive; very sticky, non-plastic (poorly ripened material); gradual, smooth boundary

C1 100-150 cm grayish brown to light brownish gray (10YR5.5/3) and dark yellowish brown (10YR4/4) sandy loam; unmottled; structure, consistence and ripening stage as horizon above

IIC2 150-180 cm light gray (10YR7/2) sandy loam; unmottled, much "riper" than the two overlying horizons.

*Range of characteristics:*

Several borings were made within about 100 m of the described profile. The Fe-pan may vary considerably in thickness and hardness; yellow mottles are locally absent.

Table 46.1

K1-1 Particle-size distribution, pH, organic C, free  $Fe_2O_3$  and sulfur fractions.

Depth (cm)	Particle-size (mm)						< 2	pH aerated	Org. $Fe_2O_3$ (d) C (%)	Waters.		Jarco SO <sub>4</sub> -S (%)			
					(μm)					100-50					
	2-1	1-0.5	0.5-0.25	0.25-0.1						50-2					
0- 13	1.3	4.4	8.4	8.4	3.3	29.7	44.5	4.7	2.3	7.8	0.01	0.05			
13- 25	6.9	12.5	13.9	12.5	5.2	33.5	15.5	3.9	0.7	40.6	0.13	0.30			
25- 35	2.5	8.8	13.5	13.8	5.4	35.5	20.5	3.4	0.5	36.3	0.13	0.47			
35- 50	2.4	9.0	17.4	18.0	6.1	29.5	17.6	3.3	0.4	26.5	0.10	0.78			
50- 70	0.9	4.9	10.0	11.4	3.9	41.5	27.4	3.5	0.2	5.1	0.02	0.90			
70- 85	1.5	6.8	13.9	20.2	3.8	26.6	27.2	3.5	0.3	3.2	0.02	0.71			
85-105	0.1	9.0	19.4	21.7	5.9	19.0	24.9	3.6	0.6	1.0	0.01	0.06			
105-130	0.5	7.2	19.0	26.6	8.0	20.5	18.2	3.8	0.7	0.1	0.01	0.03			
130-150	1.2	9.9	21.9	27.4	8.7	21.4	9.5	4.0	0.3	0.04	0.0	0.08			
150-180	1.3	10.4	21.7	26.7	7.9	19.8	12.2	4.1	0.5	0.05	0.0	0.07			

Table 46.2

K1-1 Elemental composition (weight %); a: fraction < 2 mm; b: fraction < 2  $\mu$ m.

Depth (cm)	Elemental composition (weight %)														ign. loss
	SiO <sub>2</sub>	Al <sub>2</sub> O <sub>3</sub>	Fe <sub>2</sub> O <sub>3</sub>	FeO	MnO	MgO	CaO	Na <sub>2</sub> O	K <sub>2</sub> O	TiO <sub>2</sub>	P <sub>2</sub> O <sub>5</sub>	SO <sub>3</sub>	FeS <sub>2</sub>	ign. loss	
0- 13	a. 60.2	16.3	8.79	0.54	0.07	0.16	0.07	0.27	1.00	0.55	0.12	0.15	0.00	10.9	
	b. 42.0	30.7	10.3	0.31	0.01	0.32	0.03	0.31	1.56	0.80	0.18	0.05	0.00	11.7	
13- 25	a. 31.0	5.71	48.1	0.38	0.02	0.06	0.02	0.19	0.47	0.26	0.07	1.20	0.00	12.3	
	b. 15.8	10.4	54.7	0.41	0.02	0.16	0.02	0.26	1.27	0.50	0.14	0.85	0.00	12.9	
25- 35	a. 41.8	4.11	42.8	0.29	0.01	0.08	0.01	0.18	0.57	0.31	0.06	1.45	0.00	10.0	
	b. 21.2	15.1	44.7	0.59	0.01	0.21	0.03	0.27	1.11	0.48	0.15	0.15	0.00	12.6	
35- 50	a. 57.9	4.26	28.4	0.27	0.00	0.08	0.00	0.20	0.98	0.36	0.04	2.20	0.00	8.68	
	b. 21.8	14.6	42.7	0.51	0.02	0.20	0.03	0.32	2.31	0.73	0.14	0.80	0.00	15.0	
50- 70	a. 72.6	9.61	6.28	0.16	0.02	0.07	0.02	0.29	1.37	0.61	0.01	2.55	0.00	7.60	
	b. 40.5	28.0	10.7	0.30	0.00	0.28	0.02	0.38	2.25	1.04	0.07	1.58	0.00	14.7	
70- 85	a. 79.2	8.50	4.19	0.12	0.00	0.08	0.00	0.23	1.05	0.52	0.01	1.32	0.00	5.69	
	b. 43.5	29.3	7.78	0.23	0.00	0.28	0.02	0.34	1.90	1.09	0.07	1.10	0.00	12.8	
85-105	a. 85.1	8.30	1.68	0.15	0.00	0.05	0.00	0.16	0.58	0.49	0.01	0.08	0.00	3.48	
	b. 48.8	31.8	4.56	0.30	0.00	0.22	0.02	0.30	1.71	1.25	0.07	0.00	0.00	10.7	
105-130	a. 89.3	6.16	0.53	0.13	0.00	0.05	0.00	0.10	0.46	0.43	0.01	0.05	0.00	3.10	
	b. 50.9	33.0	2.57	0.23	0.00	0.28	0.02	0.30	1.88	1.26	0.04	-	0.00	10.8	
130-150	a. 95.0	2.90	0.29	0.03	0.02	0.03	0.00	0.07	0.25	0.38	0.06	0.00	0.00	1.40	
	b. 55.1	28.9	2.28	0.30	0.00	0.27	0.06	0.29	1.76	1.66	0.05	-	0.00	9.39	
150-180	a. 94.2	3.82	0.41	0.01	0.01	0.03	0.00	0.08	0.29	0.43	0.01	0.00	0.00	1.47	
	b. 60.7	22.5	2.25	0.12	0.00	0.25	0.03	0.35	1.82	2.20	0.08	-	0.00	9.28	

Table 46.3

K1-1 Normative mineralogical composition of the fraction < 2  $\mu\text{m}$  (weight %).

Depth (cm)	Q	P	Ru	Go	Gibb	Ms	Kaol	Sm	Ab	Jar.	$\text{H}_2\text{O}^+$ rest
0- 13	1.0	0.5	0.8	11.4	0	13.1	58.9	8.8	2.6	0.2	0.2
13- 25	0	0.4	0.5	59.4	0.3	8.9	12.4	7.1	2.0	2.7	-2.8
25- 35	0	0.4	0.5	49.4	0	9.1	25.7	5.6	2.3	0.5	-1.9
35- 50	0	0.4	0.7	46.1	0.3	17.8	13.2	8.8	2.5	2.5	-0.2
50- 70	3.1	0.2	1.0	9.3	0	15.5	49.5	8.0	3.0	4.9	3.2
70- 85	4.7	0.2	1.1	6.8	0	13.5	55.9	7.3	2.7	3.4	1.6
85-105	7.3	0.2	1.3	5.1	0	14.5	61.5	7.0	2.5	0	0.1
105-130	7.8	0.1	1.4	2.9	0	15.9	62.7	7.3	2.5	0	0.3
130-150	16.7	0.1	1.7	2.5	0	14.9	53.3	7.9	2.5	0	0.4
150-180	30.5	0.2	2.2	2.5	0	15.5	37.5	5.7	3.0	0	2.6

Table 46.4

K1-1 Peak area percentages of X-ray diffractograms of the fraction < 2  $\mu\text{m}$ , treated with Mg-glycerol.

Depth (cm)	d-Value ( $\text{\AA}$ )				
	7	10	12	14	18
0- 13	.	.	.	.	.
13- 50	.	.	.	.	.
50- 70	52.5	14	3	10	20
70- 85	53	14	3	12	19
85-105	57	15	5	11	12
105-130	66	15	3.5	9	6.5
130-150	72	16	6	7	0
150-180	78	15	4	2	0

Table 46.5

K1-1 Qualitative mineralogical studies (Guinier X-ray photographs).

Depth (cm)	Material	Minerals indentified
30-80	yellow mottled soil	quartz, jarosite, goethite
13-25	soil	goethite
25-35	soil	goethite, little jarosite
35-50	soil	jarosite, goethite
13-25	red indurated soil	haematite

## Appendix C

### ANALYTICAL DATA OF WATER SAMPLES AND CALCULATED ACTIVITIES OF SOLUTES

The samples are grouped per pedon in the same order as in Appendix B, and are indicated by a site code and a serial number (sample no.). The types of samples are labelled as described in A.1.3 except for 'lei', which refers to water collected by pressure filtration from a soil sample taken inside a permanently installed poly(vinyl chloride) tube (Fig. A.1.b). The depths for groundwater samples from 'unprotected' auger holes (Fig. A.1.c) are in parenthesis, because most of these samples were contaminated by water from shallower depth.

Generally two rows of data are given under the heading Concentrations. The first row represents the analyzed concentrations corrected for excess charge by equalizing the sums of cations and anions on an equivalent basis.  $C$  represents the corrected anion concentration (expressed as percentage of the observed concentration), obtained by distributing any excess charge proportionally over cations and anions. Generally,  $C$  was very close to 100, indicating that no other major dissolved species were present, and that accuracy of the reported concentrations of major species was good.  $I$  is true ionic strength, i.e. the ionic strength calculated on the basis of various free and complexed ions in solution. The second row shows the thermodynamic concentrations, or activities, of the uncomplexed species on the same scale (mmol/litre).

$C$ ,  $I$  and the thermodynamic concentrations were calculated by a computer programme described elsewhere (van Breemen, 1973a).

#### Footnotes

- a. Water from a small (10 cm deep) ditch.
- b. Water from a large ditch or creek.
- c. I and II refer to two porous sampling cups both at 25 cm depth.
- d. pH probably too high due to loss of  $\text{CO}_2$  after sampling.
- e. Surface sea-water from the Gulf of Thailand near Pattaya, 5 km from the coast.
- f. Sampled after washing and replacement with outside surface water.
- g. Calculated assuming electroneutrality.
- h. Possibly too high due to pyrite oxidation after sampling.
- i. Surface sea-water, about 20 m from the coast.
- j. 50-100 m northeast of the described pedon.

C.1 Water samples from the Bangkok Plain.  
C.1.1 Saline acid sulfate soils.

Site no	Sample no (cm)	Depth (cm)	Date	Type	pH	$E_H/V$	Concentrations (mmol / l)						C (‰)	$I$ mol.l <sup>-1</sup>	EC (mS/cm)					
							Cl	HCO <sub>3</sub>	SO <sub>4</sub>	H <sub>4</sub> SiO <sub>4</sub>	K	Na	Mg	Ca	Fe	Al	Mn			
Standard sea-water		8.15	•		555	2.65	28.4	•	10.0	475	10.4	54.0	•	•	•	•	100.0	0.658	•	
		349	1.24	2.56	349	6.20	330	2.37	13.7	•	•	•	•	•	•	•	•	•	•	
BP-1	1	+5	69-10-23	so <sup>a</sup>	3.10	•	136	-	16.7	1.22	3.50	124	3.69	15.9	0.369	<0.0015	0.091	98.8	0.185	15.5
BP-1	4	-20	69-10-23	le	4.18	40.400	70.3	-	10.6	1.89	2.52	70.7	1.79	6.85	0.418	•	0.0564	102.8	0.101	•
BP-1	5	-110	69-10-23	le	6.61	-0.080	327	6.65	24.5	1.01	6.97	286	10.1	34.8	0.0050	•	0.0655	100.7	0.412	•
BP-1	6	(-30)	69-10-23	gr	4.42	•	148	-	17.9	1.78	4.15	139	3.76	15.9	0.892	<0.004	0.0894	100.1	0.200	16.4
BP-1	12	•	70-05-23	so	7.67	•	338	2.08	16.8	0.137	6.36	287	7.06	33.3	•	•	•	99.1	0.404	34.0
BP-1	27	(-30)	70-07-07	gr	4.50	•	255	-	17.1	1.32	5.38	221	6.18	23.9	1.02	•	0.106	98.6	0.313	26.4
BP-1	28	-70	70-07-07	fe	6.49	•	321	7.61	19.1	1.39	6.42	277	7.08	34.4	0.152	•	0.111	98.2	0.396	32.6
BP-1	29	-50	70-07-07	fe	6.29	•	214	4.58	2.46	1.39	4.21	196	1.69	8.94	0.0378	•	0.0252	•	0.0255	•
BP-1	30	-95	70-07-07	fe	6.60	•	211	5.55	2.41	1.44	6.23	272	7.03	34.7	0.280	•	0.103	97.4	0.392	32.4

BP-1	31	-10	70-07-07	1e	4.40	+0.350	353	-	23.6	1.08	6.93	308	7.43	33.7	0.129	-	0.954	90.27	0.430	-
BP-1	32	-30	70-07-07	1e	3.68	+0.415	390	-	31.7	2.24	7.56	337	10.1	43.9	0.963	-	0.252	97.2	0.488	-
BP-1	33	-60	70-07-07	1e	5.75	+0.110	379	-	29.2	1.40	7.34	318	9.64	43.7	2.45	-	0.209	98.0	0.475	-
BP-1	35	-12	70-07-24	fe	5.66	-	328	1.70	27.3	1.73	6.29	283	7.41	37.9	1.96	-	0.382	97.5	0.416	32.2
BP-1	36	-15	70-07-24	fe	4.99	-	340	6.39	27.3	1.64	6.62	290	7.48	39.0	2.40	<0.05	0.380	98.3	0.428	33.1
BP-1	38	-25	70-07-24	fe	4.98	-	329	6.31	29.3	1.77	6.50	287	7.71	39.5	-	-	0.382	97.0	0.419	32.8
BP-1	39	-50	70-07-24	fe	6.16	-	217	4.11	16.1	1.31	4.99	188	5.52	23.5	0.782	-	0.169	97.8	0.276	22.6
BP-1	40	-70	70-07-24	fe	6.30	-	150	2.58	2.58	1.31	3.40	135	1.42	6.48	0.205	-	0.422			
BP-1	41	-95	70-07-24	fe	6.30	-	247	4.87	3.05	1.48	4.62	228	2.26	10.8	0.114	-	0.0621			
BP-1	42	-12	70-08-27	fe	5.31	-	350	0.405	35.0	1.97	6.22	306	8.10	43.5	1.78	-	0.540	97.8	0.509	39.5
BP-1	43	-15	70-08-27	fe	4.20	-	262	-	13.7	1.53	4.63	215	5.05	27.7	1.75	-	0.318	103.7	0.317	26.2
							179	-	2.00	1.53	3.12	154	1.32	7.75	0.462	-	0.084			

Site	Sample no.	Depth (cm)	Date	Type	pH	$E_H/V$	C1	$HCO_3$	$SO_4$	$H_4SiO_4$	K	Na	Concentrations (mmol/l)	Mg	Fe	Al	Mn	C(%)	I mol.l <sup>-1</sup>	EC (mS/cm)
BP-1	44	-25 I <sup>c</sup>	70-08-27	fe	4.88	+	291	0.226	33.0	1.94	5.54	257	6.54	35.1	5.19	-	0.361	98.3	0.386	30.0
BP-1	45	-25 II <sup>c</sup>	70-08-27	fe	5.33	+	194	0.138	4.30	1.94	3.61	179	1.49	8.67	1.20	-	0.0938			
BP-1	46	-50	70-08-27	fe	6.30	+	207	0.625	22.8	1.27	4.41	184	4.81	23.1	4.12	-	0.274	97.7	0.276	22.4
BP-1	47	-70	70-08-27	fe	6.30	+	144	0.412	3.63	1.27	2.99	131	1.19	6.15	1.03	-	0.0588			
BP-1	48	-95	70-08-27	fe	6.60	+	199	4.82	15.6	1.14	4.57	177	5.00	21.2	0.564	-	0.174	98.4	0.256	21.2
BP-1	49	-12	70-09-24	fe	4.31	+	139	3.20	2.66	1.14	3.14	128	1.29	5.89	0.150	-	0.435			
BP-1	50	-226	70-09-24	fe	4.32	+	303	7.79	23.4	1.45	6.14	264	7.54	35.3	0.553	-	0.254	98.6	0.386	30.8
BP-1	51	-155	70-09-24	fe	4.31	+	202	4.65	3.05	1.45	4.02	186	1.76	8.97	0.135	-	0.0564			
BP-1	52	-225	70-09-24	fe	4.32	+	155	4.98	2.62	1.21	3.57	143	1.42	6.62	0.0620	-	0.0436			
BP-1	53	-345	70-09-24	fe	4.31	+	226	-	4.59	2.70	6.07	308	8.30	44.4	1.58	-	0.184	98.9	0.288	23.4
BP-1	54	-334	70-09-24	fe	4.32	+	220	-	4.64	2.68	3.87	213	1.83	10.7	0.354	-	0.120			
BP-1	55	-165	70-09-24	fe	6.20	+	242	2.18	24.8	1.13	4.79	216	5.39	26.8	4.33	-	0.534	98.0	0.455	36.8
BP-1	56	-242	70-09-24	fe	5.32	+	165	0.210	3.81	1.77	4.79	215	5.36	26.9	4.86	-	0.401	99.7	0.441	-
BP-1	57	-253	70-09-24	fe	6.50	+	173	7.66	17.3	1.28	5.31	220	6.05	28.4	0.486	-	0.179	98.8	0.320	27.0
BP-1	58	-173	70-09-24	fe	6.50	+											0.0607		0.0418	

BP-1	67	-70	70-09-24	fe	6.44	+	326	10.0	22.7	1.65	6.34	283	7.54	37.4	0.686	+	0.274	99.1	0.412	33.2
BP-1	68	-95	70-09-24	fe	6.99	+	336	12.8	19.1	1.34	6.36	291	7.47	37.1	0.0142	+	0.161	98.3	0.417	33.8
BP-1	69	-12	70-10-20	fe	4.20	+	223	7.46	2.37	1.34	4.15	205	1.75	9.47	0.0035	+	0.0344			
BP-1	70	-15	70-10-20	fe	5.18	+	315	-	36.4	2.36	5.53	279	7.14	40.8	3.07	0.102	0.351	99.6	0.418	32.6
BP-1	71	-25 <sup>I<sup>c</sup></sup>	70-10-20	fe	6.30	+	208	-	4.50	2.36	3.56	194	1.60	9.92	0.696	0.0035	0.0802			
BP-1	72	-50	70-10-20	fe	6.02	+	200	0.354	22.6	1.52	3.82	177	4.16	24.7	3.06	+	0.280	98.2	0.268	22.0
BP-1	73	-50	70-10-20	fe	6.40	+	139	0.233	3.66	1.52	2.60	127	1.03	6.58	0.766	+	0.0708			
BP-1	74	-95	70-10-20	fe	6.52	+	273	10.0	18.3	1.38	5.56	235	6.21	32.9	0.300	+	0.173	99.0	0.347	28.4
BP-1	75	-95	70-10-20	fe	6.52	+	184	6.12	2.55	1.38	3.70	167	1.50	8.60	0.0759	+	0.0387			
BP-1	76	+10	70-10-20	so	6.75	+	2.53	0.538	0.379	0.146	0.121	2.51	0.232	0.336	0.0291	+	0.0005	99.6	0.00383	0.50
BP-1	78	-50	71-01-12	fe	6.53	+	284	9.69	17.8	1.28	6.19	235	7.64	35.6	0.289	+	0.125	96.8	0.359	30.0
BP-1	79	-70	71-01-12	fe	6.49	+	191	5.81	2.40	1.28	4.11	167	1.85	9.33	0.0732	+	0.0282			
							283	8.83	17.8	1.23	5.36	235	7.43	35.1	0.629	+	0.173	97.0	0.358	29.8
							190	5.31	2.40	1.23	3.56	167	1.80	9.22	0.159	+	0.0395			

Site	Sample no.	Depth (cm)	Date	Type	pH	$E_H/V$	Concentrations (mmol/l)						C(%)	$I$ mol $^{-1}$ (mS/cm)	EC					
							Cl	HCO <sub>3</sub>	SO <sub>4</sub>	H <sub>4</sub> SiO <sub>4</sub>	K	Na	Ca	Mg	Fe	Al	Mn			
BP-1	80	-95	71-01-12	fe	6.63	-	305	11.6	17.7	1.25	6.56	255	7.86	37.3	0.0595	-	0.104	97.3	0.384	31.0
							204	6.85	2.30	1.25	4.32	180	1.88	9.68	0.0150	-	0.0228			
KD-1	1	-	69-06-09	so <sup>b</sup>	3.35	-	163	-	45.7	2.55	4.50	149	9.37	38.2	0.135	0.359	1.65	95.2	0.277	21.0
							113	-	7.02	2.55	2.98	104	2.00	8.85	0.0290	0.0102	0.365			
KD-1	2	(-50)	69-06-09	gr	3.82	-	164	-	43.4	2.61	2.94	147	7.18	38.1	3.21	-	1.79	97.5	0.275	21.2
							114	-	6.73	2.61	1.95	102	1.55	6.93	0.701	-	0.402			
KD-1	6	+30	69-08-22	so	6.58	-	13.9	4.05	0.256	0.460	0.941	10.4	0.781	2.79	-	-	-	106.2	0.0218	2.3
							78.4	-	6.29	1.71	1.86	68.6	1.40	6.33	1.69	-	0.208			
KD-1	9	-50	69-08-22	le	3.67	0.280	109	-	34.5	1.71	2.69	96.1	6.03	25.3	7.23	-	0.864	98.4	0.199	-
							193	14.6	31.5	1.29	4.80	177	6.25	36.8	0.250	-	0.965	99.9	0.293	-
KD-1	10	-140	69-08-22	le	6.40	-0.130	133	9.16	4.81	1.29	3.21	124	1.38	8.14	0.0587	-	0.195			
							81.3	-	6.36	2.51	1.86	73.3	0.992	5.78	2.32	0.0116	0.232			
KD-1	12	(-60)	69-08-22	gr	3.50	-	114	-	35.6	2.51	2.71	103	4.32	23.3	10.0	0.347	0.975	96.6	0.205	16.7
							96.0	0.597	5.99	1.90	3.09	121	4.99	27.3	8.03	-	1.03	98.6	0.229	18.8
KD-1	13	(-100)	69-08-22	gr	5.19	-	136	0.888	34.9	1.90	2.11	85.4	1.14	6.75	1.86	-	0.243			
							27.1	0.304	5.66	1.41	0.652	27.4	0.701	2.99	2.10	-	0.118	100.8	0.0931	6.5
KD-1	17	+40	69-10-23	so	6.93	-	7.37	3.88	0.110	0.406	0.452	7.03	0.432	1.46	0.0593	-	0.0462	99.6	0.0134	1.22

KD-1	18	-50	69-10-23	1e	3.73	0.080	139	-	62.1	2.49	3.22	138	8.10	36.7	14.3	-	1.55	98.3	0.283	•
KD-1	19	-70	69-10-23	1e	4.07	0.180	150	-	59.6	2.19	3.93	149	7.59	36.3	12.5	-	1.66	98.6	0.289	•
KD-1	20	-115	69-10-23	1e	5.90	-0.055	184	2.94	52.6	1.26	5.27	179	7.83	42.9	1.72	-	1.78	97.9	0.314	•
KD-1	21	-160	69-10-23	1e	6.60	-0.165	258	26.1	30.3	0.942	6.96	248	4.92	39.6	0.0041	•	0.0709	98.7	0.366	•
KD-2	5	(-10)	69-06-09	gr	7.90 <sup>d</sup>	•	496	•	18.0	0.470	9.51	407	9.79	47.8	0.0783	•	0.165	97.0	0.578	46.1
KD-2	36	•	70-02-11	so <sup>a</sup>	8.20	•	520	2.19	26.6	0.012	9.65	448	10.5	48.1	•	•	99.7	0.616	42.0	
Mc-22	1	(-50)	69-06-09	gr	5.50	•	290	•	38.6	1.00	5.55	247	9.41	45.9	1.59	•	0.518	94.6	0.368	30.2
Mc-2	1	(-50)	69-06-09	gr	5.50	•	193	•	4.85	1.00	3.58	171	2.08	11.1	0.356	•	0.117			
Mc-18	32	-5	69-11-29	1e	6.63	-0.056	24.3	6.55	0.262	0.430	0.213	18.6	2.07	3.90	0.258	•	0.052	100.7	0.037	3.42
Mc-27	44	(-15)	69-06-09	gr	8.13 <sup>d</sup>	•	709	•	•	0.620	11.4	550	13.4	66.2	0.005	•	0.275	•	•	59
Mc-28	45	(-10)	69-06-09	gr	7.90 <sup>d</sup>	•	1273	•	32.8	0.314	20.4	1000	23.8	137	0.009	•	0.130	•	•	97
T-1	1	+3	70-06-10	so	6.70	•	15.0	1.40	11.6	0.568	0.425	20.6	3.60	5.70	•	•	100.0	0.0491	3.60	

### C.1.2 Non-acid marine soils.

Site	Sample no.	Depth (cm)	Date	Type	pH	$E_H/V$	C1	$HCO_3$	$SO_4$	$H_4SiO_4$	K	Na	Ca	Mg	Fe	Al	Mn	C(%)	$I$ mol. $l^{-1}$	EC (mS/cm)
T-1	12	(-160)	70-06-10	gr	7.00	-	58.5	5.17	34.6	0.659	1.11	71.2	13.1	17.2	<0.003	-	0.0281	103.2	0.149	9.80
					43.3	3.60	7.48	0.658	0.786	51.2	2.95	4.20	-	-	-	0.0063				
T-1	30	+10	70-06-26	so	6.82	-	6.17	0.984	4.80	0.306	0.281	8.02	1.81	2.41	-	-	0.0740	99.5	0.185	12.8
					73.5	0.119	46.3	0.740	1.23	71.3	16.0	30.7	-	-	0.0740	99.5	0.185	12.8		
T-1	31	+10	70-06-26	si	5.51	-	47.3	5.10	34.6	0.662	0.875	54.9	12.1	20.3	0.451	-	0.123	100.1	0.138	9.10
					35.3	3.56	7.56	0.662	0.622	39.7	2.76	5.02	0.105	-	0.0280					
T-1	32	-20	70-06-26	fe	6.08	-	57.3	8.11	37.4	0.712	0.928	62.3	14.7	22.7	0.973	-	0.187	98.9	0.157	10.4
					42.2	5.53	7.60	0.712	0.651	44.5	3.24	5.43	0.223	-	0.0402					
T-1	33	-50	70-06-26	fe	6.30	-	47.0	6.02	30.0	0.666	0.956	53.4	12.0	16.5	0.730	-	0.0548	98.6	0.129	8.90
					35.2	4.24	6.78	0.666	0.687	39.0	2.85	4.26	0.179	-	0.0128					
T-1	34	-72	70-06-26	fe	6.50	-	47.1	5.58	26.0	0.570	0.972	52.4	10.9	14.7	0.0151	-	0.0124	99.6	0.120	8.40
					35.6	3.96	6.10	0.570	0.707	38.7	2.73	3.95	0.0039	-	0.0030					
T-1	35	-85	70-06-26	fe	6.71	-	46.1	5.92	28.6	0.591	0.980	52.8	11.9	15.9	0.0050	-	0.0191	99.4	0.125	8.50
					34.7	4.18	6.59	0.591	0.707	38.7	2.87	4.15	0.0013	-	0.0046					
T-1	36	-105	70-06-26	fe	6.63	-	47.2	6.38	27.2	0.687	1.02	51.9	11.6	15.9	0.0221	-	0.0341	99.6	0.124	8.60
					35.6	4.50	6.26	0.687	0.741	38.1	2.86	4.21	0.0056	-	0.0082					
T-1	37	-145	70-06-26	fe	6.68	-	46.1	6.74	24.9	0.660	1.08	51.7	10.7	14.1	0.0151	-	0.0525	99.1	0.118	8.20
					34.9	4.78	5.92	0.660	0.788	38.2	2.69	3.84	0.0039	-	0.0128					
T-1	38	-180	70-06-26	fe	6.80	-	9.06	2.17	5.91	0.149	0.249	11.4	2.46	3.25	-	-	0.00002	98.4	0.0294	2.20
					77.6	0.394	47.9	0.764	1.12	76.1	16.2	32.0	-	-	0.070	98.5	0.193	12.8		

T-1	41	+12	70-07-30	sf	7.25	*	9.78	2.02	6.67	0.147	0.277	12.3	2.74	35.5	*	*	<0.0002	99.2	0.0320	2.38
T-1	42	-20	70-07-30	fe	6.09	*	28.2	11.1	18.3	0.680	0.491	37.3	6.46	11.9	0.562	*	0.101	99.2	0.0885	6.1
T-1	43	-50	70-07-30	fe	6.50	*	36.4	14.5	20.8	0.541	0.749	42.6	8.49	14.2	1.84	*	0.110	100.1	0.107	7.1
T-1	44	-72	70-07-30	fe	6.52	*	49.1	6.71	28.4	0.630	0.975	55.4	11.7	16.4	0.0334	*	0.0405	98.7	0.128	8.9
T-1	45	-85	70-07-30	fe	6.50	*	46.5	6.35	25.5	0.620	0.982	52.4	10.3	14.9	0.0212	*	0.0473	99.3	0.119	8.4
T-1	46	-105	70-07-30	fe	6.48	*	46.0	6.41	26.6	0.656	0.982	53.1	10.9	14.9	0.0141	*	0.0191	99.3	0.121	8.4
T-1	47	-145	70-07-30	fe	6.40	*	46.6	7.93	28.4	0.740	1.03	53.4	12.0	16.9	0.0476	*	0.0395	98.7	0.128	8.8
T-1	48	-180	70-07-30	fe	6.50	*	49.1	7.15	26.1	0.724	1.07	54.2	10.7	15.7	0.0463	*	0.0607	97.2	0.124	8.6
T-1	49	+2	70-09-02	so	7.40	*	37.0	5.09	6.04	0.724	0.776	39.9	2.64	4.21	0.0119	*	0.0145	*	*	*
T-1	50	+2	70-09-02	si	5.31	*	31.6	0.058	8.22	0.865	0.510	38.9	2.78	4.40	*	*	0.0425	102.3	0.131	8.6
T-1	57	-20	70-09-02	fe	6.22	*	36.5	7.85	19.7	0.615	0.574	43.1	7.15	12.3	0.477	*	0.0866	99.3	0.0972	6.8
T-1	58	-50	70-09-02	fe	6.63	*	28.1	5.77	5.12	0.615	0.428	32.5	1.93	3.56	0.134	*	0.0222	*	*	*

Site	Sample no.	Depth (cm)	Date	Type	pH	$E_{H^+/V}$	Cl	HCO <sub>3</sub>	SO <sub>4</sub>	Concentrations (mmol /l)				Al	Mn	C(%)	$I$ mol.l <sup>-1</sup>	EC (mS.cm <sup>-1</sup> )	
										H <sub>4</sub> SiO <sub>4</sub>	K	Na	Ca	Mg					
T-1	59	-72	70-09-02	fe	6.70	•	49.6	7.68	26.2	0.611	1.00	53.6	11.6	15.8	0.0401	•	0.0641	99.8	0.125 8.8
							37.3	5.44	6.02	0.611	1.00	39.4	2.86	4.22	0.0103	•	0.0152		
T-1	60	-85	70-09-02	fe	6.70	•	45.7	6.64	24.9	0.625	0.934	52.3	10.3	14.0	0.0293	•	0.0575	99.1	0.117 8.2
							34.6	4.76	5.95	0.625	0.934	38.7	2.59	3.81	0.0077	•	0.0141		
T-1	61	-105	70-09-02	fe	6.72	•	45.1	7.65	25.0	0.660	0.966	52.1	10.4	14.4	0.0211	•	0.0433	99.4	0.118 8.0
							34.2	5.49	5.95	0.660	0.704	38.5	2.59	3.88	0.0055	•	0.0104		
T-1	62	-145	70-09-02	fe	6.60	•	46.5	7.74	25.8	0.780	1.03	54.0	10.6	14.5	0.199	•	0.0577	100.6	0.121 8.4
							35.1	5.54	6.09	0.780	0.751	39.8	2.63	3.88	0.0511	•	0.0137		
T-1	63	-180	70-09-02	fe	6.73	•	46.6	7.11	26.0	0.690	0.974	51.1	11.4	15.3	0.0286	•	0.0296	98.0	0.121 .
							35.2	5.01	6.06	0.690	0.709	37.7	2.83	4.10	0.0074	•	0.00712		
T-1	66	+20	70-10-01	so	7.00	•	3.93	2.15	0.621	0.270	0.074	4.30	0.560	0.916	•	•	<0.0002	101.0	0.0091 0.80
T-1	67	+20	70-10-01	si	6.60	•	46.9	1.17	34.1	0.470	0.645	52.2	12.5	19.4	•	•	0.102	97.6	0.133 9.0
							35.1	0.822	7.63	0.470	0.460	37.8	2.90	4.86	•	•	0.0240		
T-1	68	-20	70-10-01	fe	6.39	•	26.4	8.43	13.2	0.620	0.394	35.1	4.35	8.03	0.392	•	0.0621	101.5	0.0718 5.02
							20.9	6.40	3.97	0.620	0.304	27.3	1.32	2.61	0.125	•	0.0175		
T-1	69	-50	70-10-01	fe	6.92	•	25.5	11.1	10.8	0.556	0.491	35.5	3.93	7.02	0.0658	•	0.0196	101.9	0.0575 4.82
							20.3	8.48	3.36	0.556	0.382	27.9	1.23	2.35	0.0221	•	0.0055		
T-1	70	-72	70-10-01	fe	6.61	•	48.2	7.86	27.8	0.636	0.769	58.5	11.0	15.1	0.0377	•	0.0357	100.8	0.127 8.6
							36.2	5.55	6.44	0.636	0.555	42.9	2.65	3.93	0.0094	•	0.0031		
T-1	72	-85	70-10-01	fe	6.70	•	46.1	6.84	26.2	0.632	0.940	55.9	10.2	14.0	0.0139	•	0.0159	100.5	0.120 8.1
							34.9	4.91	6.24	0.632	0.683	41.2	2.51	3.73	0.0036	•	0.0038		

T-1	73	-105	70-10-01	fe	6.70	*	45.5	7.26	25.1	0.676	0.924	54.1	10.2	13.8	0.0225	*	0.0274	102.3	0.118	8.0
T-1	74	-145	70-10-01	fe	6.63	*	34.5	5.22	6.02	0.676	0.673	40.1	2.54	3.72	0.0058	*	0.0066			
T-1	75	-180	70-10-01	fe	6.74	*	46.4	7.80	27.5	0.690	0.987	56.3	10.9	15.1	0.0138	*	0.0306	101.3	0.124	8.4
T-1	76	-20	70-12-28	fe	6.50	*	35.0	5.57	6.43	0.690	0.714	41.3	2.62	3.95	0.0035	*	0.00715			
T-1	77	-50	70-12-28	fe	7.33	*	19.1	9.51	3.21	0.610	0.245	22.9	1.45	3.01	0.182	*	0.0121			
T-1	78	-72	70-12-28	fe	6.63	*	18.1	14.1	4.86	0.380	0.314	29.2	4.60	8.97	0.537	*	0.0730	98.6	0.0684	4.95
T-1	79	-85	70-12-28	fe	6.62	*	34.5	5.99	6.00	0.630	0.296	20.2	0.958	2.23	0.0131	*	0.0029			
T-1	80	-105	70-12-28	fe	6.61	*	44.7	7.10	24.9	0.640	0.887	49.7	10.2	15.2	0.0213	*	0.0399	97.7	0.121	8.6
T-1	81	-145	70-12-28	fe	6.60	*	33.9	5.08	5.92	0.640	0.648	36.8	2.57	4.13	0.0056	*	0.0095			
T-1	82	-180	70-12-28	fe	6.75	*	43.1	7.98	24.2	0.640	0.924	48.4	10.3	14.8	0.0711	*	0.0264	98.5	0.115	8.0
T-1	83	+10	70-12-28	so	7.87	*	32.8	5.72	5.81	0.640	0.676	35.9	2.59	4.04	0.0187	*	0.0064			
T-1	84	+15	70-12-28	si	7.17	*	33.4	5.67	5.98	0.665	0.679	36.5	2.64	4.18	0.0044	*	0.0094			
T-1	85	-105	70-12-28	fe	6.75	*	44.9	7.51	24.7	0.722	1.01	49.6	10.5	15.0	0.0116	*	0.0466	98.8	0.117	8.2
T-1	86	-145	70-12-28	fe	6.60	*	34.1	5.37	5.86	0.722	0.739	36.7	2.65	4.07	0.0315	*	0.0113			
T-1	87	-180	70-12-28	fe	6.75	*	51.8	1.79	36.7	0.296	0.524	55.2	13.3	22.2	0.0010	*	0.106	99.2	0.144	9.9
T-1	88	-20	70-12-28	fe	7.33	*	38.4	1.23	7.80	0.296	0.371	39.7	3.02	5.45	0.0002	*	0.0247			

Site	Sample no.	Depth (cm)	Date	Type	pH	$E_H/V$	Cl	$HCO_3$	$SO_4$	$H_4SiO_4$	K	Na	Ca	$Mg$	Fe	Al	Mn	C(%)	$I$ mol.l <sup>-1</sup>	EC (mS/cm)
T-1	85	-5	70-12-28	le	6.64	-0.153	26.7	14.9	2.51	0.333	0.234	25.1	3.75	*6.48	0.323	*	0.0548	100.4	0.0548	3.98
T-1	86	-5	70-12-28	lei	6.48	-0.130	54.3	2.20	33.8	0.390	0.562	55.5	12.5	21.1	0.285	*	0.134	100.0	0.141	9.8
					40.4	1.52	7.26	0.390	0.399	40.1	2.91	5.32	0.0674	*	0.0319					
C.1.3 Acid sulfate soils and para acid sulfate soils.																				
BK-1	3	-250	69-06-18	le	6.41	0.090	94.0	4.50	34.1	0.260	2.75	93.8	8.61	26.4	0.0039	*	0.160	100	0.186	*
BK-1	16	-200	69-07-07	le	6.32	-0.072	77.3	5.49	25.5	0.310	2.11	75.0	7.19	21.0	0.030	*	0.036			
BK-1	19	(-50)	69-07-07	gr	6.70	*	71.1	*	29.7	0.620	2.04	66.5	8.10	22.5	<0.001	*	0.241	99.7	0.151	*
BK-1	20	(-100)	69-08-11	gr	5.75	*	77.2	0.953	41.7	1.16	2.09	79.9	9.22	30.4	<0.001	*	0.362	99.4	0.149	11.0
BK-1	21	(-140)	69-08-11	gr	5.66	*	74.2	0.789	42.9	1.18	2.07	78.4	9.14	30.9	0.002	*	0.160	99.8	0.179	13.7
BK-1	24	-130	69-08-11	le	4.44	0.320	72.8	-	47.1	1.05	2.31	80.3	9.71	32.0	<0.002	*	0.463	97.2	0.185	*
BK-1	25	-150	69-08-11	le	4.55	0.189	82.0	*	58.9	1.71	2.54	90.4	12.7	38.6	1.31	*	0.101			
BK-1	29	(-100)	69-10-06	gr	5.63	*	63.7	1.29	38.8	1.12	1.81	73.5	7.91	25.6	<0.001	*	0.135	99.0	0.160	9.5
					46.8	0.896	8.09	1.12	1.26	52.4	1.75	6.12	*	0.0309						

BK-1	31	100	69-10-06	1e	5.95	0.490	67.1	1.86	40.2	0.620	2.00	76.6	8.41	26.9	<0.002	*	0.0592	97.9	0.167	*
					49.1	1.29	8.18	0.520	1.39	54.3	1.83	6.35	*	*	*	0.0133				
BK-1	32	165	69-10-06	1e	5.60	0.230	85.9	1.17	55.3	1.05	2.96	94.3	12.1	36.5	0.0503	*	1.47	97.4	0.216	*
					61.1	0.772	9.80	1.05	1.98	65.0	2.39	7.86	0.0164	*	0.301					
KR-1	1	+10	70-06-09	50	4.00	*	0.431	-	2.11	0.232	0.108	1.81	0.651	0.621	*	0.0097	0.025	103.6	0.0072	0.528
					1.11	-	1.99	0.073	0.147	2.07	0.707	0.618	*	0.0105	0.024		105.4	0.0076	0.544	
KR-1	3	+20	70-07-22	80	3.90	*	1.62	-	7.00	0.72	0.412	4.53	2.37	2.34	0.0042	0.174	0.098	96.9	0.0218	1.45
KR-1	4	+15	70-07-23	s1	3.47	*	0.877	-	1.30	0.014	0.049	1.73	0.402	0.422	0.0017	0.0107	0.0155	103.1	0.0053	0.426
KR-1	5	+17	70-08-24	80	4.05	*	2.65	-	11.5	0.89	0.542	7.30	3.68	3.90	0.016	0.440	0.157	100.1	0.0337	2.38
KR-1	6	+6	70-08-24	s1	3.18	*	0.914	-	1.51	0.030	0.081	1.80	0.460	0.451	0.0013	0.0117	0.0176	102.4	0.0059	0.488
KR-1	7	+17	70-08-24	s1 <sup>f</sup>	3.88	*	1.62	1.63	0.284	0.170	0.196	2.19	0.240	0.235	0.138	*	0.0108			
KR-1	8	-8	70-08-24	1e	5.95	-0.180	1.76	1.77	0.427	0.170	0.213	2.36	0.351	0.339	0.197	*	0.0165	96.9	0.0055	0.446
KR-1	9	-165	70-08-24	1e	3.60	+0.510	5.50	-	13.6	1.52	0.250	14.5	3.60	4.75	0.100	*	0.191	99.6	0.0423	2.70
					4.55	-	5.11	1.52	0.280	11.6	1.17	1.64	0.033	*	0.065					
KR-1	10	+20	70-09-23	80	5.20	*	0.361	*	0.601	0.011	0.039	0.826	0.174	0.168	0.0017	0.0018	0.0031	102.9	0.0024	0.194
KR-1	11	+17	70-09-23	s1	3.57	*	1.23	-	2.87	0.217	0.205	2.64	0.907	0.863	0.0028	0.054	0.0361	103.1	0.0102	0.78
KR-1	12	+68	70-10-27	80	6.81	*	1.58	0.975	0.200	0.218	0.113	1.95	0.214	0.226	0.0053	*	0.00051	97.4	0.0036	0.342
KR-1	13	+35	70-10-27	s1	6.80	*	1.78	0.791	0.92	0.245	0.154	2.26	0.559	0.433	0.0018	*	0.0056	98.8	0.0060	0.485

Site	Sample	Depth	Date	Type	pH	$E_H/V$	Concentrations (nmol/l)	Mn	C(%)	$I$	EC					
		(cm)					$H_4SiO_4$	K	Na	Ca	$mol\cdot l^{-1}$ (mS/cm)					
							Cl	HCO <sub>3</sub>	SO <sub>4</sub>	Mg	Fe	Al	Mn			
KR-1	22	65	70-10-28	gr	3.45	+	6.60	-	21.6	2.01	0.243 16.7	5.65	8.08 0.134	1.31	0.286 98.5	0.0604 4.04
KR-1	23	95	70-10-28	gr	3.30	+	7.70	-	22.7	2.05	0.306 18.7	5.45	8.30 0.125	1.70	0.275 99.7	0.0634 4.30
Mn-1	2	5	70-06-09	so	5.21	+	2.26	0.143	3.79	0.167	0.274 4.27	1.07	1.61 0.001	0.000 0.046	98.4 0.0174 1.04	
Mn-1	3	20	70-07-07	so	5.60	+	1.34	0.035	2.29	0.176	0.175 2.33	0.733	0.994 0.000	0.016 0.016	99.6 0.0089 0.62	
Mn-1	4	20	70-07-07	si	4.46	+	17.4	-	17.2	1.28	0.743 21.1	5.13	9.54 0.0004	0.048 0.293	99.6 0.0639 4.48	
Mn-1	5	+15	70-07-24	so	5.10	+	0.756	0.030	1.36	0.173	0.126 1.45	0.392	0.563 0.0050	0.0010 0.0071	99.5 0.0054 0.406	
Mn-1	6	+15	70-07-24	si	3.90	+	18.1	-	18.2	1.32	0.738 23.6	5.14	9.38 0.0004	0.096 0.319	97.4 0.0665 4.52	
Mn-1	7	-3	70-07-24	le	5.50	-0.124	2.99	1.38	4.56	0.58	0.517 5.70	1.24	2.13 0.176	+	0.089 94.8 0.0185 1.26	
Mn-1	8	-120	70-07-24	le	5.20	0.245	15.6	1.63	11.3	0.815	0.808 21.6	2.25	6.36 0.0042	+	0.131 95.9 0.0492 3.76	
Mn-1	9	-180	70-07-24	le	5.92	0.036	18.0	2.30	12.4	0.845	0.946 24.3	2.45	7.31 0.0307	+	0.135 97.8 0.0551 4.18	
Mn-1	10	+55	70-09-24	so	7.22	+	0.342	0.681	0.294	0.121	0.046 0.818	0.168	0.206	+	0.000 97.2 0.0022 0.172	
Mn-1	11	+45	70-09-24	si	3.40	+	20.6	-	18.5	1.24	0.591 26.8	4.90	9.35 0.0098	0.172 0.302	103.0 0.0696 5.04	
Mn-1	12	+76	70-10-27	so	6.63	+	0.244	0.660	0.193	0.150	0.035 0.445	0.129	0.263 0.0025	+	0.000 101.5 0.0018 0.159	

Mn-1	13	+30	70-10-27	si	3.25	*	19.3	-	17.8	1.21	0.581	24.5	4.46	9.45	0.0070	0.162	0.267	100.7	0.0666	4.96	
Mn-1	23	-35	70-10-28	gr	4.41	*	16.1	-	13.2	1.47	0.618	22.5	2.45	7.00	0.0764	0.0316	0.146	101.1	0.0528	3.96	
Mn-1	24	-65	70-10-28	gr	4.32	*	18.1	-	14.9	1.53	0.667	26.0	2.69	7.66	0.0604	0.0569	0.164	100.2	0.0589	4.44	
Mn-1	25	-100	70-10-28	gr	5.37	*	19.1	*	15.8	1.54	0.711	27.7	2.87	8.12	0.111	0.0231	0.166	99.5	0.0623	4.60	
Mn-1	26	-125	70-10-28	gr	6.11	*	19.2	1.19	15.8	1.54	0.753	27.8	2.95	8.47	0.173	*	0.165	99.0	0.0633	4.72	
Mn-2	23	(-120)	69-08-07	gr	4.08	*	33.2	*	29.5	1.06	0.679	42.4	13.1	10.9	0.091	0.240	0.200	100.2	0.107	7.70	
Mn-2	27	+70	69-09-29	so	6.93	*	0.485	2.00	0.071	0.175	0.029	0.555	0.713	0.307	*	*	*	100.9	0.0026	0.29	
Na-2	28	(-120)	69-09-30	gr	3.08	*	46.6	*	34.4	1.91	1.02	55.6	13.5	14.2	0.249	0.658	0.268	100.8	0.131	9.0	
Na-2	30	+45	69-11-26	so	7.50	*	7.60	3.94	0.071	0.150	0.086	6.32	1.22	1.42	*	*	*	102.0	0.0141	1.20	
Na-2	31	(-120)	69-11-26	gr	3.50	*	34.6	-	25.8	1.58	1.15	38.4	10.7	11.2	0.484	0.196	0.241	97.2	0.100	7.10	
Na-2	32	-2	69-11-26	le	6.63	-0.177	7.53	6.37	0.425	0.440	0.175	6.05	2.57	1.39	0.255	*	0.0386	101.1	0.0186	1.46	
Na-2	33	+2	70-06-11	so	6.71	*	26.6	-	6.45	1.58	0.847	28.4	2.77	3.12	0.126	0.0075	0.065	*	0.0183	*	
Na-2	34	+17	70-07-31	so	7.40	*	3.04	2.41	1.86	9.87	0.293	0.767	12.4	6.47	3.89	*	*	*	100.4	0.0430	3.02

Site no.	Sample	Depth (cm)	Date	Type	pH	$E_H/V$	C1	HCO <sub>3</sub>	SO <sub>4</sub>	H <sub>4</sub> SiO <sub>4</sub>	Concentrations (mmol l <sup>-1</sup> )			Al	Mn	C(%)	$I$ mol l <sup>-1</sup>	EC (mS/cm)		
											Na	Mg	Fe							
Na-2	35	+10	70-07-31	si	6.78	+	46.9	6.33	31.9	0.526	0.789	55.8	14.5	15.8	+	+	98.2	0.133	9.20	
Na-2	36	+17	70-07-31	si <sup>f</sup>	6.98	+	4.82	2.58	1.84	0.169	0.227	4.98	1.75	1.19	+	<0.0002	98.4	0.0144	1.15	
Na-2	37	+50	70-09-02	so	7.22	+	2.08	2.20	0.434	0.160	0.083	2.18	0.914	0.525	+	<0.0002	95.2	0.0067	0.534	
Na-2	38	+40	70-09-02	si	7.40	+	35.1	6.30	20.6	0.280	0.485	42.3	9.08	10.9	+	0.0032	96.9	0.0963	6.80	
Na-2	45	-	70-10-01	so	7.16	+	3.86	3.48	0.350	0.184	0.062	4.03	1.08	0.896	+	<0.0002	99.3	0.0100	0.81	
Na-2	47	-	70-10-01	si	7.40	+	45.0	6.49	26.2	0.364	0.521	50.7	12.2	14.1	+	0.033	98.3	0.119	8.40	
Na-2	48	+20	70-12-28	so	7.40	+	10.5	5.14	0.405	0.0865	0.231	9.16	1.70	1.83	0.0028	<0.0002	98.8	0.0197	1.76	
Na-2	49	+20	70-12-28	si	7.10	+	54.5	4.03	31.8	0.233	0.417	62.8	13.5	16.0	0.0023	+	0.0185	99.5	0.138	9.90
Na-2	50	-5	70-12-28	le	6.61	-0.163	23.2	19.0	10.3	0.345	0.315	29.0	8.29	7.89	0.425	+	0.123	100.1	0.0735	4.92
Na-2	51	-5	70-12-28	lei	6.63	-0.163	46.3	4.82	37.1	0.208	0.484	62.8	14.3	16.4	0.194	+	0.104	100.4	0.141	10.1
0-1	1	(-55)	70-06-05	gr	3.76	+	21.1	-	30.1	1.93	0.272	42.1	4.87	12.6	0.288	0.707	0.506	101.2	0.0952	6.10
0-1	2	(-100)	70-06-05	gr	3.76	+	16.3	-	7.99	1.93	0.200	31.1	1.18	3.29	0.0702	0.0219	0.129			
0-1	6	-135	60-06-05	le	3.50	+0.280	21.5	-	25.3	1.75	0.399	39.2	4.08	11.2	0.133	+	0.414	97.0	0.0857	.
							16.7	-	7.21	1.75	0.297	29.4	1.04	3.09	0.0341	-	0.111			

0-1	7	-160	70-06-05	1e	3.51	+0.410	22.3	-	26.4	1.57	0.485	41.3	4.07	11.5	0.346	-	0.435	97.4	0.0891 .
0-1	8	-180	70-06-05	1e	3.60	+0.170	23.4	-	26.9	1.68	0.527	41.9	4.37	11.9	0.539	-	0.433	97.5	0.0941 .
0-1	10	(-190)	70-06-05	gr	3.80	-	22.3	-	30.1	2.13	0.397	48.6	4.08	11.2	0.746	-	0.438	100.9	0.0972 6.12
0-1	26	-	70-07-15	so	4.26	-	0.377	-	0.619	0.063	0.027	0.714	0.104	0.232	<0.0004.	0.098	96.6	0.0026 .	
0-1	27	+25	70-08-14	so	5.10	-	0.178	0.150	0.253	0.0920	0.039	0.414	0.053	0.088	0.0048 .	0.045	92.3	0.0013 0.092	
0-1	28	+10	70-08-14	si	3.68	-	10.1	-	16.0	1.20	0.305	18.1	3.35	7.65	0.0061	0.445	-	98.1	0.0525 3.60
0-1	29	+25	70-08-14	si <sup>f</sup>	-	-	0.241	0.089	0.420	0.110	0.040	0.658	0.078	0.159	-	0.0064	88.2	0.0018 0.144	
0-1	30	+30	70-10-07	so	6.02	-	0.064	0.079	0.040	0.089	0.020	0.163	0.0091	0.010	-	-	-	98.6	0.0003 0.031
0-1	31	+27	70-10-07	si	3.65	-	3.37	-	5.76	0.522	0.130	6.85	1.07	2.39	0.0018	0.131	0.127	98.8	0.0203 1.45
0-1	46	-60	70-10-22	gr	3.40	-	16.9	-	24.1	2.01	0.180	30.7	3.58	11.6	0.132	0.810	0.429	100.4	0.0777 5.30
0-1	47	-75	70-10-22	gr	3.35	-	18.2	-	26.3	2.05	0.247	32.5	3.90	12.7	0.195	0.885	0.479	101.4	0.0835 5.60
0-1	48	-90	70-10-22	gr	3.32	-	20.5	-	29.8	2.13	0.288	37.5	4.23	13.9	0.485	0.950	0.502	99.8	0.0932 6.30
0-1	49	-105	70-10-22	gr	3.30	-	14.3	-	7.15	2.05	0.184	24.5	1.00	3.52	0.0507	0.0316	0.129	-	-
0-1	50	-125	70-10-22	gr	3.33	-	22.5	-	30.9	2.18	0.415	41.0	4.37	14.4	0.875	0.760	0.515	99.6	0.0984 6.80
0-1	50	-	-	-	17.3	-	7.98	-	2.18	0.304	30.3	1.05	3.75	0.212	0.0235	0.130	-	-	-

Site no.	Sample	Depth (cm)	Date	Type	pH	$E_{H^+/V}$	Cl	$HCO_3$	$SO_4$	Concentrations (mmol/l)				C (%)	$I_{mol\cdot l^{-1}}$	EC (mS/cm)				
										$H_4SiO_4$	K	Na	Ca							
0-1	51	+5	70-12-08	so	4.98	-	0.889	*	0.309	0.019	0.099	0.825	0.094	0.175	0.0046	0.0108	0.0062	101.5	0.0021	0.208
0-1	53	+20	70-12-08	si	3.73	-	4.84	-	8.07	0.830	0.159	8.81	1.60	3.72	0.0032	0.241	0.175	99.2	0.0279	2.10
0-1	54	-5	70-12-08	le	5.20	0.00	3.99	0.433	1.79	0.133	0.091	4.42	0.794	0.687	0.233	-	0.0323	96.1	0.0107	0.84
0-1	55	-5	70-12-08	lef	3.85	+0.344	8.70	-	10.9	0.715	0.238	13.2	2.30	4.85	1.10	-	0.233	100.2	0.0395	2.79
Ra-1	85	-130	69-07-30	le	3.51	+0.660	15.8	-	19.7	0.690	0.790	25.6	5.09	8.84	<0.001	-	0.173	97.3	0.0670	.
Ra-1	86	-170	69-07-30	le	3.56	+0.450	21.58	-	17.1	0.670	0.870	27.5	5.63	7.89	0.009	-	0.115	100	0.0676	.
Ra-1	99	+40	69-09-24	so	4.26	-	0.955	-	2.36	0.044	0.412	2.13	0.711	0.772	<0.001	0.0711	0.0142	98.4	0.0085	0.60
Ra-1	100	(-50)	69-09-24	gr	3.73	*	8.94	-	22.5	1.75	0.491	25.7	4.54	7.99	0.109	0.534	0.0957	102.1	0.0558	4.21
Ra-1	101	(-80)	69-09-24	gr	3.42	*	10.6	-	25.8	2.01	0.605	30.0	4.85	9.15	0.240	0.920	0.0920	100.5	0.0747	5.20
Ra-1	106	-5	69-09-24	le	4.40	+0.260	5.66	-	13.5	0.600	0.328	12.0	3.99	5.08	0.938	-	0.105	101.3	0.0425	.
Ra-1	107	-90	69-09-24	le	3.42	+0.705	10.2	-	22.7	1.85	0.558	25.3	5.08	9.15	0.0285	-	0.132	94.4	0.0682	.

Ra-1	108	-140	69-09-24 <b>1e</b>	3.53	+0.490	13.0	-	24.9	1.89	0.648	30.8	5.13	9.58	0.557	-	0.151	99.5	0.0762	.
Ra-1	109	-165	69-09-24 <b>1e</b>	3.58	+0.270	14.7	-	28.4	1.67	0.738	33.3	5.90	11.5	0.776	-	0.175	95.7	0.0855	.
Ra-1	115	+25	69-11-19 <b>8e</b>	4.30	-	0.873	-	2.19	0.031	0.076	19.1	0.770	0.836	0.0010	0.0133	0.0112	98.0	0.0081	0.57
Ra-1	116	-5	69-11-19 <b>1e</b>	4.80	+0.150	4.23	-	8.67	0.466	0.194	7.77	2.82	3.67	0.243	-	0.0570	103.0	0.0292	2.08
Ra-1	117	-110	69-11-19 <b>1e</b>	3.55	+0.580	8.33	-	24.1	1.62	0.546	25.4	5.45	9.55	0.102	-	0.159	95.6	0.0702	4.62
Ra-1	118	-130	69-11-19 <b>1e</b>	3.81	+0.492	9.96	-	23.0	1.42	0.785	17.7	7.50	10.7	0.141	-	0.196	87.67	0.0697	5.06
Ra-1	119	-170	69-11-19 <b>1e</b>	3.92	+0.126	14.0	-	26.9	1.09	0.964	31.2	5.67	11.2	0.567	-	0.152	98.0	0.0817	5.64
Ra-1	120	-210	69-11-19 <b>1e</b>	5.75	+0.030	14.5	1.49	27.6	0.948	1.18	33.5	5.36	12.4	0.318	-	0.203	97.6	0.0855	5.92
Ra-1	146	-50	70-06-15 <b>f8</b>	3.73	-	13.7	-	30.9	1.45	0.459	31.7	7.64	12.5	0.0459	0.801	0.127	103.9	0.0890	5.50
Ra-1	147	-90	70-06-16 <b>f8</b>	3.67	-	10.7	-	8.24	1.45	0.338	23.5	1.84	3.26	0.0112	0.0242	0.0323			
Ra-1	148	-110	70-06-16 <b>f8</b>	3.55	-	10.4	-	21.7	2.00	0.586	26.8	4.17	7.86	0.116	0.445	0.0884	102.7	0.0656	4.30
Ra-1	149	-140	70-06-16 <b>f8</b>	3.60	-	11.0	-	22.5	1.96	0.717	28.5	4.15	7.76	0.538	0.364	0.0879	103.6	0.0681	4.38

Site	Sample no.	Depth (cm)	Date	Type	pH	$E_{H^+/V}$	C1	HCO <sub>3</sub>	SO <sub>4</sub>	H <sub>4</sub> SiO <sub>4</sub>	K	Concentrations (mmol / l)	Ca	Mg	Fe	Al	Mn	C(%)	I mol.l <sup>-1</sup>	EC (mS/cm)
Ra-1	150	-160	70-06-16	fe	4.20	-	11.1	-	21.6	1.74	0.699	28.0	4.17	7.52	0.866	0.207	0.0935	101.6	0.0669	4.36
Ra-1	157	+15	70-06-16	so	4.80	-	1.48	-	3.06	0.112	0.165	3.09	1.07	1.09	0.0004	0.00031	0.0178	95.5	0.0112	0.78
Ra-1	160	-50	70-07-15	fe	3.82	-	4.13	-	16.0	1.48	0.396	12.1	4.60	6.05	0.140	0.450	0.0860	99.6	0.0460	2.98
Ra-1	161	-90	70-07-15	fe	3.57	-	9.83	-	20.5	2.04	0.640	23.0	4.55	7.70	0.123	0.500	0.0860	99.6	0.0622	4.22
Ra-1	162	-110	70-07-15	fe	3.52	-	10.5	-	20.5	2.08	0.681	23.0	4.75	7.70	0.284	0.527	0.0873	101.2	0.0629	4.30
Ra-1	163	-140	70-07-15	fe	3.72	-	10.6	-	21.0	2.04	0.746	23.9	4.35	7.90	0.611	0.440	0.0900	99.5	0.0642	4.38
Ra-1	164	160	70-07-15	fe	4.02	-	10.8	-	20.8	1.91	0.752	24.5	4.38	8.16	0.716	0.262	0.0947	99.2	0.0648	4.38
Ra-1	171	-	70-07-15	so	4.40	-	0.920	-	1.93	0.016	0.089	1.88	0.662	0.724	0.0004	0.0958	0.0801	96.3	0.0073	0.530
Ra-1	172	-	70-07-15	si	4.00	-	2.91	-	7.18	0.795	0.176	6.51	2.24	2.86	0.011	0.0528	0.0397	97.8	0.0238	1.60
Ra-1	175	-50	70-08-14	fe	3.50	-	11.2	-	25.7	1.62	0.534	25.4	5.92	10.8	0.171	0.680	0.111	98.2	0.0752	5.04
Ra-1	176	-90	70-08-14	fe	3.40	-	9.77	-	21.0	1.95	0.678	22.9	4.15	8.54	0.175	0.508	0.0931	96.7	0.0633	4.40
							7.83	-	6.57	1.95	0.520	17.6	1.15	2.55	0.0489	0.0207	0.0271			

Ra-1	177	-110	70-08-14	<b>fe</b>	3.40	-	9.78	-	20.6	2.01	0.685	23.2	3.95	8.07	0.286	0.508	0.0879	96.7	0.0624	4.40
Ra-1	178	-140	70-08-14	<b>fe</b>	3.55	-	10.4	-	20.9	1.98	0.754	23.9	3.93	8.22	0.624	0.414	0.0923	97.8	0.0639	4.40
Ra-1	179	-160	70-08-14	<b>fe</b>	4.00	-	10.7	-	20.5	1.76	0.785	24.4	3.77	8.21	0.754	0.223	0.0918	97.1	0.0638	4.40
Ra-1	186	+10	70-08-14	<b>so</b>	4.53	-	0.953	-	1.76	0.0170	0.081	1.78	0.611	0.683	0.0004	0.0026	0.0090	104.0	0.0068	0.526
Ra-1	187	+10	70-08-14	<b>si</b>	3.90	-	5.25	-	11.2	1.00	0.250	9.30	3.90	4.88	0.0021	0.0883	0.0661	97.7	0.0365	2.42
Ra-1	188	+10	70-08-14	<b>si<sup>f</sup></b>	4.17	-	1.05	-	2.32	0.119	0.096	2.34	0.726	0.894	0.0004	0.0020	0.0122	98.4	0.0086	0.61
Ra-1	223	+30	70-09-15	<b>si</b>	3.73	-	2.77	-	7.25	0.700	0.170	6.42	2.26	2.75	0.0074	0.0890	0.0379	96.9	0.0238	1.64
Ra-1	224	+30	70-09-15	<b>so</b>	4.67	-	0.462	-	0.968	0.0390	0.038	1.03	0.320	0.336	0.0023	0.0035	0.0095	99.8	0.0037	0.292
Ra-1	227	-50	70-10-07	<b>fe</b>	3.62	-	10.9	-	27.3	1.54	0.580	26.7	6.37	10.9	0.392	0.715	0.115	98.2	0.0783	5.01
Ra-1	228	-90	70-10-07	<b>fe</b>	3.40	-	10.2	-	21.9	1.98	0.613	25.4	4.46	8.10	0.280	0.500	0.0910	100.0	0.0659	4.32
Ra-1	229	-110	70-10-07	<b>fe</b>	3.39	-	10.3	-	21.8	1.99	0.661	25.8	4.25	7.72	0.406	0.526	0.0871	101.5	0.0655	4.32
Ra-1	230	-140	70-10-07	<b>fe</b>	3.51	-	10.6	-	21.5	1.94	0.709	26.3	3.88	7.77	0.610	0.424	0.0897	100.6	0.0654	4.40
Ra-1	231	-160	70-10-07	<b>fe</b>	3.85	-	10.9	-	21.3	1.79	0.741	26.6	3.90	7.76	0.737	0.289	0.0906	100.7	0.0656	4.40

Site	Sample no.	Depth (cm)	Date	Type	pH	$E_{H/V}$	Cl	$HCO_3$	$SO_4$	$H_4SiO_4$	K	Na	Ca	Mg	Fe	Al	Mn	C(%)	$I$ mol.l <sup>-1</sup>	EC (mS/cm)
Ra-1	239	+	70-10-07	so	5.10	+	0.505	0.025	0.920	0.016	0.044	1.21	0.260	0.295	0.001	-	0.0011	100.0	0.0036	0.29
Ra-1	240	+	70-10-07	si	3.70	+	3.51	-	8.95	0.815	0.193	8.39	2.72	3.29	0.0021	0.127	0.0456	98.3	0.0288	1.96
Ra-1	266	-50	70-12-08	fe	3.80	+	10.8	-	26.5	1.46	0.477	24.5	6.50	11.4	0.435	0.600	0.108	100.1	0.0768	4.90
Ra-1	267	-90	70-12-08	fe	3.80	+	10.2	-	20.7	1.91	0.600	22.5	4.43	8.46	0.287	0.474	0.0850	99.6	0.0632	4.42
Ra-1	268	-110	70-12-08	fe	3.67	+	10.2	-	20.8	1.91	0.681	23.2	4.16	8.35	0.443	0.465	0.0835	99.1	0.0635	4.46
Ra-1	269	-140	70-12-08	fe	3.78	+	10.4	-	20.7	1.94	0.716	23.7	3.99	8.15	0.704	0.373	0.0899	98.5	0.0636	4.48
Ra-1	270	-160	70-12-08	fe	4.68	+	10.9	-	20.5	1.71	0.638	24.3	4.08	8.34	0.820	0.178	0.0908	98.0	0.0643	4.68
Ra-1	277	+25	70-12-08	so	5.19	+	0.511	0.121	0.493	0.0270	0.094	0.335	0.153	0.183	0.0075	-	0.0006	100.6	0.0024	0.206
Ra-1	278	+25	70-12-08	si	3.84	+	4.15	-	9.88	1.04	0.202	8.62	2.99	4.13	0.0023	0.185	0.0510	100.0	0.0319	2.30
Ra-1	281	-5	70-12-08	le	5.25	-0.044	2.75	1.16	1.45	0.131	0.095	3.85	0.589	0.651	0.180	-	0.0176	96.8	0.0091	0.70
Ra-1	282	-5	70-12-08	le	4.15	0.330	9.987	-	9.32	0.570	0.330	13.1	3.13	4.02	0.373	-	0.0572	93.8	0.0369	2.56
					8.33	-	3.64	0.570	0.269	10.8	1.15	1.56	0.138	-	0.0256					

Ra-2	82	+12	69-07-30	80	4.35	+	2.51	-	5.46	0.300	0.170	4.93	2.15	1.95	<0.0001	0.0389	0.0329	100.2	0.0190	1.33
Ra-2	87	-120	69-07-30	1e	3.60	+0.500	6.66	-	10.9	0.950	0.766	12.1	3.29	4.05	0.0726	-	0.139	100.6	0.0369	.
Ra-2	88	-150	69-07-30	1e	3.86	+0.186	12.6	-	15.4	0.710	1.32	19.8	3.54	6.84	0.420	-	0.195	96.6	0.0542	.
Ra-2	89	-180	69-07-30	1e	4.98	+0.057	10.6	+	19.1	0.960	1.50	21.7	4.26	7.87	0.432	-	0.271	100.1	0.0609	.
Ra-2	102	(-60)	69-09-24	gr	3.63	+	4.32	-	15.7	2.02	0.676	15.2	3.53	5.01	0.396	0.471	0.0799	103.8	0.0455	3.00
Ra-2	103	(-100)	69-09-24	gr	3.66	+	4.54	-	16.8	2.12	0.799	16.9	3.43	5.14	0.658	0.493	0.0814	102.9	0.0483	3.40
Ra-2	110	-10	69-09-24	1e	4.37	+3.40	7.47	-	8.05	0.580	0.253	9.35	2.64	3.25	1.00	-	0.0899	105.6	0.0312	.
Ra-2	111	-130	69-09-24	1e	3.47	+0.390	5.60	-	17.4	2.07	0.755	17.8	4.03	5.69	0.786	-	0.123	100.7	0.0514	.
Ra-2	112	-180	69-09-24	1e	3.67	+0.220	6.09	-	19.5	1.73	0.818	20.0	4.08	6.58	1.22	-	0.130	100.1	0.0570	.
Ra-2	127	-5	69-11-20	1e	4.55	+0.120	6.10	+	10.8	0.461	0.335	7.46	3.43	3.93	1.73	-	0.8727	99.2	0.0368	.
Ra-2	151	-30	70-06-16	fe	4.30	+	2.80	-	8.55	0.824	0.129	8.06	2.48	3.02	0.268	0.0417	0.0476	100.8	0.0273	1.73
Ra-2	152	-50	70-06-16	fe	3.80	+	4.40	-	17.0	1.33	0.344	14.8	4.90	5.79	0.0592	0.416	0.0878	102.0	0.0487	3.06

Site	Sample no.	Depth (cm)	Date	Type	pH	$E_H/V$	Cl	$HCO_3$	$SO_4$	Concentrations (mmol/l)				C(%)	$I_{mol\cdot l^{-1}}$	EC (mS/cm)				
										$H_4SiO_4$	K	Na	Mg	Fe						
Ra-2	153	-75	70-06-16	Fe	3.52	+	3.64	-	14.6	1.66	0.433	13.2	3.73	4.99	0.0217	0.376	0.0751	101.8	0.0432	2.60
Ra-2	154	-100	70-06-16	Fe	3.47	+	4.40	-	17.6	2.08	0.601	16.1	4.27	5.82	0.147	0.521	0.087	103.4	0.0498	3.17
Ra-2	155	-120	70-06-16	Fe	3.50	+	4.04	-	14.9	1.96	0.585	14.1	3.43	4.77	0.491	0.315	0.0726	102.8	0.0433	2.79
Ra-2	156	-155	70-06-16	Fe	4.00	+	4.80	-	18.0	2.20	0.732	16.4	4.73	5.69	0.732	0.343	0.0934	104.2	0.0516	3.30
Ra-2	165	-30	70-07-15	Fe	4.52	+	2.89	+	8.80	0.860	0.141	6.86	2.80	3.16	0.694	0.0371	0.0461	99.8	0.0281	1.81
Ra-2	167	-75	70-07-15	Fe	3.70	+	2.45	+	3.69	0.860	0.117	5.73	1.08	1.27	0.268	0.00285	0.0184			
Ra-2	168	-100	70-07-15	Fe	3.50	+	3.42	-	13.2	1.61	0.439	10.9	3.68	4.67	0.0274	0.375	0.0711	97.7	0.0387	2.60
Ra-2	169	-120	70-07-15	Fe	3.71	+	2.85	-	4.94	1.61	0.353	8.84	1.22	1.65	0.0092	0.0218	0.0247			
Ra-2	170	-155	70-07-15	Fe	3.90	+	4.13	-	16.5	2.08	0.675	13.8	4.05	5.95	0.207	0.530	0.0880	100.1	0.0471	3.11
Ra-2	170	-30	70-08-14	Fe	4.48	+	2.92	-	9.50	0.810	0.149	6.83	2.97	3.44	1.01	<0.002	0.0524	97.3	0.0299	1.92
Ra-2	180	-30	70-08-14	Fe	4.48	+	2.48	-	3.89	0.810	0.123	5.67	1.11	1.36	0.379	.	0.0204			

Ra-2	161	-50	70-08-14	fe	3.54	+	3.98	-	16.1	1.49	0.402	12.3	4.41	6.14	0.214	0.436	0.0875	97.5	0.0462	3.02
Ra-2	162	-75	70-08-14	fe	3.48	+	3.40	-	13.2	1.63	0.458	10.7	3.38	5.00	0.0409	0.357	0.0695	96.8	0.0368	2.62
Ra-2	163	-100	70-08-14	fe	3.39	+	3.87	-	16.3	2.08	0.685	13.2	3.76	6.05	0.290	0.489	0.0880	96.6	0.0464	3.12
Ra-2	164	-120	70-08-14	fe	3.57	+	4.02	-	15.7	2.02	0.697	12.8	3.44	5.55	1.21	0.273	0.0813	97.6	0.0454	3.02
Ra-2	165	-155	70-08-14	fe	3.56	+	4.33	-	17.5	2.23	0.829	14.0	3.97	6.49	0.917	0.395	0.0696	98.1	0.0498	3.32
Ra-2	232	-30	70-10-07	fe	4.80	+	3.54	-	5.97	2.23	0.651	11.0	1.19	2.07	0.277	0.0156	0.0304			
Ra-2	233	-50	70-10-07	fe	3.72	+	2.85	-	10.4	0.755	0.149	7.40	3.06	3.46	1.53	-	0.0518	99.5	0.0322	2.02
Ra-2	234	-50	70-10-07	fe	3.72	+	4.01	-	16.3	1.66	0.441	13.7	4.30	5.75	0.233	0.432	0.0842	101.3	0.0466	1.91?
Ra-2	235	-75	70-10-07	fe	3.55	+	3.50	-	13.5	1.64	0.474	11.9	3.37	4.72	0.107	0.340	0.0710	99.8	0.0395	1.60?
Ra-2	236	-100	70-10-07	fe	3.40	+	2.91	-	5.05	1.64	0.381	9.61	1.11	1.65	0.0355	0.0193	0.0244			
Ra-2	237	-120	70-10-07	fe	3.75	+	3.80	-	16.1	2.07	0.651	14.2	3.63	5.49	0.470	0.443	0.0826	100.8	0.0461	3.02
Ra-2	238	-155	70-10-07	fe	3.70	+	4.48	-	18.1	2.17	0.801	16.0	3.88	6.24	0.980	0.331	0.0873	101.2	0.0480	3.08
Ra-2	239	-175	70-10-07	fe	3.64	-	3.11	-	5.87	2.08	0.556	11.3	1.13	1.79	0.403	0.0149	0.0277			

Site no.	Sample	Depth (cm)	Date	Type	pH	$E_H/V$	Cl	HCO <sub>3</sub>	SO <sub>4</sub>	Concentrations (mmol / l)					Al	Mn	C(%)	$I_{mol \cdot l^{-1}}$	EC (mS/cm)
										H <sub>4</sub> SiO <sub>4</sub>	K	Na	Ca	Mg	Fe				
Ra-2	271	-30	70-12-08	fe	6.45	•	2.93	•	8.97	0.640	0.141	6.42	3.10	3.42	0.578	•	0.0507	104.6	0.0286 1.90
Ra-2	272	-50	70-12-08	fe	3.88	•	3.83	•	16.2	1.39	0.380	11.9	4.66	6.18	0.339	0.384	0.0831	98.0	0.0464 3.05
Ra-2	273	-75	70-12-08	fe	3.80	•	3.40	•	13.3	1.58	0.419	10.6	3.58	5.08	0.180	0.314	0.0686	97.8	0.0393 2.60
Ra-2	274	-100	70-12-08	fe	3.68	•	3.80	•	15.4	1.96	0.635	12.4	3.70	5.73	0.488	0.427	0.0795	99.2	0.0445 3.04
Ra-2	275	-120	70-12-08	fe	3.71	•	4.11	•	16.6	2.06	0.719	13.2	3.79	5.98	1.17	0.318	0.0866	98.1	0.0477 3.28
Ra-2	276	-155	70-12-08	fe	4.05	•	4.54	•	17.9	2.21	0.863	15.2	4.17	6.55	0.953	0.298	0.0973	99.2	0.0514 3.34
Ra-3	84	+41	69-07-30	so	3.98	•	2.10	-	6.05	0.450	0.242	4.88	2.23	2.08	<0.0004	0.0655	0.0406	95.0	0.0200 1.29
Ra-3	90	-120	69-07-30	le	3.27	+0.657	9.48	-	16.9	1.72	1.12	14.1	5.47	7.59	0.115	•	0.358	100.8	0.0543 •
Ra-3	91	-140	69-07-30	le	3.28	•	-	-	20.8	1.84	1.14	11.9	5.43	7.50	0.274	•	0.31	•	•
Ra-3	92	-180	69-07-30	le	3.53	•	6.55	-	24.9	1.92	1.76	15.2	5.76	9.52	1.81	•	0.40	•	•
Ra-3	104	+83	69-09-24	so	4.48	•	0.583	-	0.971	0.0470	0.038	1.12	0.317	0.354	<0.0004	0.0093	0.00466	107.4	0.0039 0.36

Ra-3	113	-5	69-09-24	1e	4.30	+0.200	2.66	-	6.65	1.02	0.347	5.60	2.30	2.41	0.242	-	0.0655	99.3	0.0224	-
					2.30	-	3.07		1.02	0.294	4.77	0.962	1.05	0.102	-	0.0284				
Ra-3	114	-115	69-09-24	1e	3.20	+0.660	6.26	-	20.6	2.48	1.00	15.9	5.73	8.56	0.0464	-	0.258	97.1	0.0591	.
					5.04	-	6.53	2.48	0.773	12.3	1.61	2.59	0.0132	.	0.0763					
Ra-3	121	+70	69-11-20	so	4.20	-	0.822	-	1.85	0.032	0.089	1.74	0.667	0.657	<0.0004	0.0152	0.0097	99.0	0.0070	0.59
Ra-3	122	-5	69-11-20	1e	4.90	-0.015	2.03	*	7.49	0.679	0.295	5.26	2.21	2.38	1.08	*	0.0648	106.6	0.0239	1.60
Ra-3	124	-130	69-11-20	1e	3.51	+0.460	4.21	-	19.6	2.39	1.23	13.5	5.01	8.44	0.302	*	0.2718	96.3	0.0551	3.10
Ra-3	125	-150	69-11-20	1e	3.90	+0.190	4.27	-	21.2	2.21	1.43	13.6	4.94	9.53	0.983	*	0.238	94.7	0.0590	3.90
Ra-3	126	-210	69-11-20	1e	5.40	+0.044	6.52	2.18	22.6	1.21	1.94	13.8	10.07	8.06	0.815	*	0.213	108.0	0.0664	3.64?
Ra-3	158	+50	70-06-16	so	4.49	*	1.43	-	2.97	0.102	0.157	2.93	1.03	1.09	0.0007	0.0078	0.0176	96.3	0.0109	0.75
Ra-3	159	+50	70-06-16	si	3.44	*	2.00	-	4.42	0.580	0.255	3.66	1.51	1.65	*	0.0333	*	99.0	0.0154	1.09
Ra-3	173	*	70-07-15	so	4.30	*	0.980	-	1.92	0.0190	0.089	1.90	0.698	0.704	<0.0004	0.0657	0.0102	96.0	0.0074	0.590
Ra-3	174	*	70-07-15	si	3.22	*	2.28	-	5.14	0.743	0.236	4.24	1.66	1.90	0.0143	*	0.0338	97.1	0.0176	1.36
Ra-3	189	+50	70-08-14	so	3.97	*	0.830	-	1.76	0.011	0.086	1.68	0.595	0.635	<0.0004	0.0026	0.0093	100.3	0.0067	0.500
Ra-3	190	+50	70-08-14	si	3.27	*	2.84	-	8.54	1.23	0.282	6.04	2.82	3.22	0.0164	0.174	0.0675	101.0	0.0269	1.94
Ra-3	191	+50	70-08-14	si <sup>f</sup>	4.50	*	0.896	-	1.81	0.115	0.130	1.99	0.546?	0.637	0.0021	0.0043	0.0103	99.0	0.0069	0.550

Site	Sample no.	Depth (cm)	Date	Type	pH	$E_H/V$	Concentrations (mmol / l)						C(%)	$I$ mol.l <sup>-1</sup>	EC (mS/cm)						
							Cl	HCO <sub>3</sub>	SO <sub>4</sub>	H <sub>4</sub> SiO <sub>4</sub>	K	Na	Mg	Fe	Al	Mn					
Ra-3	225	+70	70-09-15	si	3.12	+	1.91	-	6.51	0.600	0.207	4.61	2.00	2.40	0.0708	0.0516	0.0445	98.5	0.0210	1.54	
Ra-3	226	+70	70-09-15	so	4.83	+	0.481	-	0.875	0.0370	0.046	1.07	0.262	0.268	0.0043	0.0020	0.0029	99.4	0.0035	0.256	
Ra-3	241	-	70-10-07	so	4.45	+	0.486	-	1.03	0.0180	0.056	1.23	0.296	0.318	0.0007	0.0024	0.0032	95.7	0.0040	0.308	
Ra-3	242	-	70-10-07	si	3.05	+	2.37	-	8.23	0.836	0.246	5.85	2.58	2.86	0.0127	0.111	0.0569	99.0	0.0254	1.89	
Ra-3	279	+65	70-12-08	so	6.12	+	0.459	0.130	0.502	0.0180	0.053	0.651	0.158	0.186	0.0004	0.	<0.0002	99.8	0.0024	0.208	
Ra-3	280	+65	70-12-08	si	3.32	+	2.74	-	9.78	1.16	0.295	6.45	3.09	3.92	0.0115	0.191	0.0774	97.6	0.0299	2.28	
Ra-3	283	-5	70-12-08	le	5.40	-0.090	4.35	1.84	2.32	0.313	0.114	5.90	1.03	1.17	0.185	0.	0.0217	96.6	0.0141	1.04	
Ra-3	284	-5	70-12-08	lei	5.09	-0.066	7.31	0.621	4.01	0.629	0.284	8.39	1.38	1.71	0.522	0.	0.0112	0.	0.035	108.5	0.0206
Mc-3	3	+120	69-11-06	so	6.43	+	-	-	-	-	-	-	-	-	-	-	-	-	0.43		
Mc-3	4	-5	69-11-06	le	5.36	-0.045	4.04	0.503	5.25	0.540	0.212	6.08	1.92	1.47	0.949	0.	0.035	108.5	0.0206	0.	
Mc-4	5	+120	69-11-06	so	6.79	+	-	-	-	-	-	-	-	-	-	-	-	-	0.10		
Mc-4	6	-5	69-11-06	le	6.41	-0.200	1.64	4.58	0.665	0.380	0.231	2.28	1.42	0.803	0.269	0.	0.0268	108.3	0.0101	0.	

Mc-5	7	+80	69-11-06	so	6.46	*	*	*	*	*	*	*	*	*	*	*	*	*	*	0.10		
Mc-5	8	-5	69-11-06	1e	5.63	-0.032	1.47	2.53	0.661	0.250	0.065	1.72	0.812	0.631	0.296	*	*	*	*	0.0258	104.6	0.0073 .
Mc-6	9	+20	69-11-06	so	7.00	*	*	*	*	*	*	*	*	*	*	*	*	*	*	0.23		
Mc-6	10	-5	69-11-06	1e	6.43	-0.133	3.33	5.28	1.84	0.410	0.180	4.56	2.37	1.23	0.133	*	0.0380	105.4	0.0161 .			
Mc-7	11	+20	69-11-06	so	6.30	*	*	*	*	*	*	*	*	*	*	*	*	*	*	0.44		
Mc-7	12	-5	69-11-06	1e	4.50	+0.020	1.20	-	3.79	0.660	0.085	2.46	1.35	0.531	1.21	*	0.0241	99.8	0.0131 .			
Mc-8	13	+20	69-11-06	so	5.38	*	*	*	*	*	*	*	*	*	*	*	*	*	*	0.11		
Mc-8	14	-5	69-11-06	1e	5.30	+0.050	2.61	*	2.08	0.540	0.072	2.73	0.809	0.859	0.286	*	0.0322	111.7	0.0973 .			
Mc-9	15	*	69-11-06	so	4.21	*	*	*	*	*	*	*	*	*	*	*	*	*	*	0.15		
Mc-9	16	-5	69-11-06	1e	4.44	+0.240	2.67	-	2.21	0.430	0.103	3.17	0.845	1.02	0.0245	*	0.0263	110.1	0.0101 .			
Mc-10	17	+60	69-11-06	so	7.00	*	*	*	*	*	*	*	*	*	*	*	*	*	*	0.22		
Mc-10	18	-5	69-11-06	1e	5.85	+0.006	7.01	2.47	3.28	0.410	0.304	7.23	1.25	2.64	0.318	*	0.0424	103.7	0.0209 .			

Site no.	Sample	Depth (cm)	Date	Type	pH	$E_H^{\prime \prime} / V$	Concentrations (mmol / l)						Al	Mn	C(%)	$I_{mol \cdot l^{-1}}$ (mS/cm)	EC			
							Cl	$HCO_3$	$SO_4$	$H_4SiO_4$	K	Na	Ca	Mg						
Mc-11	19	+15	69-11-29	so	6.58	•	•	•	•	•	•	•	•	•	•	•	0.38			
Mc-11	20	-5	60-11-29	le	4.80	+0.320	2.54	•	13.1	0.460	0.167	3.07	7.87	3.92	0.893	•	0.102	89.6	0.0385	2.70
Mc-12	21	+45	69-11-29	so	7.12	•	•	•	•	•	•	•	•	•	•	•	0.0359			
Mc-12	22	-5	69-11-29	le	6.47	+0.002	4.39	6.02	0.872	0.300	0.260	5.83	1.59	1.33	0.0718	•	0.0439	100.3	0.0151	•
Mc-15	25	+70	69-11-29	so	7.39	•	•	•	•	•	•	•	•	•	•	•	0.0212			
Mc-15	26	-5	69-11-29	le	4.97	+0.221	1.60	1.50	2.11	0.360	0.140	2.26	1.43	0.988	0.0209	•	0.0219	100.3	0.0105	•
Mc-16	27	+70	69-11-29	so	7.52	•	•	•	•	•	•	•	•	•	•	•	0.0121			
Mc-16	28	-5	69-11-29	le	6.24	-0.060	2.99	4.94	0.577	0.220	0.126	4.83	1.08	0.846	0.111	•	0.0272	102.9	0.0091	0.70
Mc-17	29	+150	69-11-29	so	7.01	•	•	•	•	•	•	•	•	•	•	•	0.0143			
Mc-17	30	-5	69-11-29	le	5.17	+0.150	2.97	1.37	3.88	0.700	0.220	4.76	1.78	1.38	0.285	•	0.116	112.4	0.0167	•

## C.2 Water samples from the Cha-am Laguna.

Ca-1	34	*2	69-08-07	80	7.75	.	112	.0.6222	5.43	0.151	1.82	96.3	2.91	9.90	.	.	.	98.7	0.136	12.6
Ca-1	35	(-100)	69-08-07	gr	3.45	.	903	-	41.5	1.91	12.7	740	20.1	93.4	0.972	1.00	0.800	98.6	1.07	76.5
Ca-1	36	-2	69-08-07	1e	6.35	+0.080	186	5.56	10.9	0.270	2.31	154	4.60	22.6	0.0094	.	0.993	95.6	0.236	20
Ca-1	37	-90	69-08-07	1e	3.30	+0.420	941	-	38.2	0.520	13.4	765	20.5	97.5	0.0917	.	1.31	97.9	1.10	81
Ca-1	38	-130	69-08-07	1e	3.67	+0.426	959	-	38.3	0.820	13.7	789	19.1	95.6	0.727	.	0.979	99.0	1.12	60
Ca-1	39	-150	69-08-07	1e	4.14	+0.034	881	-	39.1	0.570	13.1	714	20.3	93.4	1.31	.	0.949	98.0	1.04	79
Ca-1	40	-170	69-08-07	1e	5.78	-0.050	846	*	43	0.640	13.2	691	20.5	91.3	1.39	*	1.04	97.7	1.01	77
Ca-1	43	*20	69-09-30	80	7.30	.	11.5	0.983	0.855	0.230	0.259	10.6	0.600	1.08	.	.	.	98.3	0.0163	1.62
Ca-1	44	(-100)	69-09-30	gr	3.40	*	925	-	52.1	2.07	12.4	774	20.8	98.0	0.0911	1.02	0.698	98.8	1.10	70?
Ca-1	45	(-200)	69-09-30	gr	3.97	.	549	-	53.4	1.93	11.9	780	19.4	93.9	1.64	0.395	0.705	101.3	1.09	68
Ca-1	46	-85	69-09-30	1e	3.25	+0.725	939	-	57.7	1.36	12.7	798	30.7	100	0.0133	.	0.878	99.0	1.13	.
Ca-1	47	-115	69-09-30	1e	3.35	+0.500	900	-	53.9	1.47	12.6	754	21.2	97.5	0.753	.	0.884	99.4	1.08	.

Site	Sample no.	Depth (cm)	Date	Type	pH	$E_H/V$	Cl	HCO <sub>3</sub>	SO <sub>4</sub>	Concentrations (mmol/l)				Al	Mn	C(%)	$I \text{ mol} \cdot \text{l}^{-1}$	EC (mS/cm)		
										H <sub>4</sub> SiO <sub>4</sub>	K	Na	Mg	Fe						
Ca-1	48	-140	69-09-30 le		4.60	+0.086	875	*	56.9	1.26	13.0	728	22.6	96.1	4.21	*	0.910	98.9	1.06	
Ca-1	63	+5	69-11-26 so		6.60	*	7.62	0.187	0.342	0.0310	0.253	6.27	0.231	0.753	*	*	*	103.6	0.097	1.00
Ca-1	64	-2	69-11-26 le		6.72	-0.310	31.8	2.75	1.45	0.296	0.549	27.6	0.857	3.52	0.0850	*	0.191	103.4	0.0422	4.10
Ca-1	65	-90	69-11-26 le		3.31	+0.570	952	-	50.1	1.18	13.1	789	20.1	103	0.571	*	0.829	96.7	1.13	
Ca-1	66	-110	69-11-26 le		3.41	+0.495	931	-	49.9	1.48	13.0	769	20.0	101	1.92	*	0.894	99.5	1.11	
Ca-1	67	-130	69-11-26 le		5.15	+0.040	864	0.218	47.9	1.15	13.0	706	20.6	97.3	2.03	*	0.847	99.2	1.04	
Ca-1	69	-170	69-11-26 le		5.69	+0.041	849	0.049	49.6	1.15	13.0	693	21.3	96.4	1.98	*	1.03	98.1	1.02	
Ca-1	70	(-100)	69-11-26 gr		3.51	*	838	-	43.9	1.72	11.3	691	17.9	91.3	0.521	*	0.787	97.6	1.00	
Ca-1	90	+20	70-12-23 so		7.02	*	8.53	0.556	1.02	0.160	0.282	7.78	0.457	1.07	*	*	0.178	0.132	1.30	
Ca-2 <sup>a</sup>	30	*	69-08-07 so		7.74	*	524	3.16	27.2	0.090	10.4	449	11.8	49.3	0.005	*	0.003	100.7	0.624	51.9
Ca-2 <sup>a</sup>	56	*	69-09-30 so		7.79	*	58.6	1.36	3.31	0.160	1.35	51.5	1.38	5.51	*	*	*	97.1	0.0737	70

Ca-2	57	(-20)	69-09-30	gr	7.43	.	504	11.8	22.3	0.630	10.0	435	9.31	48.3	0.0101	.	0.0152	98.8	0.599	46.8
							321	6.22	2.16	0.630	6.29	304	2.11	12.2	0.0024	.	0.0032			
Ca-2	58	-70	69-09-30	1e	6.62	-0.192	542	4.78	32.1 <sup>h</sup>	0.460	12.1	471	10.4	53.2	0.0051	.	0.0522	97.7	0.651	.
							341	2.49	2.92	0.460	7.48	326	2.34	13.3	0.0012	.	0.0114			
Ca-2	59	-60	69-09-30	1e	6.67	-0.184	574	5.09	34.1 <sup>h</sup>	0.680	12.3	495	12.4	57.7	0.0082	.	0.0748	97.6	0.692	.
							359	2.59	2.97	0.680	7.59	342	2.76	14.4	0.0019	.	0.0162			
Ca-2	60	-100	69-09-30	1e	6.68	-0.177	577	7.29	31.7 <sup>h</sup>	0.970	12.0	497	12.1	57.2	0.0081	.	0.0741	98.5	0.693	.
							362	3.71	2.75	0.970	7.38	345	2.70	14.3	0.0019	.	0.0158			
Ca-2	77	-30	60-11-26	1e	6.55	-0.172	248	10.0	7.27	0.697	6.06	216	4.51	20.7	0.0214	.	0.0204	98.2	0.293	25.0
							171	6.46	1.14	0.697	4.14	157	1.20	5.90	0.0060	.	0.0049			
Ca-2	78	-60	69-11-26	1e	6.56	-0.168	331	10.5	14.6	0.785	7.49	293	6.05	28.7	0.0412	.	0.0201	99.6	0.396	31.0
							220	6.32	1.91	0.785	4.93	208	1.47	7.57	0.0105	.	0.0045			
Ca-2	79	(-20)	69-11-26	gr	7.29	.	367	4.13	16.9	0.270	7.14	311	7.29	35.7	0.0865	.	0.0163	98.3	0.437	36.0
							242	2.38	2.04	0.270	4.65	220	1.77	9.43	0.0216	.	0.0039			
Ca-2 <sup>b</sup>	80	.	69-11-26	so	7.81	.	452	2.08	22.8	0.0180	8.74	384	8.96	44.4	.	.	.	98.9	0.536	42.2
Ca-3	19	-50	69-08-07	1e	6.13	-0.167	994	5.82	50.4	0.370	18.5	839	19.9	101	0.0113	.	0.174	98.7	1.17	86
							591	2.39	2.88	0.370	10.8	588	4.52	27.2	0.0026	.	0.0377			
Ca-3	20	-90	69-08-07	1e	6.05	-0.084	941	3.06	50.8	0.460	17.5	794	19.9	97.0	0.0277	.	0.236	97.6	1.12	84
							562	1.28	3.00	0.460	10.3	554	4.49	25.8	0.0064	.	0.0518			
Ca-3	21	-130	69-08-07	1e	6.23	.	915	6.28	48.6	0.880	17.1	783	18.0	91.0	0.122	.	0.153	98.4	1.08	81
							548	2.70	2.95	0.880	10.0	546	4.03	2.39	0.0282	.	0.0326			

Site	Sample	Depth	Date	Type	pH	$E_H/V$	Cl	$\text{HCO}_3$	$\text{SO}_4$	$\text{H}_4\text{SiO}_4$	K	Na	Ca	Mg	Fe	Al	Mn	C(%)	$I$	EC
no.		(cm)																	mol.l <sup>-1</sup>	(mS/cm)
Ca-3	22	-170	69-08-07	1e	6.48	-0.108	998	5.79	42.5	0.590	18.8	834	20.7	96.9	0.0188	0.198	96.0	1.16	83	
Ca-3	24	(-30)	69-08-07	gr	6.50	+	916	7.17	37.1	0.910	16.2	757	19.6	92.2	0.121	98.9	1.07	75.5		
Ca-3	50	(-40)	69-09-30	gr	6.68	+	917	6.16	50.4	1.14	18.0	776	19.2	95.7	0.0461	0.0972	97.7	1.09	69	
Ca-3	51	(-60)	69-09-30	gr	6.72	+	910	6.64	49.3	1.24	17.5	768	20.8	93.8	0.0891	0.106	97.7	1.08	71	
Ca-3	52	(-100)	69-09-30	gr	6.72	+	922	6.61	49.3	1.37	17.5	784	19.2	93.8	0.0973	0.115	98.6	1.09	71	
Ca-3	73	(-40)	69-11-26	gr	7.00	+	671	7.20	34.2	0.864	11.0	574	13.7	66.5	0.172	0.200	98.6	0.798	59	
Ca-3A	23	+10	69-08-07	so	7.50	-	582	5.21	26.4	0.230	10.7	486	13.2	58.1	0.0041	0.133	97.7	0.690	54.4	
Ca-3A	26	-10	69-08-07	1e	6.92	-0.191	800	9.19	30.6	0.280	14.6	668	16.1	77.6	0.0551	0.122	98.1	0.935	72	
Ca-3A	27	-50	69-08-07	1e	6.49	-0.124	827	5.31	33.4	0.320	15.0	692	15.3	80.2	0.0135	0.155	96.5	0.965	74	
Ca-3A	28	-90	69-08-07	1e	6.37	-0.100	898	3.71	41.3	0.560	16.7	752	17.3	90.4	0.136	0.152	98.8	1.06	80	

Ca-3A	29	(-20)	69-08-07 gr	6.37	•	937	9.48	40.4	1.20	17.1	782	20.1	93.8	0.0406	•	0.152	98.4	1.10	80.4
Ca-3A	49	+20	69-09-30 so	8.07	•	281	3.77	15.2	0.390	5.08	241	6.29	28.0	•	•	98.8	0.340	28.5	
Ca-3A	53	(-40)	69-09-30 gr	6.68	•	804	7.33	45.3	1.16	15.2	679	16.6	87.3	0.0308	•	0.0977	97.3	0.964	64
Ca-3A	54	(-60)	69-09-30 gr	6.70	•	487	3.26	3.00	1.16	9.05	471	3.66	22.3	0.0071	•	0.0206			
Ca-3A	55	(-100)	69-09-30 gr	6.64	•	843	7.56	47.1	1.20	15.5	723	16.4	86.3	0.0553	•	0.100	99.5	1.00	62
Ca-3A	74	+15	69-11-26 so	7.88	•	508	3.34	3.03	1.20	9.16	502	3.62	22.2	0.0127	•	0.0211			
Ca-3A	91	•	70-12-23 so	7.08	•	912	8.17	50.7	1.27	16.6	786	17.9	91.2	0.0966	•	0.124	99.5	1.08	69
Ca-4 <sup>i</sup>	31	•	69-08-07 so	8.27	•	531	2.13	27.0	0.028	10.9	455	10.6	50.1	•	•	96.8	0.629	51	
Ca-4 <sup>i</sup>	81	•	69-11-26 so	7.97	•	447	2.09	22.9	0.026	8.75	381	8.78	43.8	•	•	98.8	0.532	•	
C.3 Water samples from the Songkhla-Patran region.																			
Nk-1	11	(-75)	70-12-19 gr	3.00	•	10.1	-	6.64	1.74	0.255	9.76	1.23	1.36	0.196	2.11	0.0315	101.9	0.0282	2.32
Nk-1	13	(-70)	70-12-19 gr	2.80	•	16.5	-	11.2	2.04	0.591	18.4	1.41	2.72	1.41	2.12	0.0454	101.6	0.0455	3.80
Nk-2	20	(-100)	70-12-19 gr	2.90	•	54.1	-	6.32	0.710	0.616	44.7	2.87	5.00	0.742	0.746	0.0550	98.1	0.0768	0.0219
						42.6	-	1.75	0.710	0.480	35.4	1.04	1.92	0.217	0.0768	0.0219			

Site	Sample no.	Depth (cm)	Date	Type	pH	$E_{H^+}/V$	Concentrations (mmol / l)						C(%)	$I_{mol \cdot l^{-1}}$	EC (mS/cm)					
							Cl	$HC O_3$	$SO_4$	$H_4SiO_4$	K	Na	Ca	Mg	Fe	Al	Mn			
Sa-1	1	+5	70-12-20	so	6.50	-	1.13	0.258	0.210	0.142	0.076	1.26	0.126	0.109	-	-	-	99.1	0.0022	0.220
Sa-1	2	(-50)	70-12-20	gr	3.49	-	46.7	-	6.88	1.37	0.840	41.5	1.14	4.73	1.86	0.760	0.0320	100.1	0.0693	6.20
Sa-1	3	(-40)	70-12-20	gr	3.50	-	38.8	-	6.18	1.18	0.800	33.2	1.09	4.00	2.34	0.645	0.0320	100.2	0.0595	5.54
Sa-1							31.2	-	1.92	1.18	0.636	26.8	0.414	1.60	0.894	0.682	0.0124			

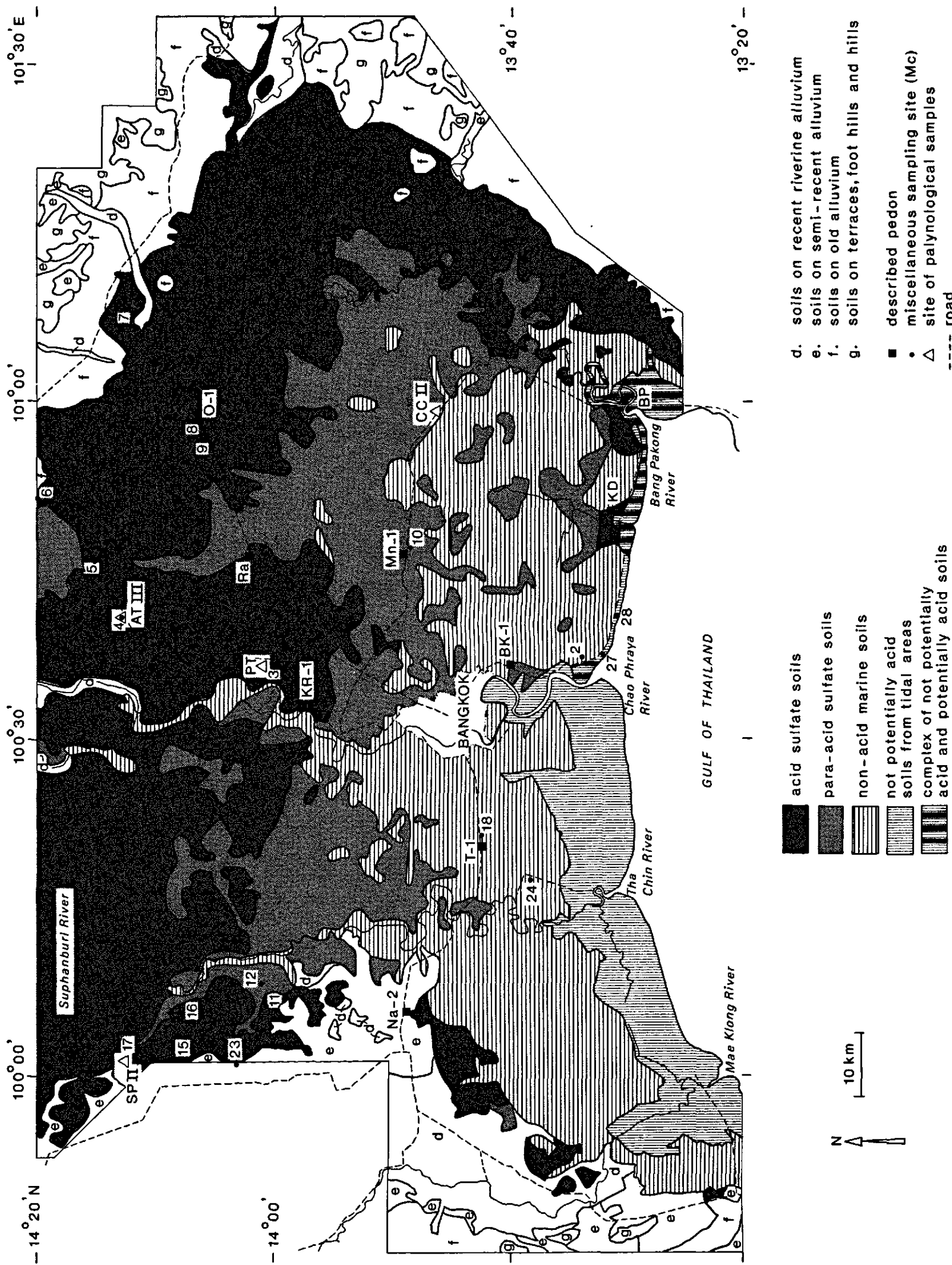
C.4 Water samples from the Southeast Coast Region.

Ch-1	16	-35	69-08-21	1e	3.20	+0.454	384	-	24.3	2.14	5.03	318	7.49	39.0	7.84	-	0.111	99.5	0.471
Ch-1	17	-50	69-08-21	1e	3.80	+0.235	294	-	22.9	1.51	5.57	244	6.29	30.8	7.77	-	0.0971	97.5	0.371
Ch-1	18	-70	69-08-21	1e	4.65	+0.086	280	-	21.1	1.32	5.26	229	6.56	29.5	7.73	-	0.0912	97.6	0.354
Ch-1	19	-90	69-08-21	1e	4.68	-0.006	285	-	21.2	1.34	5.21	234	6.08	29.4	8.63	-	0.0725	97.9	0.359
Ch-1	20	-130	69-08-21	1e	4.50	+0.095	290	-	26.3	0.970	5.10	243	6.52	31.9	8.71	-	0.0836	98.1	0.374
Ch-1	21	-170	69-08-21	1e	4.50	+0.041	301	-	27.3	0.780	5.60	254	6.72	32.1	8.70	-	0.127	98.2	0.387
Ch-1	23	(-60)	69-08-21	gr	3.97	-	277	-	22.2	1.63	5.10	230	5.36	28.0	9.82	-	0.0541	97.6	0.352
							187	-	3.01	1.63	3.37	163	1.31	7.38	2.43	-	0.0134		

Ch-1	24	(-100)	69-08-21	gr	4.28	+	278	-	24.9	1.46	5.26	232	5.81	28.3	10.1	-	0.0617	97.3	0.359	31.3	
Ch-1 <sup>b</sup>	29	-	69-08-21	so	3.14	+	167	-	5.65	1.25	2.83	138	2.98	15.4	0.420	0.110	0.0110	100.4	0.197	19.0	
Ch-1	37	-35	69-10-22	1e	3.02	+0.527	394	-	34.6	2.21	5.84	334	7.29	49.6	0.940	-	0.116	99.7	0.499	-	
Ch-1	38	-70	69-10-22	1e	4.60	+0.041	291	+	26.4	1.54	5.54	249	6.50	32.0	6.01	-	0.0742	98.3	0.374	-	
Ch-1	39	-130	69-10-22	1e	4.26	+0.087	301	-	29.3	0.895	5.57	255	7.07	35.1	7.09	-	0.114	98.7	0.391	-	
Ch-1	40	-170	69-10-22	1e	4.50	+0.054	299	-	31.3	0.650	5.20	258	7.06	34.7	6.87	-	0.0679	100.2	0.392	-	
Ch-1	41	(-40)	69-10-22	gr	3.82	+	285	-	24.3	2.01	5.28	244	5.43	28.3	8.28	-	0.0646	0.0507	100.6	0.363	28.7
Ch-1 <sup>b</sup>	42	-	69-10-22	so	3.63	+	66.4	-	34.1	0.483	1.45	57.0	1.36	5.96	0.0100	0.0190	0.0030	100.2	0.081	7.70	
Ch-1	61	-40	71-01-11	gr	4.03	+	238	-	18.3	1.53	4.08	197	5.03	24.9	7.05	0.0077	0.0439	98.9	0.302	25.6	
Ch-1 <sup>b</sup>	62	-	71-01-11	so	6.70	+	436	1.36	22.1	0.066	7.45	367	8.58	45.0	-	-	97.3	0.521	42.0		
Ch-2A	30	(-40)	69-08-21	gr	4.10	+	39.8	-	4.16	0.330	0.512	35.3	0.711	3.15	2.15	0.0801	0.0090	99.9	0.0548	5.16	
Ch-2A	31	(-80)	69-08-21	gr	3.20	+	135	-	8.24	1.36	1.86	109	3.00	14.2	1.08	0.965	0.0289	100.6	0.170	16.1	

Site no.	Sample	Depth (cm)	Date	Type	pH	$E_H/V$	Cl	HCO <sub>3</sub>	SO <sub>4</sub>	H <sub>4</sub> SiO <sub>4</sub>	Concentrations (mmol/l)				Al	Mn	C (%)	$I$ mol.l <sup>-1</sup>	EC
											K	Na	Ca	Mg					
Ch-2B 32	(-60)	69-08-21	gr	3.15	.	445	-	38.2	2.06	4.45	382	11.0	50.6	5.45	.	0.0935	98.2	0.562	46
						285	-	3.79	2.06	2.78	263	2.44	12.4	1.23	.	0.0211			
Ch-2B 33	(-80)	69-08-21	gr	3.31	.	446	-	36.1	2.40	4.77	377	11.8	50.0	5.94	.	0.0884	99.5	0.560	46
						286	-	3.58	2.40	2.99	261	2.64	12.4	1.35	.	0.0201			
Ch-2B 45	(-60)	69-10-21	gr	3.00	.	384	-	32.4	2.30	4.04	330	9.20	41.0	4.25	1.64	0.0730	100.1	0.486	39.4
						250	-	3.50	2.30	2.57	229	2.10	10.2	9.86	0.0606	0.0169			
Ch-2C 34	(-50)	69-08-21	gr	3.72	.	720	-	44.0	1.19	9.78	607	13.6	75.4	5.72	0.733	0.0763	101.0	0.870	63
						441	-	3.13	1.19	5.87	420	3.04	19.3	1.30	0.0227	0.0171			
Ch-2C 46	+15	69-10-22	so	6.78	.	35.3	0.302	1.41	0.062	0.789	31.0	0.585	2.75	.	.	.	100.8	0.0422	4.08
Ch-3 25	(-50)	69-08-21	gr	3.40	.	108	-	5.63	1.20	2.08	95.4	1.51	8.04	0.862	0.166	0.0049	98.8	0.130	12.9
						81.1	-	1.33	1.20	1.55	73.0	0.498	2.80	0.285	0.0153	0.0016			
Ch-6 47	(-60)	69-10-22	gr	4.00	.	522	-	28.6	1.80	8.94	447	11.8	50.6	0.820	0.110	0.0150	100.3	0.626	46.5
						330	-	2.66	1.80	5.57	311	2.72	13.0	0.192	0.0040	0.0035			
Ch-7 48	(-50)	69-10-22	gr	5.23	.	379	0.359	35.0	1.75	6.46	322	8.53	42.1	9.70	.	0.0702	99.7	0.486	35.6
						247	0.207	3.86	1.75	4.11	223	1.92	10.4	2.22	.	0.0160			
Ch-7 49	-30	69-10-22	le	3.50	0.486	412	-	32.5	1.53	5.69	359	8.86	42.0	4.07	0.180	0.0960	99.9	0.512	.
						267	-	3.48	1.53	3.61	249	2.01	10.5	0.940	0.0065	0.0221			

K1-1 <sup>j</sup>	2	(-100)	69-08-23	gr	4.45	*	0.24	-	0.32	0.42	0.029	0.55	0.092	0.053	0.005	*	0.004	123.9	0.0014	0.103
K1-1 <sup>j</sup>	3	(-80)	69-10-23	gr	3.90	*	1.13	-	0.187	0.370	0.038	0.906	0.106	0.058	0.0116	0.0260	0.0039	103.8	0.0019	0.215
K1-1	63	(-140)	71-01-11	gr	3.92	*	3.43	-	1.09	0.602	0.259	3.84	0.294	0.315	0.0639	*	0.0077	98.4	0.0071	0.670
K1-1	76	(-110)	71-01-11	gr	4.00	*	1.72	-	0.969	0.615	0.227	2.16	0.231	0.164	0.0043	0.122	0.0048	104.3	0.0049	0.424
					1.60	-	0.646	0.615	0.210	2.00	0.156	0.112	0.0029	0.0383	0.0033					



Generalized soil map of the Southern Central Plain (after van der Kervie & Yenmanas, 1972) showing the sampling sites